Non-additive effects of multiple global-change drivers on aquatic ecosystems of both hemispheres

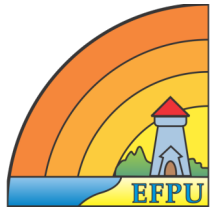

Department of Ecology
&
Estación de Fotobiología Playa Unión (EFPU)
&
Universitary Institute of Water Research

PhD Programme: **Fundamental and Systems Biology**

PhD Thesis:

A Thesis submitted by **Marco Jabalera Cabrerizo** for the degree of Doctor of Philosophy in the University of Granada

Granada, February 2017

Editor: Universidad de Granada. Tesis Doctorales
Autor: Marco Jabalera Cabrerizo
ISBN: 978-84-9163-503-1
URI: http://hdl.handle.net/10481/48124

The doctoral candidate Marco Jabalera Cabrerizo and the thesis supervisors Presentación Carrillo Lechuga and E. Walter Helbling guarantee, by signing this doctoral thesis, that the work has been done by the doctoral candidate under the direction of the thesis supervisor's, as far as our knowledge reaches, in the performance of the work, the rights of other authors to be cited (when their results or publications have been used) have been respected.

Granada, February 2017

Doctoral candidate

Signed: **Mr. Marco Jabalera Cabrerizo**

Thesis supervisors

Signed: **Dra. Presentación Carrillo**

Signed: **Dr. E. Walter Helbling**

The present work have been conducted between the group of Ecología Funcional (RNM 367) of the Department of Ecology of University of Granada and Universitary Institute of Water Research and Estación de Fotobiología Playa Unión. This research has been supported by:

- Ministerio de Economía y Competitividad (MINECO) and Fondo Europeo de Desarrollo Regional (FEDER) (CGL2011–23681 and CGL2015–67682–R)
- Junta de Andalucía (Excelencia projects P09–RNM–5376 and P12–RNM–327)
- Agencia Nacional de Promoción Científica y Tecnológica – ANPCyT (PICT 2012–0271 and PICT 2013–0208)
- Consejo Nacional de Investigaciones Científicas y Técnicas – CONICET (PIP N° 112–201001–00228)
- Fundación Playa Unión

Marco Jabalera Cabrerizo was supported by Ministerio de Educación, Cultura y Deporte through a "Formación de Profesorado Universitario" PhD fellowship (AP12/01243) and a short-term placement fellowship (EST13/0666), by Campus de Excelencia Interacional – University of Granada (CeiBiotic - UGR) (call. 2015) and by Fundación Playa Unión.

A Mari Paz,
por recordarme la esencia
por ser faro y brújula
por ser el alma donde quiero reflejarme
por esta vida y todo lo que conlleva

A tí, para tí y por tí.

General index

Chapter I. Introduction **17**

The complex nature of global change 18

Impacts of global-change drivers on food webs 22

The metabolic balance of aquatic ecosystems in a global-change context 25

Thesis outline and objectives 28

References 31

Chapter II. General Methodology **39**

Remote-sensing parameters 40

Physical parameters 40

Chemical parameters 41

Biological parameters 42

Data analysis and artwork 45

References 45

Chapter III. Current and predicted global change impacts of UVR, temperature and nutrient inputs on photosynthesis and respiration of key marine phytoplankton groups 49

Abstract 50

Introduction 50

Material and Methods 53

Results 58

Discussion 74

Conclussion 78

References 79

Chapter IV. Differential impacts of global change variables on coastal South Atlantic phytoplankton: Role of seasonal variations 87

Abstract 88

Introduction 88

Material and Methods 91

Results 98

Discussion 107

Conclussion 111

References 111

Chapter V. Rising nutrient-pulse frequency and high UVR strengthen microbial interactions 119

Abstract 120

Introduction 120

Material and Methods 124

Results 130

Discussion 139

Conclusion 141

References 142

Supplementary information 149

Chapter VI. Saharan dust inputs and high UVR levels jointly alter the metabolic balance of marine oligotrophic ecosystems 171

Abstract 172

Introduction 172

Material and Methods 175

Results 183

Discussion 191

Conclusion 193

References 194

Supplementary information 201

Chapter VII. Increased dust deposition and riverine nutrients under high UVR decrease the CO_2-sink capacity of coastal South Atlantic waters **211**

Abstract 212

Introduction 212

Material and Methods 214

Results 224

Discussion 234

Conclusion 237

References 237

Supplementary information 246

Chapter VIII. Synthesis **253**

Chapter IX. Conclussions **259**

Agradecimientos **263**

List of papers

1. Cabrerizo et al. 2017. Rising nutrient-pulse frequency and high UVR strengthen microbial interactions. *Sci. Rep.* **7**, 43615.

2. Cabrerizo et al. 2017. Differential impacts of global change variables on coastal South Atlantic phytoplankton: Role of seasonal variations. *Mar. Environm. Res.* **125**, 63-72.

3. Cabrerizo et al. 2016. Saharan dust inputs and high UVR levels jointly alter the metabolic balance of marine oligotrophic ecosystems. *Sci. Rep.* **6**, 35892.

4. Cabrerizo et al. 2014. Current and predicted global change impacts of UVR, temperature and nutrient inputs on photosynthesis and respiration of key marine phytoplankton groups. *J. Exp. Mar. Biol. Ecol.* **461**, 371-380.

5. Cabrerizo et al. Increased dust deposition and riverine nutrients under high UVR decrease the CO_2-sink capacity of coastal South Atlantic waters. Manuscript ready for submission.

Chapter I

Introduction

The complex nature of global change

Aquatic ecosystems worldwide are being confronted with sharp alterations by several environmental drivers which are triggering changes never seen before in the communities inhabiting these systems (Parmesan & Yohe, 2003). As a consequence of all these unpredictable situations, multiple lines of evidence forecast shifts in the ranges of geographical distribution of species (Malviya et al., 2016; Parmesan, 2006), changes in the ecological interactions within and among trophic levels as well as in the strength of these interactions (Griffiths et al., 2016; Pincebourde et al., 2012) or even species extinction (McCauley et al., 2015). However, one of the major obstacles and current challenges in the global-change research is their complex nature. Overall, on a global scale, aquatic ecosystems are undergoing three major changes: (1) increasing solar radiation exposure due to shallower upper mixed layers (UML) caused by ongoing stratification of water column during periods of time more and more extensive (Williamson et al., 2014), (2) higher nutrient (Nut) concentrations by continental runoff (Rabalais et al., 2009) or atmospheric dust inputs (Jickells & Moore, 2015), and (3) rising temperatures (T) in surface waters by the increasing heat waves and concentrations of carbon dioxide (CO_2) derived from burning fossil fuels (Nagelkerken & Connell, 2015).

The growing interest during the last four decades in evaluating the impact on aquatic ecosystems of these global change drivers has multiplied the number of publications. In this sense, to identify the gaps in knowledge, we quantify the number of studies that have assessed responses to these drivers in aquatic ecosystems by conducting systematic literature searches in Scopus, and the results are presented in the Table 1. Our goal in conducting these searches was identify which targets and temporal scales are receiving the most attention and which potentially important combinations of drivers might require more consideration. Thus, we focused on studies that measured responses to experimentally manipulated abiotic conditions, and we therefore excluded correlational field studies (database is available at: *www.dropbox.com/sh/56hlr2lyrue70gd/AABc5U5reWI6uIlDWwEqXLkka?dl=0*).

Table 1: Results from experimental studies published from 1972-2016 assessing single [ultraviolet radiation (UVR), nutrient (Nut) inputs and temperature (T)] and interactive effects on organisms and / or communities in aquatic (freshwater and marine) ecosystems at short (< day) and mid- and long-term scales (from days or weeks to years). Numbers in bold represent the number of studies found and numbers between parentheses the percentage of these studies respect to the total number of studies for each environmental driver considered as well as their interaction. Note that the total number of studies considered for each single global-change driver or their interaction were: UVR (n = 136), Nut (n = 90), T (n = 38), UVR × Nut (n = 18), UVR × T (n = 14), Nut × T (n = 11) and UVR × Nut × T (n = 3).

	Community	
Environmental factor	Short-term	Mid/Long-term
UVR	**32** (23.5%)	**25** (18.4%)
Nut	**17** (18.9%)	**60** (66.7%)
T	**8** (21.1%)	**17** (44.7%)
UVR×Nut	**1** (5.6%)	**13** (72.2%)
UVR×T	**0** (0%)	**7** (50%)
Nut×T	**0** (0%)	**7** (70%)
UVR×Nut×T	**2** (66.7%)	**0** (0%)
	Organism	
UVR	**42** (30.9%)	**32** (23.5%)
Nut	**5** (5.6%)	**5** (5.6%)
T	**2** (5.3%)	**9** (23.7%)
UVR×Nut	**1** (5.6%)	**3** (16.7%)
UVR×T	**7** (50%)	**0** (0%)
Nut×T	**2** (20%)	**1** (10%)
UVR×Nut×T	**1** (33.3%)	**0** (0%)
	Community + Organism	
UVR	**3** (2.2%)	**2** (1.5%)
Nut	**2** (2.2%)	**1** (1.1%)
T	**0** (0%)	**2** (5.3%)
UVR×Nut	**0** (0%)	**0** (0%)
UVR×T	**0** (0%)	**0** (0%)
Nut×T	**0** (0%)	**0** (0%)
UVR×Nut×T	**0** (0%)	**0** (0%)

The main targets explored through the biological-organization levels are the responses of populations and communities to individual drivers, since such responses match their consideration as stress bioindicators or as tools to evaluate the ecological risk to stress factors (Boyd & Brown, 2015; Woodward et al., 2010). Our extensive literature analysis on 310 peer-reviewed papers in which experimental manipulations of UVR, Nut and T were performed highlights that (i) more than 85% of the results reported came from studies that assessed the impacts of global-change drivers in isolation on natural communities and / or specific groups of organisms; and (ii) in most of these studies the variable most often manipulated was the ultraviolet radiation (UVR) (ca. 52%) followed by nutrient (Nut) concentration (34%) and temperature (14%). Although these invaluable studies have helped to define the many ramifications of altering even just one environmental driver (Boyd & Hutchins, 2012), recent reports are increasingly realizing that the experiments manipulating only one variable may not be adequate to evaluate the complex impacts of global change on communities and ecosystems (Boyd et al., 2016; Gunderson et al., 2016; Wernberg et al., 2012). The reason behind this proposal is that interaction among multiple global-change drivers may generate net effects that fall below (i.e., antagonism) or exceed (i.e., synergism) their expected additive effect (Christensen et al., 2006; Crain et al., 2008; Folt et al., 1999; Piggott etal., 2015; Vinebrooke et al., 2004). Hence, from the total of studies considered ca. 14% assessed the combined impact of two of the mentioned drivers, whereas only 1% of them evaluated the interaction of the three drivers.

Other crucial aspects to considerer in the evaluation of the impact of environmental drivers are the temporal scale of exposure (i.e., from hours to years) as well as the response of the organisms. These aspects are key because the nature and magnitude of the interaction can change during the experiment period, as organisms can adapt or acclimate in order to cope with changing environmental conditions (Häder & Gao, 2015). Thus, previous studies have tested the impact of UVR, T and Nut impacts over shorter periods of time (< day) (5 – 33%) when conducted with species (Table 1) but on mid- or long-term scales (from days and weeks to months

or years) when performed at community or ecosystems levels (50 – 72.2%).

However, when we specifically examined studies that assessed interactive effects of the three drivers considered, we found most of these works to be centred also on specific groups of organisms and mostly on phytoplankton groups (50 – 72%), followed by heterotrophs as zooplankton (7.1 – 22.2%), crabs and fishes (7.1 – 27.3%) and with minor frequency on bacteria (9.1%) (Table 2). Surprisingly, studies at a higher level of complexity such as plankton communities, including the interaction between trophic levels (e.g., phytoplankton – bacteria) within the ecosystems proved to be comparatively rarer (9 – 33%).

Table 2: Results from experimental studies published from 1972-2016 assessing interactive effects of ultraviolet radiation (UVR), nutrient (Nut) inputs and / or temperature (T) on specific groups of organisms such as phytoplankton, bacteria or zooplankton, on the planktonic community or other groups of organisms distinct than those previously considered. Numbers in bold represent the number of studies performed and numbers between parentheses the percentage of these studies respect to the total number of studies for each interaction considered. Note that the total number of studies considered for each interaction were: UVR × Nut (n = 18), UVR × T (n = 14), Nut × T (n = 11) and UVR × Nut × T (n = 3).

Interaction	Phytoplankton	Bacteria	Zooplankton	Plankton community	Other groups
UVR×Nut	**9** (50%)	**0** (0%)	**4** (22.1%)	**5** (27.9%)	**0** (0%)
UVR×T	**10** (71.5%)	**0** (0%)	**1** (7.1%)	**2** (14.3%)	**1** (7.1%)
Nut×T	**6** (54.5%)	**1** (9.1%)	**0** (0%)	**1** (9.1%)	**3** (27.3%)
UVR×Nut×T	**2** (66.7%)	**0** (0%)	**0** (0%)	**1** (33.3%)	**0** (0%)

Also, the results of the analysis show that these studies have usually been focused on specific processes (or targets) both in single (e.g., UVR – physiological; Nut and T – metabolic) as well as in multi-driver manipulations (e.g., UVR × T – physiological; Nut × T and UVR × Nut × T – metabolic) rather than evaluating different processes (or targets) through the biological organizational level used to gain a more integrated view on the impacts of global change (Table 3). Therefore, research focused on the global change should strive to conduct more interactive studies on different biolog-

ical organizational levels, with exposure regimes based on temporal scales appropriate to the organisms and food webs under study.

Table 3: Results from experimental studies published from 1972-2016 that tested the single and interactive effects of ultraviolet radiation (UVR), nutrient (Nut) inputs and temperature (T) on physiological and metabolic processes. Numbers in bold represent the number of studies found that tested the impacts of drivers mentioned on the variables showed, whereas the numbers between parentheses is the percentage of these studies respect to the total number of studies considered for each environmental driver and their interaction. Note that one study can have assessed the single and interactive effects of UVR, Nut and T on more than one of variables shown here. UVR (n = 136), Nut (n = 90), T (n = 38), UVR × Nut (n = 18), UVR × T (n = 14), Nut × T (n = 11) and UVR × Nut × T (n = 3). Physiological processes were considered those such as DNA repair, enzymatic activities, production of cyclobutane pyrimidine dimmers or PSII performance, whereas metabolic processes were the primary production, net community production, community respiration, bacterial production, bacterial respiration, release of organic carbon, bacterial carbon demand, among others.

Environmental factor	Physiological	Metabolic
UVR	**58** (42.6%)	**36** (26.5%)
Nut	**5** (5.6%)	**32** (35.6%)
T	**1** (2.6%)	**20** (51.3%)
UVR×Nut	**9** (50%)	**9** (50%)
UVR×T	**8** (57.1%)	**3** (21.4%)
Nut×T	**0** (0%)	**6** (54.5%)
UVR×Nut×T	**1** (33.3%)	**2** (66.7%)

Impacts of global-change drivers on food webs

All living organisms in the biosphere are tightly (directly and / or indirectly) connected to each other through a complex web of interactions, and hence the impact affecting one species can be transmitted to others in the system through multiple pathways that may differ in strength (Wootton & Emmerson, 2005). In fact, such interactions are so relevant that they can strongly shape the structure and functioning of communities and conse-

quently modulate the metabolic balance of the ecosystem, from autotrophy to heterotrophy or vice versa, going by the stable equilibrium (Begon et al., 2006).

Despite supporting 1% of the photosynthetic biomass on the Earth, aquatic ecosystems are responsible for approximately half of the global primary production (PP) of the biosphere (Field et al., 1998). Through the oxygenic photosynthesis, primary producers, commonly called phytoplankton, contribute to the redox state of the planet and the global cycles of carbon (C) and oxygen (O_2), affecting the global climate and generating the suitable conditions for others organisms can habitable the Earth (Falkowski & Godfrey, 2008). Furthermore phytoplankton, heterotrophic prokaryotes – that is, 'bacteria' collectively – numerically dominate the aquatic planktonic community in oceans and freshwater ecosystems (Sarmento & Gasol, 2012), and are responsible of immobilizing and (re) mineralizing the most of inorganic elements that play any role in the global biogeochemical cycles to make them available at higher trophic levels (Schlesinger & Bernhardt, 2013). Together with the inorganic nutrients, the dissolved organic C released by phytoplankton (EOC) or by cellular lysis is the major energy source driving heterotrophic growth and respiration (Agustí & Duarte, 2000; Lasternas & Agustí, 2014; Medina-Sánchez et al., 2010). Although processes (e.g., zooplankton excretion) other than the EOC by phytoplankton are needed to balance the bacterial carbon demands (BCD), it is generally accepted that phytoplankton exudates are the main organic-C source consumed by bacteria in autotrophic ecosystems (Baines & Pace, 1991; Becker et al., 2014; Carrillo et al., 2002). Based on these premises, the nature of the producer-decomposer relationship can be highly diverse (Fig. 1). This can reportedly vary from comensalism when bacterial production (BP) is sustained by the photosynthetic EOC (Mayali & Azam, 2004; Ribalet et al., 2008), to a competition when inorganic nutrients, mainly nitrogen (N) and phosphorus (P), are limiting (Joint et al., 2002; Van Mooy et al., 2009). Nevertheless, the phytoplankton-bacteria interaction can also be mutualistic when phytoplankton satisfy the BCD through EOC, but also phytoplankton obtain inorganic nutrients through phagotrophy (Medina-

Sánchez et al., 2004; Mitra et al., 2014). This latter kind of interaction between the two planktonic compartments has taken on remarkable importance in recent years both in freshwater (Carrillo et al., 2006; Medina-Sánchez et al., 2004) as well as marine (Fischer et al., 2016; Ptacnik et al., 2016) ecosystems because it appears to be greatly stimulated under climate-change conditions (Wilken et al., 2013). This increasingly interest is due mainly to mixotrophic phytoplankton, which can simultaneously combine into a single-cell phototrophy, to obtain energy or C, and phagotrophy to taken in limiting inorganic nutrients, increasing the energy-transfer efficiency from nutrient regeneration to PP, and enabling a direct by-pass for the support of PP from BP (Medina-Sánchez et al., 2004; Mitra et al., 2014; Ptacnik et al., 2016).

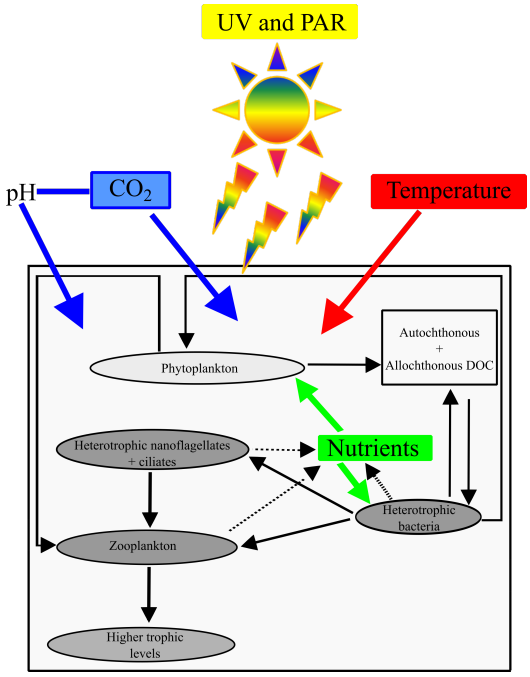

Figure 1: Simplified food web with a focus on potential multiple global-change drivers affecting their responses as well as their interaction with other trophic levels.

Despite that the interaction between phytoplankton-bacteria constitutes one of the main regulators of both groups, global change may also influence the strength of this interaction, strengthening or weakening it (Fig. 1). Recent results in different aquatic ecosystems have shown that a rise in EOC by phytoplankton under high UVR levels (Carrillo et al., 2002; Carrillo et al., 2015), increased T (Morán et al., 2006) or due to the interaction of both drivers (Durán et al., 2016) can satisfy the BCD and stimulate the bacterial growth and production, strengthening the coupling between the two trophic levels. Therefore, if we make predictions about the impact of global change on aquatic ecosystems but neglect the strength of interactions among different trophic levels of food webs, such inferences become unrealistic for any system with a relative degree of complexity (Montoya & Raffaelli, 2010) and thus would fail to predict how global change alters the role of aquatic ecosystems as sources or sinks of CO_2.

The metabolic balance of aquatic ecosystems in a global-change context

At the ecosystem level, from the total organic matter produced by phytoplankton, part is respired in surface waters either to support their maintenance costs or to support the heterotrophic activities of other organisms. The oxidation of this organic matter not only counterbalances C and O_2 fluxes but also reduces the total amount of organic matter available for higher trophic levels (Serret et al., 2015). The difference between the total amount of photosynthesis, called gross primary production (GPP), and respiration (CR) by the total community including those by auto- and heterotrophs, is the net community production (NCP). The NCP is an ecosystem-level process that integrates responses of different groups of eukaryotes, prokaryotes, and protists, and it also determines the capacity to fix carbon dioxide (CO_2) of ecosystems (Ducklow & Doney, 2013). A positive NCP (NCP > 0) reflects the surplus of organic matter production that

is available for lateral (e.g., mesopelagic zone) or vertical (e.g., deep ocean zone) exportation (Fig. 2), whereas a negative NCP (NCP ≤ 0) denotes a deficit of organic C available for food web due to increased consumption by R.

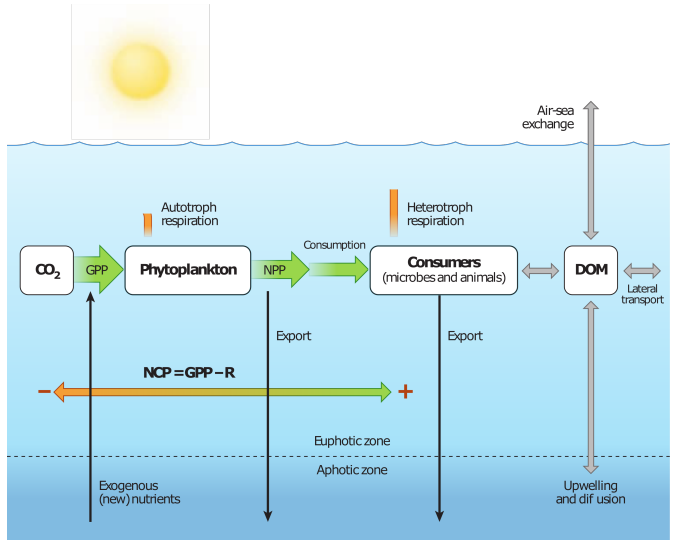

Figure 2: Metabolic exchanges, transformations and related processes that influences the balance between net autotrophy and heterotrophy into aquatic ecosystems (taken from Ducklow & Doney 2013).

The idea concerning the metabolic state of ecosystems was already present in the seminal work of Odum (1956), which proposed that heterotrophy could be considered as a dysfunctional characteristic of ecosystems whereas autotrophy would signal that an ecosystem is healthy. From Odum's work, the pioneer studies by del Giorgio et al. (1997) and Duarte & Agustí (1998) established the notion that plankton communities of aquatic ecosystems are net heterotrophic because the BCD usually tend to exceed NCP. Moreover, Westberry et al. (2012) estimated that approximately 52% of the total ocean surface area are net heterotrophic regions (Fig. 3); however, recent

studies challenge this idea, proposing that these are net autotrophic areas (Ducklow & Doney, 2013; Williams et al., 2013), or even that the metabolic balance of these ecosystems are neither autotrophic nor heterotrophic but metabolically diverse (Serret et al., 2015), thus alternating between auto- and heterotrophic metabolic states.

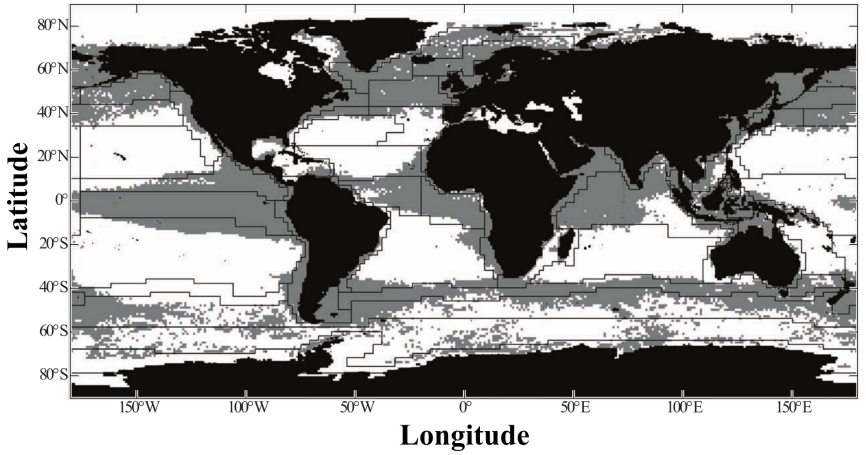

Figure 3: Global distribution of the net community production based on the production *vs.* respiration relationship. The autotrophic zones are shown in grey while the heterotrophic zones are shown in white (modified from Westberry et al., 2012).

Despite the enormous interest and fundamental scientific questions that continue to arise concerning the metabolic balance of ecosystems, the few studies perfomed to date intended to test the effects of global change have been focused primarily on their single effects (e.g., UVR, Nut or T) while the combined effects remain largely unknown. On one hand, experimental results have shown that, for example, high UVR levels can augment the NCP in autotrophic communities or, contrarily, diminish it in heterotrophic communities (García-Corral et al., 2014; 2016). Also, increased nutrient concentrations can boost autotrophy (Rodríguez et al., 2016) or even alter the metabolic balance from hetero- to autotrophy (Martínez-García et al.,

2013). Conversely, according to the metabolic theory of Ecology (Brown et al., 2004), warming tends to differentially benefit the heterotrophic as opposed to autotrophic processes; thus, experimental studies in freshwater and marine ecosystems have reported greater heterotrophy by augmented CR under warming (García-Corral et al., 2015; Yvon-Durocher et al., 2010). On the other hand, the scarce reports assessing the interaction between several global-change drivers on the metabolic balance have found that the responses can vary from a strong heterotrophy (e.g., UVR × warming, García-Corral et al., 2015) to an absence of effect with respect to current conditions (e.g., warming × nutrients, Rodríguez et al., 2016). Therefore, given the contrasting findings reported and the fact that the current global-change scenario affecting all ecosystems worldwide due to anthropogenic or climate-driven changes may alter this balance, a key unresolved question in Ecology that must be solved is: What direction will the planktonic responses take (towards auto- or heterotrophy)?.

Thesis outline and objectives

Great advances has been made to understand the effects of variables associated with global change on ecosystems (see review by Häder et al. 2014). However, as pointed out above, we have meagre and contrasting information about how these combined impacts occurring at organism's level might be scaled up to an ecosystem level. Moreover, considering the strong asymmetries existing between aquatic ecosystems of Northern and Southern Hemispheres (e.g., ozone concentrations, atmospheric aerosols), we might expect a differential forcing of selection and adaptation of organisms to the ongoing impacts of global change (Agustí et al., 2014) and therefore, variable responses. Notwithstanding, currently it is poorly understood how aquatic ecosystems of both hemispheres could respond to the same situation of global change. Within the biosphere, temperate aquatic environments (30-60° North and South) constitute the most productive areas into the planet, together with the terrestrial ecosystems (Falkowski et

al., 2000; Field et al., 1998). At the climatic level, temperate areas have a marked seasonality over the year with respect to tropical and polar areas both in terms of solar radiation received as in the surface T (Rousseaux & Gregg, 2014). The surface layers of the aquatic ecosystems in these areas undergo alternating periods of high (spring – summer) and low (fall – winter) UVR and photosynthetically active radiation (PAR) levels and warm and cold conditions which determine the biology and organisms that can inhabit these areas (Agustí et al., 2014; Chen, 2015). Nevertheless, in the Northern Hemisphere the surface T are *a priori* more variable than the Southern Hemisphere with mean differences of ca. 12 and 3°C, respectively, due to a higher land:ocean surface ratio and thus, a lower specific calorific capacity (Trenberth, 2002). The two hemispheres differ not only in the proportion of continents *vs.* ocean surface but also in the UVR levels reaching the Earth's surface (i.e., increases from the Equator towards the poles; Tittensor et al., 2010), or in the climatology, including phenomena such as the North Atlantic Oscillation [NAO] and El Niño Southern Oscillation [ENSO]. These latitudinal variations, which are being intensified by the global change, result in dissimilarities in the local weather and climate, generating seasonal, spatial, and non-linear responses of communities that alter the distribution and dispersion of organisms (Stenseth et al., 2003).

In addition to being highly dynamic ecosystems, temperate areas also sustain the greatest impact on the Earth by human activities (agriculture, livestock, herding), as they are the most populated areas on the planet with more than 50% of world population living less than 100 km from the coastline (Gattuso et al., 1998). Thus, the increasing human-induced pressures on ecosystems are resulting in steadily greater inputs of nutrients to surface waters (Peñuelas et al., 2013). These higher nutrient inputs through rivers together with altered patterns of atmospheric dust deposition are causing nutrient overenrichment with unpredictable cascading effects on aquatic ecosystems (Mahowald et al., 2008; Rabalais et al., 2009). Based in all these premises, this thesis focuses on assessing the non-additive effects that multiple drivers associated with the global change exert on temperate aquatic ecosystems of both hemispheres. The approach combines

laboratory and field experiments together with observational and remote-sensing data to test the responses of aquatic planktonic communities to future global-change scenarios on a regional and global scale. To achieve this main goal, in this thesis a gradualist approach is established at different biological organization levels and temporal scales with four specific research objectives:

1. To understand the underlying mechanisms that modulate the responses of Bacillariophyceae, Chlorophyceae, Dinophyceae, and Haptophyceae faced with a future scenario of increased nutrient (Nut) inputs and temperature (T) under UVR (Chapter III): "**Current and predicted global change impacts of UVR, temperature, and nutrient inputs on photosynthesis and respiration of key marine phytoplankton groups**".

2. To quantify how the natural environmental dynamic alter the phytoplankton responses to UVR, Nut and T through the seasonal succession (Chapter IV): "**Differential impacts of global change variables on coastal South Atlantic phytoplankton: Role of seasonal variations**".

3. To assess how variations in the frequency of nutrient inputs under high UVR levels affects the strength interaction in microbial food webs (Chapter V): "**Rising nutrient-pulse frequency and high UVR strengthen microbial interactions**".

4. To evaluate the impact of Saharan dust inputs and / or riverine inputs and high UVR levels on the metabolic balance of marine areas with contrasted trophic state in ecosystems of both hemispheres (Chapter VI): "**Saharan dust inputs and high UVR levels jointly alter the metabolic balance of marine oligotrophic ecosystems**" and (Chapter VII): "**Increased dust deposition and riverine nutrients under high UVR decrease the CO_2-sink capacity of coastal South Atlantic waters**".

Finally, in the Chapters VIII and IX summarize the main findings throughout this thesis as well as their conclusions.

References

Agustí, S., Duarte, C.M., 2000. Strong seasonality in phytoplankton cell lysis in the NW Mediterranean littoral. *Limnol. Oceanogr.* **45**, 940-947.

Agustí, S., Llabrés, M., Carreja, B., Duarte, C.M., 2014. Contrasting sensitivity of marine biota to UV-B radiation between southern and northern hemispheres. *Estuar. Coast.* **38**, 1126-1133.

Baines, S.B., Pace, M.L., 1991. The production of dissolved organic matter by phytoplankton and its importance to bacteria: Patterns across marine and freshwater systems. *Limnol. Oceanogr.* **36**, 1078-1090.

Becker, J.W., Berube, P.M., Follett, C.L., Waterbury, J.B., Chisholm, S.W., DeLong, E.F., Repeta, D.J., 2014. Closely related phytoplankton species produce similar suites of dissolved organic matter. *Front. Microbiol.* **5**, 111.

Begon, M., Townsend, C.R., Harper, J.L., 2006. Ecology: From individuals to ecosystems, 4th ed. Blackwell Publishing, Malden (USA).

Boyd, P.W., Brown, C.J., 2015. Modes of interactions between environmental drivers and marine biota. *Front. Mar. Sci.* **2**, 9.

Boyd, P.W., Dillingham, P.W., McGraw, C.M., Armstrong, E.A., Cornwall, C.E., Feng, Y.-y., Hurd, C.L., Gault-Ringold, M., Roleda, M.Y., Timmins-Schiffman, E., Nunn, B.L., 2016. Physiological responses of a Southern Ocean diatom to complex future ocean conditions. *Nat. Clim. Change* **6**, 207-213.

Boyd, P.W., Hutchins, D.A., 2012. Understanding the responses of ocean biota to a complex matrix of cumulative anthropogenic change. *Mar. Ecol. Prog. Ser.* **470**, 125-135.

Brown, J.P., Gillooly, F., Allen, A.P., Savage, V.M., West, G.B., 2004. Toward a metabolic theory of ecology. *Ecology* **85**, 1771-1789.

Carrillo, P., Medina-Sánchez, J.M., Durán, C., Herrera, G., Villafañe, V.E., Helbling, E.W., 2015. Synergistic effects of UVR and simulated stratification on commensalistic algal-bacterial relationship in two optically contrasting oligotrophic Mediterranean lakes. *Biogeosciences* **12**, 697-712.

Carrillo, P., Medina-Sánchez, J.M., Villar-Argaiz, M., 2002. The interaction of phytoplankton and bacteria in a high mountain lake: Importance of the spectral composition of solar radiation. *Limnol. Oceanogr.* **47**, 1294-1306.

Carrillo, P., Medina-Sánchez, J.M., Villar-Argaiz, M., Delgado-Molina, J.A., Bullejos, F.J., 2006. Complex interactions in microbial food webs: Stoichiometric and functional approaches. *Limnetica* **25**, 189-204.

Crain, C.M., Kroeker, K., Halpern, B.S., 2008. Interactive and cumulative effects of multiple human stressors in marine systems. *Ecol. Lett.* **11**, 1304-1315.

Chen, B., 2015. Patterns of thermal limits of phytoplankton. *J. Plankton Res.* **37**, 285-292.

Christensen, M.R., Graham, M.D., Vinebrooke, R.D., Findlay, D.L., Paterson, M.J., Turner, M.A., 2006. Multiple anthropogenic stressors cause ecological surprises in boreal lakes. *Glob. Change Biol.* **12**, 2316–2322.

del Giorgio, P.A., Cole, J.J., Cimbleris, A., 1997. Respiration rates in bacteria exceed phytoplankton production in unproductive aquatic systems. *Nature* **385**, 148-151.

Duarte, C.M., Agustí, S., 1998. The CO_2 balance of unproductive aquatic ecosystems. *Science* **281**, 234-236.

Ducklow, H.W., Doney, S.C., 2013. What is the metabolic state of the oligotrophic ocean? A debate. *Ann. Rev. Mar. Sci.* **5**, 525-533.

Durán, C., Medina-Sánchez, J.M., Herrera, G., Carrillo, P., 2016. Changes in the phytoplankton-bacteria coupling triggered by joint action of UVR, nutrients, and warming in Mediterranean high-mountain lakes. *Limnol. Oceanogr.* **61**, 413-429.

Falkowski, P.G., Godfrey, L.V., 2008. Electrons, life and the evolution of Earth's oxygen cycle. *Philos. T. Roy. Soc. B* **363**, 2705-2716.

Falkowski, P.G., Scholes, R.J., Boyle, E., Canadell, J., Canfield, D., Elser, J.J., Gruber, N., Hibbard, K., Högberg, P., Linder, S., Mackenzie, F.T., Moore Iii, B., Pedersen, T., Rosenthal, Y., Seitzinger, S., Smetacek, V., Steffen, W., 2000. The global carbon cycle: A test of our knowledge of Earth as a system. *Science* **290**, 291-296.

Field, C.B., Behrenfeld, M.J., Randerson, J.T., Falkowski, P., 1998. Primary production of the Biosphere: Integrating terrestrial and oceanic components. *Science* **281**, 237-240.

Fischer, R., Giebel, H.-A., Hillebrand, H., Ptacnik, R., 2016. Importance of mixotrophic bacterivory can be predicted by light and loss rates. *Oikos* **in press**.

Folt, C.L., Chen, C.Y., Moore, M.V., Burnaford, J.L., 1999. Synergism and antagonism among multiple stressors. *Limnol. Oceanogr.* **44**, 864-877.

García-Corral, L.S., Agustí, S., Regaudie-de-Gioux, A., Luculano, F., Carrillo-de-Albornoz, P., Wassmann, P., Duarte, C.M., 2014. Ultraviolet radiation enhances Arctic net plankton community production. *Geophys. Res. Lett.* **41**, 1-8.

García-Corral, L.S., Holding, J., Carrillo-de-Albornoz, P., Steckbauer, A., Pérez-Lorenzo, M., Navarro, N., Serret, P., Duarte, C.M., Agustí, S., 2017. Effects of UVB radiation on net community production in the upper global ocean. *Glob. Ecol. Biogeogr.* **26**, 54-64.

García-Corral, L.S., Martínez-Ayala, J., Duarte, C.M., Agustí, S., 2015. Experimental assessment of cumulative temperature and UV-B radiation effects on Mediterranean plankton metabolism. *Front. Mar. Sci.* **2**, 48.

Gattuso, J.P., Frankignoulle, M., Wollast, R., 1998. Carbon and carbonate metabolism in coastal aquatic ecosystems. *Ann. Rev. Ecol. Syst.* **29**, 405-434.

Griffiths, J.R., Hajdu, S., Downing, A.S., Hjerne, O., Larsson, U., Winder, M., 2016. Phytoplankton community interactions and environmental sensitivity in coastal and offshore habitats. *Oikos* **125**, 1134-1143.

Gunderson, A.R., Armstrong, E.J., Stillman, J.H., 2016. Multiple stressors in a changing world: The need for an improved perspective on physiological responses to the dynamic marine environment. *Ann. Rev. Mar. Sci.* **8**, 357-378.

Häder, D.-P., Gao, K., 2015. Interactions of anthropogenic stress factors on marine phytoplankton. *Front. Environ. Sci.* **3**, 14.

Häder, D.P., Villafañe, V.E., Helbling, E.W., 2014. Productivity of aquatic primary producers under global climate change. *Photochem. Photobiol. Sci.* **13**, 1370-1392.

Jickells, T.D., Moore, C.M., 2015. The importance of atmospheric deposition for ocean productivity. *Ann. Rev. Ecol. Evol. Syst.* **46**, 481-501.

Joint, I., Henriksen, P., Fonnes, G.A., Bourne, D., Thingstad, T.F., Riemann, B., 2002. Competition for inorganic nutrients between phytoplankton and bacterioplankton in nutrient manipulated mesocosms. *Aquat. Microb. Ecol.* **29**, 145-159.

Lasternas, S., Agustí, S., 2014. The percentage of living bacterial cells related to organic carbon release from senescent oceanic phytoplankton. *Biogeosciences* **11**, 6377-6387.

Mahowald, N., Jickells, T.D., Baker, A.R., Artaxo, P., Benitez-Nelson, C.R., Bergametti, G., Bond, T.C., Chen, Y., Cohen, D.D., Herut, B., Kubilay, N., Losno, R., Luo, C., Maenhaut, W., McGee, K.A., Okin, G.S., Siefert, R.L., Tsukuda, S., 2008. Global distribution of atmospheric phosphorus sources, concentrations and deposition rates, and anthropogenic impacts. *Glob. Biogeochem. Cy.* **22**, GB4026.

Malviya, S., Scalco, E., Audic, S., Vincent, F., Veluchamy, A., Poulain, J., Wincker, P., Iudicone, D., de Vargas, C., Bittner, L., Zingone, A., Bowler, C., 2016. Insights into global diatom distribution and diversity in the world's ocean. *Proc. Natl. Acad. Sci.* **113**, 1516-1525.

Martínez-García, S., Fernández, E., Calvo-Díaz, A., Cermeño, P., Marañón, E., Morán, X.A.G., Teira, E., 2013. Differential response of microbial plankton to nutrient inputs in oligotrophic versus mesotrophic waters of the North Atlantic. *Mar. Biol. Res.* **9**, 358-370.

Mayali, X., Azam, F., 2004. Algicidal bacteria in the Sea and their impacts on Algal Blooms. *J. Eukaryot. Microbiol.* **51**, 139-144.

McCauley, D.J., Pinsky, M.L., Palumbi, S.R., Estes, J.A., Joyce, F.H., Warner, R.R., 2015. Marine defaunation: Animal loss in the global ocean. *Science* **347**, 1255651.

Medina-Sánchez, J.M., Carrillo, P., Delgado-Molina, J.A., Bullejos, F.J., Villar-Argaiz, M., 2010. Patterns of resource limitation of bacteria along a trophic gradient in Mediterranean inland waters. *FEMS Microbiol. Ecol.* **74**, 554-565.

Medina-Sánchez, J.M., Villar-Argaiz, M., Carrillo, P., 2004. Neither with nor without you: A complex algal control on bacterioplankton in a high mountain lake. *Limnol. Oceanogr.* **49**, 1722-1733.

Mitra, A., Flynn, K.J., Burkholder, J.M., Berge, T., Calbet, A., Raven, J.A., Granéli, E., Glibert, P.M., Hansen, P.J., Stoecker, D.K., Thingstad, F., Tilmann, U., Vage, S., Wilken, S., Zubkov, M.V., 2014. The role of mixotrophic protist in the biological carbon pump. *Biogeosciences* **11**, 995-1005.

Montoya, J.M., Raffaelli, D., 2010. Climate change, biotic interactions and ecosystem services. *Philos. T. Roy. Soc. B* **365**, 2013-2018.

Morán, X.A.G., Sebastián, M., Pedrós-Alió, C., Estrada, M., 2006. Response of Southern Ocean phytoplantkton and bacterioplankton production to short-term experimental warming. *Limnol. Oceanogr.* **51**, 1791-1800.

Nagelkerken, I., Connell, S.D., 2015. Global alteration of ocean ecosystem functioning due to increasing human CO_2 emissions. *Proc. Natl. Acad. Sci.* **112**, 13272-13277.

Odum, H.T., 1956. Primary production in flowing waters. *Limnol. Oceanogr.* **2**, 101-117.

Parmesan, C., 2006. Ecological and evolutionary responses to recent climate change. *Ann. Rev. Ecol. Evol. Syst.* **37**, 637-669.

Parmesan, C., Yohe, G., 2003. A globally coherent fingerprint of climate change impacts across natural systems. *Nature* **421**, 37-42.

Peñuelas, J., Poulter, B., Sardans, J., Ciais, P., van der Velde, M., Bopp, L., Boucher, O., Godderis, Y., Hinsinger, P., Llusia, J., Nardin, E., Vicca, S., Obersteiner, M., Janssens, I.A., 2013. Human-induced nitrogen-phosphorus imbalances alter natural and managed ecosystems across the globe. *Nat. Commun.* **4**, 2934.

Piggott, J., Townsend, C. R., Matthaei, C.D., 2015. Reconceptualizing synergism and antagonism among multiple stressors. *Ecol. Evol.* **5**, 1538-1547.

Pincebourde, S., Sanford, E., Casas, J., Helmuth, B., 2012. Temporal coincidence of environmental stress events modulates predation rates. *Ecol. Lett.* **15**, 680-688.

Ptacnik, R., Gomes, A., Royer, S.-R., Berger, S.T., Calbet, A., Nejstgaard, J.C., Gasol, J.M., Isari, S., Moorthi, S.D., Ptacnikova, R., Striebel, M., Sazhin, A.F., Tsagaraki, T.M., Zervoudaki, S., Altoja, K., Dimitriou, P.D., Laas, P., Gazihan, A., Martínez, R.A., Schabhüttl, S., Santi, I., Sousoni, D., Pitta, P., 2016. A light-induced shortcut in the planktonic microbial loop. *Sci. Rep.* **6**, 29286.

Rabalais, N.n., Turner, R.E., Díaz, R.J., Justic, D., 2009. Global change and eutrophication of coastal waters. *ICES J. Mar. Sci.* **66**, 1528-1537.

Ribalet, F., Intertaglia, L., Lebaron, P., Casotti, R., 2008. Differential effect of three polyunsaturated aldehydes on marine bacterial isolates. *Aquat. Toxicol.* **31**, 249-255.

Rodríguez, P., Byström, P., Geibrink, E., Hedström, P., Rivera-Vasconcelos, F., Karlsson, J., 2016. Do warming and humic river runoff alter the metabolic balance of lake ecosystems? *Aquat. Sci.* **78**, 717-725.

Rousseaux, C.S., Gregg, W.W., 2014. Interannual variation in phytoplankton primary production at a global scale. *Remote Sens.* **6**, 1-19.

Sarmento, H., Gasol, J.M., 2012. Use of phytoplankton-derived dissolved organic carbon by different types of bacterioplankton. *Environ. Microbiol.* **14**, 2348-2360.

Schlesinger, W.H., Bernhardt, E.S., 2013. Biogeochemistry: An analysis of global change, Third edition ed. Academic Press. Elsevier, Oxford, United Kingdom.

Serret, P., Robinson, C., Aranguren-Gassis, M., García-Martín, E.E., Gist, N., Kitidis, V., Lozano, J., Harris, C., Thomas, R., 2015. Both respiration and photosynthesis determine the scaling of plankton metabolism in the oligotrophic ocean. *Nat. Commun.* **6**, 6961.

Stenseth, N.C., Ottersen, G., Hurrell, J.W., Mysterud, A., Lima, M., Chan, K.-S., Yoccoz, N.G., Ådlandsvik, B., 2003. Studying climate effects on ecology through the use of climate indices: The North Atlantic Oscillation, El Niño Southern Oscillation and beyond. *Proc. Roy. Soc. Lon. B* **270**, 2087-2096.

Tittensor, D.P., Mora, C., Jetz, W., Lotze, H.K., Ricard, D., Vanden Berghe, e., Worm, B., 2010. Global patterns and predictors of marine biodiversity across taxa. *Nature* **466**, 1098-1101.

Trenberth, K., 2002. Earth system processes, in: MacCracken, M.C., Perry, J.S. (Eds.), Encyclopedia of global environmental change. John Wiley & Sons, Chichester, pp. 13-30.

Van Mooy, B.A.S., Fredricks, H.F., Pedler, B.E., Dyhrman, S.T., Karl, D.M., Koblizek, M., Lomas, M.W., Mincer, T.J., Moore, L.R., Moutin, T., Rappé, M.S., Webb, E.A., 2009. Phytoplankton in the ocean use non-phosphorus lipids in response to phosphorus scarcity. *Nature* **458**, 69-72.

Vinebrooke, R.D., Cottingham, K.L., Norberg, J., Scheffer, M., Dodson, S.I., Maberly, S.C., Sommer, U., 2004. Impacts of multiple stressors on biodiversity and ecosystem functioning: The role of species co-tolerance. *Oikos* **104**, 451-457.

Wernberg, T., Smale, D.A., Thomsen, M.S., 2012. A decade of climate change experiments on marine organisms: procedures, patterns and problems. *Glob. Change Biol.* **18**, 1491-1498.

Westberry, T.K., Williams, P.J.l.B., Behrenfeld, M.J., 2012. Global net community production and the putative net heterotrophy of the oligotrophic oceans. *Glob. Biogeochem. Cy.* **26**, GB4019.

Wilken, S., Huisman, J., Naus-Wiezer, S., Van Donk, E., 2013. Mixotrophic organisms become more heterotrophic with rising temperature. *Ecol. Lett.* **16**, 225-233.

Williams, P.J.l.B., Quay, P.D., Westberry, T.K., Behrenfeld, M.J., 2013. The oligotrophic ocean is autotrophic? *Ann. Rev. Mar. Sci.* **5**, 535-549.

Williamson, C.E., Zepp, R.G., Lucas, R.M., Madronich, S., Austin, A.T., Ballaré, C.L., Norval, M., Sulzberger, B., Bais, A.F., McKenzie, R.L., Robinson, S.A., Häder, D.P., Paul, N.D., Bornman, J.F., 2014. Solar ultraviolet radiation in a changing climate. *Nat. Clim. Change* **4**, 434-441.

Woodward, G., Perkins, D.M., Brown, L.E., 2010. Climate change and freshwater ecosystems: impacts across multiple levels of organization. *Philos. T. Roy. Soc. B* **365**, 2093-2106.

Wootton, J.T., Emmerson, M., 2005. Measurement of interaction strength in nature. *Ann. Rev. Ecol. Evol. Syst.* **36**, 419-444.

Yvon-Durocher, G., Jones, J.I., Trimmer, M., Woodward, G., Montoya, J.M., 2010. Warming alters the metabolic balance of ecosystems. *Philos. T. Roy. Soc. B* **365**, 2117-2126.

Chapter II

General Methodology

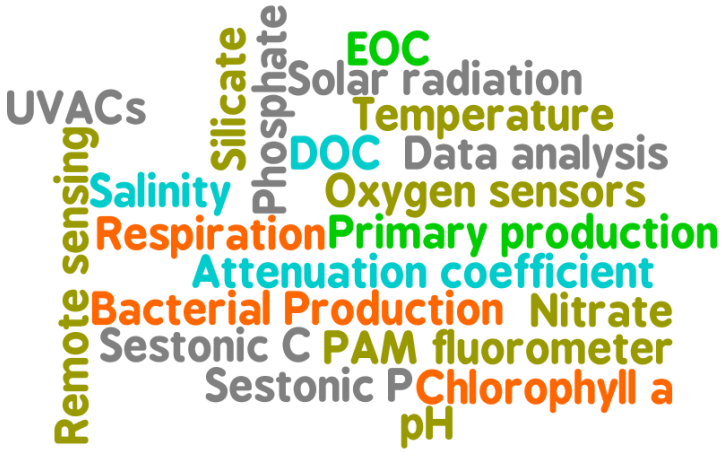

From the five independent experiments that forming part of this thesis, the common methodology used in them is summarized in five main sections: **Remote-sensing data**, **physical**, **chemical** and **biological parameters** and **statistical analyses** and **artwork**. The specific material and methods as well as the experimental designs are detailed in the corresponding chapter.

Remote-sensing parameters

Original data from daily aerosol index (AI, relative units) (Chapters V, VI and VII) and surface shortwave radiation fluxes (in W m^{-2}) (Chapter VI) from 1979 to 2015 period for South Western (SW) Mediterranean Sea, and daily AI from 1996 to 2015 and from 2010 to 2015 period for South Atlantic Ocean (SAO) and La Caldera Lake (Sierra Nevada National Park, Spain), respectively, were downloaded from Ozone Monitoring Instrument (OMI), Total Ozone Mapping Spectrometer-Earth Probe (TOMS-EP) and Nimbus satellites through Giovanni v 4. 18. 3 Earth database of National Aeronautics and Space Administration (NASA) (Acker & Leptoukh, 2007). The same database was used to download particulate organic carbon data (POC, mg C m^{-3}) (Chapter VII) for SAO over the 1999-2016 period.

Physical parameters

For micro and mesocosm experiments, the daily incident solar irradiances were monitored using an European Light Dosimeter Network broadband filter radiometer (ELDONET, Real Computers, Germany) with three broadband channels, one for ultraviolet B (UV-B, 280-315 nm), one for ultraviolet A (UV-A, 315-400 nm) and other for photosynthetically active radiation (PAR, 400-700 nm) (chapter VII) or with a BIC Compact multichannel radiometer (Biospherical Instruments Inc., CA, USA) with three channels for

UVR portion (305 [UV-B], 320 and 380 [UV-A] nm) and one broadband channel for PAR (Chapters V and VI). Historical data of daily doses of PAR (Chapter VII) measured using an ELDONET radiometer for the 1999-2015 period in coastal SAO waters were obtained from the online database of Estación de Fotobiología Playa Unión (see http://www.efpu.org.ar). However, for laboratory experiments, the irradiances received by the species or communities during the exposure period in an environmental test chamber (Sanyo MLR-350, Japan) were measured using an Ocean Optics model HR 2000CG-UV-spectroradiometer (Chapters III and IV). Underwater profiles of solar radiation in the study sites were made using a submergible BIC Compact multichannel radiometer (Biospherical Instruments Inc., CA, USA) with three channels for UVR (305, 320 and 380 nm) and one for PAR portion (chapters V and VI). Vertical profiles of temperature, salinity, conductivity and pH were done with two different multiparameter probes, a Yellow Spring Instruments model 600 XLM (USA) (Chapters IV and VII) and a Hanna HI9828-0 (Chapter V), or with a sealogger CTD SBE 25 (Sea-Bird Electronics, Inc., WA, USA) (Chapter VI).

Chemical parameters

The analysis of the main fractions of nutrients contained in water samples, including as (i) total nitrogen (TN), total dissolved nitrogen (TDN) or nitrate + nitrite ($NO_2^- + NO_3^-$) in the case of the N compartment; (ii) total phosphorus (TP), total dissolved phosphorus (TDP), soluble reactive phosphorus (SRP) or as phosphate (PO_4^{-3}) in the case of P and (iii) the silicate (SiO_2^{-3}) for Si were done following the standard methodologies collected into the American Public Health Association (APHA, 1992) in the case of freshwater ecosystems (chapter V), and following to Strickland & Parssons (1972) and Koroleff (1977) in the case of marine ecosystems (Chapters VI and VII). Dissolved organic carbon (DOC) (Chapters V and VI) analyses were done filtering water samples through pre-combusted GF/F Whatman filters (25 mm diameter), which were then acidified with HCL 1N (2%) and

measured following the methodology proposed by Benner & Strom (1993).

Biological parameters

Stoichiometric variables

The sestonic C and P (Chapter V) were quantified from filtered water samples into pre-combusted GF/B Whatman filters (25 mm diameter) and measured using either an elemental analyser (Perkin Elmer 2400, USA) or the persulfate digested technique proposed by Murphy & Riley (1962), respectively.

Structural variables

Chlorophyll *a* (Chl *a*) concentrations (Chapters III to VII) were quantified from water samples filtered through GF/F Whatman or MG-F Muntkell filters (25 mm diameter) and extracting the photosynthetic pigments in absolute methanol (Holm-Hansen & Riemann 1978) or in acetone (APHA 1992). After this, the supernatant was scanned between 250-750 nm using a spectrophotometer (Hewlett Packard, model 8453E, USA) or measured using a fluorometer (Perkin Elmer LS 55, USA or Turner Designs, model TD 700). Chl *a* concentrations were calculated using the equations of Porra (2002) and APHA (1992). The cellular abundance of the planktonic communities was quantified and separated into three main compartments; autotrophic nanoplankton (ANP), autotrophic picoplankton (APP) and heterotrophic picoplankton (HPP). The ANP fraction was quantified either through classical microscopic techniques, sedimenting an aliquot of the original sample and following the procedure described by Villafañe & Reid (1995) or by Utermöhl (1958) (Chapters IV to VII). APP and HPP fractions were quantified through flow cytometry using a FACSCanto II (Becton Dickin-

son Biosciences, Oxford, UK), being each picoplanktonic group identified using phycoerithrin and Chl *a* fluorescence signals (Chapters VI and VII). From cellular abundances it was also estimated the carbon biomass. In the case of ANP, the cell volume was approximated to their geometric shape (Carrillo, et al. 1995; Hillebrand, et al. 1999) and converted it into C content using the equations of Rocha & Duncan (1985) and Strathmann (1967). For APP, the biovolume was calculated following Ribés et al. (1999) and Zubkov et al. (1998), whereas that for HPP the works of Posch et al. (2001) and Zubkov et al. (1998). From biovolume, it was converted into C biomass following suitable conversion factors for each fraction [APP (Booth 1988; Verity et al., 1992); and HPP (Bjørnsen 1986; Posch et al., 2001)].

Functional variables

The planktonic physiological and metabolic responses quantified in this thesis were measured to different cellular levels. On one hand, the *in vivo* Chl *a* fluorescence to photosystem II (PSII) level was measured at short-term during light and dark periods as well as through diel cycles under solar radiation at dawn, noon at dusk in phytoplankton species or communities using a pulse amplitude modulated (PAM) fluorometer (Walz, Water PAM, Effeldrich, Germany) equipped with WinControl v. 2.0.8. software. The samples were measured six times after sampling and without dark adaptation, being each sample measured during 1 minute in total. From these measurements, the effective photochemical quantum yield of Photosystem II (Φ_{PSII}) (Genty, et al. 1989; Maxwell & Johnson 2000) and the non-photochemical quenching (NPQ) values were obtained. From Φ_{PSII} values, it was calculated the inhibition (k) and recovery (r) PSII-rates over the time (Chapters III, IV and VII), whereas NPQ values measured (Chapter III) were used as a proxy of the photoprotective capacity of phytoplankton to dissipate of the excess of energy absorbed as heat.

On the other hand, the metabolic processes of organisms and communities presented in the following chapters were quantified through a dual

approach: (1) using oxygen (O_2) sensors coupled with a fiber optic oxygen transmitter and (2) using radiotracers. In the first case, O_2 concentration measurements were performed over short-term exposures during light and dark periods in phytoplankton species and communities as well as during diel cycles under solar radiation with plankton communities using a Presens system (Presens GmbH, Germany) consisting of sensor-spots (SP-PSt3-NAU-D5-YOP) glued to the base of Narrow mouth Teflon bottles (Nalgene, USA) and an optic-fiber oxygen transmitter (Fibox 3) equipped with Oxyview v. 6.02 software. From these measurements, photosynthesis and respiration rates for phytoplankton species (Chapter III), and the total planktonic metabolism of communities (i.e., auto and heterotrophs) including the net community production (NCP) (Chapter IV) and / or net primary production (NPP) and the community respiration (CR) were quantified (Chapters IV, VI and VII). Finally, the bacterial community respiration (BR) (Chapter V) in darkness was also quantified using the same methodology than described above from filtered water samples through 0.7 μm filters (Whatman GF/F, 25 mm diameter).

Secondly, two radiotracers, ^{14}C as $NaH_{14}CO_3$ (DHI Water and Environment, Germany) to quantify the C-incorporation and the release of organic carbon (EOC) by phytoplankton (Chapters V and VI) and ^{3}H-thymidine (Perkin Elmer, USA) to measure the bacterial production (BP) (Chapter V). The C-incorporation was measured following the method of Steemann-Nielsen (1952). For that, water samples were filtered through 1 or 0.7-μm Whatman GF/F filters (25 mm diameter) and through 0.2 μm filters (Nucleopore, USA) to quantify both the particulate organic carbon (POC) as the phytoplankton exudates incorporated by HPP, respectively. EOC was calculated as the sum of DOC and phytoplankton exudates used by HPP. The BP was measured using the radio-labelled method of Fuhrman & Azam (1982). Both types of samples were measured using a scintillation counter equipped with autocalibration (Beckman LS 6000 TA). In the case of BP, the incorporated traces were converted into C using suitable conversion factors (Bell 1993; Lee & Fuhrman 1987).

Data analysis and artwork

The statistical analyses contained in this thesis which include: Normality (by Kolmogorov-Smirnov and Shapiro-Wilk), Homocedasticity (by Cochran and Levene) and Sphericity (by Mauchly) test's, (2) analysis of variance (ANOVA) and *post hoc* test's (Bonferroni and Least Significant Differences), (3) Student *t*-test's and (4) structural equation modeling (SEM) and Goodness-of-Fit (χ^2, Bentler-Bonnet Normed Fit Index [NFI] and the Goodness-of-Fit Index [GFI]) analysis were performed using Statistica v.7.0 and 10.0 (StatSoft Inc., 2005-2010). Linear, non-linear and multiple linear regression analysis were performed using Origin Pro v.9.0 (OriginLab, 2013). The artwork that form part of this thesis was done or edited using Inkscape v.0.92 (2015) whereas figures from Chapters III to VII were done using Grapher v.12 (Golden software, 2015) and Ocean Data view v.4.7.9 (Schlitzer 2015).

References

Acker, J. G., Leptoukh, G., 2007. Online analysis enhance NASA Earth science data. *EOS, Trans. AGU* **88**, 14-17.

APHA. 1992. Standard methods for the examination of water and wastewater. American Public Health Association, Washington.

Bell, R. T. 1993. Estimating production of heterotrophic bacterioplankton via incorporation of tritiated thymidine. Pages 495-503 in P. F. Kemp, B. F. Sherr, and J. J. Cole, editors. Handbook of methods in aquatic microbial ecology. Lewis Publishers, Boca Ratón, Florida, USA.

Benner, R., Strom, M., 1993. A critical evaluation of the analytical blank asociated with DOC measurements by high-temperature catalytic oxidation. *Mar. Chem.* **41**, 153-160.

Bjørnsen, P. K. 1986. Automatic determination of bacterioplankton biomass by image analysis. *Appl. Environ. Microbiol.* **51**, 1199-1204.

Booth, B. C. 1988. Size classes and major taxonomic groups of phytoplankton at two locations in the subarctic Pacific Ocean in May and August, 1984. *Mar. Biol.* **97**, 275-286.

Carrillo, P., Reche, I., Sánchez-Castillo, P. M., Cruz-Pizarro. L., 1995. Direct and indirect effects of grazing on the phytoplankton seasonal succession in an oligotrophic lake. *J. Plankton Res.* **17**, 1363-1379.

Fuhrman, J. A., Azam, F., 1982. Thymidine incorporation as a measure of heterotrophic bacterioplankton production in marine surface waters: Evaluation and field results. *Mar. Biol.* **66**, 109-120.

Genty, B. E., Briantais, J. M., Baker, n. R., 1989. The relationship between the quantum yield of photosynthetic electron transport and quenching of chlorophyll fluorescence. *Biochim. Biophys. Acta* **990**, 87-92.

Hillebrand, H., Dürselen, C. D., Kirschtel, D., Pollingher, U., Zohary, T., 1999. Biovolume calculation for pelagic and benthic microalgae. *J. Phycol.* **35**, 403-424.

Holm-Hansen, O., Riemann, B., 1978. Chlorophyll *a* determination: Improvements in methodology. *Oikos* **30**, 438-447.

Koroleff, F. 1977. Simultaneous persulphate oxidation of phosphorous and nitrogen compounds in water. in K. Grasshoff, editor. Report on the Baltic intercalibration workshop, Kiel, Germany.

Lee, S., Fuhrman, J. A., 1987. Relationships between biovolume and biomass of naturally derived marine bacterioplankton. *Appl. Environ. Microbiol.* **53**, 1298-1303.

Maxwell, K., Johnson, M. G., 2000. Chlorophyll fluorescence - a practical guide. *J. Exp. Bot.* **51**, 659-668.

Murphy, J., Riley, J. P., 1962. A modified single solution method for the determination of phosphate in natural waters. *Anal. Chim. Acta* **27**, 31-36.

Porra, R. J. 2002. The chequered history of the development and use of simultaneous equations for the accurate determination of chlorophylls *a* and *b*. *Photosynth. Res.* **73**, 149-156.

Posch, T., Loferer-Krößbacher, M., Gao, G., Alfreider, A., Pernthaler, J., Psenner, R., 2001. Precision of bacterioplankton biomass determination: a comparison of two fluorescent dyes, and of allometric and linear volume-to-carbon conversion factors. *Aquat. Microb. Ecol.* **25**, 55-63.

Ribés, M., Coma, R., Maria-Gili, M., 1999. Seasonal variation of particulate organic carbon, dissolved organic carbon and the contribution of microbial communities to live particulate organic carbon in a shallow near-bottom ecosystem at the Northwestern Mediterranean Sea. *J. Plankton Res.* **21**, 1077-1100.

Rocha, O., Duncan, A., 1985. The relationship between cell carbon and cell volume in freshwater algal species used in zooplankton studies. *J. Plankton Res.* **7**, 279-294.

Schlitzer, R. 2015. Ocean Data View. http://odv.awi.de.

Steemann-Nielsen, E., 1952. The use of radio-active carbon (C^{14}) for measuring organic production in the sea. *J. Cons. Perm. Int. Explor. Mer.* **18**, 117-140.

Strathmann, R. R. 1967. Estimating the organic carbon content of phytoplankton from cell volume or plasma volume. *Limnol. Oceanogr.* **12**, 411-418.

Strickland, J. D. H., Parsons, T. R., 1972. A practical handbook of seawater analysis. *Fish. Res. Board Can. Bull.* **167**, 1-310.

Utermöhl, H. 1958. Zur Vervollkommnung der quantitativen Phytoplankton-Methodik. *Internationale Vereinigung fur Theoretische und Angewandte Limnologie* **9**, 1-38.

Verity, P. G., Robertson, C. Y., Tronzo, C. R., Andrews, M. G., Nelson, J. R., Sieracki, M. E., 1992. Relationships between cell volume and the carbon and nitrogen content of marine photosynthetic nanoplankton. *Limnol. Oceanogr.* **37**, 1434-1446.

Villafañe, V. E., Reid, F. M. H., 1995. Métodos de microscopía para la cuantificación del fitoplancton. Pages 169-185 in K. Alveal, M. E. Ferrario, E. C. Oliveira, and E. Sar, editors. Manual de Métodos Ficológicos. Universidad de Concepción, Concepción, Chile.

Zubkov, M. V., Sleigh, M. A., Tarran, G. A., Burkill, P. H., Leakey, R.J. G., 1998. Picoplanktonic community structure on an Atlantic transect from 50°N to 50°S. *Deep Sea Res. Pt. I* **45**, 1339-1355.

Chapter III

Current and predicted global change impacts of UVR, temperature and nutrient inputs on photosynthesis and respiration of key marine phytoplankton groups

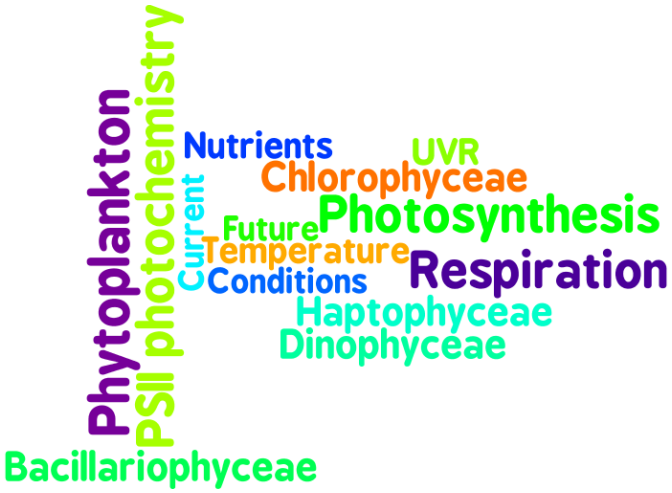

Abstract

Multiple stressors are altering primary production in coastal and estuarine systems; however, it is difficult to predict their combined impacts due to the scarcity of multifactorial experiments. Photosynthesis, respiration, and PSII photochemical performance of *Alexandrium tamarense*, *Chaetoceros gracilis*, *Dunaliella salina* and *Isochrysis galbana* were studied during daily cycles using a combination of two radiation treatments (UVR + PAR and PAR), two nutrients concentrations, and three temperatures (14, 17 and 20°C). UVR exerted a negative impact in all species decreasing photosynthesis and quantum yield of PSII under low nutrients concentrations and temperatures up to 20°C. At higher temperatures (global change scenario of 4°C increase), increased UVR and nutrients, *C. gracilis* and *I. galbana* reversed their responses increasing photosynthesis and repair rates, respectively; they also showed a decrease in respiration rates. By contrast, *A. tamarense* and *D. salina* showed further decrease in photosynthesis and repair rates as compared to present conditions. Our modeled responses to warming under a scenario of increased nutrients and UVR, suggest that diatoms and haptophytes will benefit from these conditions and possibly will outcompete chlorophytes and dinoflagellates. If this is a generalized response, it might influence primary production and affect food web interactions in coastal ecosystems.

Introduction

Phytoplankton are responsible for ca. 50 % of the global primary production (Field et al., 1998) and coastal systems, including estuaries, are among the most productive areas of the planet (Cloern et al., 2014); therefore, coastal phytoplankton has been the focus of many investigations aiming to understand the effects of multiple stressors associated to global change (Kennish et al., 2014). Many studies were devoted to evaluate the effects

and impacts of higher fluxes of ultraviolet radiation (UVR, 280-400 nm), either due to depletion of the ozone layer or as the result of increased stratification (Häder et al., 2011; Helbling & Zagarese, 2003; McKenzie et al., 2011); the increase in surface seawater temperature associated to global warming (Häder et al., 2011; Luo et al., 2008; Winder & Sommer, 2012); and the increase of nutrients inputs into coastal marine ecosystems by rivers or atmospheric deposition due, in turn, to increased rainfall and / or stronger and more frequent wind events (IPCC, 2013).

It is already known that UVR produce negative effects on phytoplankton e.g., by affecting photosynthesis and respiration (Beardall & Raven, 2004; Beardall et al., 1997) and damaging vital cellular targets such as the DNA molecule (Buma et al., 2003), proteins and membrane lipids (Abo-Shady et al., 2008; Arts & Rai, 1997; Guihéneuf et al., 2010; Skerratt et al., 1998). However UV-A (315-400 nm) has been shown to stimulate photosynthesis under low Photosynthetic Active Radiation (PAR, 400-700 nm) or under fast mixing (Barbieri et al., 2002; Helbling et al., 2003), and has also be involved in photorepairing UV-B (280-315 nm)-induced DNA damage (Buma et al., 2003). Higher nutrient inputs, on the other hand, generally benefit primary production (Lagaria et al., 2011), the growth of algae (Toseland et al., 2013) and decrease photoinhibition (Bergmann et al., 2002); although it has also been reported that high nutrients unmask the negative UVR-effects on algal development (Carrillo et al., 2008; Korbee et al., 2012). Recent studies have determined variable effects of increased temperature, increasing the maximum quantum yield of PSII in the dinoflagellate *Symbiodinium* sp. (Takahashi et al., 2013), producing shifts towards smaller-size species (Thomas et al., 2012) or reducing UVR-induced photoinhibition in the diatom *Thalassiosira pseudonana* (Sobrino & Neale, 2007). This is probably due to the increases in depoxidation rate of the xantophyll pigment cycle and consequently higher repair rates of PSII (Dimier et al., 2009; Kulk et al., 2013) or higher RUBISCO activity (Helbling et al., 2011). In contrast, increased temperature resulted in inhibition of growth of some tropical diatoms (Halac et al., 2013) and exacerbated the harmful UVR effects on effective photochemical quantum yield in some sub-Antarctic brown-algae

(Cruces et al., 2013). These contrasting findings are due not only to different experimental conditions, but also to the species-specificity of responses. Moreover, the effects of a single factor (or stressor) on a particular organism or process is usually different than when considered in combination with other factors, due to the antagonistic or synergistic nature of interactions (Folt et al., 1999). Another potential cause of differences in responses to multiple stressors lies on the evolutionary traits achieved through time i.e., allowing acclimation, that in turn result in differential sensitivity to changing environmental factors.

The aim of this study is to evaluate the photosynthetic and respiratory responses, together with PSII photochemical activity, of key marine phytoplankton species, representatives of four different phytoplankton phyla, under the combination of UVR, temperature and nutrients, considering a global change context. In particular, it was hypothesized that a combined increase in temperature and nutrients will exacerbate the potential negative UVR-effects on photosynthesis-respiration and photochemical activity on phytoplankton compared with current ambient conditions. To test this hypothesis, experiments were carried out in which monospecific cultures of different phytoplankton groups characteristic of coastal areas were exposed to different combinations of variables associated to global change i.e., two radiation, two nutrients and three temperature conditions and the photosynthetic / photochemical and respiratory responses during short term incubations were followed. The data obtained, in turn, allowed to predict the responses of key phytoplankton species in a future global change scenario as expected by the year 2100 (IPCC, 2013).

Material and Methods

Culture conditions

Experiments were carried out during the Austral Autumn (March-June, 2013). The phytoplankton species used in this study were isolated from the Patagonian coast and maintained in the Algal Culture Collection of Estación de Fotobiología Playa Unión (EFPU). The dinoflagellate *Alexandrium tamarense* (Lebour) Balech, the diatom *Chaetoceros gracilis* Schütt, the chlorophyte *Dunaliella salina* (Dunal) Teodoresco and the haptophyte *Isochrysis galbana* Parke were grown and maintained in exponential growth (chlorophyll *a* [Chl *a*] values ranging between 50-60 μg L^{-1}) in either a high-nutrient (f/2) (hereafter HN) or a low-nutrient (f/40) medium (hereafter LN) (Guillard & Ryther 1962), under three experimental temperatures, 14 ºC, 17 and 20°C, inside an environmental illuminated chamber (Minicella, Argentina). Control treatments of nutrient and temperature represent either the mean values of the contributions of nitrate, nitrite, phosphate and silicate of the Chubut River during low-tide (f/40) and the average sea water temperatures (14°C) through end-March to mid-May (Helbling et al., 1992; Helbling et al., 2010).

Semi-continuous cultures were maintained in non-aerated 1-L bottles, filled up to 50% of their volume and maintained in exponential growth by diluting them every day with 250 mL of fresh medium, to maintain the initial volume. The cultures were pre-acclimated for seven days to both, temperature and nutrient conditions as described above, before being used in experimentation. During this acclimation period the cultures grew under a 12 hL:12 hD photoperiod, under illumination provided by fluorescent tubes (Phillips daylight), receiving 300 μmol photons m^{-2} s^{-1} of Photosynthetic Active Radiation (PAR, 400-700 nm).

Experimental set up

In order to assess the combined impact of UVR (i.e., factor Rad), nutrient (i.e., factor Nut) and temperature (i.e., factor Temp) on the four species (i.e., factor Spp) considered in this study, a 2 × 2 × 3 × 4 matrix was implemented. Triplicate samples for each radiation and nutrient condition were placed into 40 mL round quartz vessels for measurements of photosynthesis and respiration, while another set of triplicate samples were placed in 40 mL quartz tubes to measure fluorescence parameters. The two radiation treatments were: (1) PAB, with samples receiving UVR+PAR (> 280 nm), uncovered quartz tubes, and (2) P, with samples receiving only PAR (> 400 nm), quartz tubes covered with Ultraphan film (UV Opak 395 filter, Digefra). The two nutrients treatments consisted in HN and LN media, while the three temperature treatments were 14, 17 and 20°C, as mentioned above for the pre-acclimation period. The samples were placed in an illuminated culture chamber (Sanyo MLR-350, Japan) that kept the wanted temperature constant, while the radiation conditions were provided by 10 Philips daylight fluorescent tubes for PAR and 5 tubes Q-Pannel UVA-340 for UVR. The cultures were exposed to irradiances of 164.1 (754.9 μmol photons m^{-2} s^{-1}), 42.8, and 0.7 W m^{-2} for PAR, UV-A and UV-B, respectively, which represent the mean daily values for the experimental period (Helbling et al., 2005). The spectral output of the lamps was checked with a spectroradiometer (Ocean Optics model HR 2000CG-UV-NIR), and no UV-C radiation output was measured. The radiation exposure period lasted 6 h in order to get a radiation dose comparable with natural daily doses during the period of experimentation. Therefore samples received a daily dose of 3.5 MJ m^{-2} for PAR, 910 kJ m^{-2} for UV-A and 15 kJ m^{-2} for UV-B. After exposure, the cultures were maintained inside the chamber for another 8 h in darkness; this time period was chosen based on preliminary measurements, and also to obtain various data points to calculate respiration.

Analysis and measurements

Photosynthesis and respiration measurements

Oxygen concentration (O_2) was measured using a Presens system (PreSens GmbH, Germany) consisting of sensor-spot optodes (SP-PSt3-NAU-D5-YOP) and an optic-fiber oxygen transmitter (Fibox 3) connected to a computer equipped with an Oxyview 6.02 software to register the data. The system was calibrated by a two-point calibration, together with data of atmospheric pressure and temperature before each experiment, following the manufacturer's recommendations. Measurements were made at the initial time (t_0) and then every hour during the 6 h of exposure to artificial radiation, every 30 min during the first two hours of darkness, and then every 1.5 h until the end of the dark period (8 h).

PSII fluorescence measurements

In vivo photochemical parameters were obtained using a pulse amplitude modulated (PAM) fluorometer (Walz, Water PAM, Effeltrich, Germany). Aliquots of 3 mL of sample were taken every 15 min during the first hour of exposure, and then with the same periodicity as mentioned before for oxygen measurements; the samples were placed in a cuvette, and measured six times immediately after sampling, without any dark-adaptation. The quantum yield of PSII (Φ_{PSII}) was calculated using the equations of Genty et al. (1990) and Maxwell & Johnson (2000) as:

$$\Phi_{PSII} = \Delta F/F'm = (F'm - Ft)/F'm$$

where F′m is the maximum fluorescence induced by a saturating light pulse (ca. 5300 μmol photons m^{-2} s^{-1} in 0.8 s) and Ft the current steady state fluorescence induced by a weak actinic light ca. 492 μmol photons m^{-2} s^{-1} in light-adapted cells.

The non-photochemical quenching (NPQ) of chlorophyll *a* (Chl *a*) fluorescence, used as a proxy of the dissipation of the excess light energy, was obtained directly using the PAM fluorometer. The software stores the Fm value that is then used with every sample, to calculate the NPQ. In this study Fm values for each species was determined and stored them, every time just before any exposure to solar radiation using a few dark-acclimated samples, and thus the NPQ data obtained with the PAM software based on these values were routinely used. Previous studies carried out by our group (Halac et al., 2010) showed that there were no significant differences between NPQ values calculated when Fm was determined for each individual sample and those obtained directly using the PAM fluorometer software.

Chl *a* concentrations and UV-absorbing compounds

Aliquots of 50 mL of sample were filtered onto GF-C filters (Munktell, Sweden) and photosynthetic pigments and UV-absorbing compounds were extracted in 5 mL of methanol. The tubes containing the methanolic extract were firstly sonicated at 20°C for 20 min, followed by 40 min of extraction. After this, the samples were centrifuged for 20 min at 2000 rpm and the absorption spectra of the supernatant were obtained by doing scans between 250 and 750 nm with a spectrophotometer (Hewlett Packard, model HP 8453E). Chl *a* concentration was calculated with the equation of Porra (2002) and the same sample was used to calculate Chl *a* concentration from the fluorescence of the extract (Holm-Hansen & Riemann 1978) before and after acidification (1 N HCl) using a fluorometer (Turner Designs, model TD 700). There were no differences between Chl *a* concentration determined by the two methods, thus values calculated with the equation of Porra (2002) were used. Once the scans (250-750 nm) for UV-absorbing compounds (UVAC) were obtained, the raw data were processed using a baseline correction and considering the entire area delimited under the peak at 337 nm and the peak high. Since there were no differences between both values, the peak high at 337 nm was used as previously described in Helbling

et al. (1996).

Data and statistical analysis

Photosynthesis and respiration rates (in μmol O_2 μg Chl a^{-1} h^{-1}) were calculated as the slope of the regression line of chlorophyll-specific oxygen concentrations versus time.

The net UVR effect on photosynthesis and / or respiration was calculated as:

$$\text{UVR effect} = [O_2]\text{PAB} - [O_2]\text{P}$$

where $[O_2]$PAB is the photosynthesis or respiration rates in the PAB-treatment, and $[O_2]$P is the photosynthesis or respiration rates in the P-treatment.

Inhibition (k – in min^{-1}) and recovery (r – in min^{-1}) rates were estimated as the decrease and increase, respectively, in Φ_{PSII} by applying an exponential regression fit during the radiation exposure (inhibition) and darkness (recovery) periods to the data:

$$\Phi_{PSII} = \text{A} \times \text{e}^{-kt} \text{ or}$$

$$\Phi_{PSII} = \text{A} \times \text{e}^{rt}$$

where Φ_{PSII} is the quantum yield of PSII, A is a constant, k / r represents inhibition / recovery, respectively, and t is the time.

The net UVR effect on k and r of PSII was calculated as:

$$\text{UVR effect} = (k)_{PAB} - (k)_P \text{ and}$$

$$\text{UVR effect} = (r)_{PAB} - (r)_P$$

where k and r are the mean values of inhibition and recovery for any of the measurements done in the PAB and P radiation treatments.

A four-way analysis of variance (ANOVA) was used to determine interactions among radiation, nutrients, temperature and species on photosynthesis, respiration, inhibition and recovery rates. The normality (by Shapiro-Wilks' test or Kolgomorov-Smirnov) and homoscedasticity (using Cochran, Hartley & Bartlett or Levene's tests) were checked for each data group before the ANOVA application. A *post hoc* test (Fisher Least Significant Difference, LSD) was used to determine significant differences within and among the different factors. A 95% confidence limit was used in all tests and all analyses were performed with the STATISTICA v.7.0 software (Statsoft Inc., 2005). Based on the photosynthesis and respiration rates, the UVR effect for each experimental condition for each species was calculated, and such values were fitted using a polynomial model. Error propagations was used to calculate the variance of the UVR effects. The model was also used to extend a prediction of the combined effects of temperature and nutrients at temperatures higher than the experimental 20°C used in our study (i.e., up to 24°C).

Results

Dynamics of photosynthesis and respiration

Representative data of oxygen evolution (i.e., production and respiration) at 17°C, normalized to the initial Chl *a* concentration, for the four species studied are shown in Fig. 1 (only this temperature is shown for simplicity,

as the trends were similar at 14, 17 and 20°C). For all species, the general pattern was of an increase in chlorophyll-specific photosynthesis (i.e., production) during the radiation exposure period, whereas the concentration was reduced (i.e., respiration) towards stabilization during the dark period. However, the responses were clearly species-specific, according to the radiation and nutrient treatment imposed to the samples. Overall, two clear and distinct patterns were observed: In the case of *A. tamarense* (Fig. 1A), nutrient concentration had greater impact on photosynthesis than radiation conditions, resulting in higher O_2 concentrations in cells grown under HN, regardless the radiation treatment. Instead, as in the case of *C. gracilis* (Fig. 1B), *D. salina* (Fig. 1C), and *I. galbana* (Fig. 1D), radiation exposure caused more significant effects than nutrient concentration, and thus samples incubated under the P-treatment had higher oxygen concentration than those under the PAB-treatment, regardless the nutrient concentration.

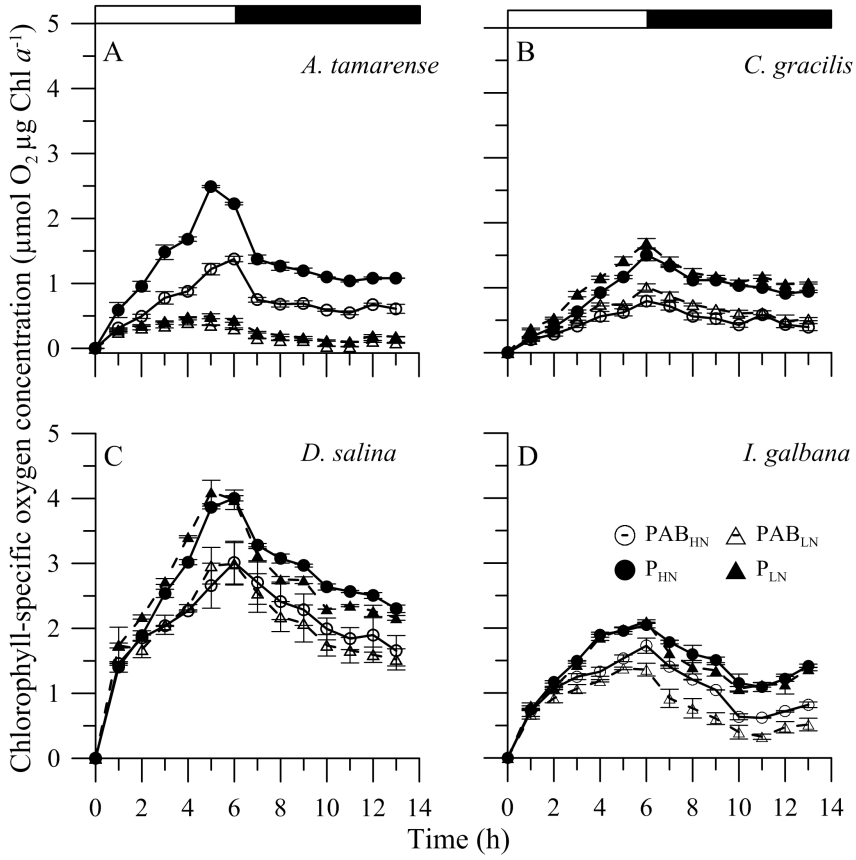

Figure 1: Mean chlorophyll-specific oxygen concentration (in μmol O_2 μg Chl a^{-1}) of *Alexandrium tamarense* (A), *Chaetoceros gracilis* (B), *Dunaliella salina* (C) and *Isochrysis galbana* (D) during 6 h exposure to UVR+PAR (PAB, open symbols) and PAR only (P, black symbols), and 8 h of darkness at 17°C. The horizontal white and black bars on the top indicate the radiation (exposure) and dark periods, respectively. Samples were grown and incubated at high (HN, circles) and low nutrients (LN, triangles) conditions. Each symbol represents the mean of triplicate samples while the vertical lines indicate the standard deviation.

The species-specific responses to each variable and condition are best seen in the rates of photosynthesis and respiration (Fig. 2). There were significant interactions between factors (i.e., Rad × Nut; Rad × Temp; and Nut × Temp) with the exception of Rad × Nut on photosynthesis (Table 1). For *A. tamarense* (Fig. 2A) and under HN treatment, photosynthesis rates were higher at high temperatures (20°C), with values of ca. 0.36 and 0.44 μmol O_2 μg Chl a^{-1} h^{-1} under PAB and P, respectively; an opposite trend was observed under LN conditions, with photosynthesis rates being lower at high temperatures. Similarly to photosynthesis, absolute respiration rates were somehow higher at 20°C under HN conditions whereas they were lower at higher temperature under LN conditions. *C. gracilis* (Fig. 2B) under HN conditions, showed an increase in production rates with increasing temperature; however the highest production (ca. 0.46 μmol O_2 μg Chl a^{-1} h^{-1}) was determined at 14°C in the LN treatment. For this species, and under HN conditions, no significant changes were observed in absolute respiration rates however, they were lower with increasing temperature at LN conditions. In *D. salin*a (Fig. 2C) photosynthetic rates were significantly lower at 14 and 20°C as compared to 17 ^{o}C in both nutrient conditions. In this species, absolute respiration rates were higher at high temperatures in the HN condition, and maximal values were determined at 17°C under LN conditions. Finally, *I. galbana* (Fig. 2D) exhibited a clear trend of increasing photosynthesis rates with increasing temperature under both nutrient conditions. Absolute respiration rates also were higher with increasing temperature in both nutrient conditions.

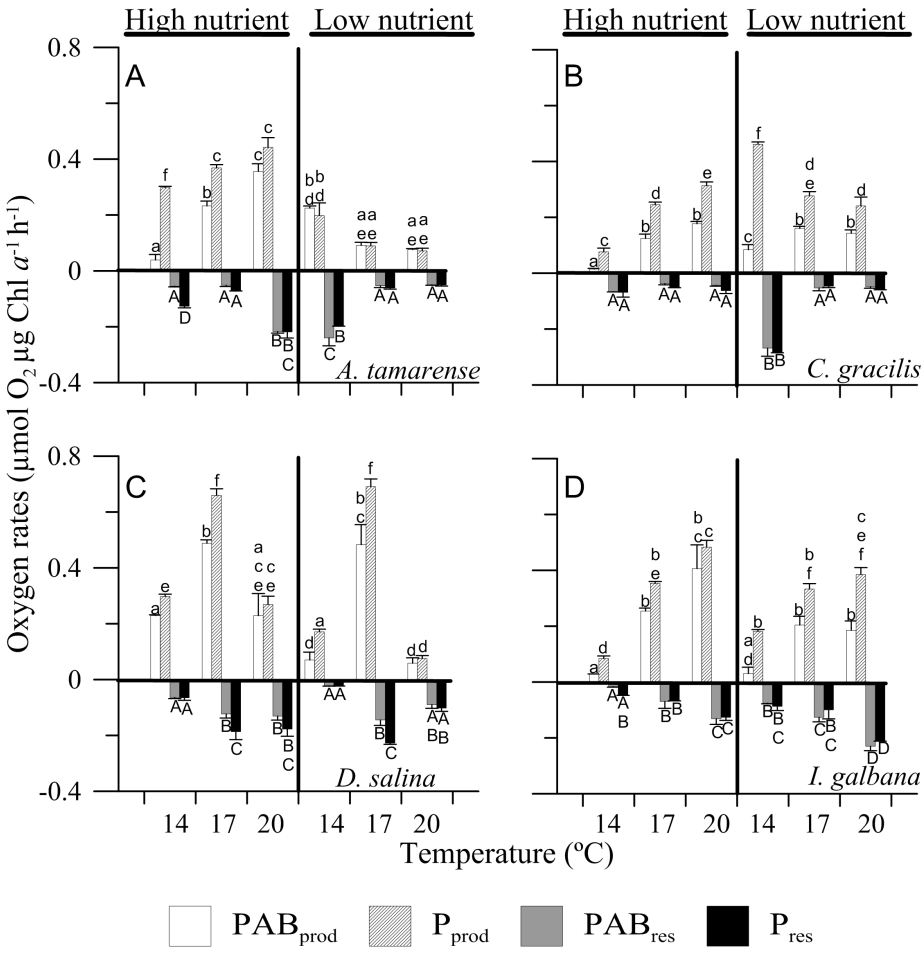

Figure 2: Rates (in μmol O_2 μg Chl a^{-1} h^{-1}) of photosynthesis (positive values) and respiration (negative values) of *Alexandrium tamarense* (A), *Chaetoceros gracilis* (B), *Dunaliella salina* (C) and *Isochrysis galbana* (D). Samples were grown and incubated at high (HN) and low nutrients (LN) conditions; three temperatures: 14, 17, and 20°C, and exposed to two radiation treatments: UVR+PAR (PAB, white and grey bars) and PAR only (P, dashed and black bars). The lines on the top of the bars indicate the standard deviation. Significance of *post hoc* comparisons between radiation treatments for each nutrients condition and temperature are represented with small and capital letters for production and respiration rates, respectively.

Table 1: Results of statistical analysis for the effects of radiation (Rad), nutrients (Nut), temperature (T), and species (Spp), and their interactions, on photosynthesis and respiration. All F values are rounded to two significant digits. Radiation (PAB and P), Nutrient (HN and LN), Temperature (14, 17 and 20°C). df, degrees of freedom; n.s., not significant, and the asterisks *, ** and *** represent the $p < 0.05$, $p < 0.01$ and $p < 0.001$, respectively.

		Photosynthesis	Respiration
Treatment	df	F	F
Rad	1	104.08***	6.38*
Nut	1	21.78***	21.42***
T	2	57.72***	15.96***
Spp	3	23.88***	15.93***
Rad×Nut	1	0.19	4.57*
Rad×T	2	4.15*	0.33
Nut×T	2	40.99***	48.62***
Rad×Spp	3	1.59	1.99
Nut×Spp	3	18.90***	29.12***
Temp×Spp	6	32.88***	69.31***
Rad×Nut×T	2	0.65	0.33
Rad×Nut×Spp	3	3.01*	1.77
Rad×T×Spp	6	2.62*	3.39**
Nut×T×Spp	6	4.82***	26.71***
Rad×Nut×T×Spp	6	1.97	1.76

For all species UVR had, in general, a negative impact on photosynthesis rates, under both nutrient conditions, up to 20°C (Figs. 3A, B, dotted area). The responses at higher predicted temperatures varied among species with (i) an antagonistic effect among UVR and temperature on *D. salina*, with increasing temperatures counteracting the negative UVR effect under both nutrient conditions (Fig. 3A). A similar effect was observed in *A. tamarense* under the LN condition (Fig. 3A) and *I. galbana* under the HN condition (Fig. 3B); (ii) a synergistic effect of temperature and UVR in *C. gracilis* and *I. galbana* under LN (Fig. 3A, dotted area) and for *A.*

tamarense and *C. gracilis* under HN (Fig. 3B, dotted area). Overall, at predicted increased temperatures, high nutrient inputs together with UVR would benefit the photosynthesis of *C. gracilis* and *I. galbana*, while they would decrease the photosynthesis of *A. tamarense* and *D. salina* (Fig. 3C, striped bar). In the case of respiration (Figs. 3D, E and F), the four species would have a continuous increase of UVR impact under predicted higher temperatures and under LN conditions (Fig. 3D, striped bar), being this effect more accentuated in *C. gracilis*. By contrast, little effect as compared to current conditions would be observed under HN conditions for all species (Fig. 3E). Finally, and in contrast to photosynthesis, the net effect of UVR and high nutrients would exert a positive effect on respiration, decreasing it significantly in all cases, with the exception of *I. galbana* where it would be slightly increased (Fig. 3F).

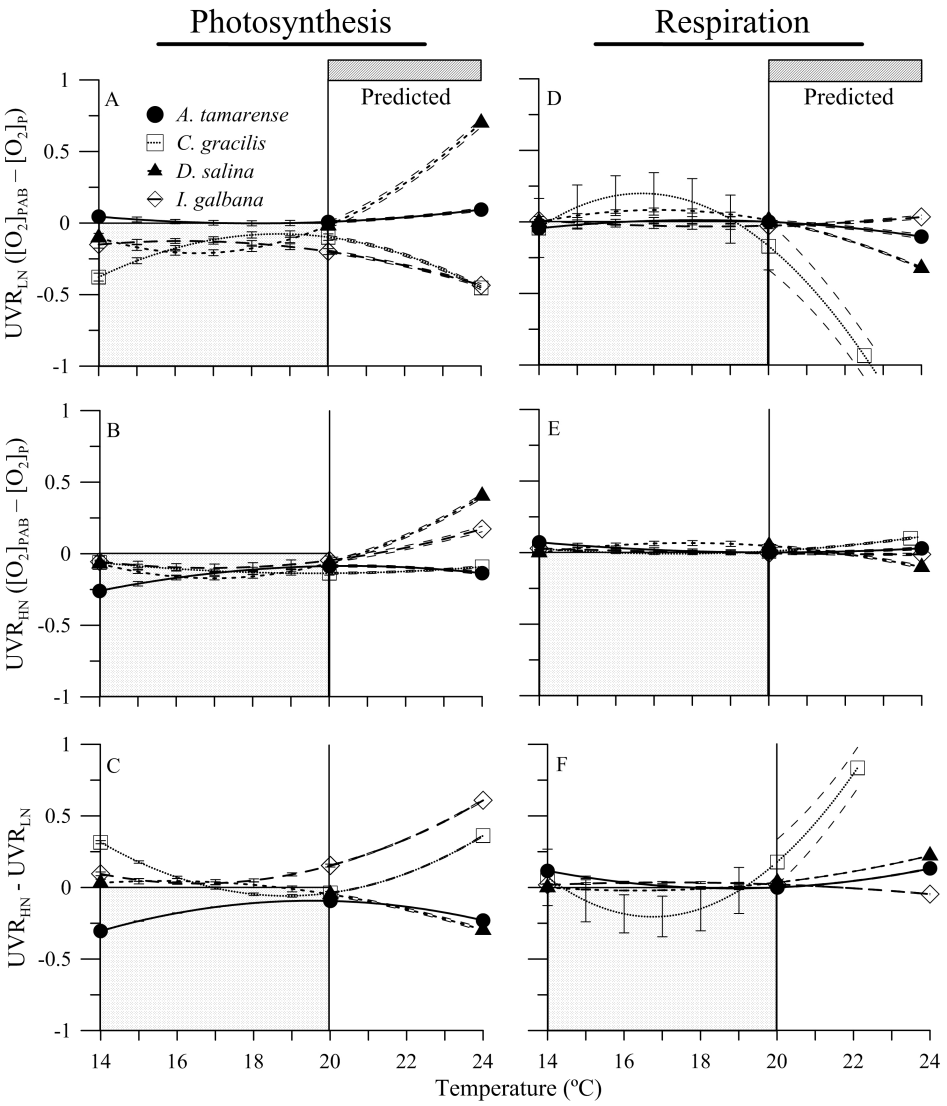

Figure 3: UVR effect, evaluated as the difference between PAB and P treatments, on photosynthesis (A, B) and respiration (D, E) rates as a function of temperature, for *Alexandrium tamarense* (circles), *Chaetoceros gracilis* (squares), *Dunaliella salina* (triangles), and *Isochrysis galbana* (diamonds) within the experimental temperature interval (temperatures up to 20°C) and within the increased temperature (i.e., predicted values, temperatures up to 24°C). Samples were grown and incubated at high (HN) and low nutrients (LN) conditions, and three temperatures, 14, 17, and 20°C. The net effect of high nutrients under UVR within the experimental (temperatures up to 20°C) and predicted temperature interval (i.e., predicted values, temperatures up to 24°C) on photosynthesis (C) and respiration (F) is shown. The lines (solid and broken) represent the best fit using a polynomial function, while the vertical lines represent 95 % confidence intervals, shown every 1°C in the 14 – 20°C interval and continuously in the 20 – 24°C interval.

Dynamics of photochemical parameters

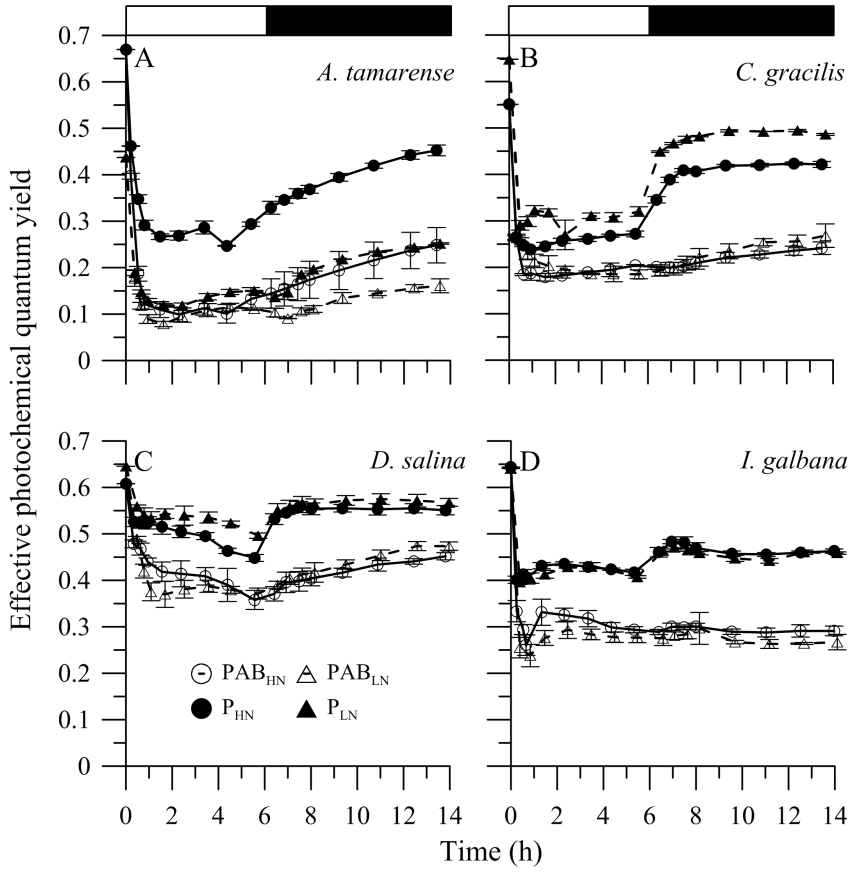

Figure 4: Mean effective photochemical quantum yield of *Alexandrium tamarense* (A), *Chaetoceros gracilis* (B), *Dunaliella salina* (C) and *Isochrysis galbana* (D) during the 6 h exposure to UVR+PAR (PAB, open symbols) and PAR only (P, black symbols), and 8 h of darkness. The horizontal white and black bars on the top indicate the radiation (exposure) and dark periods, respectively. Samples grown and incubated at high (HN, circles) and low nutrients (LN, triangles) conditions. Each symbol represents the mean of triplicate samples while the vertical lines indicate the standard deviation.

The dynamics of the quantum yield of PSII (Φ_{PSII}) for the four species studied showed a similar behavior at 17°C (only this temperature is shown for simplicity, as the trends were similar at 14, 17 and 20°C) (Fig. 4). All species displayed a decrease in Φ_{PSII} as soon as the radiation exposure started, with values remaining low during the exposure, followed by a partial or total recovery in darkness.

In general, and although there was some variability in the responses among species, radiation was the factor that most affected Φ_{PSII}, with values under P being higher than those under the PAB-treatment, regardless of the nutrient conditions. Based on the decrease and recovery of Φ_{PSII}, the inhibition (k) and recovery (r) rates (in min^{-1}) for all species under the different treatments were calculated (Fig. 5). As expected, significant variability among species and treatments were determined. The general trend, however, was of higher absolute k values as compared to r, and also of higher values under the PAB as compared to P treatments, for any temperature and nutrient condition. A significant interaction Rad × Nut × Temp × Spp on k and r was found (Table 2). For *A. tamarense* (Fig. 5A) absolute k and r values decreased with increasing temperature under HN, whereas the opposite occurred under LN. For *C. gracilis* (Fig. 5B) and *I. galbana* (Fig. 5D) there was a general trend of decreasing inhibition with increasing temperature under both nutrient conditions, except for *C. gracilis* grown at LN that had similar inhibition at all temperatures. In regard to recovery rates of *C. gracilis* and *I. galbana*, there were in general no significant differences among temperatures under both nutrient conditions. Finally, in the case of *D. salina* (Fig. 5C), the inhibition increased with temperature under both nutrient conditions, while there were no differences in recovery rates.

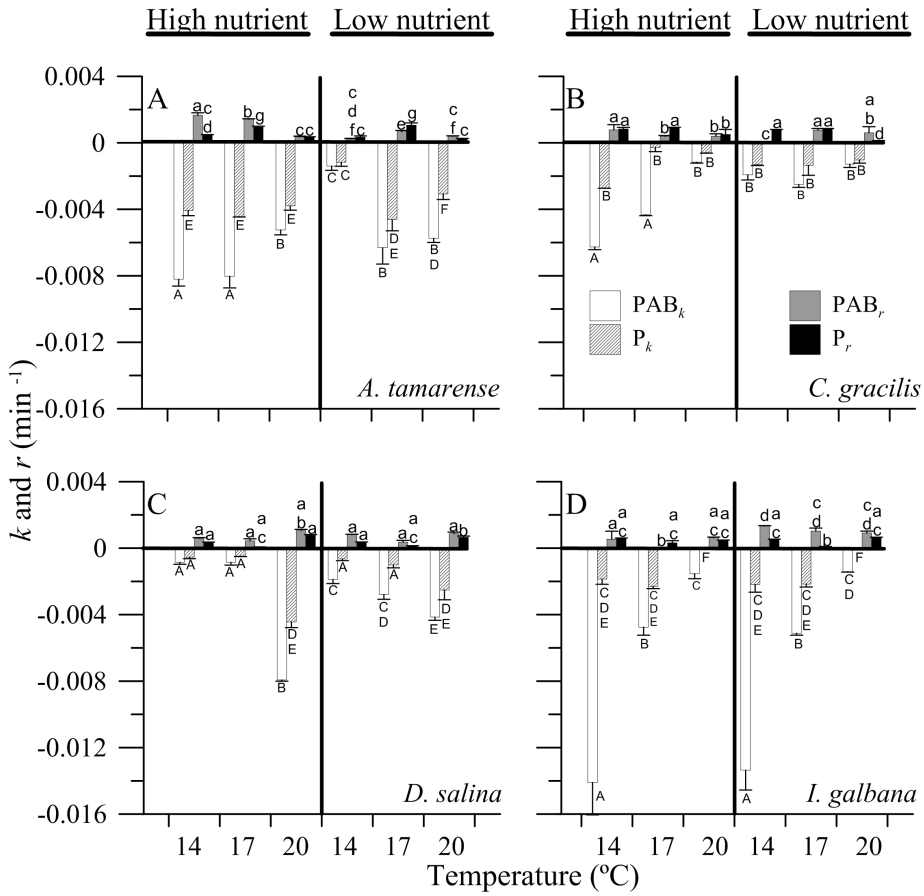

Figure 5: Inhibition (k) (negative values) and recovery (positive values) (r) rates (in min^{-1}) of *Alexandrium tamarense* (A), *Chaetoceros gracilis* (B), *Dunaliella salina* (C) and *Isochrysis galbana* (D). Samples were grown and incubated at two nutrient conditions, HN and LN; three temperatures: 14, 17, and 20°C, and exposed to two radiation treatments: UVR+PAR (PAB, white and grey bars) and PAR only (P, dashed and black bars). The lines on the top of the bars indicate the standard deviation. Significance of post hoc comparisons between radiation treatments for each nutrients condition and temperature are represented with small and capital letters for r and k rates, respectively.

Table 2: Results of statistical analysis for the effects of radiation (Rad), nutrients (Nut), temperature (Temp), and species (Spp), and their interactions, on inhibition (k) and recovery (r). All F values are rounded to two significant digits. Radiation (PAB and P), Nutrient (HN and LN), Temperature (14, 17 and 20°C). df, degrees of freedom; n.s., not significant, and the asterisks *, ** and *** represent the $p < 0.05$, $p < 0.01$ and $p < 0.001$, respectively.

		Inhibition (k)	Recovery (r)
Treatment	df	F	F
Rad	1	201.00***	3.28
Nut	1	16.50***	0.00
Temp	2	10.86***	1.38
Spp	3	36.07***	1.80
Rad×Nut	1	5.75*	0.23
Rad×Temp	2	2.23	0.07
Nut×Temp	2	5.92**	3.89*
Rad×Spp	3	18.73***	4.30**
Nut×Spp	3	11.32***	10.72***
Temp×Spp	6	58.98***	20.63***
Rad×Nut×Temp	2	0.32*	4.60*
Rad×Nut×Spp	3	3.00*	13.61***
Rad×Temp×Spp	6	8.81***	5.92***
Nut×Temp×Spp	6	7.75***	2.18
Rad×Nut×Temp×Spp	6	2.72*	8.36***

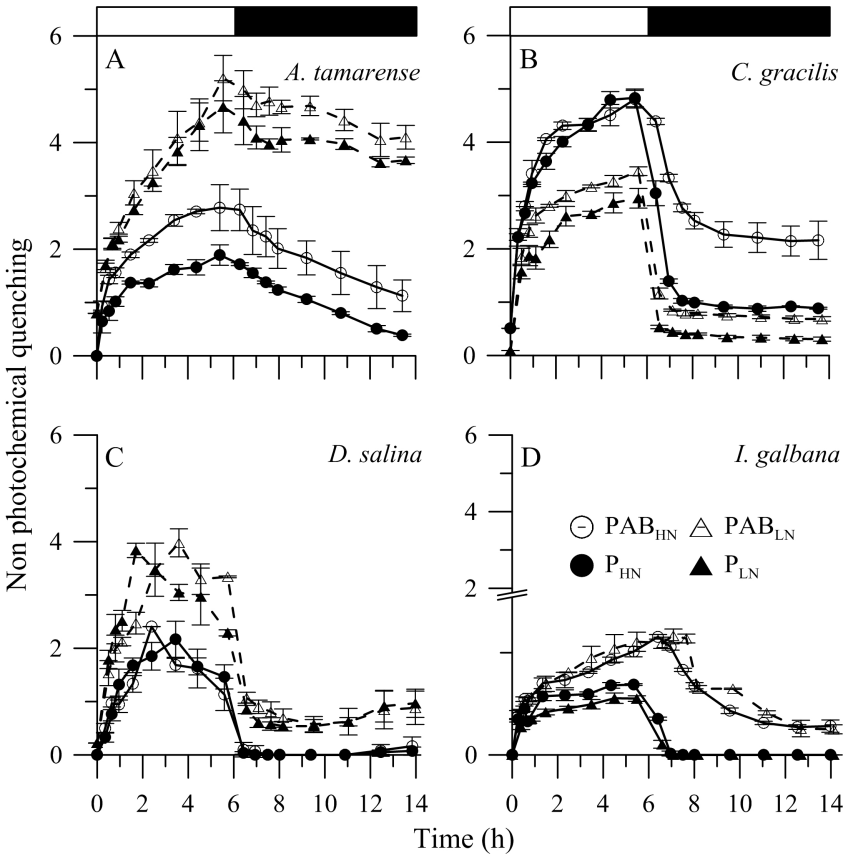

Figure 6: Mean non photochemical quenching (NPQ) of *Alexandrium tamarense* (A), *Chaetoceros gracilis* (B), *Dunaliella salina* (C) and *Isochrysis galbana* (D) during the 6 h of exposure to UVR+PAR (PAB, open symbols) and PAR only (P, black symbols), and 8 h of darkness. The horizontal white and black bars on the top indicate the radiation (exposure) and dark periods, respectively. Samples were grown and incubated at high (HN, circles) and low nutrients (LN, triangles) conditions. Each symbol represents the mean of triplicate samples while the vertical lines indicate the standard deviation.

Fig. 6 shows a representative example of the variations in non photochemical quenching (NPQ) throughout the radiation exposure and recovery in darkness. In general, NPQ showed somehow opposite responses as Φ_{PSII} (Fig. 4), with increasing values during the radiation exposure period, and decreasing during darkness. There was important species-specific variability in NPQ responses, as seen in samples incubated at 17°C (Fig. 6). Higher NPQ values were determined in *A. tamarense* (Fig. 6A) and *D. salina* (Fig. 6C) in samples under LN as compared to those under HN. By contrast, *C. gracilis* (Fig. 6B) had higher NPQ values in samples grown under HN as compared to those under LN conditions. Finally, in *I. galbana* (Fig. 6D) a strong radiation effect was determined, with high NPQ values in samples under the PAB treatment, regardless the nutrient condition. Overall, the lowest NPQ values were determined either in samples under HN (i.e., *A. tamarense*, Fig. 6A and *D. salina*, Fig. 6C), LN (i.e., *C. gracilis*, Fig. 6B) or under the P-treatment (i.e., *I. galbana*, Fig. 6D).

To estimate the effectiveness of NPQ as a mechanism to cope with excess energy, the rates of inhibition (k) vs. NPQ values were compared for the different temperature and nutrient treatments (data not shown). It was observed that for *A. tamarense*, *C. gracilis* and *I. galbana* under the PAB-treatment and grown under HN conditions as well as of *I. galbana* under LN conditions, higher inhibition with decreasing temperature was associated to increasing NPQ values. This pattern was not clear in samples under the P-treatment that had lower k values than when receiving UVR for both nutrient conditions in all species. The net effect of UVR on k and r values as a function of temperature for the two nutrients conditions is shown in Fig. 7. As observed with the photosynthesis, species-specific responses were found: UVR had a negative impact on Φ_{PSII}, increasing the inhibition rates in all species, regardless of the nutrient conditions, up to 20°C (Figs. 7A, B, dotted area). At predicted increased temperatures it was found that: (i) Under LN conditions (Fig. 7A, striped bar), a synergistic effect of UVR and temperature was determined for *I. galbana* as with higher temperatures inhibition rates increased. However, increasing temperatures had antagonistic effects with UVR counteracting its nega-

tive impact in *C. gracilis*. Increased temperature did not modify the UVR inhibitory effect in *A. tamarense* and *D. salina* (i.e., striped bar). ii) Under HN conditions (Fig. 7B, striped bar), increased temperature enhanced the UVR inhibition (i.e., synergistic effect – dotted area) in *D. salina* and *I.galbana*, but it counteracted the negative UVR effects in *A. tamarense* and *C. gracilis*. Overall, a combination of increased temperature and nutrients will significantly counteract UVR inhibition in *A. tamarense* and *C. gracilis* but will enhance it in *I. galbana* and *D. salina* (Fig. 7C, striped bar). In the case of r under LN conditions (Fig. 7D), increasing temperatures resulted in an increase in recovery for all species, with the exception of *I. galbana*, that presented an opposite effect. The addition of nutrients changed this pattern, with *C. gracilis* and *I. galbana* (Fig. 7E) benefiting from the increase in temperature and thus having higher recovery rates than under LN conditions. *A. tamarense* and *D. salina*, on the other hand, had in general a decrease of r as temperature increased. These patterns between LN and HN conditions resulted in an increased recovery capacity of *C. gracilis* and *I. galbana*, but not of *A. tamarense* and *D. salina*, under net increased nutrients and predicted temperature (Fig. 7F).

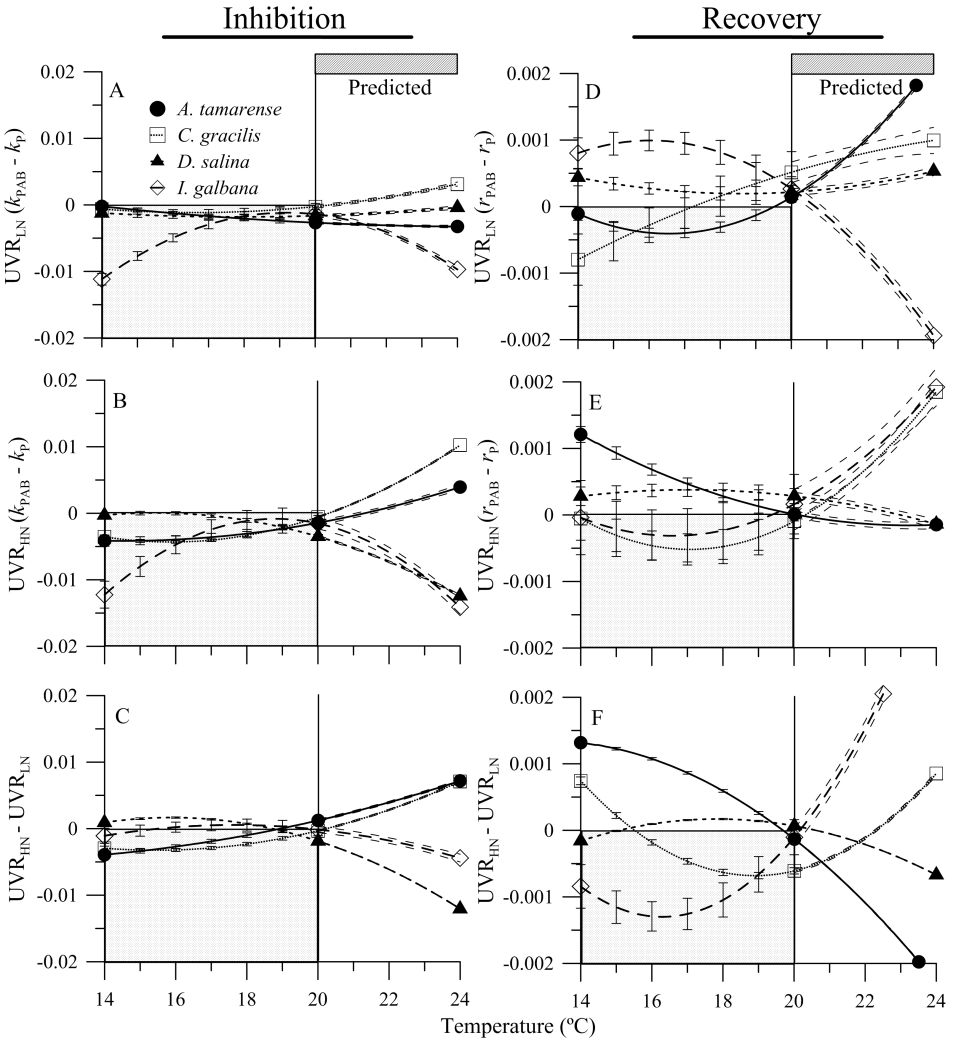

Figure 7: UVR effect, evaluated as the difference between PAB and P treatments, on inhibition (A, B) (k) and recovery (D, E) (r) rates of *Alexandrium tamarense* (circles), *Chaetoceros gracilis* (squares), *Dunaliella salina* (triangles), and *Isochrysis galbana* (diamonds) within the experimental temperature interval (temperatures up to 20°C) and within the increased temperature (i.e., predicted values, temperatures up to 24°C). Samples were grown and incubated at high (HN) and low (LN) nutrients conditions, and three temperatures, 14, 17, and 20°C. The net effect of high nutrients under UVR within the experimental (temperatures up to 20°C) and increased temperature interval (i.e., predicted values, temperatures up to 24°C) on inhibition (C) and recovery (F) is shown. The lines (solid and broken) represent the best fit using a polynomial function, while the vertical lines represent 95 % confidence intervals, shown every 1°C in the 14 – 20°C interval, and continuously in the 20 – 24°C interval.

Discussion

The main goal of this study was to simultaneously evaluate the impact of multiple variables (i.e., UVR exposure, nutrient inputs and temperature) on photosynthetic responses and respiration of key phytoplankton species representative of four marine taxa found in estuarine and coastal waters. To the best of our knowledge, this is the first study that evaluated these responses considering both, a current and a future environmental scenario in a context global change. Our study also highlights the importance to carry out multifactorial experiments to better predict interactive effects among global change variables as well as their impact on aquatic organisms.

Current environmental scenario

Overall, our study shows a synergistic UVR-effect under current ambient conditions of relatively low nutrients and temperatures $< 20°C$ (Fig. 8, white-rectangle arrows) as all species have a reduction in photosynthesis (Fig. 8, P). It has been reported that the oxygen evolving complex (OEC) seems to be UVR-sensitive, especially to UV-B (Kataria et al., 2014). Vass et al. (1996) measured the effects of UVR on different components of PSII, and found that OEC appeared to be the most sensitive, concluding that the primary damage by UVR occurs in this complex. In this sense, any damage in the OEC due to UVR would produce an alteration in the water-splitting reaction, triggering a decrease in photosynthesis (i.e., oxygen production) as shown in all of our species tested (Fig. 8, P; white-rectangle arrows). Besides, the decrease in photosynthesis was coupled with a strong inhibition in PSII (Fig. 8, k). Radiation damages the PSII, and the increase in PSII-photoinhibition could be due to: (i) a direct UVR-impact on PSII (i.e., increasing damage and decreasing repair rates) and (ii) an indirect consequence of an alteration in the OEC. Such alteration in the OEC could also produce a decrease in the proton gradient, which is involved in NPQ-activation (Lavaud et al., 2012), resulting in low NPQ values observed in

all species under current conditions. This mechanism of dissipation of excess energy decreased in the four species tested, in almost all conditions as temperature increased. Similar results were obtained in other studies working with diatoms (Helbling et al., 2011; Li et al., 2012), and the decrease of NPQ with increasing temperature was related to increasing metabolic pathways (i.e., RUBISCO) resulting in a better utilization of radiation and thus reaching higher production (Helbling et al., 2011). The evaluation of the presence of UVACs (data not shown) revealed no significant amounts of these compounds in our experiments with the exception of a small peak in *A. tamarense*. These UVACs, which could help to mitigate the harmful effects produced by UVR have been determined both in isolated species (Hannach & Sigleo, 1998) as well as in phytoplankton communities (Oubelkheir et al., 2013) and have a well-known photoprotective role. A slight synergistic effect of UVR on respiration (i.e., increase) was only observed in *C. gracilis* (Fig. 8, R) but not in the other three species. This lack of UVR effect on respiration rates were observed in other studies carried out with microalgae, that suggested that respiration is not appreciably altered during short-term exposures to UVR (hours) due to a low damage or by relatively fast repair once the damage had occurred, therefore without a measurable signal (Heraud & Beardall, 2002; Larkum & Wood, 1993). However, the results obtained in our study partially agree (Fig. 8, R in *C. gracilis*) with those carried out by Beardall et al. (1994) that reported an enhancement in respiration rates after pre-exposure to high photon fluxes in two microalgae species.

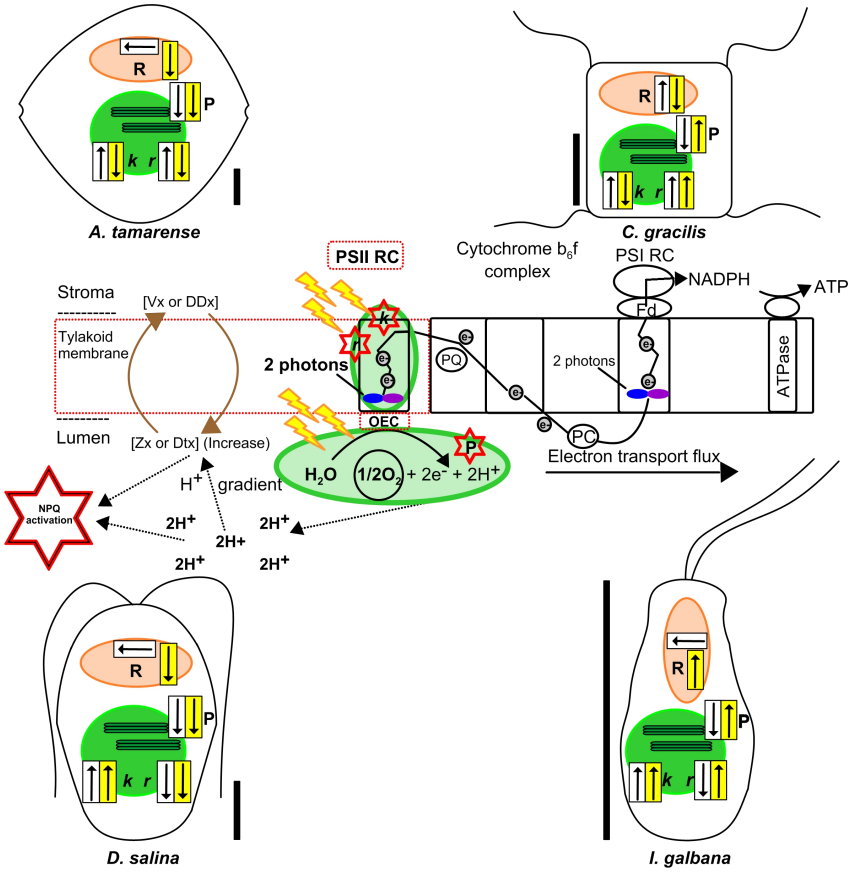

Figure 8: Conceptual graphical model on the combined impact of UVR, nutrient inputs and increased temperature on photosynthetic and respiratory processes in *Alexandrium tamarense*, *Chaetoceros gracilis*, *Dunaliella salina* and *Isochrysis galbana*. Within each cell we represented a chloroplast (green), and a mitochondria (orange) and the processes evaluated in these organelles: photosynthesis (P), respiration (R), inhibition (k) and recovery (r) under current (white-rectangle with arrows) and predicted (yellow-rectangle with arrows) conditions of UVR, nutrients and temperature. The middle panel shows in detail the specific location and development of these processes, as well as, the underlying-related mechanisms that are occurring in the photosystem II. The scale bar represents 5 μm.

Predicted global change scenario

Under predicted environmental conditions an antagonistic UVR-effect will be observed under increased concentrations of nutrients and higher temperatures (Fig. 8, yellow-rectangle arrows) as compared to current conditions. The changes included an increase in photosynthesis of *C. gracilis* and *I. galbana* (Fig. 8, P), whereas respiration will decrease in all species, except for *I. galbana*, probably due to an increase in metabolic oxygen demand with increasing temperature (Clarke, 2003) (Fig. 8, r). On the other hand, the combined effects of increasing nutrients and temperature would result in higher UVR inhibition of PSII in *D. salina* and *I. galbana* (Fig. 8, k), while recovery would diminish in *D. salina* and *A. tamarense* (Fig. 8, r). Despite the variability in the responses among the studied species, our results suggest that under the expected global change scenario, diatoms (*C. gracilis*) and haptophytes (*I. galbana*) would be benefited as the combined impact of increasing Rad × Nut × Temp would improve both photosynthesis (i.e., increasing oxygen production) and photochemical performance (i.e., increasing repair rates). For dinoflagellates (*A. tamarense*), and while photosynthesis would decrease, the rate of photosynthetic inhibition would decrease as well, and this, in the short term, might be associated with the content of UVACs. By contrast, chlorophytes (*D. salina*) would be the most damaged group as predicted conditions would cause greater inhibition and an overall decrease in photosynthesis. This could be related to the fact that chlorophytes have a xanthophyll-cycle acquired through evolution based exclusively on Violaxanthin (Vx), whereas in the others groups it is based on Diadinoxanthin (Ddx) or even though they have low levels of the Vx cycle. The Vx-cycle comprises two de-epoxidations while to Ddx-cycle involves only one de-epoxidation (Goss & Jakob, 2010), and thus reduce the response time to cope with any damage. Besides, algae with Ddx-cycle can also synthesize the xantophylls of Vx-cycle, but in both cases the pigments of Vx-cycle can only be available when algae are illuminated for long-periods (Lohr & Wilhelm, 1999). This supports our view of their low acclimation capacity over short-term exposures under the expected envi-

ronmental changes imposed in our experiments. By contrast, and as seen in Fig. 8, an increase in photosynthesis seems to be a consequence of a suitable functioning of OEC (e.g., by favoring the water-splitting), which could produce: (i) an increase in the proton gradient, that will entail an activation of NPQ, dissipating the excess of energy received as heat and, (ii) an increase in electron gradient. Both gradients could indirectly explain the increase in photosynthesis observed and in the PSII-repair rates for *C. gracilis* and *I. galbana*. The observed metabolic changes under UVR might also be a consequence of a faster response and higher tolerance of small species (*C. gracilis* and *I. galbana*) as compared to large cells, as observed when assessing impact on photosynthesis (Helbling et al., 2001). Partially in agreement with our results, previous studies have found a beneficial temperature-effect in small-sized species (Daufresne et al., 2009; Halac et al., 2013), which also agrees with the temperature-size rule (Hessen et al., 2013). Besides, it cannot be discarded that part of the variability in the observed responses are also related to the nutrient conditions, as cell volume is also a major determinant of nutrient uptake (Tambi et al., 2009). Small cells have generally higher uptake affinities for nutrients as compared to large cells due to their higher surface area to volume quotient (Finkel et al., 2007).

Conclussion

In summary, it was found that an increase in nutrients and temperature will counteract the UVR-inhibition on photosynthesis and photochemical performance of two (i.e., diatoms and haptophytes) out of four groups of marine phytoplankton. Since the interaction between UVR, nutrients and temperature conditions has not been previously examined by experimental manipulation on different phytoplanktonic groups, it is clear that more research is necessary to fully understand the responses by primary producers in a scenario of global change. Modeling and experimental approaches such as these developed in this study would help to improve our under-

standing about the interactive effects of global change variables on key eco-physiological processes. Although the approach used in this study constitutes a simplification of the events occurring in nature, it could be considered a novel way to explore and evaluate the acclimation to the future global change in phytoplankton key groups. These changes would not only affect the photosynthesis and primary production in estuaries and coastal areas, but it might also influence trophic interactions due to a future scenario under these conditions could favor differentially smaller size organisms (diatoms and haptophytes) blooms-development in contrast to other larger size taxonomic groups.

References

Abo-Shady, A.M., El-Sheekh, M.M., El-Naggar, A.H., Abomohra, A.E.-F., 2008. Effect of UV-B radiation on growth, photosynthetic activity and metabolic activities of *Chlorococcum* sp. *Ann. Microbiol.* **58**, 21-27.

Arts, M.T., Rai, H., 1997. Effects of enhanced ultraviolet-B radiation on the production of lipid, polysaccharide and protein in three freshwater algal species. *Freshwater Biol.* **38**, 597-610.

Barbieri, E.S., Villafañe, V.E., Helbling, E.W., 2002. Experimental assessment of UV effects upon temperate marine phytoplankton when exposed to variable radiation regimes. *Limnol. Oceanogr.* **47**, 1648-1655.

Beardall, J., Raven, J.A., 2004. The potential effects of global climate change on microalgal photosynthesis, growth and ecology. *Phycologia* **43**, 26-40.

Beardall, J., Berman, T., Markager, S., Martinez, R., Montecino, V., 1997. The effects of ultraviolet radiation on respiration and photosynthesis in two species of microalgae. *Can. J. Fish. Aquat. Sci.* **54**, 687-696.

Beardall, J., Burger-Wiersma, T., Rijkeboer, M., Sukenik, A., Lemoalle, J., Dubinsky, Z., Fontvielle, D., 1994. Studies on enhanced post-illumination respiration in microalgae. *J. Plankton Res.* **16**, 1401-1410.

Bergmann, T., Richardson, T.L., Paerl, H.W., Pinckney, J.L., Schofield, O., 2002. Synergy of light and nutrients on the photosynthetic efficiency of phytoplankton populations from the Neuse River estuary, North Carolina. *J. Plankton Res.* **24**, 923-933.

Buma, A.G.J., Boelen, P., Jeffrey, W.H., 2003. UVR-induced DNA damage in aquatic organisms. In: Helbling, E.W., Zagarese, H.E. (Eds.), UV effects in aquatic organisms and ecosystems. The Royal Society of Chemistry, Cambridge, pp. 291-327.

Carrillo, P., Delgado-Molina, J.A., Medina-Sánchez, J.M., Bullejos, F.J., Villar-Argaiz, M., 2008. Phosphorus inputs unmask negative effects of ultraviolet radiation on algae in a high mountain lake. *Glob. Change Biol.* **14**, 423-439.

Clarke, A., 2003. Costs and consequences of evolutionary temperature adaptation. *Trends Ecol. Evol.* **18**, 573-581.

Cloern, J.E., Foster, S.Q., Kleckner, A.E., 2014. Review: Phytoplankton primary production in the world's estuarine-coastal ecosystems. *Biogeosciences* **11**, 2477-2501.

Cruces, E., Huovinen, P., Gomez, I., 2013. Interactive effects of UV radiation and enhanced temperature on photosynthesis, phlorotannin induction and antioxidant activities of two sub-Antarctic brown algae. *Mar. Biol.* **160**, 1-13.

Daufresne, M., Lengfellner, K., Sommer, U., 2009. Global warming benefits the small in aquatic ecosystems. *Proc. Natl. Acad. Sci.* **106**, 12788-12793.

Dimier, C., Giovanni, S., Ferdinando, T., Brunet, C., 2009. Comparative ecophysiology of the xanthophyll cycle in six marine phytoplankton species. *Protist* **160**, 397-411.

Field, C.B., Behrenfeld, M.J., Randerson, J.T., Falkowski, P.G., 1998. Primary production of the biosphere: Integrating terrestrial and oceanic components. *Science* **281**, 237-240.

Finkel, Z.V., Sebbo, J., Feist-Burkhardt, S., Irwin, A.J., Katz, M.E., Schofield, O.M.E., Young, J.R., Falkowski, P.G., 2007. A universal driver of macroevolutionary change in the size of marine phytoplankton over the Cenozoic. *Proc. Natl. Acad. Sci.* **104**, 20416-20420.

Folt, C.L., Chen, C.Y., Moore, M.V., Burnaford, J.L., 1999. Synergism and antagonism among multiple stressors. *Limnol. Oceanogr.* **44**, 864-877.

Genty, B.E., Briantais, J.M., Baker, N.R., 1989. The relationship between the quantum yield of photosynthetic electron transport and quenching of chlorophyll fluorescence. *Biochim. Biophys. Acta* **990**, 87-92.

Goss, R., Jakob, T., 2010. Regulation and function of xantophyll cycle-dependent photoprotection in algae. *Photosynth. Res.* **106**, 103-122.

Guihéneuf, F., Fouqueray, M., Mimouni, V., Ulmann, L., Jacquette, B., Tremblin, G., 2010. Effect of UV stress on the fatty acid and lipid class composition in two marine microalgae *Pavlova lutheri* (Pavlovophyceae) and *Odontella aurita* (Bacillariophyceae). *J. Appl. Phycol.* **22**, 629-638.

Guillard, R.R.L., Ryther, J.H., 1962. Studies of marine planktonic diatoms. I. *Cyclotella nana* Husted, and *Detonula confervacea* (Cleve) *Gran. Can. J. Microbiol.* **8**, 229-239.

Häder, D.-P., Helbling, E.W., Williamson, C.E., Worrest, R.C., 2011. Effects of UV radiation on aquatic ecosystems and interactions with climate change. *Photochem. Photobiol. Sci.* **10**, 242-260.

Halac, S.R., Villafañe, V.E., Helbling, E.W., 2010. Temperature benefits the photosynthetic performance of the diatoms *Chaetoceros gracilis* and *Thalassiosira weissflogii* when exposed to UVR. *J. Photochem. Photobiol. B: Biol.* **101**, 196-205.

Halac, S.R., Guendulain-García, S.D., Villafañe, V.E., Helbling, E.W., Banaszak, A.T., 2013. Responses of tropical plankton communities from the Mexican Caribbean to solar ultraviolet radiation exposure and increased temperature. *J. Exp. Mar. Biol. Ecol.* **445**, 99-107.

Hannach, G., Sigleo, A.C., 1998. Photoinduction of UV-absorbing compounds in six species of marine phytoplankton. *Mar. Ecol. Prog. Ser.* **174**, 207-222.

Helbling, E.W., Barbieri, E.S., Marcoval, M.A., Gonçalves, R.J., Villafañe, V.E., 2005. Impact of solar ultraviolet radiation on marine phytoplankton of Patagonia, Argentina. *Photochem. Photobiol.* **81**, 807-818.

Helbling, E.W., Buma, A.G.J., Boelen, P., van der Strate, H.J., Fiorda Giordanino, M.V., Villafañe, V.E., 2011. Increase in Rubisco activity and gene expression due to elevated temperature partially counteracts ultraviolet radiation–induced photoinhibition in the marine diatom *Thalassiosira weissflogii*. *Limnol. Oceanogr.* **56**, 1330-1342.

Helbling, E.W., Buma, A.G.J., de Boer, M.K., Villafañe, V.E., 2001. *In situ* impact of solar ultraviolet radiation on photosynthesis and DNA in temperate marine phytoplankton. *Mar. Ecol. Prog. Ser.* **211**, 43-49.

Helbling, E.W., Chalker, B.E., Dunlap, W.C., Holm-Hansen, O., Villafañe, V.E., 1996. Photoacclimation of antarctic marine diatoms to solar ultraviolet radiation. *J. Exp. Mar. Biol. Ecol.* **204**, 85-101.

Helbling, E.W., Gao, K., Gonçalves, R.J., Wu, H., Villafañe, V.E., 2003. Utilization of solar UV radiation by coastal phytoplankton assemblages off SE China when exposed to fast mixing. *Mar. Ecol. Prog. Ser.* **259**, 59-66.

Helbling, E.W., Pérez, D.E., Medina, C.D., Lagunas, M.G., Villafañe, V.E., 2010. Phytoplankton distribution and photosynthesis dynamics in the Chubut River estuary (Patagonia, Argentina) throughout tidal cycles. *Limnol. Oceanogr.* **55**, 55-65.

Helbling, E.W., Santamarina, J.M., Villafañe, V.E., 1992. Chubut river estuary (Argentina): Estuarine variability under different conditions of river discharge. *Rev. Biol. Mar.* **27**, 73-90.

Helbling, E.W., Zagarese, H.E., 2003. UV effects in aquatic organisms and ecosystems. The Royal Society of Chemistry, Cambridge, 1-575 pp.

Heraud, P., Beardall, J., 2002. Ultraviolet radiation has no effect on respiratory oxygen consumption or enhanced post-illumination respiration in three species of microalgae. *J. Photochem. Photobiol. B: Biol.* **68**, 109-116.

Hessen, D.O., Daufresne, M., Leinaas, H.P., 2013. Temperature-size relations from the cellular-genomic perspective. *Biol. Rev.* **88**, 476-489.

Holm-Hansen, O., Riemann, B., 1978. Chlorophyll *a* determination: Improvements in methodology. *Oikos* **30**, 438-447.

IPCC, 2013. Climate Change 2013. The Physical Science Basis: Working Group I Contribution to the Fifth Assessment Report of the Intergovernmental Panel on Climate Change. Cambridge University Press, New York. USA, 1552 pp.

Kataria, S., Jajoo, A., Guruprasad, K.N., 2014. Impact of increasing Ultraviolet-B (UV-B) radiation on photosynthetic processes. *J. Photochem. Photobiol. B: Biol.*, **137**, 55-66.

Kennish, M.J., Brush, M.J., Moore, K.A., 2014. Drivers of change in shallow coastal photic systems: An introduction to a special issue. *Estuar. Coast.* **37**, 3-19.

Korbee, N., Carrillo, P., Mata, M.T., Rosillo, S., Medina-Sánchez, J.M., Figueroa, F.L., 2012. Effects of ultraviolet radiation and nutrients on the structure–function of phytoplankton in a high mountain lake. *Photochem. Photobiol. Sci.* **11**, 1087-1098.

Kulk, G., De Vries, P., Van de Poll, W., Ronald, J., Buma, A.G.J., 2013. Temperature-dependent photoregulation in oceanic picophytoplankton during excessive irradiance exposure. In: Dubinsky, Z. (Ed.), Photosynthesis. InTech, http://www.intechopen.com/books pp. 209-228.

Lagaria, A., Psarra, S., Lefèvre, D., Van Wanbeke, F., Courties, C., Pujo-Pay, M., Oriol, L., Tanaka, T.Y., Christaki, U., 2011. The effects of nutrient additions on particulate and dissolved primary production and metabolic state in surface waters of three Mediterranean eddies. *Biogeosciences* **8**, 2595-2607.

Larkum, A.W.D., Wood, W.F., 1993. The effect of UV-B radiation on photosynthesis and respiration of phytoplankton, benthic macroalgae and seagrasses. *Photosynth. Res.* **36**, 17-23.

Lavaud, J., Materna, A.C., Sturm, S., Vugrinec, S., Kroth, P.G., 2012. Silencing of the violaxanthin de-epoxidase gene in the diatom *Phaeodactylum tricornutum* reduces diatoxanthin synthesis and non-photochemical quenching. *PloS One* **7**, e36806.

Li, Y., Gao, K., Villafane, V.E., Helbling, E., 2012. Ocean acidification mediates photosynthetic response to UV radiation and temperature increase in the diatom *Phaeodactylum tricornutum*. *Biogeosciences* **9**, 3931-3942.

Lohr, M., Wilhelm, C., 1999. Algae displaying the diadinoxanthin cycle also possess the violaxanthin cycle. *Proc. Natl. Acad. Sci.* **96**, 8784-8789.

Luo, Y., Gerten, D., Le Maire, G., Parton, W.J., Weng, E., Zhou, X., Keough, C., Beier, C., Ciais, P., Cramer, W., Dukes, J.S., Emmett, B., Hanson, P.J., Knapp, A., Linder, S., Nepstad, D., Rustad, L., 2008. Modeled interactive effects of precipitation, temperature, and [CO_2] on ecosystem carbon and water dynamics in different climatic zones. *Glob. Change Biol.* **14**, 1986–1999.

Maxwell, K., Johnson, G.N., 2000. Chlorophyll fluorescence - a practical guide. *J. Exp. Bot.* **51**, 659-668.

McKenzie, R., Aucamp, P.J., Bais, A., Björn, L.O., Ilyas, M., Madronich, S., 2011. Ozone depletion and climate change: Impacts on UV radiation. *Photochem. Photobiol. Sci.* **10**, 182-198.

Oubelkheir, K., Clementson, L., Moore, G.F., Tilstone, G.H., 2013. Production of mycosporine-like amino acids by phytoplankton under ultraviolet radiation exposure in the Sub-Antarctic zone south of Tasmania. *Mar. Ecol. Prog. Ser.* **494**, 41-63.

Porra, R.J., 2002. The chequered history of the development and use of simultaneous equations for the accurate determination of chlorophylls *a* and *b*. *Photosynth. Res.* **73**, 149-156.

Skerratt, J.H., Davidson, A.D., Nichols, P.D., McMinn, T.A., 1998. Effect of UV-B on lipid content of three Antarctic marine phytoplankton. *Phytochem.* **49**, 999-1007.

Sobrino, C., Neale, P.J., 2007. Short-term and long-term effects of temperature on photosynthesis in the diatom *Thalassiosira pseudonana* under UVR exposures. *J. Phycol.* **43**, 426-436.

Takahashi, S., Yoshioka-Nishimura, M., Nanba, D., Badger, M.R., 2013. Thermal acclimation of the symbiotic alga *Symbiodinium* spp. alleviates photobleaching under heat stress. *Plant Physiol.* **161**, 477-485.

Tambi, H., Fonnes-Flaten, G.A., J.K., E., Bødtker, G., Jacobsen, A., Thingstad, T.F., 2009. Relationship between phosphate affinities and cell size and shape in various bacteria and phytoplankton. *Aquat. Microb. Ecol.* **57**, 311-320.

Thomas, M.K., Kremer, C.T., Klausmeier, C.A., Litchman, E., 2012. A global pattern of thermal adaptation in marine phytoplankton. *Science* **338**, 1085-1088.

Toseland, A., Daines, S.J., Clark, J.R., Kirkham, A., Strauss, J., Uhlig, C., Lenton, T.M., Valentin, K., Pearson, G.A., Moulton, V., Mock, T., 2013. The impact of temperature on marine phytoplankton resource allocation and metabolism. *Nat. Clim. Change* **3**, 979-984.

Vass, I., László, S., Spetea, C., Bakou, A., Ghanotakis, D.F., Petrouleas, V., 1996. UV-B-induced inhibition of photosystem II electron transport studied by EPR and chlorophyll fluorescence. Impairment of donor and acceptor side components. *Biochem.-US* **35**, 8964-8973.

Winder, M., Sommer, U., 2012. Phytoplankton response to a changing climate. *Hydrobiologia* **698**, 5-16.

Chapter IV

Differential impacts of global change variables on coastal South Atlantic phytoplankton: Role of seasonal variations

Abstract

Global change is associated to the increase in temperature (T), nutrient inputs (Nut) and solar radiation in the water column. To address their joint impact on the net community production [NCP], respiration [CR] and PSII performance (Φ_{PSII}) of coastal phytoplankton communities from the South Atlantic Ocean over a seasonal succession, we performed a factorial design. For this, we used a $2 \times 2 \times 2$ matrix set-up, with and without UVR, ambient and enriched nutrients, and *in situ* T and *in situ* T + 3°C. The future scenario of global change exerted a dual impact, from an enhancement of NCP and Φ_{PSII} during the pre-bloom to an inhibition of both processes towards the bloom period, when the *in situ* T and irradiances were lower and the community was dominated by diatoms. The increased inhibition of NCP and Φ_{PSII} during the most productive stage of the annual succession could produce significant alterations of the CO_2-sink capacity of coastal areas in the future.

Introduction

Coastal areas represent a small fraction (ca. 5%) of the total oceanic surface, however, they constitute the most productive ecosystems on Earth (Rousseaux & Gregg, 2014; Uitz et al., 2010). These areas are also considered biogeochemical hot spots because they receive large inputs of nutrients (Nut) and organic carbon from land and open ocean thus supporting high metabolism and primary production (Cloern et al., 2014). Coastal areas also present highly variable environmental conditions e.g., light, temperature (T) among others, making them particularly interesting model systems to evaluate the responses of organisms in a scenario of global change. Global change is a process largely related to human-derived activities e.g., the release of high amounts of CO_2 into the atmosphere due to industrialization (IPCC, 2013). Such atmospheric changes derive in more acidified and

warmer water bodies, receiving higher levels of solar radiation (including ultraviolet radiation [UVR, 280-400 nm]) due to increased stratification of the water column (Williamson et al., 2014). In addition, due to the increasing human pressures through agriculture, livestock, and industry, higher population densities in areas close to the coast, and consequently higher waste removal (Cloern et al., 2016), coastal areas are incurring greater nutrient inputs through rivers, and these inputs expected to intensify during the next few decades (Rabalais et al., 2009).

The effects of variables associated to global change on coastal communities have been largely explored individually in both, laboratory and field studies. The validity of such approaches, however, is being challenged by recent research that reveals interactive effects among environmental variables that affect the responses as compared to the individual effects (Boyd et al., 2015; 2016). Thus, studies assessing multi-variable impacts are more appropriate as they provide more reliable information about future impacts of global change on aquatic ecosystems. For example, solar UVR is an abiotic factor that strongly influences the responses of phytoplankton under global change conditions. Although a huge body of literature has shown the negative effects of UVR on several targets (e.g., photosystem II [Φ_{PSII}], proteins, DNA) and processes (e.g., growth, nutrients uptake, photosynthesis, respiration) (Häder et al., 2015) other studies have also found positive effects (e.g., higher photorepair of DNA, enhanced photosynthesis; Barbieri et al., 2002; Gao et al., 2007). Part of these contrasting responses, however, occurs due to the interaction of UVR with other variables. In this sense, nutrient enrichment generally tends to counteract the negative effects of solar UVR exposure (Agustí et al., 2009; Harrison & Smith, 2013; Villafañe et al., 2014) therefore acting antagonistically. Increased temperature frequently acts in an antagonistic manner with UVR either on short- (e.g. Sobrino & Neale, 2007) and mid-term scales (Helbling et al., 2011). This antagonistic effect improves phytoplankton photochemical performance (Helbling et al., 2011; Villafañe et al., 2015; Wong et al., 2015), increasing growth rates (Morán et al., 2010) or even protein synthesis and nitrogen uptake (Toseland et al., 2013), especially when the tested organisms are below their

optimal thermal limit.

In spite of the ecological and socio-economic importance that implies the prediction of the effects of multiple global change variables on aquatic ecosystems, up to date scarce experimental studies have considered how the interaction between UVR, Nut and T could impact on primary producers (Cabrerizo et al., 2014; Doyle et al., 2005; Durán et al., 2016). These studies have reported a wide range of effects under a multi-factor scenario, ranging from inhibition of phytoplankton growth (Doyle et al., 2005) to enhancement of photosynthesis and of excretion of organic carbon (Durán et al., 2016). One study carried by our group (Cabrerizo et al., 2014) further highlighted the species-specificity of responses under the joint effect of these variables – UVR, Nut and T. Moreover, most of the studies simulating a scenario of global change, however, have been performed during rather short periods of time, neglecting the natural environmental heterogeneity that can also alter the biological responses of phytoplankton. This is especially important, as aquatic ecosystems experience natural variations in their physical and chemical parameters, together with a temporal succession of species. Thus, and to address this gap of knowledge i.e., the responses of organisms to global change conditions tied to the natural variability of the environment, we designed experiments to quantify how a future scenario of UVR under increased Nut and T could alter the physiology of phytoplankton communities during the pre-bloom to bloom period in coastal South Atlantic Ocean waters. Thus we worked not only with communities that changed along the season but that also had different light and thermal history due to variable irradiances/mixing conditions, and *in situ* T due to the transition from fall to winter. We performed experiments during almost three months, manipulating simultaneously the Nut concentrations, T and radiation quality. Over this period, we measured the net community production [NCP], community respiration [CR]) and the effective photochemical quantum yield (Φ_{PSII}) on different phytoplankton communities of Patagonian coastal waters.

Despite that between 6-11% of the global primary productivity occurs in the South Atlantic Basin (Rousseaux & Gregg, 2014; Uitz et al., 2010) and although Patagonian waters constitute one of the most important fishery areas of the Atlantic Ocean Basin (De Carli et al., 2012; Góngora et al., 2012), they continue to be a relatively unexplored area. The area has continuous inputs of nutrients from the river into the sea due to agricultural and urban activities (Helbling et al., 2010), and a clear bloom (dominated by diatoms, mainly *Odontella aurita*) during winter time and pre- and post-bloom periods (dominated by pico-nanoplankton cells, mainly flagellates) have also been reported for this site (Villafañe et al., 2004; 2013). With this background in mind, our working hypothesis was that a future global change scenario will reduce the NCP and Φ_{PSII} performance, and will enhance the CR in the pre-bloom as compared to the bloom communities, as increased T will displace such communities above of the optimal growing temperatures experienced inside the annual thermal limits (17 – 9°C). Thus, through our simulations of future global change conditions we tested the impacts of a multi-variable scenario on the communities varying during the seasonal succession.

Material and Methods

Study site and sampling

Water samples were collected at the seawater side of the Chubut River estuary, in Patagonian coastal waters (Chubut Province, South Atlantic Ocean, Argentina) (Fig. 1). The experiments were done during the period April 5 to June 14, 2013, with field samples collected every week (10 experiments in total). Surface seawater (salinities > 31) samples (ca. 20 L) were collected in the afternoon-evening of the day previous to the experimentation at Egi station (43° 20.5′ S, 65° 02.0′ W) (Fig. 1) during high tide. The samples were pre-screened through a 180 μm Nitex mesh to eliminate

meso-zooplankton, and put into an acid-cleaned (1N HCl) opaque container and immediately transported to the Estación de Fotobiología Playa Unión (EFPU, 10-15 min away from the sampling site) where experiments were performed as described below. Once at the laboratory, samples were pre-acclimated to the *in situ* T registered during the sampling moment or either to the *in situ* T + 3°C overnight before being used in experimentation.

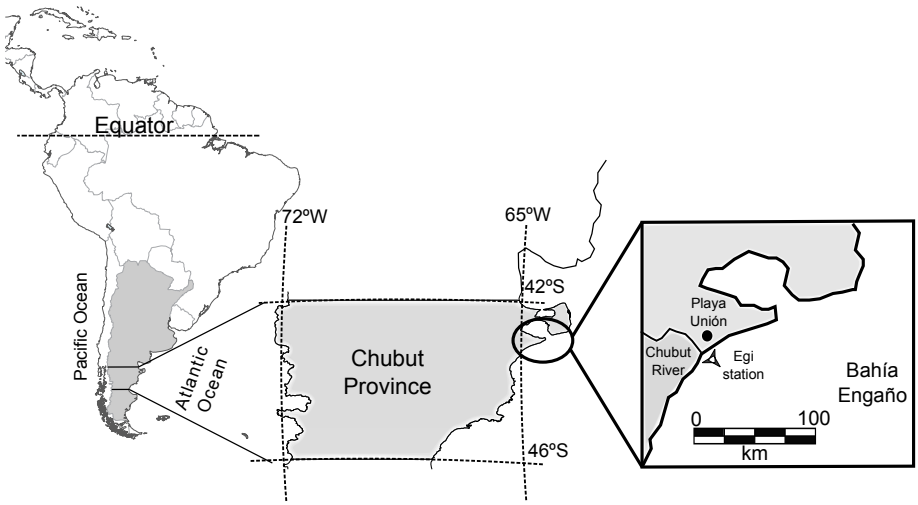

Figure 1: Map of South America indicating the relative location of the Chubut province, Argentina. The enlarged area shows the sampling site (Egi station) outside the Chubut River estuary in Bahía Engaño.

Experimental set up

The UVR × Nut × T effects on NCP, CR and Φ_{PSII} were assessed using a factorial design set up with a 2 × 2 × 2 matrix. All experimental units were run in triplicate. The original seawater sample was divided in two sub-samples that were put into two opaque containers. In one of them, the

nutrients were kept under ambient conditions (i.e., without modification, as at the time of collection) whereas the other was enriched in macronutrients by 45 μM for nitrate + nitrite, 1.8 μM for phosphate, and 5.5 μM for silicate over their respective ambient concentration, simulating larger inputs by the Chubut river. Samples from these two Nut conditions were placed in 50 mL quartz round vessels, 24 for oxygen and 24 for Φ_{PSII} measurements, and exposed to: a) two radiation treatments, PAB (UVR+PAR, > 280 nm), uncovered vessels, and P (PAR, > 400 nm) vessels covered with UV Opak 395 filter (Difegra); and, b) two T treatments (*in situ* and *in situ* + 3°C). The increase in 3°C represents predicted values by the end of century for South Atlantic surface waters by IPCC (2013) (scenario RCP 8.5). All vessels containing the samples were put in a rotating system, to ensure homogeneous exposures, inside an illuminated environmental chamber (Sanyo MLR-350, Japan). The chamber kept the desired temperature *in situ* or *in situ* + 3°C constant for each experimental condition. Due to logistical limitations inside the environmental test chamber, it was first set to the *in situ* water temperature and the following day to the increased temperature. To avoid alterations in the acclimation conditions and in the physiological state of the communities, we took new samples for the *in situ* + 3°C experiments. We found no significant differences between samples taken during two consecutive days for each experiment (data not shown). Radiation levels were provided by 10 Philips daylight fluorescent tubes for PAR and 5 Q-Pannel UVA-340 tubes for UVR. The samples were exposed to constant irradiances of 164.1, 42.8 and 0.7 W m^{-2} for PAR, UV-A and UV-B, respectively. The spectral output of the lamps was checked using a spectroradiometer (Ocean Optics HR 2000CG-UV-NIR); no UV-C output was measured. The radiation exposure period lasted 6 h hence samples received a daily dose of 3.5 MJ m^{-2} for PAR, 910 kJ m^{-2} for UV-A and 15 kJ m^{-2} for UV-B, and the response to UVR of all samples was tested under the same conditions although the samples had a different light history (and different taxonomic composition) as the season progressed. After the exposure period, the experimental units were maintained for 8 h in darkness for respiration measurements (see below).

Analysis and measurements

Net community production and community respiration

Oxygen concentration (O_2) was measured using an optode-probe system (Fibox 3, PreSens GmbH, Germany) equipped with fiber optics and sensor-spots (SP-PSt3-NAU-D5-YOP) together with the Oxyview 6.02 software to register the data. The system was initially calibrated using a two-point calibration for 100% and 0% oxygen saturation, at the desired temperature and at atmospheric pressure. Oxygen concentration measurements were done at the beginning of each experiment (t_0); then, every hour during the 6 h light-exposure period to determine the NCP rates. In addition, measurements of oxygen concentration were done every 30 min during the first 2 h of darkness and then every 1.5 h until finishing the 8 h dark period to determine CR rates.

Fluorescence measurements

Sub-samples of 3 mL were taken (with the same frequency as for oxygen concentration measurements) to measure in vivo chlorophyll *a* (Chl *a*) fluorescence, using a pulse amplitude modulated (PAM) fluorometer (Walz, Water PAM, Effeltrich, Germany). Each sample was measured six times immediately after sampling, with each measurement lasting 10 seconds, therefore the total time for measuring each sample was 1 min. The effective photochemical quantum yield of PSII (Φ_{PSII}) was calculated using the equations of Genty et al. (1989) and Maxwell & Johnson (2000) as:

$$\Phi_{PSII} = \Delta F/F'm = (F'm - Ft)/F'm$$

where F′m is the maximum fluorescence induced by a saturating light pulse (ca. 5300 μmol photons m^{-2} s^{-1} in 0.8 s) and Ft the current steady state

fluorescence induced by a weak actinic light ca. 492 µmol photons m^{-2} s^{-1} in light-adapted cells.

Chlorophyll *a* (Chl *a*)

The Chl *a* content of the samples was measured by filtering two aliquots (50 mL) of the original sample onto MG-F glass fiber filters (25 mm, Munktell, Sweden) and the photosynthetic pigments were extracted in absolute methanol (Holm-Hansen & Riemann, 1978). After 1 h of extraction and 10 min of centrifugation at 2000 rpm, the supernatant was scanned (250 to 700 nm) using a spectrophotometer (Hewlett Packard, model 8453E, USA). The Chl *a* concentration was calculated from these scans using the equation of Porra (2002).

Taxonomic analyses

Aliquots from the original samples were placed in 125 mL brown glass bottles and fixed with buffered formaline (0.4% final concentration of formaldehyde in the sample). Sub-samples of 25 mL were settled in a Utermöhl chamber (Hydro-Bios GmbH, Germany) for 24 h to ensure complete sedimentation of cells. The samples were counted under 200× for microplankton (>20 μm) and under 400× magnification for nanoplankton cells (<20 μm); a drop of Rose Bengal was added to the sample to better distinguish between organic material and detritus. Species were identified and enumerated using an inverted microscope (Leica, model DM IL, Germany) following the technique described in Villafañe & Reid (1995). The biovolumes of the phytoplankton cells groups analyzed were calculated following Hillebrand et al. (1999). Biovolumes were converted into carbon content (i.e., biomass) using the equations of Strathmann (1967).

Solar radiation, temperature and conductivity

Incident solar radiation was continuously monitored using an European Light Dosimeter Network broadband filter radiometer (ELDONET, Real Time Computers, Germany) that measures UV-B (280-315 nm), UV-A (315-400 nm) and PAR (400-700 nm) every second and averages the data over a 1 min interval. The radiometer is permanently installed on the roof of the Estación de Fotobiología Playa Unión and is calibrated every year using a clear sky solar calibration procedure together with model outputs (Björn & Murphy, 1985). Seawater temperature and conductivity was measured for every field sampling day using a multiparameter probe (Yellow Spring Instruments, model 600 XLM, USA).

Data and statistical analyses

NCP and CR rates were calculated as the slope of the regression fit of increases (for NCP, light period) and decreases (for CR, dark period) in the oxygen concentration versus time. As the community structure and species changed along the study period, we normalized the NCP and CR rates (in μmol O_2 L^{-1} h^{-1}) by the Chl *a* concentration to be able to compare the oxygen rates (in μmol O_2 μg Chl a^{-1} h^{-1}). Inhibition (k, in h^{-1}) and recovery (r, in h^{-1}) rates of Φ_{PSII} were estimated by applying an exponential regression fit to the data obtained during the light or dark periods, respectively, as:

$$\Phi_{PSII} = A \times e^{-kt} \text{ or}$$

$$\Phi_{PSII} = A \times e^{rt}$$

where Φ_{PSII} is the quantum yield of PSII, A is a constant, k / r represents inhibition / recovery, respectively, and t is the time.

We calculated the single effects of UVR, Nut and T on NCP, CR, k and r as:

$$\text{Single effect } (\%) = (\text{control} - \text{variable}_{single})/(\text{control}) \times 100$$

where the control represents samples under the P treatment, ambient nutrient and *in situ* temperature in all cases, and variable single represents: (i) samples under the PAB treatment, ambient nutrient and *in situ* temperature for UVR effects, (ii) samples under the P treatment, enriched nutrients and *in situ* temperature for Nut enrichment effects and, (iii) samples under the P treatment, ambient nutrients and *in situ* temperature + 3°C for increased T effects.

The interactive effect of UVR × Nut × T on NCP, CR, k or r rates were calculated as:

$$\text{Interactive effect } (\%) = (\text{control} - \text{variable}_{multiple})/(\text{control}) \times 100$$

where the control represents samples under the P treatment, ambient nutrient and *in situ* temperature, and the variable multiple represents samples under the PAB treatment, enriched nutrients and *in situ* temperature + 3°C treatments. Error propagation was used to calculate the variance of single and interactive effects (%). The single and interactive effects on k and CR were multiplied by -1; thus, negative values represent an enhancement whereas positive values an inhibitory effect on the process considered.

A four-way ANOVA were used to determine differences on NCP, CR and Φ_{PSII} performance (as k and r) rates with UVR, Nut and T and sampling days (Date) as factors. Assumptions of normality and homoscedasticity were checked for each data set before ANOVA application (Zar, 1999). When significant differences were determined, a Bonferroni *post hoc* test's was performed. Due to the multiple comparisons possible between treatments for NCP, CR, k and r rates it was impractical to add all symbols

in the figures to denote significances; hence they are mentioned in the text only when it is appropriate.

We used fordward stepwise multiple linear regression (MLR) analyses to assess the relative strength of abiotic (i.e., *in situ* T and previous light history) and biotic variables (i.e., biomass of diatoms and flagellates) to explain the variability observed in the single and interactive effects of UVR, Nut and T on NCP, CR, r and k rates over the experimental period. The previous light history received by the communities was assessed as the mean daily solar irradiance of the previous 5-7 days of the sampling day, as this period has been shown enough for acclimation of the cells (Buma et al., 2009). Previous to the MLRs analyses, assumptions of linearity were verified through residual analyses. Multicolinearity among independent variables was also verified by correlation analysis and controlled by specifying 0.6 as the minimum acceptable tolerance; homocedasticity was verified through normal probability scatter-plot analysis.

Results

Seasonal physical and biological conditions

The study period was characterized by variable radiation conditions, although with a predominance of cloudy days. Also, a characteristic trend of decreasing daily doses over time was determined, from 5.39 to 1.97 MJ m^{-2}, 0.72 to 0.24 MJ m^{-2} and 14.14 to 3.10 kJ m^{-2}, for PAR, UV-A and UV-B, respectively (Figs. 2A, B). The mean daily irradiances during this period varied between ca. 111-33 (Fig. 2C), ca. 13-4 and 0.30-0.04 W m^{-2} (Fig. 2D) for PAR, UV-A and UV-B, respectively.

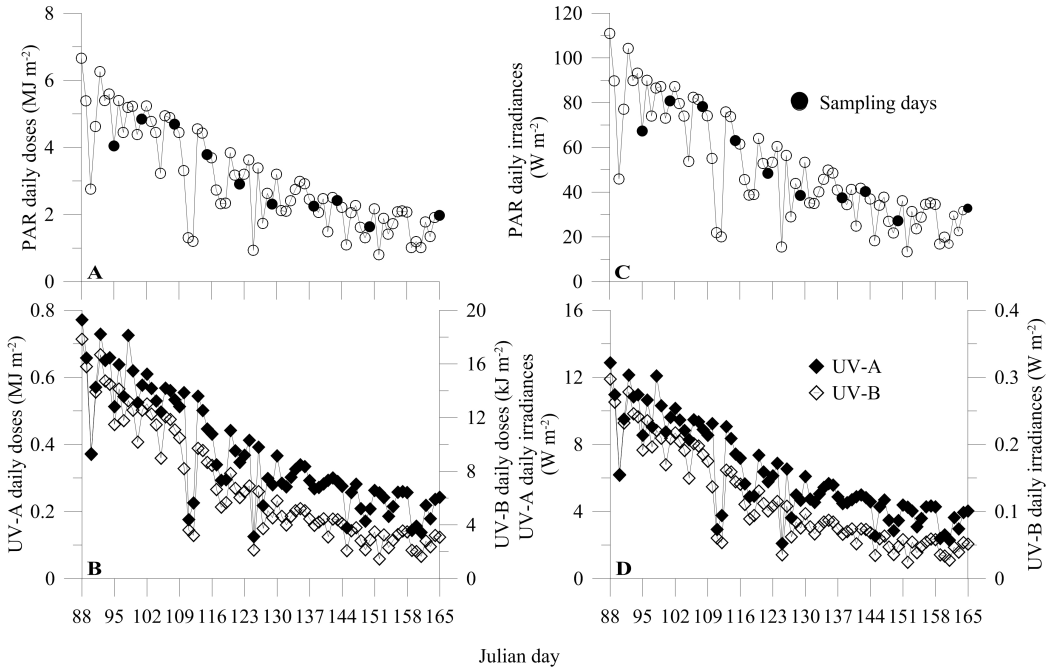

Figure 2: Daily doses (in MJ or kJ m^{-2}) (A, B) and mean daily irradiances (in W m^{-2}) (C, D) for photosynthetically active radiation (PAR) and ultraviolet radiation A (UV-A, 315-400 nm) and B (UV-B, 280-315 nm) from Julian day 88 to 165. The solid circles represent the sampling days and the open circles the previous light-history of communities sampled.

Seawater temperature, Chl *a* and the biomass of the different phytoplankton groups (Fig. 3) also varied during the study period. Temperature continuously decreased from 16.9°C in early April to 9.8°C in mid-June (Fig. 3A). Although Chl *a* concentrations generally ranged between 6 and 10 μg L^{-1}, two clear peaks (i.e., 20 in late April and ca. 45 μg L^{-1} in late May) were found, supporting the idea of a transition from a pre-bloom (March – May) to a bloom period (late May – June). During the study period, the proportion of nanoplankton cells (< 20 μm in diameter) ranged between ca. 15-72 % of the total biomass (Fig. 3B). The biomass of di-

atoms was higher than that of flagellates, especially in the two Chl *a* peaks, where it reached values of ca. 70 and 80 μg C L^{-1}, respectively (Fig. 3B). The dominating diatoms during these Chl *a* peaks that occurred in the two different stages of the succession were mostly chains of *Thalassiosira* species (10 – 50 μm) in the first peak (pre-bloom), and *Odontella aurita* in the second peak (bloom). The contribution of dinoflagellates (e.g., small naked species, *Prorocentrum micans* and *Alexandrium tamarense*) was very low throughout the study period, accounting for < 1% of the total cellular biomass.

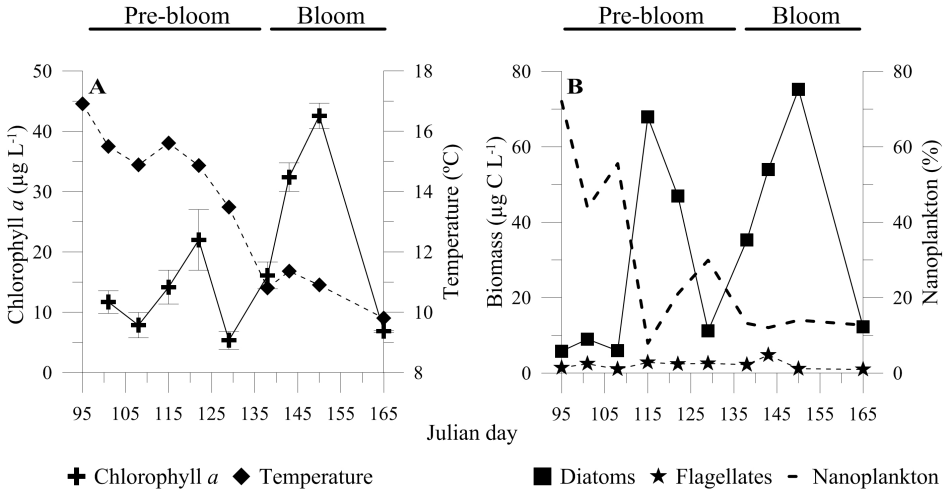

Figure 3: Chlorophyll *a* concentration (in μg L^{-1}) and *in situ* temperature (in °C) (A); biomass of flagellates and diatoms (in μg C L^{-1}) (B), together with the percentage (%) of the pico-nanoplankton (< μm 20) fraction during the study period.

Impact of multiple global change variables on phytoplankton physiology

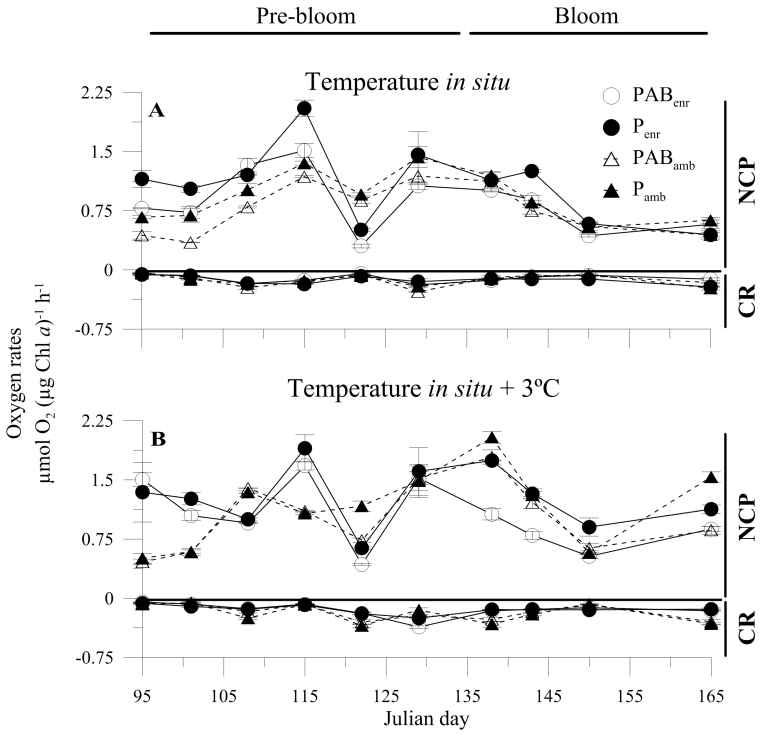

Figure 4: Normalized net community production (NCP) and community respiration (CR) rates (in μmol O_2 μg Chl a h^{-1}) as a function of time for samples under UVR + PAR (PAB) and PAR (P), two nutrient treatments: ambient (dashed lines) and enriched (solid lines) and two temperature treatments: (A) *in situ* and (B) *in situ* + 3°C. Each symbol represents the mean of triplicate samples whereas vertical lines indicate the standard deviation.

Overall, NCP rates (Fig. 4) were significantly higher under nutrient enrichment than under ambient treatments during the pre-bloom (Bonferroni *post hoc*, $p < 0.05$) but as the season progressed, these differences were not significant. Nevertheless, a significant UVR × Nut × T × date effect was found on NCP rates (Table 1). At the *in situ* T, NCP rates were significant lower (Bonferroni *post hoc*, $p < 0.01$) under UVR than under PAR during most of the pre-bloom (Fig. 4A), but this difference between treatments decreased towards the bloom. At the increased T (Fig. 4B), the UVR effect was lower than that observed at the *in situ* T during the pre-bloom; however, this inhibitory UVR effect increased during the bloom, particularly under enriched treatments (Bonferroni *post hoc*, $p < 0.05$). CR rates did not exhibit any clear response pattern neither under UVR, nutrient nor T treatments throughout the season, with mean CR rates being -0.12 (± 0.06) and -0.16 (± 0.09) μmol O_2 μg Chl a^{-1} h^{-1} for the *in situ* T and *in situ* + 3°C, respectively.

Table 1: Results of four-way ANOVA for the single and interactive effects of ultraviolet radiation (UVR), nutrients (Nut), temperature (T) and Date on normalized net community production (NCP) and community respiration (CR), inhibition (k) and recovery (r) rates. All F values which represent F-test are rounded to two significant digits. Radiation (PAB and P), Nutrient (ambient and enriched), Temperature (*in situ* and *in situ* + 3°C) and sampling day (Date). df, degress of freedom; n.s., not significant, and the asterisks *****, ****** and ******* represent the $p < 0.05$, $p < 0.01$ and $p < 0.001$, respectively.

		NCP	CR	Inhibition *(k)*	Recovery *(r)*
Treatment	df	F	F	F	F
Rad	1	73.93***	3.47***	21.24***	18.30***
Nut	1	117.04***	108.32***	0.17	0.11
T	2	168.67***	70.30***	7.69**	10.52**
Date	8	996.36***	1199.52***	21.01***	7.58***
Rad×Nut	1	0.43	2.08	12.55***	0.01
Rad×T	2	5.48*	1.50	1.82	2.19
Rad×Date	8	4.14***	20.25***	1.56	2.36*
Nut×T	1	3.56	10.08***	0.01	0.01
Nut×Date	8	90.86***	46.63***	8.41***	4.33***
T×Date	8	17.27***	19.34***	8.01***	4.76***
Rad×Nut×Date	8	3.48***	0.98	1.36	1.06
Rad×T×Date	8	10.52***	19.97***	0.93	1.22
Rad×Nut×T	1	0.73	17.85***	3.79	0.02
Nut×T×Date	8	44.97***	50.98***	7.14***	1.32
Rad×Nut×T×Date	8	4.38***	11.48	1.13***	0.71

A significant UVR × Nut × T × date interaction for Φ_{PSII} rates (Table 1) was only found on k. However, although k rates showed a slight increase during the season it was only significant towards the end of the bloom period under PAB, independently of the nutrients treatment considered at the *in situ* T, and under PAB and ambient nutrients treatment under increased temperature (Bonferroni *post hoc*, $p < 0.05$) (Fig. 5). In contrast, r rates did not show a clear response pattern, exhibiting similar values under all experimental conditions throughout the study period.

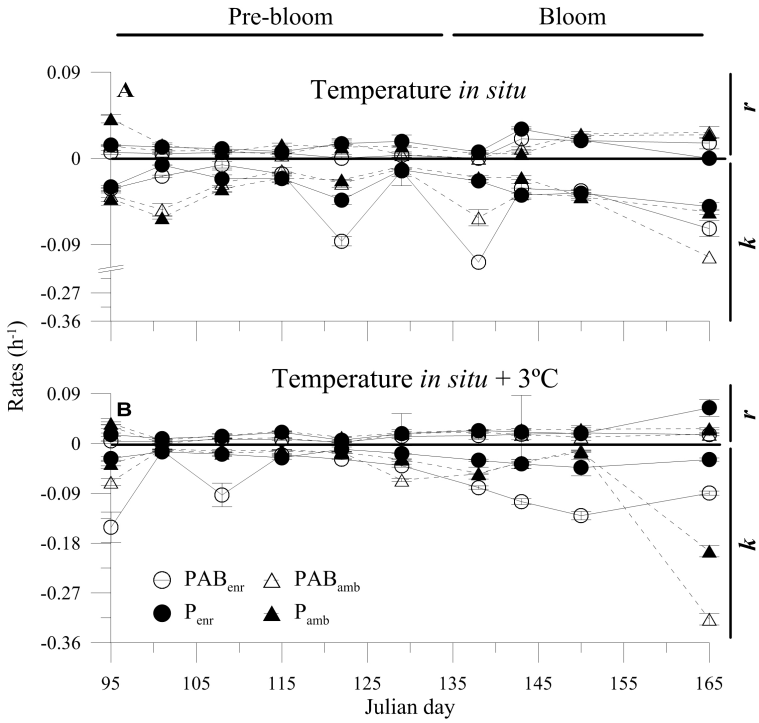

Figure 5: Photosystem II inhibition (k) and recovery (r) rates (in h^{-1}) as a function of time for samples under UVR + PAR (PAB) and PAR (P), two nutrient treatments: ambient (dashed lines) and enriched (solid lines) and two temperature treatments: (A) *in situ* and (B) *in situ* + 3°C. Each symbol represents the mean of triplicate samples whereas vertical lines indicate the standard deviation.

Modeling of single and interactive effects of multiple global change variables

MLR analyses (Fig. 6, open symbols) showed that from all potential predictors assayed, only the previous light history of phytoplankton communities, the *in situ* T, and the diatom and flagellates biomass significantly explained the variability of the NCP and k. Thus, these variables were the only con-

sidered in the analysis of the modeled single and interactive effects of UVR, Nut and T on NCP and k (Table 2). The previous light history and the *in situ* T had opposite relationships (negative *vs.* positive coefficients, Table 2) hence both abiotic factors had an opposite impact on the magnitude of the effects of the variables tested (with the exception of UVR on NCP) and their interaction on NCP and k. Moreover, the inhibitory effect of UVR × Nut × T under the future scenario on NCP and k was increasing and significantly higher towards the bloom which matched with higher diatoms biomass (93% ± 4%) than that observed during the pre-bloom (81% ± 6%).

Table 2: Results of forward stepwise multiple linear regression (MLR) analysis with the best-fitting models for single (UVR, Nut and T) and interactive effects (UVR × Nut × T) on the normalized net community production (NCP) and Φ_{PSII} inhibition (k) rates. Parameters (in bold) include the daily mean photosynthetically active radiation received by communities the previous week of the experimentation (light history), diatoms and flagellates biomass, and *in situ* temperature (T), as predictor variables, whereas numbers in parentheses represent the percentage of variance explained by each predictor variable. F represents F-test values, * $p < 0.05$, ** $p < 0.01$ and *** $p < 0.001$ and R^2 determination coefficient. Note that one experimental day was excluded in all cases.

Net community production (NCP)						
Effect	Light history	Flagellates	Diatoms	T	F	R^2
UVR	**0.09** (9%)	**2.95** (1%)	**-0.43** (44%)	**1.45** (1%)	38.53***	0.86
Nut	**-1.17** (27%)	**-8.18** (16%)	**-0.02** (1%)	**6.33** (1%)	3.56*	0.45
T	**-0.16** (1%)	**19.35** (19%)	**-0.32** (1%)	**21.89** (81%)	77.93***	0.93
Interactive	**0.01** (2%)	**-0.76** (3%)	**1.01** (13%)	**-3.13** (27%)	3.07*	0.93
Inhibition (k)						
UVR	**1.35** (1%)	**-4.24** (1%)	**0.70** (1%)	**-35.83** (68%)	13.38***	0.71
T	**6.23** (5%)	**22.01** (3%)	**-4.18** (22%)	**4.89** (61%)	53.99***	0.91
Interactive	**-7.64** (13%)	**130.48** (12%)	**-7.42** (18%)	**47.85** (29%)	14.66***	0.72

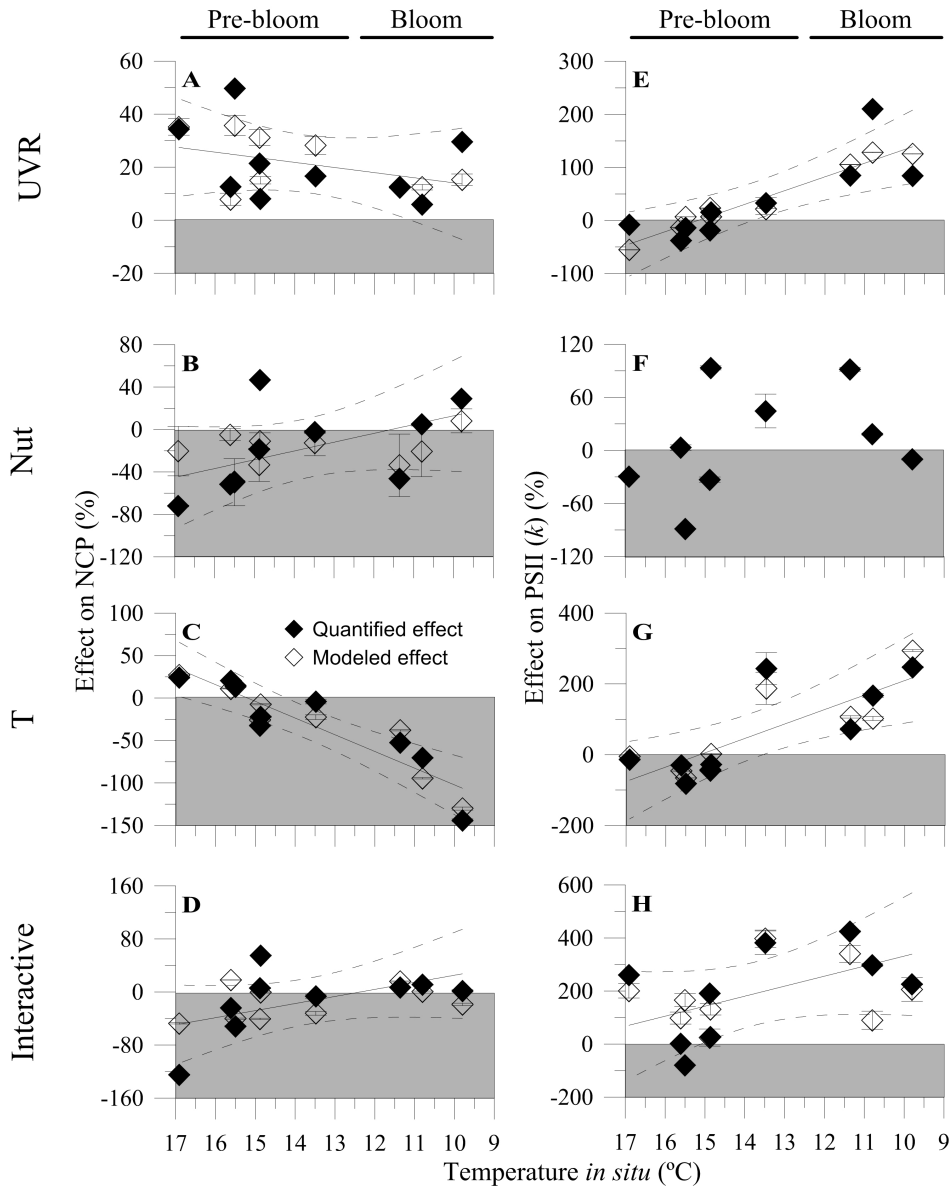

Figure 6: Single and interactive quantified effects (solid symbols) and modeled (open symbols) by multiple linear regression for ultraviolet radiation (UVR) (A, E), nutrients (Nut) enrichment (B, F), increased temperature (T) (C, G), and interactive effects on the normalized net community production (NCP) and inhibition (k) rates (D, H) throughout the experimental period as a function of the *in situ* temperature. The solid line indicates the regression fit for quantified effects and the dashed lines indicate the 95% confidence limits for the quantified values. Vertical lines in quantified and modeled values indicate the standard deviation calculated using error propagation. Positive values (white area) indicate an inhibitory effect and negative values (grey area) an enhancement effect.

Overall, the inhibitory UVR effect on NCP rates decreased significantly (ca. 10%) as the seawater temperature was cooling towards the winter (Fig. 6A). The Nut effect on NCP rates (Fig. 6B) changed from a stimulation during the pre-bloom (negative values) to an inhibition towards the bloom (positive values) when the temperature decreased below 13.5°C. The T effect (Fig. 6C) also decreased significantly as the seawater temperature decreased, resulting in inhibition of NCP rates during pre-bloom (*in situ* temperatures > 15°C) and stimulation towards the bloom (*in situ* temperatures < 13.5°C). The interaction of all variables studied (Fig. 6D) exerted an enhancement of NCP rates during the first half of the study period (negative values) hereafter caused an inhibitory effect under *in situ* water temperatures $< 13.5°C$.

The single effect of the studied variables on k changed from negative values during the pre-bloom (temperature > 15°C) to positive values towards the bloom (temperature < 13.5°C) for UVR (Fig. 6E) and T (Fig. 6G) denoting higher inhibition of PSII when the *in situ* T decreased. No significant relationship was found for Nut effects as a function of the seawater temperature (Fig. 6F). The interactive effect of all factors had an increasing negative effect on k (positive values Fig. 6H) throughout the experimental period, with maximal inhibition at lower temperatures.

Discussion

The effects that global change variables could have on phytoplankton greatly depend on the physiological status of the cells. The changes in the community composition also need to be considered together with the differential responses of species which in turn is tied up to the environmental conditions experienced. In fact, the characteristic phytoplanktonic succession of Patagonian coastal waters with strong winter phytoplankton blooms is explained by the stability of the water column and by the shallow UML due to low wind speeds and frequencies (Helbling et al., 2005). Moreover,

phytoplankton also tends to be low-light and low-temperature adapted during the winter as compared to summer or spring due to the lower incident solar irradiance penetrating the water column and the fact that the cells undergoing temperatures of ca. 7°C during this stage of the year as compared with those that occurs during summer (ca. 18°C) (Helbling et al., 2010); thus, organisms would have higher growth under summer temperatures as compared to those occurring during winter. Therefore one cannot expect that a given variable or a combination of several of them would have the same effect throughout the year. Thus, it is not surprising that our study demonstrated that a future scenario of increased UVR, Nut and T exerts a dual impact on coastal phytoplankton as the seasonal succession progressed.

Specifically, we have found that both CR and recovery of Φ_{PSII} (r) were not significantly affected by global change variables (individually or interacting) at any time of the seasonal succession. These findings contrast with previous studies that showed that CR increased under high UVR levels (Agustí et al., 2014; Carrillo et al., 2015), nutrient inputs (Smith & Kemp, 2003) and/or warming (Yvon-Durocher et al., 2010). It is possible that the lack of a clear pattern in respiration or Φ_{PSII} (r) throughout our study could be due to a low chronic damage during the short-term exposures as reported by Heraud & Beardall (2002) and that any potential damage was quickly repaired (i.e., dynamic inhibition) as shown for diatoms under a global change condition (Cabrerizo et al., 2014). On the other hand, the same global change variables tested here had a differential impact on NCP and Φ_{PSII} (k) at the same stage of the seasonal succession, and conversely, the impact was different when considering the same process at different times of the study period (i.e., pre-bloom *vs.* bloom). Contrary to our initial hypothesis, we found a positive impact, with an increase in NCP (Fig. 6D) during the pre-bloom, and a negative impact, with a significant inhibition of NCP and Φ_{PSII} during the bloom (Fig. 6H). When considering the timing of these effects, it is seen that the increasing inhibition in both physiological processes under the future conditions imposed in our study came together with a decrease in solar radiation levels, lower *in situ* T

and higher dominance of large diatoms. In the following paragraphs we will discuss how the individual effects of climate change related variables changed along the season but most important, how the interactive effects of them deviated or not from the single effects.

Our results show that the UVR impact on Φ_{PSII} of the pre-bloom phytoplankton community (Fig. 6E) was significantly lower than that during the bloom, and this is in agreement with previous studies assessing the effects of these wavebands on different cellular targets for photosynthesis (Helbling et al., 2011; Villafañe et al., 2013). This could be a consequence of the light acclimation towards darker conditions during the transition from fall to winter (Fig. 2) or the fact that during winter the communities are dominated mostly by diatoms instead of flagellates, which possess siliceous cell walls with optical qualities similar to quartz, and therefore, are highly transparent to UVR. Thus, a low-light acclimation together with cells highly transparent to radiation may translate as increased sensitivity to harmful effects of enhanced UVR levels, as proposed in a previous study by Llabrés & Agustí (2010). This increased sensitivity to UVR could explain the higher PSII-k found during the bloom than pre-bloom period. In addition, the constant radiation intensities used in our experimental set-up throughout the study period could have exacerbated the observed impact of UVR on our communities, as the UV-A and UV-B levels were higher than mean daily irradiances (Fig. 2C, D) and thus, mean daily doses received by organisms towards bloom during our exposures were between 3- (for UV-A) and 4-fold (UV-B) higher than those received in the environment (Fig. 2A, B). However, this behavior was not clearly seen in the NCP (Fig. 6A) as the inhibitory effect of UVR slightly decreased towards the bloom. Part of the differences in the UVR impact on Φ_{PSII} at different times during the seasonal succession was previously attributed to the reduced repair rates of Φ_{PSII} during the winter bloom (Villafañe et al., 2004; 2013). The increasing inhibitory effect on Φ_{PSII} towards the bloom might also partially be related to the lower *in situ* T occurring at this time of the year, due to the fact that with lower temperatures the excitation pressure on PSII tends to increase (Derks et al., 2015; Maxwell et al., 1995). One

interesting point is that the increased temperature simulated in our future condition did not counteract the higher excitation pressure during the low *in situ* T period, and in fact, the inhibition of Φ_{PSII} increased towards the bloom (Fig. 6G). On the other hand, increased temperatures of the future scenario resulted in enhancement of NCP as the *in situ* T decreased (Fig. 6C), supporting the view that an increase in T was more effective at lower *in situ* T to enhance the cell metabolism, as also seen in studies carried out in marine ecosystems worldwide (García-Corral et al., 2014; Holding et al., 2013). There was not a clear effect of Nut enrichment on Φ_{PSII} during the study period (Fig. 6F), contrasting with previous studies that showed an enhancement of Φ_{PSII} performance under such conditions (Harrison & Smith, 2013; Marcoval et al., 2007). The different responses observed between those studies and ours could be related to the fact that species need time to acclimate to the new experimental conditions whereas our short-term experimental study did not allow for such acclimation. Despite that we found no nutrient effect over the season, a recent study by Villafañe et al. (2016) in tropical coastal waters has shown that the short-term impact of nutrient addition is highly dependent on the type of community tested. For example, these authors found that diatom-dominated communities exhibited a significant increase in the Φ_{PSII} (ca. 10%) within a few hours of nutrient addition, but when these communities were dominated by flagellates such increases in the Φ_{PSII} performance were not detected nor at mid-term scales. Still, there was a slight inhibitory effect of Nut in NCP towards the winter (Fig. 6B). In the study area, nutrient concentrations are generally high and do not seem to be a limiting factor, but this depends on the continuous riverine input (Helbling et al., 2010). However, the phytoplanktonic bloom is dominated by large diatoms (Fig. 3) that generally has low ability to uptake nutrients as compared to flagellates (Mercado et al., 2014). Besides, nutrient uptakes are T-dependent and the half-saturation constant increase with T (Litchman et al., 2015) hence it could have been reduced or, in the worst case, even inhibited under the low *in situ* T experienced by communities during the bloom. Thus it is probable that in this condition of cold *in situ* T, the increased temperature was not enough to counteract this inhibitory effect.

Conclusion

Overall, in the present study we call on attention to the fact that the effects of global change variables on communities should be centered not only on their interactions on diverse biological targets (e.g., oxygen-evolving complex and Φ_{PSII}) but also on the timing and length of the experimentation. This is important, as the seasonal variations concurs with global change variables conditioning the physiological status of phytoplankton and hence their responses. Although our results should be interpreted cautiously as we did not assess the potential acclimation of communities to global change variables (Villafañe et al., 2016; Yvon-Durocher et al., 2010) an increased inhibition of Φ_{PSII} performance and NCP, due to the interaction of multiple variables, during the most productive stage of the phytoplankton succession could severely alter the current key role that coastal ecosystems are playing in the global carbon cycle as CO_2 sinks.

References

Agustí, S., Duarte, C., Llabrés, M., Agawin, N.S.R., Kennedy, H., 2009. Response of coastal Antarctic phytoplankton to solar radiation and ammonium manipulation: An *in situ* mesocosm experiment. *J. Geophys. Res.: Biogeosciences* **114**, 1-16.

Agustí, S., Regaudie-de-Gioux, A., Arrieta, J.M., Duarte, C.M., 2014. Consequences of UV-enhanced community respiration for plankton metabolic balance. *Limnol. Oceanogr.* **59**, 223-232.

Barbieri, E.S., Villafañe, V.E., Helbling, E.W., 2002. Experimental assessment of UV effects upon temperate marine phytoplankton when exposed to variable radiation regimes. *Limnol. Oceanogr.* **47**, 1648-1655.

Björn, L.O., Murphy, T.M., 1985. Computer calculation of solar ultraviolet radiation at ground level. *Physiol. Veg.* **23**, 555-561.

Boyd, P.W., Dillingham, P.W., McGraw, C.M., Armstrong, E.A., Cornwall, C.E., Feng, Y.-y., Hurd, C.L., Gault-Ringold, M., Roleda, M.Y., Timmins-Schiffman, E., Nunn, B.L., 2016. Physiological responses of a Southern Ocean diatom to complex future ocean conditions. *Nat. Clim. Change* **6**, 207-213.

Boyd, P.W., Lennartz, S.T., Glover, D.M., Doney, S.C., 2015. Biological ramifications of climate-change-mediated oceanic multi-stressors. *Nat. Clim. Change* **5**, 71-79.

Buma, A.G.J., Visser, R.J., Van de Poll, W., Villafañe, V.E., Janknegt, P.J., Helbling, E.W., 2009. Wavelength-dependent xanthophyll cycle activity in marine microalgae exposed to natural ultraviolet radiation. *Eur. J. Phycol.* **44**, 515-524.

Cabrerizo, M.J., Carrillo, P., Villafañe, V.E., Helbling, E.W., 2014. Current and predicted global change impacts of UVR, temperature and nutrient inputs on photosynthesis and respiration of key marine phytoplankton species. *J. Exp. Mar. Biol. Ecol.* **461**, 371-380.

Carrillo, P., Medina-Sánchez, J.M., Herrera, G., Durán, C., Segovia, M., Cortés, D., Salles, S., Korbee, N., Figueroa, F.L., Mercado, J.M., 2015. Interactive effect of UVR and phosphorus on the coastal phytoplankton community of the Western Mediterranean Sea: Unravelling eco-physiological mechanisms. *PloS One* **10**, e0142987.

Cloern, J.E., Abreu, P.C., Carstensen, J., Chauvaud, L., Elmgren, R., Grall, J., Greening, H., Johansson, J.O., Kahru, M., Sherwood, E.T., Xu, J., Yin, K., 2016. Human activities and climate variability drive fast-paced change across the world's estuarine-coastal ecosystems. *Glob. Change Biol.* **22**, 513-529.

Cloern, J.E., Foster, S.Q., Fleckner, A.E., 2014. Phytoplankton primary production in the world's estuarine-coastal ecosystems. *Biogeosciences* **11**, 2477-2501.

De Carli, P., Braccalenti, J.C., García-de-León, F.J., Acuña-Gómez, E.P., 2012. La pesquería del langostino argentino *Pleoticus muelleri* (Crustacea: Penaeidae) en Patagonia, ¿Un único stock?. *An. Inst. Patagon.* **40**, 103-112.

Derks, A., Schaven, K., Bruce, D., 2015. Diverse mechanisms for photoprotection in photosynthesis. Dynamic regulation of photosystem II excitation in response to rapid environmental change. *Biochim. Biophys. Acta: Bioenergectics* **1847**, 468-485.

Doyle, S.A., Saros, J.E., Williamson, C.E., 2005. Interactive effects of temperature and nutrient limitation on the response of alpine phytoplankton growth to ultraviolet radiation. *Limnol. Oceanogr.* **50**, 1362-1367.

Durán, C., Medina-Sánchez, J.M., Herrera, G., Carrillo, P., 2016. Changes in the phytoplankton-bacteria coupling triggered by joint action of UVR, nutrients, and warming in Mediterranean high-mountain lakes. *Limnol. Oceanogr.* **61**, 413-429.

Gao, K., Li, G., Helbling, E.W., Villafañe, V.E., 2007. Variability of UVR effects on photosynthesis of summer phytoplankton assemblages from a tropical coastal area of the South China Sea. *Photochem. Photobiol.* **83**, 802-809.

García-Corral, L.S., Regaudie-de-Gioux, A., Sal, S., Holding, J., Agustí, S., Navarro, N., Mozetic, P., Duarte, C.M., 2014. Temperature dependence of planktonic metabolism in the subtropical North Atlantic Ocean. *Biogeosciences* **11**, 4529-4540.

Genty, B.E., Briantais, J.M., Baker, N.R., 1989. The relationship between the quantum yield of photosynthetic electron transport and quenching of Chlorophyll fluorescence. *Biochim. Biophys. Acta* **990**, 87-92.

Góngora, M.E., González-Zevallos, D., Pettovello, A., Mendía, L., 2012. Caracterización de las principales pesquerías del golfo de San Jorge Patagonia, Argentina. *Lat. Am. J. Aquat. Res.* **40**, 1-11.

Häder, D.-P., Williamson, C.E., Wängberg, S.-A., Rautio, M., Rose, K.C., Gao, K., Helbling, E.W., Sinha, R.P., Worrest, R., 2015. Effects of UV radiation on aquatic ecosystems and interactions with other environmental factors. *Photochem. Photobiol. Sci.* **14**, 108-126.

Harrison, J.W., Smith, R.E.H., 2013. Effects of nutrients and irradiance on PSII variable fluorescence of lake phytoplankton assemblages. *Aquat. Sci.* **75**, 399–411.

Helbling, E.W., Barbieri, E.S., Marcoval, M.A., Gonçalves, R.J., Villafañe, V.E., 2005. Impact of solar ultraviolet radiation on marine phytoplankton of Patagonia, Argentina. *Photochem. Photobiol.* **81**, 807-818.

Helbling, E.W., Buma, A.G.J., Boelen, P., van der Strate, H.J., Fiorda Giordanino, M.V., Villafañe, V.E., 2011. Increase in Rubisco activity and gene expression due to elevated temperature partially counteracts ultraviolet radiation–induced photoinhibition in the marine diatom *Thalassiosira weissflogii*. *Limnol. Oceanogr.* **56**, 1330-1342.

Helbling, E.W., Pérez, D.E., Medina, C.D., Lagunas, M.G., Villafañe, V.E., 2010. Phytoplankton distribution and photosynthesis dynamics in the Chubut River estuary (Patagonia, Argentina) throughout tidal cycles. *Limnol. Oceanogr.* **55**, 55-65.

Heraud, P., Beardall, J., 2002. Ultraviolet radiation has no effect on respiratory oxygen consumption or enhanced post-illumination respiration in three species of microalgae. *J. Photochem. Photobiol. B: Biol.* **68**, 109-116.

Hillebrand, H., Dürselen, C.D., Kirschtel, D., Pollingher, U., Zohary, T., 1999. Biovolume calculation for pelagic and benthic microalgae. *J. Phycol.* **35**, 403-424.

Holding, J.M., Duarte, C.M., Arrieta, J.M., Vaquer-Suyner, R., Coello-Camba, A., Wassmann, P., Agusti, S., 2013. Experimentally determined temperature thresholds for Arctic plankton community metabolism. *Biogeosciences* **10**, 357-370.

Holm-Hansen, O., Riemann, B., 1978. Chlorophyll *a* determination: Improvements in methodology. *Oikos* **30**, 438-447.

IPCC, 2013. Climate Change. The Physical Science Basis. Cambridge University Press, New York, USA.

Litchman, E., Edwards, K.F., Klausmeier, C.A., 2015. Microbial resource utilization traits and trade-offs: Implications for community structure, functioning, and biogeochemical impacts at present and in the future. *Front. Microbiol.* **6**, 254.

Llabrés, M., Agustí, S., 2010. Effects of ultraviolet radiation on growth, cell death and the standing stock of Antarctic phytoplankton. *Aquat. Microb. Ecol.* **59**, 151-160.

Marcoval, M.A., Villafañe, V.E., Helbling, E.W., 2007. Interactive effects of ultraviolet radiation and nutrient addition on growth and photosynthesis performance of four species of marine phytoplankton. *J. Photochem. Photobiol. B: Biol.* **89**, 78-87.

Maxwell, D.P., Falk, S., Huner, N.P.A., 1995. Photosystem II excitation pressure and development of resistance to photoinhibition. *Plant Physiol.* **107**, 687-694.

Maxwell, K., Johnson, G.N., 2000. Chlorophyll fluorescence - a practical guide. *J. Exp. Bot.* **51**, 659-668.

Mercado, J.M., Sala, I., Salles, S., Cortés, D., Ramírez, T., Liger, E., Yebra, L., Bautista, B., 2014. Effects of community composition and size structure on light absorption and nutrient uptake of phytoplankton in contrasting areas of the Alboran Sea. *Mar. Ecol. Progr. Ser.* **499**, 47-64.

Morán, X.A.G., López-Urrutia, A., Calvo-Díaz, A., Li, W.K.W., 2010. Increasing importance of small phytoplankton in a warmer ocean. *Glob. Change Biol.* **16**, 1137-1144.

Porra, R.J., 2002. The chequered history of the development and use of simultaneous equations for the accurate determination of chlorophylls *a* and *b*. *Photosynth. Res.* **73**, 149-156.

Rabalais, N.n., Turner, R.E., Díaz, R.J., Justic, D., 2009. Global change and eutrophication of coastal waters. *ICES J. Mar. Sci.* **66**, 1528-1537.

Rousseaux, C.S., Gregg, W.W., 2014. Interannual variation in phytoplankton primary production at a global scale. *Remote Sens.* **6**, 1-19.

Smith, E.M., Kemp, W.M., 2003. Planktonic and bacterial respiration along an estuarine gradient: Responses to carbon and nutrient enrichment. *Aquat. Microb. Ecol.* **30**, 251-261.

Sobrino, C., Neale, P.J., 2007. Short-term and long-term effects of temperature on photosynthesis in the diatom *Thalassiosira pseudonana* under UVR exposures. *J. Phycol.* **43**, 426-436.

Strathmann, R.R., 1967. Estimating the organic carbon content of phytoplankton from cell volume or plasma volume. *Limnol. Oceanogr.* **12**, 411-418.

Toseland, A., Daines, S.J., Clark, J.R., Kirkham, A., Strauss, J., Uhlig, C., Lenton, T.M., Valentin, K., Pearson, G.A., Moulton, V., Mock, T., 2013. The impact of temperature on marine phytoplankton resource allocation and metabolism. *Nat. Clim. Change* **3**, 979-984.

Uitz, J., Claustre, H., Gentili, B., Stramski, D., 2010. Phytoplankton class- specific primary production in the world's oceans: Seasonal and interannual variability from satellite observations. *Glob. Biogeochem. Cy.* **24**, GB3016-3035.

Villafañe, V.E., Banaszak, A.T., Guendulain-García, S.D., Strauch, S.M., Halac, S.R., Helbling, E.W., 2013. Influence of seasonal variables associated with climate change on photochemical diurnal cycles of marine phytoplankton from Patagonia (Argentina). *Limnol. Oceanogr.* **58**, 203-214.

Villafañe, V.E., Barbieri, E.S., Helbling, E.W., 2004. Annual patterns of ultraviolet radiation effects on temperate marine phytoplankton off Patagonia, Argentina. *J. Plankton Res.* **26**, 167-174.

Villafañe, V.E., Cabrerizo, M.J., Erzinger, G.S., Bermejo, P., Strauch, S.M., S., V.M., Helbling, E.W., 2016. Photosynthesis and growth of temperate and sub-tropical estuarine phytoplankton in a scenario of nutrient enrichment under solar ultraviolet radiation exposure. *Estuar. Coast.*, **in press**.

Villafañe, V.E., Erzinger, G.S., Strauch, S.M., Helbling, E.W., 2014. Photochemical activity of PSII of tropical phytoplankton communities of Southern Brazil exposed to solar radiation and nutrient addition. *J. Exp. Mar. Biol. Ecol.* **459**, 199-207.

Villafañe, V.E., Guendulain-García, S.D., Valadez, F., Rosiles-González, G., Helbling, E.W., Banaszak, A.T., 2015. Antagonistic and synergistic responses to solar ultraviolet radiation and increased temperature of phytoplankton from cenotes (sink holes) of the Yucatán Peninsula, Mexico. *Freshwater Sci.* **34**, 1282-1292.

Villafañe, V.E., Reid, F.M.H., 1995. Métodos de microscopía para la cuantificación del fitoplancton, in: Alveal, K., Ferrario, M.E., Oliveira, E.C., Sar, E. (Eds.), Manual de Métodos Ficológicos. Universidad de Concepción, Concepción, Chile, pp. 169-185.

Williamson, C.E., Zepp, R.G., Lucas, R.M., Madronich, S., Austin, A.T., Ballaré, C.L., Norval, M., Sulzberger, B., Bais, A.F., McKenzie, R.L., Robinson, S.A., Häder, D.P., Paul, N.D., Bornman, J.F., 2014. Solar ultraviolet radiation in a changing climate. *Nat. Clim. Change* **4**, 434-441.

Wong, C.-Y., Teoh, M.-L., Phang, S.-M., Lim, P.-E., Beardall, J., 2015. Interactive effects of temperature and UV radiation on photosynthesis of *Chlorella* strains from polar, temperate and tropical environments: Differential impacts on damage and repair. *PloS One* **10**, e0139469.

Yvon-Durocher, G., Jones, J.I., Trimmer, M., Woodward, G., Montoya, J.M., 2010. Warming alters the metabolic balance of ecosystems. *Philos. T. Roy. Soc. B* **365**, 2117-2126.

Zar, J.H., 1999. Biostatistical analysis, 4th ed. Prentice Hall, Englewood Cliffs, NJ.

Chapter V

Rising nutrient-pulse frequency and high UVR strengthen microbial interactions

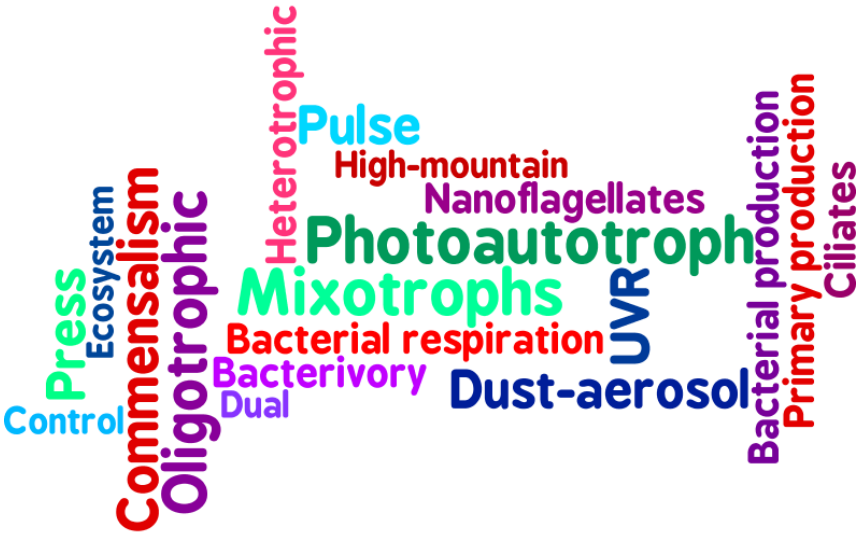

Abstract

Solar radiation and nutrient pulses regulate the ecosystem's functioning. However, little is known about how a greater frequency of pulsed nutrients under high ultraviolet radiation (UVR) levels, as expected in the near future, could alter the responses and interaction between primary producers and decomposers. In this report, we demonstrate through a mesocosm study in lake La Caldera (Spain) that a repeated (*press*) compared to a one-time (*pulse*) schedule under UVR prompted higher increases in primary (PP) than in bacterial production (BP) coupled with a replacement of photoautotrophs by mixotrophic nanoflagellates (MNFs). The mechanism underlying these amplified phytoplanktonic responses was a dual control by MNFs on bacteria through the excretion of organic carbon and an increased top-down control by bacterivory. We also show across a 6-year whole-lake study that the changes from photoautotrophs to MNFs were related mainly to the frequency of pulsed nutrients (e.g., desert dust inputs). Our results underscore how an improved understanding of the interaction between chronic and stochastic environmental factors is critical for predicting ongoing changes in ecosystem functioning and its responses to climatically driven changes.

Introduction

Nutrients and light are two key factors that regulate the ecosystem's functioning. Nutrient pulses are stochastic events of brief resource availability that have strong effects on a huge variety of ecological processes (e.g., growth, primary production [PP], consumer-resource interaction) in a range of ecosystems worldwide (Yang, 2004; 2010). Although Yang et al. (2008) have clearly defined pulsed resources, a major unresolved question is how the increasing frequency of such events due to global climate change (IPCC, 2013) could alter ecosystem dynamics in the future. Specifically, the heavy

transport of atmospheric dust due to severe droughts related to climate change and positive anomalies in the North Atlantic Oscillation Index (+NAO) implies greater mineral inputs to aquatic ecosystems worldwide (Jickells & Moore, 2015). These higher mineral inputs to ecosystems may be particularly relevant in the Mediterranean region due to its proximity with the Sahara Desert, which constitutes the largest global dust-export source of mineral nutrients, especially inorganic phosphorus (P) (Gallisai et al., 2014; Mahowald et al., 2008). These potential increases in the P inputs may be particularly critical in severely nutrient-limited aquatic environments such as open-sea areas (Cabrerizo et al., 2016; Moore et al., 2013) or oligotrophic high-mountain lakes (Carrillo et al., 2008a; Williamson et al., 2009), because of the relatively greater exposure to atmospheric deposition and / or the minimal influence of catchment vegetation (Mladenov et al., 2011). Brief events of pulsed nutrients in these ecosystems can account for a large proportion of all available resources, which can have persistent repercussions for primary producers, consumers and decomposers (Lennon & Cottingham, 2008; Yang, 2008). These persistent effects result from the altered cell size and structure of the microbial community (Lekunberri et al., 2010; Martínez-García et al., 2015) as well as from altered key processes such as PP and trophic interaction within the microbial loop (Carrillo et al., 2008b; Ridame et al., 2014).

Ever since the pioneering study by Azam et al. (1983), information has been progressively amassed concerning the complex interactions between the nutritional–physicochemical environment and the components of the microbial food web in oligotrophic ecosystems. Surges in nutrient availability are known to reduce competition between phytoplankton and bacteria and stimulate their growth (Danger et al., 2008). This stimulatory effect on both compartments and the reported increase in the excretion of organic carbon (EOC) by phytoplankton (Durán et al., 2016; Medina-Sánchez et al., 2013), can be propagated from the microbial loop (Carrillo et al., 2008b; Duarte et al., 2005) to the grazing chain (Cottingham et al., 1997). Therefore, the microbial loop development depends on the coupling between phytoplankton and bacteria. This coupling is defined as the

capacity of the carbon (C) released by the phytoplankton to support the bacterial C requirement (Morán et al., 2002) and the degree of coupling differs depending on the inorganic nutrient availability (López-Sandoval et al., 2011; Medina-Sánchez et al., 2013), ultraviolet radiation (UVR) exposure (Carrillo et al., 2015a), temperature (Durán et al., 2016) or stoichiometric balances (Daufresne et al., 2008; Medina-Sánchez et al., 2006). However, this traditional paradigm of food-web structure are being challenged by a current of thought that suggests an alternative new paradigm in which the bulk of the base of this food web is supported by protist planktonic communities that are mixotrophic, combining phagotrophy and phototrophy within the same organism, instead of photoautotrophic phytoplankton (Mitra et al., 2014). In fact, an increasing number of studies show the prevalence of mixotrophs in natural communities, particularly in surface waters of oligotrophic ecosystems (i.e., freshwater and marine), where they tend to predominate due to having an advantage on photoautotrophic phytoplankton by obtaining limiting nutrients (e.g., P) through phagotrophy (Hartmann et al., 2012; Medina-Sánchez et al., 2004; Unrein et al., 2014; Zubkov & Tarran, 2008). In addition to their flexible nutrition, mixotrophs seem also to be favoured by high light conditions (Medina-Sánchez et al., 2006; Ptacnik et al., 2016), and hence it would be expected that, under stabler and shallower upper mixed layers (UMLs) due to global change situation, they would be strongly benefited with respect to photoautotrophic groups by greater exposure to radiation.

Solar radiation including the UVR region of the spectrum, is another key factor that controls ecosystem functioning and their communities by acting upon several biotic targets (e.g., DNA, photosystems or membranes) and metabolic processes in planktonic organisms (e.g., photosynthesis, respiration, growth) (Beardall & Raven, 2004; Häder et al., 2015). Thus, the biological effects of UVR may be particularly striking in clear environments (e.g., open ocean areas and high-mountain lakes) (Moore et al., 2013; Sommaruga, 2001) because the high transparency of the water column allows the ambient UVR and photosynthetically active radiation (PAR) intensities to be sufficient to cause near-surface photoinhibition (Harrison & Smith,

2009).

Despite the ecological relevance of each of these environmental factors, the community responses to a single factor are frequently altered by synergistic or antagonistic interactions among them (Häder & Gao, 2015). For example, some authors have reported that nutrient pulses can unmask the harmful UVR effects on phytoplankton and/or bacterial production (BP) (Carrillo et al., 2015b; Korbee et al., 2012; Pausz & Herndl, 2002), altering the trophic interactions within the microbial loop (Durán et al., 2016). Contrarily, other studies contend that nutrient pulses can attenuate the damage that UVR inflicts on PP and BP (Bergmann et al., 2002; Helbling et al., 2013; Medina-Sánchez et al., 2006). However, no available study to date has experimentally quantified how the interaction between an increased nutrient-pulse frequency and high UVR levels will affect the commensalistic phytoplankton–bacteria interactions, community dynamics (e.g., dominance and/or succession in the microbial community) and the ecosystem productivity in the future global-change scenario. To address these questions, we conducted a field mesocom experiment in lake La Caldera (Spain; Fig. S1) where we manipulated (1) the schedule of nutrient inputs (*press* [5 μg P L^{-1} $\times$ 6 times] vs. *pulse* [30 μg P L^{-1} once]), while maintaining the total amount of nutrients (i.e., P) at the end of the experiment, and (2) the spectrum of radiation received (with and without UVR). The rationale behind this approach was to mimic future increases in the frequency of atmospheric dust depositions rich in P from the Sahara Desert and high solar radiation levels (UVR and / or PAR) undergone by planktonic communities as if they were trapped in the top layer of the water column due to a potential stratification induced by global warming. We examine the structural, stoichiometric, and metabolic responses of phytoplankton and heterotrophic bacteria as well as the interaction between these two groups. In addition, we compare these experimental responses together with the microbial community dynamics and the natural variability in the atmospheric dust-deposition inputs entering the ecosystem via a 6-year seasonal and interannual observational study.

Material and Methods

Study site

La Caldera is a high-mountain lake situated above the treeline (3050 m a.s.l.) in the Sierra Nevada National Park (southern Spain, 36° 55′–37° 15′ N, 2° 31′–3° 40′ W) on siliceous bedrock in a glacial cirque. The site has been previously described in terms of its physical, chemical, and biological characteristics, highlighting its high transparency to solar radiation, strong limitation by P and relatively simple pelagic community (Dorado-García et al., 2014).

Measurements of natural inputs of pulsed nutrients: Remote sensing

As a measure of aerosol content in the troposphere, we used the ultraviolet (UV) aersolos index (UV-AI) produced by the Giovanni online data system, developed and maintained by the NASA GES DISC (Acker & Leptoukh, 2007) (Supplementary text S1) as a proxy for natural nutrient inputs into the ecosystem.

Observational approach: Field sampling in the water column from 2010–2015

Sampling was conducted during the ice-free periods (1 June to 15 November) from 2010 to 2015. For each sampling day, a lake sample was constructed from equal volumes of lake-water samples collected with a 6-L horizontal Van Dorn sampler from three depths, spaced evenly within the photic layer at least affected by 1% PAR. From this composite lake sample, subsamples of 125 mL for phytoplankton taxonomic composition and 500

mL for ciliates and heterotrophic nanoflagellates (HNFs) were preserved using alkaline Lugol's reagent.

Experimental approach

An *in situ* experimental setup consisted of 18 UVR-transparent low-density polyethylene mesocosms (0.58 m in diameter, LDPE, Plasticos Andalucia), closed at the bottom and the top, with a total volume of 0.1 m^3. The LDPE used transmits > 70% of UVR and > 85% of PAR. A water pump was used to fill each mesocosm with 45 μm of filtered lake water (excluding zooplankton), which was collected from the first meter in depth. Once filled, the mesocosms were set in six racks 4 m long × 3 m wide (three for UVR and three for PAR, see below) made of 3-cm polyvinyl chloride pipe, and placed under a thin water layer in the lake (1 m deep). Thus, the cells were exposed to the worst-case scenario of solar radiation (i.e., as if they were in the top layer of the water column due to a shallower (UML), as is expected due to global warming (Behrenfeld et al., 2006; Boyce et al., 2010). The six racks were set approximately 25 m apart to avoid shading effects and were secured to a buoy attached to an anchored rope. The radiation treatments were performed by using a cover of polyethylene arranged on the mesocosms that transmitted > 70% of UVR and > 85% of PAR in the case of the UVR treatment, whereas the PAR treatment was performed by using a cover of UV-filter foil (UV-Process Supply Inc., IL, USA) arranged on the mesocosms that transmitted > 90% of PAR but blocked UVR (> 400 nm).

The experiment was conducted from 31 August to 18 September 2011 using a 2 × 3 full-factorial matrix (in triplicate) with: a) two radiation treatments, PAB (> 280 nm) and PAR (P, > 400 nm); and b) three nutrient conditions: (1) ambient (amb); (2) *press* (5 μg P L^{-1} × 6 times); and (3) *pulse* (30 ×g P L^{-1} × 1 time). When we integrated over the experimentation period, both the *press* and *pulse* treatments had the same quantity of nutrients added. To ensure that P (as NaH_2PO_4) remained as the limiting

nutrient in the enclosures, inorganic N (as NH_4NO_3) was added to mesocosms to reach an N:P molar ratio of 30. The rationale for using nutrient additions (N and P) as a proxy of Saharan dust deposition was because: (1) mineral aerosols are the dominant source of atmospheric TP on a global scale (82%) (Mahowald et al., 2008) and (2) previous studies in the Sierra Nevada National Park area established clear connections between TP loads and Saharan dust depositions (Morales-Baquero et al., 2006). Also, the addition of inorganic N to reach an N:P molar ratio of 30 mimics the mean value of the molar TN:TP ratio also found in total atmospheric deposition (Morales-Baquero et al., 2006). At the beginning of the experiment, nutrients were added for both treatments (5 μg P L^{-1} for the *press* treatment and 30 μg P L^{-1} for the *pulse* treatment), and on days 4, 7, 9, 12, and 15 of September in the case of the *press* treatment until a final concentration of 30 μg P L^{-1} was reached. The duration of the experiment was based upon the regional frequency of atmospheric deposition events that are involved with the release of P into lake La Caldera (Morales-Baquero et al., 2006) and with the microbial community dynamics (Supplementary text S2). Samples for the different analysis and measurements outlined below were taken early in the morning (and before the nutrient additions in the case of the *press* treatment) in each experimental day using a water pump connected to a silicone tube inserted into each mesocosm during the incubation period to prevent tampering.

Analyses and measurements

Stoichiometric variables

To determine sestonic carbon (C) and phosphorus (P), we filtered water samples from each mesocosm (500 mL) through pre-combusted (1 h at 550°C) GF/B Whatman filters (25-mm diameter). For sestonic P, filters were placed in acid-washed vessels, persulfate digested at 120°C for 30 min and immediately analysed as SRP following Murphy & Riley (1962). For

sestonic C, filters were desiccated (24 h at 60°C) and analysed using an elemental analyser (Perkin Elmer 2400, USA).

Structural variables

Water samples (250 mL) for Chlorophyll *a* (Chl *a*) determination were filtered through GF/F Whatman filters (25-mm diameter) and frozen at –20°C until analysis. For the Chl *a* analyses, filters were placed in centrifuge tubes (15 mL) with 5 mL of 90% acetone for 24 h at 4°C in darkness. After this, the samples were centrifuged and the supernatant fluorescence was measured with a fluorometer (Perkin Elmer LS 55, USA) (APHA, 1992). The abundance of phytoplankton (photoautotrophs and mixotrophic nanoflagellates [MNFs]), HNFs and ciliates were quantified following the procedure described by Straskrabová et al. (1999). Bacterial abundance was determined by the flow-cytometry technique (FACSCanto II, Becton Dickinson Biosciences, Oxford, UK). Previously, 1.5 mL of sampling water was fixed with 75 μL of particle-free 20% (w/v) paraformaldehyde (1% final concentration) and frozen in liquid nitrogen to be stored at –80°C until analysed (Kamiya et al., 2007; Zubkov et al., 2007) (Supplementary text S3).

Functional variables

PP was measured with the ^{14}C-incorporation method (Steemann-Nielsen, 1952). Briefly, sets of four 50-mL quartz vessels (three clear and one dark) by treatment, with 0.37 MBq of $NaH_{14}CO_3$ (DHI Water and Environment, Germany) added, were placed *in situ* at 1 m under the surface, receiving a radiation treatment identical to that of the mesocosms, and incubated for 4 h symmetrically distributed around noon. Total organic carbon (TOC) was measured in 4-mL subsamples collected before filtration. Particulate PP was determined by serial filtration of the entire content of each quartz

vessel (50 mL) through 1-μm (particulate organic carbon, POC_1) and 0.2-μm (particulate organic carbon, POC_2) pore-size Nucleopore filters of 25 mm in diameter. EOC was calculated as the sum of DOC and POC_2 (Supplementary text S4).

BP was measured using the radio-labelled thymidine-incorporation technique (Fuhrman & Azam, 1982). A set of five (3 + 2 blanks) acid-cleaned and sterilised tubes per treatment containing 1.5 mL of sample were inoculated with ^{3}H-thymidine (SA = 48 – 50 Ci mmol^{-1}, Perkin Elmer) to a final saturating concentration of 12 nM. After this, tubes were incubated at the *in situ* temperature for 1 h in darkness (Supplementary text S4). Samples for BR (< 0.7-μm fraction) were filtered through Whatman GF/F filters (25-mm diameter), placed in sealed 25-mL glass vessels equipped with optode sensor-spots (SP-PSt3-NAU-D5-YOP) and incubated in darkness in a temperature-controlled bath to maintain the same temperature as the lake and to measure the oxygen concentration over time using an oxygen optode (Fibox 3, PreSens GmbH, Germany; Supplementary text S4). BGE was estimated as BP divided by the sum of BP and BR (del Giorgio & Cole, 1998; Vidal et al., 2011). As autochthonous C (measured as EOC) is the C source preferentially used by bacteria (Durán et al., 2016; Kritzberg et al., 2005; Medina-Sánchez et al., 2002), and given the feasibility of segregating microbial fractions through filtration, we estimated the PEGA as

$$\text{PEGA } (\%) = 100\times(POC_2+BR)/(EOC)$$

This represents a direct measurement of the strength of the interaction between phytoplankton and bacteria.

Data and statistical analysis

The effect of nutrients (ambient, *press* and *pulse*) on initial C biomass was tested by one-way analysis of variance (ANOVA). The interactive effect of

UVR and P on phytoplankton and bacteria biomass and Chl *a* over time was tested by two-way repeated measures ANOVA (RM-ANOVA). The interactive effects of UVR and P evaluated as the intensity (moderate vs. intense) and frequency (*press* vs. *pulse*) of the pulse on stoichiometric (sestonic P and sestonic C:P ratio) and functional variables (BP, PP, EOC, BR, BGE, and %PEGA) were tested by a two-way ANOVA. Shorter- and longer-term responses were analysed separately because of the different nutrient concentrations present in the mesocosms each day. Sphericity (by Mauchly's test), homoscedasticity (by Cochran's and Levene's tests) and normality (by Shapiro-Wilk's test) were checked for each variable to verify the ANOVA and RM-ANOVA assumptions, respectively. When interactive effects were significant, Bonferroni's *post hoc* test was used to denote statistical differences among and within treatments. Structural equation modeling (SEM) analysis was used to test whether the pool of the main resources (i.e., TDP and dissolved organic carbon [DOC]) influenced the relationship between MNFs and bacteria biomass at the end of the experimental period under the two 'natural' scenarios considered (i.e., *press* × UVR and *pulse* × UVR, supplementary text S5).

Results

Long-term biological and climatic data

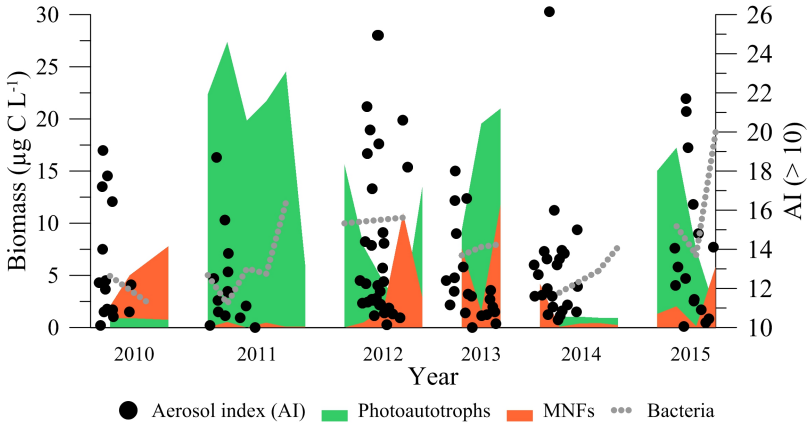

Figure 1: Dynamics of the biomass contribution (in μg C L^{-1}) of main phytoplankton groups (mixotrophic nanoflagellates [MNFs, orange area] and photoautotrophs [green area]) and bacterial community [grey dotted line]) and aerosol index (AI in relative units, solid circles) with events > 10 for the 2010-2015 ice-free period (from 1 June to 15 November) in lake La Caldera. Note that AI $\geq$ 10 is a measure of intense atmospheric dust deposition inputs and that frequency is denoted with the degree of clustering of solid circles.

The temporal dynamics from 2010 – 2015 showed that phytoplankton predominated over bacteria in terms of biomass (except for 2015) and reflected two clear response patterns related to the intensity and frequency of aerosol inputs (i.e., Aerosol Index [AI]). Thus, when aerosol inputs were intense (AI > 10), as in the case of years 2011, 2013, and 2015, the biomass of photoautotrophs (mainly *Monoraphidium* sp.) considerably increased, whereas the biomass of MNFs (dominated by *Chromulina nevadensis*) remained low and unaltered (< 5 μg C L^{-1}). By contrast, when aerosol inputs increased in frequency during 2010 and 2012 (i.e., the clusters of black dots in Fig.

1) the opposite pattern resulted, as reflected by the dominance of MNFs over photoautotrophs in La Caldera lake (Fig. 1). Ciliates and HNFs were not detected on any sampling date during the 6-year period studied.

Experimental approach

The lake's physico-chemical conditions

The water temperature in the water column showed no thermal stratification (Fig. S2; Supplementary text S6). According to the attenuation coefficients of solar radiation ($kd_{305} = 0.61$; $kd_{320} = 0.52$; $kd_{380} = 0.34$), the first two meters received ca. 90% of incident UVR. Similarly, PAR also penetrated deep into the lake ($kd_{PAR} = 0.25$) with $\geq 10\%$ of incident radiation reaching the bottom of the lake. Mesocosms in the experiments, incubated at 1-m depth, received mean irradiances 2- to 3-fold higher than those received by organisms in the water column (e.g., 11.04 vs. 4.06 [320 nm] μW cm^{-2} nm^{-1} and 908.60 vs. 468.86 [PAR] μmol photons m^{-2} s^{-1}). Dissolved nutrients (total dissolved phosphorus [TDP] and total dissolved nitrogen [TDN], supplementary Table S1) slowly decreased over time to non-detectable levels in the lake whereas DOC remained relatively unchanged (Table S2).

Nutrient and Chl *a* dynamics in mesocosms

In ambient nutrient treatments, we found a slight but significant rise in TDP (ca. 0.16 μM P) at mid-term, followed by a significant fall at the end of the experimental period (Tables S1, S3). In nutrient-enriched treatments, two well-differentiated patterns were discerned, depending on how nutrients were amended: (1) in *press* treatments, TDP increased up to 0.30 ($\pm$ 0.04) μM P under UVR at the end of the experimental period; and (2) in *pulse* treatments, TDP decreased after the nutrient pulse was added from ca. 0.40

(±0.05) μM P to concentrations similar to those registered before nutrient additions (31 August; Table S1). TDN remained relatively unchanged over the experimental period under ambient and *press* treatments (except for PAR_{press}), whereas it was significantly higher under *pulse* treatments (Tables S1, S3). Therefore, these results suggest that N was in excess and was not a limiting factor. DOC concentrations were low over the experimental period, particularly under ambient nutrient treatments (Tables S2, S3); however, a continuous increase occurred under PAR_{pulse} treatment during the experiment. An interactive UVR × P × Time effect on TDP, TDN, and DOC was found (Table S3). Similarly, there was a UVR × P × Time interactive effect on Chl *a* (Tables S4, S5). By contrast, as a single factor, UVR did not exert a significant effect under ambient or enriched nutrient treatments (except for the final incubation day), whereas the addition of nutrients prompted a significantly steady increase in Chl *a* compared to ambient treatments.

Nutrient-pulse frequency and UVR effects on the microbial community

Phytoplankton dominated the biomass of the nanoplanktonic food web both in ambient and nutrient-amended treatments over the experiment (Fig. 2A–C; Tables S5, S6). However, as for the lake, ciliates and HNFs were not found in any of the mesocosms. Bacterial biomass remained relatively stable (values < 13 μg C L^{-1}) over the experiment regardless of the nutrient and radiation treatments considered (insert in Figs. 2B, C; Tables S5, S6). Two phytoplankton species dominated the community under all experimental conditions (see below), *Monoraphidium* sp. (a photoautotroph) and *C. nevadensis* (a MNF), which comprised over 95% of the total phytoplankton biomass during the experiment. The rest of the total biomass was represented by Bacillariophyeae (i.e., *Cyclotella* sp.), Dinophyceae (i.e., *Gymnodinium* sp.), and Cryptophyceae (i.e., *Rhodomonas* and *Cryptopmonas* sp.). At the beginning of experiment, no significant differences (F

= 2.25, p = 0.19) were found in the total phytoplankton (photoautotrophs and MNFs) biomass between the ambient (20.40 ± 3.82 μg C L^{-1}) and nutrient-enriched treatments (*press* = 26.79 ± 4.83 and *pulse* = 19.96 ± 4.52 μg C L^{-1}). However, over the experiment, the photoautotrophs and MNFs biomass decreased in ambient treatments whereas they increased in the *press* and *pulse* treatments. Thus, photoautotrophs dominated the microbial community in the ambient nutrient treatments, contributing between ca. 6 to ca. 28 μg C L^{-1}, while MNFs biomass did not exceed 1 μg C L^{-1} (Fig. 2A). In both nutrient treatments (*press* and *pulse*) photoautotrophs were replaced by MNFs, although with different timing, as they dominated on day 13 in the case of *press* treatments and on day 16 for *pulse* treatments. In fact, in the *pulse* treatments, independently of the radiation treatment, photoautotrophs grew exponentially up to day 7 (ca. 200 μg C L^{-1}), after which they progressively declined towards the end of the experiment. By contrast, MNFs followed the opposite pattern, from an initially low biomass (< 20 μg C L^{-1}) to a maximum of ca. 110 μg C L^{-1} at the end of the experiment under UVR. In the case of the *press* treatment under UVR, photoautotrophs showed a unimodal response and reached their maximum biomass by day 10. The subsequent decline in biomass after this date was coupled with a sharp increase in MNFs towards the end of the experiment. A similar unimodal response pattern was observed for MNFs under PAR-treatment, although biomass peaked by day 13 (ca. 400 μg C L^{-1}), whereas the photoautotrophs biomass remained fairly constant throughout the experiment (Fig. 2C; Table S5, S6).

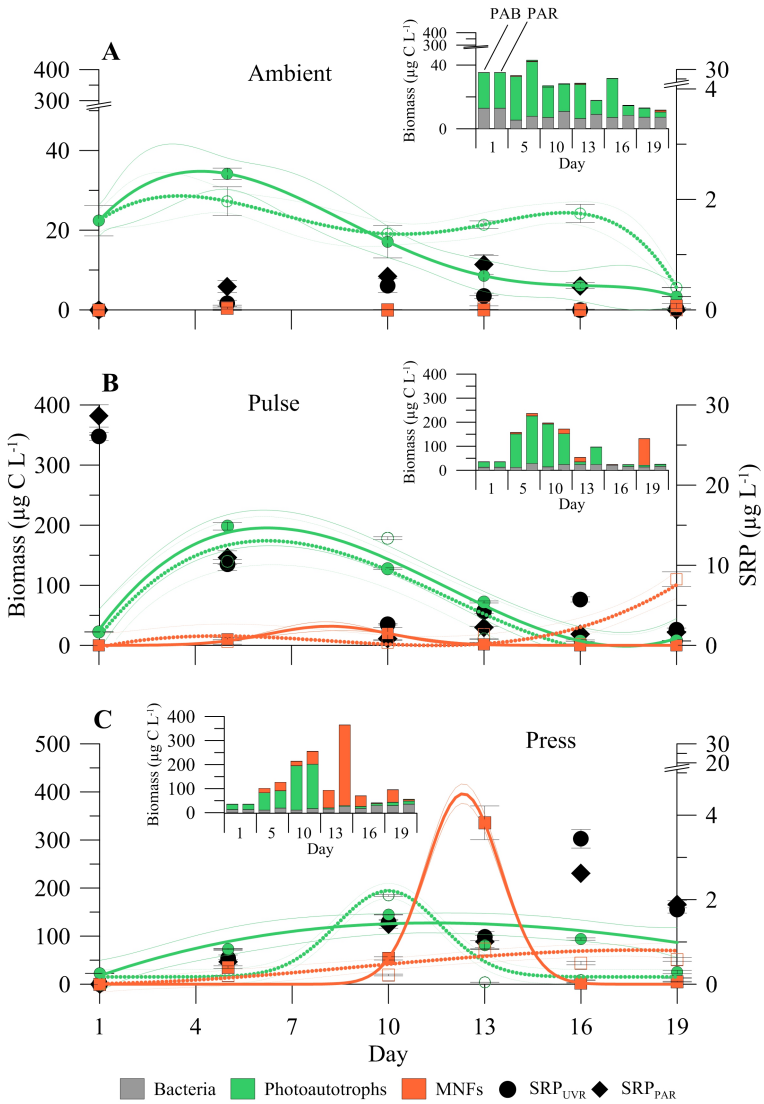

Figure 2: Non-linear regression of the dynamics of the main phytoplankton groups (in μg C L^{-1}), mixotrophic nanoflagellates (MNFs, orange lines) and photoautotrophs (green lines) during the experiment under (A) ambient, (B) *press* and (C) *pulse* treatments. Dashed and solid thick lines (green and orange) represent samples under UVR (> 280 nm) and PAR (> 400 nm), respectively, whereas thin dashed and solid lines (green and orange) indicate 95% interval confidence for each regression fitted by peak-Gaussian: $y = y_0 + a \exp(-0.5((x - b) / w^2))$ or cubic: $y = ax^3 + bx^2 + cx + d$. Solid diamonds and circles in A, B and C panels represent the temporal variation of soluble reactive phosphorus (SRP, in μg L^{-1}) over the experiments under two radiation treatments: PAB (> 280 nm) and PAR (> 400 nm), respectively. Inserted figures in A, B, and C represent total community biomass including bacterial compartment (in μg C L^{-1}; grey) under the two radiation treatments mentioned previously.

Nutrient-pulse frequency and UVR effects on metabolic variables

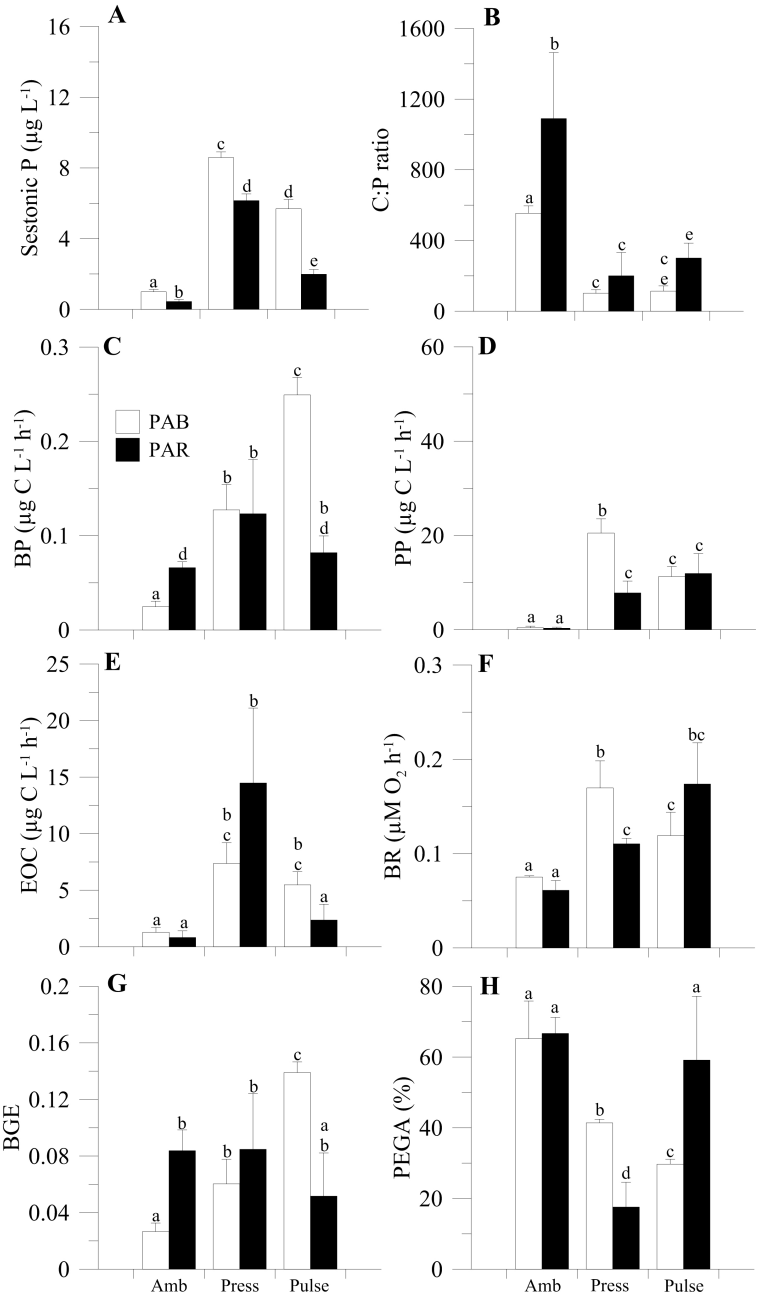

Figure 3: (A) Sestonic phosphorus (P) concentrations (in μg L^{-1}), (B) sestonic carbon : phosphorus ratio (C:P ratio), (C) bacterial production (BP, in μg C L^{-1} h^{-1}), (D) primary production (PP, in μg C L^{-1} h^{-1}), (E) excretion of organic carbon (EOC, in μg C L^{-1} h^{-1}), (F) bacterial respiration (BR, μM O_2 h^{-1}), (G) bacterial growth efficiency (BGE) and (H) percentage of photosynthetic excreted gross assimilation (%PEGA) in lake La Caldera under two radiation treatments: PAB (> 280 nm, white bars) and PAR (P, > 400 nm, black bars) and three nutrient treatments: ambient (amb), *press* and *pulse*. The bars represent mean values of three replicates and lines in top of the bars are the standard deviation. Letters indicate differences among treatments by Bonferroni *post hoc* test. Note that these results represent responses observed over the longer term, when communities received the same amount of nutrients but at different frequencies.

At the end of experiment, when samples had received the same amount of nutrients but at different frequencies, the percentage of photosynthetic excreted carbon gross assimilation (%PEGA) exhibited values < 100% in all cases (Fig. 3H), as did the ratio bacterial carbon demand:excreted organic carbon (BCD:EOC ratio; Fig. S3A), and showed the same pattern of response to UVR and nutrient treatments as the BCD:EOC ratio (Fig. S3A; Table S7). In addition, values < 100% for PEGA and the BCD:EOC ratio were also found in the shorter term, when both communities had received a different intensity of nutrient pulses (moderate and intense treatments; Figs. S3B; Table S7; S8 and Supplementary text S7).

Sestonic P, PP, bacterial respiration (BR), and %PEGA (Fig. 3; Table S9) were significantly higher under the *press* treatment when compared to the *pulse* treatment and UVR; however, the opposite was true for BP and the bacterial growth efficiency (BGE), where the lowest values corresponded to the *press* treatment. By contrast, under UVR, the sestonic C:P ratio and EOC were similar between the *press* and *pulse* treatments. In this sense, and partially contrasting with the findings over the shorter term (moderate and intense treatments; Fig. S4; Table S8 and Supplementary text S7), our results show that the *press* or *pulse* input counteracted (e.g., C:P ratio, BP, BGE) or reversed (e.g., sestonic P, PP, BR, %PEGA) the negative UVR effects, except for the %PEGA, for which a *pulse* input unmasked the negative effects mentioned above.

Relationship between the microbial community and its environment

Due to the variation in the interaction strength of the microbial community and the changes in the taxonomic composition throughout the incubation period, a structural equation modelling (SEM) analysis was performed to test the potential top-down (by MNFs) vs. bottom-up (by DOC and TDP) control on the bacterial biomass under the two simulated natural scenarios considered in this study (*press* × UVR and *pulse* × UVR). The two SEM analyses exhibited a good fit with the observed data for both scenarios, as indicated by their non-significant χ^2 ($p > 0.05$) and by the two Goodness-of-fit indices (NFI and GFI > 0.9 in both cases; Fig. 4 and supplementary text S5). Regardless of the nutrient treatment, SEM yielded positive and significant ($p < 0.05$) standardized path coefficients for the effects of DOC and TDP on bacteria (*press*, 0.48 and 0.59; *pulse*, 0.39 and 0.62, respectively), whereas they were negative and non-significant ($p > 0.05$) for MNFs. In addition, both resources were positively correlated in the *pulse* × UVR scenario ($p < 0.001$) (Fig. 4B). SEM analysis showed negative and significant standardized path coefficients for conditions (i.e., low P) favouring MNFs, resulting in an increased MNFs bacterivory on the bacterial biomass, which was 2.5-fold higher in the *press* compared to the *pulse* × UVR scenario (*press*, -0.72 and $p < 0.001$; *pulse*, -0.29 and $p < 0.01$).

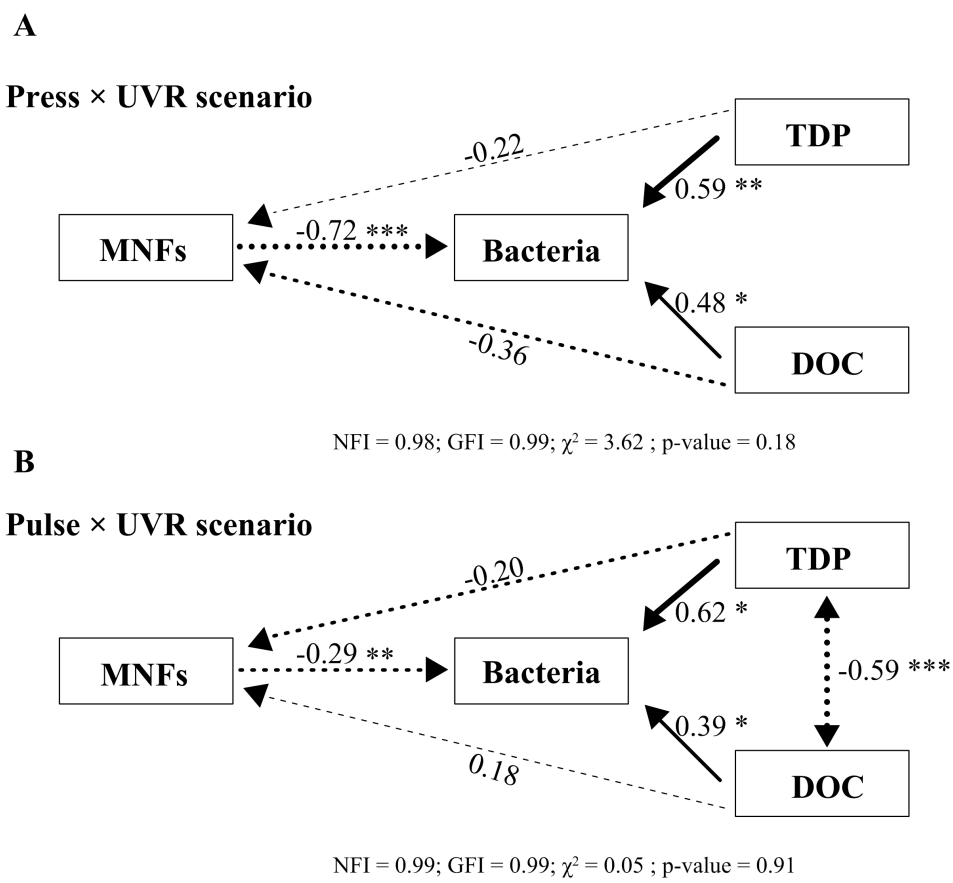

Figure 4: Graphic path model representing the relationship between mixotrophic nanoflagellates (MNFs) and bacterial biomass and the dynamics of nutrients (total dissolved phosphorus, TDP and dissolved organic carbon, DOC) in lake La Caldera under the two 'natural' scenarios of frequency of pulsed nutrients considered, (A) *press* × UVR and (B) *pulse* × UVR. Arrow widths are proportional to path coefficients; the two-headed arrow denotes correlations and the one-headed arrow causal relationship. Negative effects are indicated by dashed lines and positive effects by solid black lines. Numbers join to the paths indicate standardized paths coefficients. Significance p-values are denoted with ***** (p-value < 0.05), ****** (p-value < 0.01) and ******* (p-value < 0.001). Fit statistics (Goodness-of-fit index, GFI; normal-fit index, NGI; χ^2; p-value).

Discussion

This study responds to the increasing need for forecasts on how the growing frequency of climatically driven nutrient pulses and their interaction with other stressors alters the structure and the strength of biotic interactions in food webs (Yang et al., 2010). Our findings show that under UVR the *press* conditions, more than *pulse* conditions, stimulated PP and phytoplankton biomass. Although previous studies also reported a concomitant microbial loop development after nutrient inputs in oligotrophic ecosystems (Carrillo et al., 2008b; Cotner & Biddanda, 2002), our results show that this may not generally be the case for all oligotrophic ecosystems, supporting previous studies in this ecosystem that found only a transitory development of this compartment after nutrient pulses (Dorado-García et al., 2014; Medina-Sánchez et al., 2013.)

Surprisingly, the limited bacterial development and the absence of ciliates and HNFs was counterbalanced by the increased development of MNFs, particularly under UVR and *press* conditions. In fact, under *pulse* conditions, photoautotrophs dominated the community exhibiting a characteristic domed-curve dynamic probably due to the rapid and high levels of nutrient availability that caused an overshoot of the consumer-carrying capacity, generating rapid community growth followed by substantial declines, which in some cases, even lead to population extinctions (Holt, 2008). By contrast, the early and sustained development of MNFs under the *press* conditions (particularly under UVR) is consistent with previous findings, both in laboratory and field studies (Fischer et al., 2016; Hartmann et al., 2012; Mitra et al., 2014; Rothhaupt, 1996) showing that MNFs are most successful when nutrients are scarce and solar radiation plentiful. This is indicative that the *press* conditions maintained nutrient scarceness (as actual availability) below the threshold that would elicit a bloom-development of photoautotrophic phytoplankton. Our field survey on a seasonal and inter-annual scale and our experimental results show a consistent response pattern with the prevalence of MNFs under low but frequent nutrient in-

puts, whereas photoautotrophs responded to high nutrient inputs, denoting the differential growth strategy that both groups adopted with the nutrient-input schedule. However, in neither approach was there a clear development of bacteria nor was the presence of ciliates or HNFs detected, a finding that we attribute to a higher competitive advantage of MNFs over ciliates and HNFs (not found here), because MNFs have a lower minimum threshold of bacteria abundance to grow (Havskum & Riemann, 1996). In addition, as Mitra et al. (2014) recently suggested, the synergistic co-operation between phototrophy (to obtain C) and phagotrophy (to obtain nutrients) within the same organism also confer higher competitive advantage to MNFs over photoautotrophs. This is particularly relevant under high light intensities and low nutrient concentrations, conditions which favour increased bacterivory rates (Medina-Sánchez et al., 2004) and positive net growth rates (Fischer et al., 2016) of MNFs.

In relation to the joint effects of pulsed nutrients and UVR on primary producers, bacteria and their commensalistic interaction, our results show that PP and BP were stimulated several-fold over the shorter term (different intensity of nutrient inputs; Fig. S4 and Supplementary text S7) and over the longer term of the experiment (equal intensity of nutrient inputs; Fig. 3). The reported increases in PP were consistently coupled with increases in the sestonic P content and decreases in the sestonic C:P ratio, indicating a more balanced elemental content of phytoplankton to growth (Carrillo et al., 2015b). Despite the EOC satisfying the BCD in both nutrient-input schedules, the BCD (and BR) was higher (2–fold) and the BP (and BGE) was lower in the *press* × UVR than in the *pulse* × UVR scenario (Fig. 3C). These findings suggest that *press* conditions caused bacteria to use most of their C uptake for energy expenditure rather than for biomass production. Moreover, this lower BP found under a *press* than *pulse* × UVR scenario could be due to a higher bacterivory by MNFs on bacteria, a possibility supported by the fact that the negative SEM coefficients for the MNF–bacteria interaction were 2–fold higher under the *press* × UVR scenario, hence denoting an intensive top-down control of bacterial compartment by MNFs. These results support our previous findings on

the dominance of MNFs in oligotrophic ecosystems, and are in line with a newly proposed microbial food-web paradigm (Medina-Sánchez et al., 2004; Mitra et al., 2014) where MNFs dominate the microbial community and are responsible for most C fixation, while also controlling the bacterial biomass due to their phagotrophic metabolism. Therefore, the energetic constraint of bacteria (i.e., a higher respiratory cost) together with a higher top-down control under *press* conditions could help to explain the steadiness of the heterotrophic compartment over the time.

Conclussion

From the above, we conclude that the growing frequency of pulsed nutrients entering into the ecosystems together with high UVR fluxes can reinforce the dual control that MNFs exert on bacteria via increased photosynthetic C release, a share of which can be recycled through phagotrophy following the MNF–bacteria–MNF sequence. This dual form of control favours the bypass or short circuit between the two functional groups, as described by Carrillo et al. (2006) and Medina-Sánchez et al. (2004) in freshwater ecosystems and by Ptacnik et al. (2016) in marine ecosystems. This mutualistic interaction underpins the mixotrophic strategy reported in this study, as a high frequency of low nutrient inputs under high UVR levels benefits the growth of MNFs. Therefore, the combination of these two factors could explain the inter-annual persistence of MNFs in this and other freshwater and marine clear-water ecosystems (Hartmann et al., 2012; Medina-Sánchez et al., 2004; Sanders & Gast, 2011).

The present study has three major implications. First, current changes that are occurring in resources (e.g., the increasing frequency of pulsed nutrients) and energy fluxes (i.e., higher solar radiation under shallower UMLs) in many oligotrophic areas worldwide may cause a shift in the dominance of the planktonic community from photoautototrophs to mixotrophs coupled with higher primary productivity rates in these ecosystems. Sec-

ond, such changes in planktonic community structure could reinforce the top-down control on heterotrophic bacteria through mixotrophic metabolism. Third, it is critical to consider the interaction between chronic and stochastic environmental stressors to more accurately predict and understand how population and communities will respond to the predicted climate-driven changes.

References

Acker, J.G., Leptoukh, G., 2007. Online analysis enhance NASA Earth science data. *EOS, Trans. AGU* **88**, 14-17.

APHA, 1992. Standard methods for the examination of water and wastewater. American Public Health Association, Washington.

Azam, F., Fenchel, T., Field, J.G., Gray, J.S., Meyer-Reil, L.A., Thingstad, F., 1983. The ecological role of water-column microbes in the sea. *Mar. Ecol. Prog. Ser.* **10**, 257-263.

Beardall, J., Raven, J.A., 2004. The potential effects of global climate change on microalgal photosynthesis, growth and ecology. *Phycologia* **43**, 26-40.

Behrenfeld, M.J., O'Malley, R.T., Siegel, D.A., McClain, C.R., Sarmiento, J.L., Feldman, G.C., Milligan, A.J., Falkowski, P.G., Letelier, R.M., Boss, E.S., 2006. Climate-driven trends in contemporary ocean productivity. *Nature* **444**, 752-755.

Bergmann, T., Richardson, T.L., Paerl, H.W., Pinckney, J.L., Schofield, O., 2002. Synergy of light and nutrients on the photosynthetic efficiency of phytoplankton populations from the Neuse River Estuary, North Carolina. *J. Plankton Res.* **24**, 923-933.

Boyce, D.G., Lewis, M.R., Worm, B., 2010. Global phytoplankton decline over the past century. *Nature* **466**, 591-596.

Cabrerizo, M.J., Medina-Sánchez, J.M., González-Olalla, J.M., Villar-Argaiz, M., Carrillo, P., 2016. Saharan dust and high UVR jointly alter the metabolic balance in marine oligotrophic ecosystems. *Sci. Rep.* **6**, 35892.

Carrillo, P., Delgado-Molina, J.A., Medina-Sánchez, J.M., Bullejos, F.J., Villar-Argaiz, M., 2008a. Phosphorus inputs unmask negative effects of ultraviolet radiation on algae in a high mountain lake. *Glob. Change Biol.* **14**, 423-439.

Carrillo, P., Medina-Sánchez, J.M., Durán, C., Herrera, G., Villafañe, V.E., Helbling, E.W., 2015a. Synergistic effects of UVR and simulated stratification on commensalistic algal-bacterial relationship in two optically contrasting oligotrophic Mediterranean lakes. *Biogeosciences* **12**, 697-712.

Carrillo, P., Medina-Sánchez, J.M., Herrera, G., Durán, C., Segovia, M., Cortés, D., Salles, S., Korbee, N., Figueroa, F.L., Mercado, J.M., 2015b. Interactive effect of UVR and phosphorus on the coastal phytoplankton community of the Western Mediterranean Sea: Unravelling eco-physiological mechanisms. *PloS One* **10**, e0142987.

Carrillo, P., Medina-Sánchez, J.M., Villar-Argaiz, M., Delgado-Molina, J.A., Bullejos, F.J., 2006. Complex interactions in microbial food webs: Stoichiometric and functional approaches. *Limnetica* **25**, 189-204.

Carrillo, P., Villar-Argaiz, M., Medina-Sánchez, J.M., 2008b. Does microorganism stoichiometry predict microbial food web interactions after a phosphorus pulse? *Microb. Ecol.* **56**, 350-363.

Cotner, B.J., Biddanda, B.A., 2002. Small players, large role: Microbial influence on biogeochemical processes in pelagic aquatic ecosystems. *Ecosystems* **5**, 105-121.

Cottingham, K.L., Knight, S.E., Carpenter, S.R., Cole, J.J., Pace, M.L., Wagner, A.E., 1997. Response of phytoplankton and bacteria to nutrients and zooplankton: A mesocosm experiment. *J. Plankton Res.* **19**, 995-1010.

Danger, M., Daufresne, T., Lucas, F., Pissard, S., Lacroix, G., 2008. Does Liebig's law of the minimum scale up from species to communities? *Oikos* **117**, 1741-1751.

Daufresne, T., Lacroix, G., Benhaim, D., Loreau, M., 2008. Coexistence of algae and bacteria: A test of the carbon hypothesis. *Aquat. Microb. Ecol.* **53**, 323-332.

del Giorgio, P.A., Cole, J.J., 1998. Bacterial growth efficiency in natural aquatic systems. *Ann. Rev. Ecol. Syst.* **29**, 503-541.

Dorado-García, I., Medina-Sánchez, J.M., Herrera, G., Cabrerizo, M.J., Carrillo, P., 2014. Quantification of carbon and phosphorus co-limitation in bacterioplankton: New insights on an old topic. *PloS One* **9**, e99288.

Duarte, C.M., Agustí, S., Vaqué, D., Agawin, N.S.R., Felipe, J., Casamayor, E.O., Gasol, J.M., 2005. Experimental test of bacteria-phytoplankton coupling in the Southern Ocean. *Limnol. Oceanogr.* **50**, 1844-1854.

Durán, C., Medina-Sánchez, J.M., Herrera, G., Carrillo, P., 2016. Changes in the phytoplankton-bacteria coupling triggered by joint action of UVR, nutrients, and warming in Mediterranean high-mountain lakes. *Limnol. Oceanogr.* **61**, 413-429.

Fischer, R., Giebel, H.-A., Hillebrand, H., Ptacnik, R., 2016. Importance of mixotrophic bacterivory can be predicted by light and loss rates. *Oikos* **in press**.

Fuhrman, J.A., Azam, F., 1982. Thymidine incorporation as a measure of heterotrophic bacterioplankton production in marine surface waters: Evaluation and field results. *Mar. Biol.* **66**, 109-120.

Gallisai, R., Peters, F., Volpe, G., Basart, S., Baldasano, J.M., 2014. Saharan dust may affect phytoplankton growth in the Mediterranean Sea at ecological time scales. *PloS One*, e110762.

Häder, D.-P., Gao, K., 2015. Interactions of anthropogenic stress factors on marine phytoplankton. *Front. Environ. Sci.* **3**, 14.

Häder, D.-P., Williamson, C.E., Wängberg, S.-A., Rautio, M., Rose, K.C., Gao, K., Helbling, E.W., Sinha, R.P., Worrest, R., 2015. Effects of UV radiation on aquatic ecosystems and interactions with other environmental factors. *Photochem. Photobiol. Sci.* **14**, 108-126.

Harrison, J.W., Smith, R.E.H., 2009. Effects of ultraviolet radiation on the productivity and composition of freshwater phytoplankton communities. *Photochem. Photobiol. Sci.* **8**, 1218-1232.

Hartmann, M., Grob, C., Tarran, G.A., Martin, A.P., Burkill, P.H., Scanlan, D.J., Zubkov, M.V., 2012. Mixotrophic basis of Atlantic oligotrophic ecosystems. *Proc. Natl. Acad. Sci.* **109**, 5756-5760.

Havskum, H., Riemann, B., 1996. Ecological importante of bacterivorous, pigmented flagellates (mixotrophs) in the Bay of Aarhus, Denmark. *Mar. Ecol. Progr. Ser.* **17**, 17-27.

Helbling, E.W., Carrillo, P., Medina-Sánchez, J.M., Durán, C., Herrera, G., Villar-Argaiz, M., Villafañe, V.E., 2013. Interactive effects of vertical mixing, nutrients and ultraviolet radiation: *in situ* photosynthetic responses of phytoplankton from high mountain lakes in Southern Europe. *Biogeosciences* **10**, 1037-1050.

Holt, R.D., 2008. Theoretical perspectives on resource pulses. *Ecology* **89**, 671-681.

IPCC, 2013. Climate Change. The Physical Science Basis. Cambridge University Press, New York, USA.

Jickells, T.D., Moore, C.M., 2015. The importance of atmospheric deposition for ocean productivity. *Ann. Rev. Ecol. Evol. Syst.* **46**, 481-501.

Kamiya, E., Izumiyama, S., Nishimura, M., Mitchell, J.G., Kogure, K., 2007. Effects of fixation and storage on flow cytometric analysis of marine bacteria. *J. Oceanogr.* **63**, 101-112.

Korbee, N., Carrillo, P., Mata, M.T., Rosillo, S., Medina-Sánchez, J.M., Figueroa, F.L., 2012. Effects of ultraviolet radiation and nutrients on the structure–function of phytoplankton in a high mountain lake. *Photochem. Photobiol. Sci.* **11**, 1087-1098.

Kritzberg, E.S., Cole, J.J., Pace, M.L., Granéli, W., 2005. Does autochthonous primary production drive variability in bacterial metabolism and growth efficiency in lakes dominated by terrestrial C inputs? *Aquat. Microb. Ecol.* **38**, 103-111.

Lekunberri, I., Leport, T., Romero, E., Vázquez-Domínguez, E., Romera-Castillo, C., Marrasé, C., Peters, F., Weinbauer, M., Gasol, J.M., 2010. Effects of a dust deposition event on coastal marine microbial abundance and activity, bacterial community structure and ecosystem function. *J. Plankton Res.* **32**, 381-396.

Lennon, J.T., Cottingham, K.L., 2008. Microbial productivity in variable resource environments. *Ecology* **89**, 1001-1014.

López-Sandoval, D.C., Fernández, A., Marañón, E., 2011. Dissolved and particulate primary production along a longitudinal gradient in the Mediterranean Sea. *Biogeosciences* **8**, 815-825.

Mahowald, N., Jickells, T.D., Baker, A.R., Artaxo, P., Benitez-Nelson, C.R., Bergametti, G., Bond, T.C., Chen, Y., Cohen, D.D., Herut, B., Kubilay, N., Losno, R., Luo, C., Maenhaut, W., McGee, K.A., Okin, G.S., Siefert, R.L., Tsukuda, S., 2008. Global distribution of atmospheric phosphorus sources, concentrations and deposition rates, and anthropogenic impacts. *Glob. Biogeochem. Cy.* **22**, GB4026.

Martínez-García, S., Arbones, B., García-Martín, E.E., Teixeira, I.G., Serret, P., Fernández, E., Figueiras, F.G., Teira, E., Álvarez-Salgado, X.A., 2015. Impact of atmospheric deposition on the metabolism of coastal microbial communities. *Estuar. Coast. S. Sci.* **153**, 18-28.

Medina-Sánchez, J.M., Delgado-Molina, J.A., Bratbak, G., Bullejos, F.J., Carrillo, P., 2013. Maximum in the middle: Nonlinear response of microbial plankton to ultraviolet radiation and phosphorus. *PloS One* **8**, e60223.

Medina-Sánchez, J.M., Villar-Argaiz, M., Carrillo, P., 2002. Modulation of the bacterial response to spectral solar radiation by algae and limiting nutrients. *Freshwater Biol.* **47**, 2191-2204.

Medina-Sánchez, J.M., Villar-Argaiz, M., Carrillo, P., 2004. Neither with nor without you: A complex algal control on bacterioplankton in a high mountain lake. *Limnol. Oceanogr.* **49**, 1722-1733.

Medina-Sánchez, J.M., Villar-Argaiz, M., Carrillo, P., 2006. Solar radiation - nutrient interaction enhances the resource and predation algal control on bacterioplankton: A short-term experimental study. *Limnol. Oceanogr.* **51**, 913-924.

Mitra, A., Flynn, K.J., Burkholder, J.M., Berge, T., Calbet, A., Raven, J.A., Granéli, E., Glibert, P.M., Hansen, P.J., Stoecker, D.K., Thingstad, F., Tilmann, U., Vage, S., Wilken, S., Zubkov, M.V., 2014. The role of mixotrophic protist in the biological carbon pump. *Biogeosciences* **11**, 995-1005.

Mladenov, N., Sommaruga, R., Morales-Baquero, R., Laurion, I., Camarero, L., Diéguez, M.C., Camacho, A., Delgado, A., Torres, O., Chen, Z., Felip, M., Reche, I., 2011. Dust inputs and bacteria influence dissolved organic matter in clear alpine lakes. *Nat. Commun.* **2**, 405.

Moore, C.M., Mills, M.M., Arrigo, K.R., Berman-Frank, I., Bopp, L., Boyd, P.W., Galbraith, E.D., Geider, R.J., Guieu, C., Jaccard, S.L., Jickells, T.D., La Roche, J., Lenton, T.M., Mahowald, N.M., Marañón, E., Marinov, I., Moore, J.K., Nakatsuka, T., Oschlies, A., Saito, M.A., Thingstad, T.F., Tsuda, A., Ulloa, O., 2013. Processes and patterns of oceanic nutrient limitation. *Nat. Geosci.* **6**, 701-710.

Morales-Baquero, R., Pulido-Villena, E., Reche, I., 2006. Atmospheric inputs of phosphorus and nitrogen to the southwest Mediterranean region: Biogeochemical responses of high mountain lakes. *Limnol. Oceanogr.* **51**, 830-837.

Morán, X.A.G., Estrada, M., Gasol, J.M., Pedrós-Alió, C., 2002. Dissolved primary production and the strength of phytoplankton-bacterioplankton coupling in contrasting marine regions. *Microb. Ecol.* **44**, 217-223.

Murphy, J., Riley, J.P., 1962. A modified single solution method for the determination of phosphate in natural waters. *Anal. Chim. Acta* **27**, 31-36.

Pausz, C., Herndl, G.J., 2002. Role of nitrogen versus phosphorus availability on the effect of UV radiation on bacterioplankton and their recovery from previous UV stress. *Aquat. Microb. Ecol.* **29**, 89-95.

Ptacnik, R., Gomes, A., Royer, S.-R., Berger, S.T., Calbet, A., Nejstgaard, J.C., Gasol, J.M., Isari, S., Moorthi, S.D., Ptacnikova, R., Striebel, M., Sazhin, A.F., Tsagaraki, T.M., Zervoudaki, S., Altoja, K., Dimitriou, P.D., Laas, P., Gazihan, A., Martínez, R.A., Schabhüttl, S., Santi, I., Sousoni, D., Pitta, P., 2016. A light-induced shortcut in the planktonic microbial loop. *Sci. Rep.* **6**, 29286.

Ridame, C., Dekaezemacker, J., Guieu, C., Bonnet, S., L'Helguen, S., Malien, F., 2014. Contrasted saharan dust events in LNLC environments: Impact on nutrient dynamics and primary production. *Biogeosciences* **11**, 4783-4800.

Rothhaupt, K.O., 1996. Laboratory experiments with a mixotrophy Chrysophyte and obligately phagotrophic and phototrophic competitors. *Ecology* **77**, 716-724.

Sanders, R.W., Gast, R.J., 2011. Bacterivory by phototrophic picoplankton and nanoplankton in Artic waters. *FEMS Microb. Ecol.* **82**, 242-253.

Sommaruga, R., 2001. The role of solar UV radiation in the ecology of alpine lakes. *J. Photochem. Photobiol. B: Biol.* **62**, 35-42.

Steemann Nielsen, E., 1952. The use of radio-active carbon (C^{14}) for measuring organic production in the sea. *J. Cons. Perm. Int. Explor. Mer.* **18**, 117-140.

Straškrabová, V., Callieri, C., Carrillo, P., Cruz-Pizarro, L., Fott, J., Hartman, P., Macek, M., Medina-Sánchez, J.M., Nedoma, J., Šimek, K., 1999. Investigations on pelagic food webs in mountain lakes - aims and methods. *J. Limnol.* **58**, 77-87.

Unrein, F., Gasol, J.M., Not, F., Forn, I., Massana, R., 2014. Mixotrophic haptophytes are key bacterial grazers in oligotrophic coastal waters. *ISME J.* **8**, 164-176.

Vidal, L.O., Granéli, W., Daniel, C.B., Heiberg, L., Roland, F., 2011. Carbon and phosphorus regulating bacterial metabolism in oligotrophic boreal lakes. *J. Plankton Res.* **33**, 1747-1756.

Williamson, C.E., Saros, J.E., Schindler, D.W., 2009. Sentinels of change. *Science* **323**, 887-888.

Yang, L.H., 2004. Periodical cicadas as resource pulses in North American Forests. *Science* **306**, 1565-1568.

Yang, L.H., 2008. Pulses of dead periodical cicadas increase herbivory of american bellflowers. *Ecology* **89**, 1497-1502.

Yang, L.H., Bastow, J., Spence, K.O., Wright, A.N., 2008. What can we learn from resource pulses? *Ecology* **89**, 621-634.

Yang, L.H., Edwards, K.F., Byrnes, J.E., Bastow, J.L., Wright, A.N., Spence, K.O., 2010. A meta-analysis of resource pulse-consumer interactions. *Ecol. Monogr.* **80**, 125-151.

Zubkov, M.V., Burkill, P.H., Topping, J.N., 2007. Flow cytometric enumeration of DNA-stained oceanic planktonic protists. *J. Plankton Res.* **29**, 79-86.

Zubkov, M.V., Tarran, G.A., 2008. High bacterivory by the smallest phytoplankton in the North Atlantic Ocean. *Nature* **455**, 224-226.

Supplementary information

Supplementary text S1

Measurements of natural inputs of pulsed nutrients: Remote sensing

Aerosol data were successfully used for the study of Saharan dust inputs in previous studies of this freshwater ecosystem, due to the highly positive correlation of TOMS aerosol index (AI) with total phosphorus (TP) (Bullejos et al., 2010; Morales-Baquero et al., 2006). We used TOMS AI data for the 2010-2015 ice-free period at lake La Caldera (37.5°N, 3.5°W). We considered that values of AI $\geq$ 10 represent intense deposition events. Original data for this study were downloaded from Giovanni database web (Acker & Leptoukh, 2007).

Supplementary text S2

Experimental approach

The integrated approach used here is sufficiently realistic to unravel the underlying mechanisms that govern the interaction between nutrient pulses, UVR, and the microbial community in the ecosystem because (i) the incubation period extended over three weeks, allowing us quantify the microbial loop response and changes in phytoplankton community; (ii) the UVR and nutrients pulse applied reproduced the natural optical conditions in the water column and the intensity and frequency of atmospheric deposition of aerosol in this area (Bullejos et al., 2010; Morales-Baquero et al., 2006); and (iii) the absence of zooplankton in the mesocosms did not alter the response pattern of the microbial community structure with respect to natural lake conditions, suggesting a negligible net effect of zooplankton on

the response of the microbial dynamics.

Supplementary text S3

Phytoplankton abundances

An aliquot of 50 mL from each sample was settled in an Utermöhl chamber of 2.6 cm diameter for 48 h to ensure complete sedimentation of the smallest phytoplankton species and counted at 400× and 1000× magnification under an inverted microscope (Carl Zeiss AX10, LCC, USA). For each sample, at least 400 cells of the more abundant phytoplanktonic species were counted, and 20 cells per species were measured for each date to estimate cell volume according to a corresponding geometrical shape. Phytoplankton biomass was estimated by approximating the cell volume to their geometric shape (Carrillo et al., 1995) and transform it to carbon (C) units following (Rocha & Duncan, 1985). For ciliates and heterotrophic nanoflagellates (HNFs), an aliquot of 300-mL of each sample was allowed to settle for 72 h, and the supernatant was removed by suction with a Pasteur pipette coupled to a low-pressure pump. The remaining 50 mL were again settled in an Utermöhl chamber with the same procedure as described above for phytoplankton counting.

Bacteria abundances

Before analyses, the samples were unfrozen and stained with Sybr–Green I DNA (Sigma-Aldrich) 1:5000 final dilution of initial stock (Gasol & del Giorgio, 2000; Zubkov et al., 2007). A standard concentration of yellow-green 1-μm beads (10^5 particles mL^{-1}) (Fluoresbrite Microparticles, Polysciences, Warrington, PA, USA) was added in order to determine absolute cell concentrations (Zubkov et al., 2007; Zubkov & Burkill, 2006). Bacterial biomass was estimated by approximating cell volume to their geometric

shape and to transform it to C units following suitable conversion factors (Posch et al., 2001).

Supplementary text S4

Primary production (PP)

All filtrations were done under low vacuum pressure (< 100 mm Hg) to minimize cell breakage. All the filters were placed in scintillation vials and also acidified with 1 N HCl (2%) for 24 h to remove inorganic radiocarbon before the addition of liquid scintillation cocktail (Ecoscint A). After this, all samples were measured using a scintillation counter equipped with autocalibration (Beckman LS 6000 TA). The filtrate < 0.2 μm obtained was also treated as described for the total organic carbon (TOC, see main text). Because of the absence of photoautotrophic picoplankton (Dorado-García et al., 2014) and not significant retention of bacteria in 1-μm pore-size filters, the organic ^{14}C retained on the 0.2-μm pore filters corresponded to the phytoplankton exudates incorporated by heterotrophic bacteria (POC_2) (Carrillo et al., 2002; Medina-Sánchez et al., 2006).

Bacterial respiration (BR)

Oxygen-concentration measurements (O_2) were made in darkness using an optic-fiber oxygen transmitter (Fibox 3; PreSens GmbH, Germany) with temperature compensation to register any change in the bath temperature, and connected to a computer with Oxyview 6.02 software to register the data. Prior to experimentation, the system was submitted to a two-point calibration, together with data of atmospheric pressure and temperature. Firstly, 0% O_2 concentration was determined by adding sodium sulfite (Na_2SO_3) to sterilized-distilled water to a final concentration > 0.1 mg mL^{-1}. To achieve the 100% O_2 saturation, wet cotton wool was put

into the closed flask to ensure that the air was over-saturated with O_2 by water vapor. BR rates were calculated from least-square regressions after confirming that oxygen fitted a linear model during the first 24 h after sampling.

Bacterial carbon demand (BCD)

BCD was calculated as the sum of BP plus BR.

Supplementary text S5

Structural equation modeling (SEM)

We performed a SEM analysis to test the top-down (mixotrophic nanoflagellates, MNFs) *vs.* bottom-up control (DOC and TDP) on bacteria biomass under the two scenarios considered in this study (*press* × UVR and *pulse* × UVR), due to the variation in the interaction strength of the microbial community and the changes in the taxonomic composition through incubation. As the sample size was relatively small (18 data per variable), we followed the recommendations of Tanaka et al. (1987). Previously, all variables considered were assessed for normality before statistical analysis. Suitable transformation (log) was performed for bacterial biomass to improve normality according to Zar (1999). The GLS ⇒ ML method with 300 iterations was used to estimate standardized path coefficients in our models, and the χ^2 to test the degree of fit of the model to the observed data. Non-significant χ^2 indicates that the pattern predicted by the hypothesis is not different from the observed data, and thus the model can be accepted (Iriondo et al., 2003). Notwithstanding, it is generally accepted that the χ^2 test should be interpreted with caution and supplemented with other Goodness-of-fit indices (Lohelin, 1992). Therefore, two additional other Goodness-of-fit indices were used, such as the Bentler-Bonnet Normed Fit

Index (NFI) and the Goodness-of-Fit Index (GFI).

Supplementary text S6

Measurements of physical-chemical variables

Vertical profiles of solar radiation in the water column were measured at noon during the first experimental day using a submersible BIC Compact 4-Channel radiometer (Biospherical Instruments Inc., CA, USA) with three channels in the UVR region (305, 320, and 380 nm) and one broad-band channel for PAR (400-700 nm). Diffuse attenuation coefficients for downward irradiance (k_d) were determined from the slope of the linear regression of the natural logarithm of downwelling irradiance vs. depth for each wavelength range considered (n > 300, $R^2 > 0.90$). Temperature profiles were recorded using a multiparametric probe (Hanna HI9828-0).

Water samples for the chemical determination of total dissolved phosphorus (TDP), soluble reactive phosphorus (SRP), and total dissolved nitrogen (TDN) were also collected, and prior to determination were filtered through GF/F Whatman filters (25-mm diameter). Samples for TDP were persulfate digested at 120°C for 30 min and determined (as for SRP) using 10 cm quartz cuvettes, following the acid molybdate technique (APHA, 1992). TDN samples were also persulphate digested and measured as NO_3^- following the ultraviolet spectrophotometric method (APHA, 1992). Water samples for dissolved organic carbon (DOC) determination were filtered through pre-combusted (2 h at 500°C) GF/F Whatman filters (25-mm diameter); after this, they were acidified with 1N HCl (2%) and stored in darkness at 4°C until analysis. DOC concentrations were measured with the high-temperature catalytic oxidation method in a TOC analyzer (Shimadzu, model 5000) (Benner & Strom, 1993).

Supplementary text S7

Nutrients pulse intensity and UVR effects on metabolic variables

The percentage of photosynthetic excreted gross assimilation (%PEGA), from a direct measurement of carbon (C) incorporated by bacteria of photosynthetic origin, was consistently $< 100\%$ in all treatments, and showed a similar pattern to that of the bacterial carbon demand: excreted organic carbon (BCD: EOC) ratio (Fig. S3A; Table S7), suggesting that the C released by phytoplankton was the main C source supporting BCD. In general, the addition of a moderate or intense pulse increased sestonic P and all metabolic variables, but decreased sestonic carbon: phosphorus (C:P) ratio with respect to ambient conditions. However, a combined impact of UVR and a moderate pulse counteracted (e.g., EOC, BGE) or reversed (e.g., BP, BR) the negative UVR effects, whereas an intense nutrient pulse unmasked (e.g., sestonic P, PP, BR, %PEGA) or even enhanced (e.g., BP, EOC) these negative UVR effects (Fig. S4; Table S8).

Supplementary tables

Table 1: Mean concentration (± SD) of total dissolved phosphorous (TDP) and nitrogen (TDN) (in μM) measured during the incubation period in each experimental treatment (radiation [PAB, > 280 nm; PAR, > 400 nm] and nutrients [ambient (amb), *press*, and *pulse*]) and in the water column of lake La Caldera. Data from 31 August represent concentrations before nutrient additions. n. d. represents non-detectable TDP or TDN concentrations.

Total dissolved phosphorus (TDP)							
Day	Lake	PAB_{amb}	PAR_{amb}	PAB_{press}	PAR_{press}	PAB_{pulse}	PAR_{pulse}
31 August	0.06 (±0.01)	0.06 (±0.01)	0.06 (±0.01)	0.06 (±0.01)	0.06 (±0.01)	0.06 (±0.01)	0.06 (±0.01)
4 September	0.06 (±0.00)	0.03 (±0.01)	0.04 (±0.01)	0.03 (±0.01)	0.08 (±0.01)	0.41 (±0.03)	0.39 (±0.07)
9 September	0.02 (±0.01)	0.15 (±0.03)	0.14 (±0.00)	0.25 (±0.03)	0.12 (±0.07)	0.27 (±0.06)	0.11 (±0.03)
12 September	0.01 (±0.00)	0.16 (±0.00)	0.01 (±0.00)	0.16 (±0.02)	0.09 (±0.01)	0.23 (±0.04)	0.08 (±0.02)
15 September	0.01 (±0.00)	0.10 (±0.08)	0.01 (±0.00)	0.23 (±0.03)	0.08 (±0.01)	0.16 (±0.00)	0.06 (±0.01)
18 September	n.d.	0.04 (±0.00)	0.02 (±0.00)	0.30 (±0.04)	0.07 (±0.01)	0.08 (±0.03)	0.05 (±0.01)
Total dissolved nitrogen (TDN)							
31 August	20.00 (±1.43)	20.00 (±1.43)	20.00 (±1.43)	20.00 (±1.43)	20.00 (±1.43)	20.00 (±1.43)	20.00 (±1.43)
4 September	17.86 (±2.86)	12.86 (±24.28)	1.43 (±1.42)	24.30 (±40.71)	n.d.	21.43 (±41.43)	0.71 (±0.00)
9 September	18.57 (±0.07)	17.14 (±24.29)	20.00 (±20.43)	20.01 (±32.14)	5.71 (±2.14)	30.00 (±35.71)	0.71 (±0.02)
12 September	14.30 (±0.01)	12.14 (±25.00)	20.01 (±40.79)	12.14 (±36.43)	0.71 (±5.00)	40.71 (±32.86)	40.71 (±1.43)
15 September	9.70 (±3.57)	15.00 (±32.14)	50.71 (±25.50)	14.28 (±32.85)	0.72 (±4.29)	19.29 (±32.85)	1.43 (±2.86)
18 September	n.d.	20.00 (±45.71)	50.72 (±20.43)	30.00 (±33.57)	21.43 (±2.86)	47.86 (±27.14)	16.43 (±2.14)

Table 2: Mean concentration (± SD) of dissolved organic carbon (DOC, in μM) measured during the incubation period in each experimental treatment (radiation [PAB, > 280 nm; PAR, > 400 nm] and nutrients [ambient (amb), *press*, and *pulse*]) and in the water column of lake La Caldera. Data from 31 August represent concentrations before nutrient additions. n. m. represents not measured.

Dissolved organic carbon (DOC)							
Day	Lake	PAB_{amb}	PAR_{amb}	PAB_{press}	PAR_{press}	PAB_{pulse}	PAR_{pulse}
31 August	49.16 (±11.67)	49.16 (±11.67)	49.16 (±11.67)	49.16 (±11.67)	49.16 (±11.67)	49.16 (±11.67)	49.16 (±11.67)
4 September	25.83 (±1.67)	25.83 (±1.67)	n.m.	52.50 (±7.50)	41.67 (±4.17)	46.67 (±5.00)	54.0 (±15.00)
9 September	70.00 (±4.17)	25.83 (±1.61)	44.17 (±12.50)	71.67 (±6.67)	73.33 (±5.00)	62.50 (±1.67)	79.17 (±20.00)
12 September	n.m.	27.50 (±2.50)	40.83 (±5.00)	65.83 (±7.50)	66.67 (±9.17)	65.00 (±3.33)	85.00 (±7.50)
15 September	74.17 (±11.67)	29.17 (±1.67)	36.67 (±5.83)	60.83 (±3.33)	60.83 (±3.33)	66.67 (±9.17)	90.01 (±0.00)
18 September	n.m.	29.17 (±3.33)	31.67 (±5.82)	110.00 (±20.83)	67.50 (±6.67)	49.17 (±11.67)	111.67 (±21.67)

Table 3: Results of two-way repeated-measures analysis of the variance (RM-ANOVA) of the interactive effects of ultraviolet radiation (Rad) and frequency of pulsed nutrients (Nut; treatments: ambient [amb], *press*, and *pulse*) on total dissolved phosphorus (TDP), total dissolved nitrogen (TDN) and dissolved organic carbon (DOC). F represents F-test values, and the asterisks *****, ****** and ******* represent the $p < 0.05$, $p < 0.01$ and $p < 0.001$, respectively.

	TDP	TDN	DOC
Treatment	F	F	F
Rad	21.95***	30.01***	0.50
Nut	0.96	38.13***	32.15***
Date	6.38***	112.06***	59.40***
Rad×Nut	0.08	2.87	4.27*
Rad×Date	12.82***	27.08***	21.85***
Nut×Date	2.93**	186.65***	29.21***
Rad×Nut×Date	2.17*	16.64***	24.56***

Table 4: Mean concentration (± SD) of chlorophyll *a* (Chl *a*, in μg L^{-1}) measured during the incubation period in each experimental treatment (radiation [PAB, > 280 nm; PAR, > 400 nm] and nutrients [ambient (amb), *press*, and *pulse*]) and in the water column of lake La Caldera. Data from 31 August represent concentrations before nutrient additions.

Day	PAB_{amb}	PAR_{amb}
31 August	3.19 (±0.41)	3.19 (±0.41)
4 September	3.89 (±0.21)	4.37 (±0.27)
9 September	3.91 (±0.08)	2.08 (±1.26)
12 September	3.85 (±0.26)	1.84 (±0.14)
15 September	4.53 (±0.69)	2.14 (±0.31)
18 September	2.96 (±0.04)	1.69 (±0.11)
	PAB_{press}	PAR_{press}
31 August	3.19 (±0.41)	3.19 (±0.41)
4 September	12.52 (±0.85)	13.61 (±3.03)
9 September	26.72 (±5.05)	25.60 (±0.50)
12 September	11.48 (±0.00)	10.51 (±2.95)
15 September	12.55 (±0.00)	11.32 (±2.99)
18 September	23.03 (±0.14)	10.33 (±4.53)
	PAB_{pulse}	PAR_{pulse}
31 August	3.19 (±0.41)	3.19 (±0.41)
4 September	13.54 (±0.32)	17.91 (±1.06)
9 September	25.02 (±2.42)	25.36 (±3.04)
12 September	4.36 (±0.01)	15.62 (±3.60)
15 September	5.33 (±1.58)	3.38 (±0.95)
18 September	13.78 (±2.36)	4.99 (±2.69)

Table 5: Results of two way-repeated measures analysis of variance (RM-ANOVA) of the interactive effect of ultraviolet radiation (Rad) and frequency of pulsed nutrients (Nut; treatments: ambient [amb], *press*, and *pulse*) on Chlorophyll *a* (Chl *a*), total phytoplankton (PB) and bacteria biomass (BB). *F* represents *F*-test values, and the asterisks *, ** and *** represent the $p < 0.05$, $p < 0.01$ and $p < 0.001$, respectively.

	Chl *a*	PB	BB
Treatment	*F*	*F*	*F*
Rad	0.13	3.24	16.25***
Nut	130.29***	58.23**	85.98***
Date	457.65***	160.66***	146.91***
Rad×Nut	0.92	5.09*	0.07
Rad×Date	47.29***	20.91***	6.10***
Nut×Date	126.37***	52.17***	6.70***
Rad×Nut×Date	24.50***	11.65***	3.69***

Table 6: Results of the non-linear fitting through cubic ($y = ax^3 + bx^2 + cx + d$) and peak-Gaussian functions ($y = y_0 + a \exp(-0.5((x - b) / w^2))$) for mixotrophic nanoflagellates (MNFs) and photoautotrophs during the incubation period in each experimental treatment ([PAB, > 280 nm; PAR, > 400 nm] and nutrients [ambient (amb), *press*, and *pulse*]). R^2 represent the determination coefficient, - means not-significant relationship, and the asterisks *, ** and *** represent the $p < 0.05$, $p < 0.01$ and $p < 0.001$, respectively.

	MNFs	Photoautotrophs
Treatment	R^2	R^2
PAB_{amb}	-	0.90***
PAR_{amb}	-	0.92***
PAB_{press}	0.76***	0.70**
PAR_{press}	0.98***	0.66***
PAB_{pulse}	0.79***	0.75***
PAR_{pulse}	0.98***	0.86***

Table 7: Results of two-way analysis of variance (ANOVA) of the interactive effect of ultraviolet radiation (Rad) and intensity (ambient [amb], moderate [mod], and intense [int]) or frequency (ambient [amb], *press*, and *pulse*) of pulsed nutrients (P) on bacterial carbon demand : excretion of organic carbon ratio (BCD:EOC ratio). *F* represents *F*-test values, and the asterisks *****, ****** and ******* represent the $p < 0.05$, $p < 0.01$ and $p < 0.001$, respectively.

	Intensity	Frequency
Treatment	*F*	*F*
Rad	5.39	0.36
Nut	14.64***	10.22**
Rad×Nut	1.83	3.97*

Table 8: Results of two-way analysis of variance (ANOVA) of the interactive effect of ultraviolet radiation (Rad) and intensity of pulsed nutrients (Nut; treatments: ambient [amb], moderate [Mod], and intense [Int]) on sestonic P, sestonic carbon:phosphorus ratio (C:P), bacterial production (BP), primary production (PP), excretion of organic carbon (EOC), bacterial respiration (BR), bacterial growth efficiency (BGE), and gross assimilation of excreted photosynthetic carbon by bacteria (%PEGA). F represents F-test values, and the asterisks *, ** and *** represent the $p < 0.05$, $p < 0.01$ and $p < 0.001$, respectively.

Variable	Treatment	F
Sestonic P		
	Rad	182.03***
	Nut	3116.80***
	Rad×Nut	115.21***
C:P ratio		
	Rad	676.51**
	Nut	149.13***
	Rad×Nut	42.50***
BP		
	Rad	9.37**
	Nut	33.50***
	Rad×Nut	20.96***
PP		
	Rad	121.44***
	Nut	262.91***
	Rad×Nut	12.77***
EOC		
	Rad	54.02***
	Nut	27.06***
	Rad×Nut	0.47
BR		
	Rad	0.01
	Nut	26.13***
	Rad×Nut	25.66***
BGE		
	Rad	15.90**
	Nut	7.70**
	Rad×Nut	14.43**
%PEGA		
	Rad	0.97
	Nut	4.64**
	Rad×Nut	1.93

Table 9: Results of two-way analysis of variance (ANOVA) of the interactive effect of ultraviolet radiation (Rad) and frequency of pulsed nutrients (Nut; treatments: ambient [amb], *press*, and *pulse*) on sestonic P, sestonic carbon:phosphorus ratio (C:P), bacterial production (BP), primary production (PP), excretion of organic carbon (EOC), bacterial respiration (BR), bacterial growth efficiency (BGE) and gross assimilation of excreted photosynthetic carbon by bacteria (%PEGA). F represents F-test values, and the asterisks *, ** and *** represent the $p < 0.05$, $p < 0.01$ and $p < 0.001$, respectively.

Variable	Treatment	F
Sestonic P		
	Rad	212.93***
	Nut	634.05***
	Rad×Nut	36.16***
C:P ratio		
	Rad	18.19***
	Nut	88.13***
	Rad×Nut	33.12***
BP		
	Rad	6.50*
	Nut	20.89***
	Rad×Nut	15.64***
PP		
	Rad	7.74*
	Nut	189.36***
	Rad×Nut	7.62**
EOC		
	Rad	0.69
	Nut	40.89***
	Rad×Nut	5.93*
BR		
	Rad	0.98
	Nut	9.71**
	Rad×Nut	3.01
BGE		
	Rad	0.03
	Nut	4.72*
	Rad×Nut	16.70***
%PEGA		
	Rad	0.41
	Nut	6.08**
	Rad<Nut	2.46

Supplementary figures

Figure 1: (A) Map of the study site showing a general view of lake La Caldera in Sierra Nevada National Park with the Mulhacen peak (3484 m.a.s.l.) in the background. (B) *In situ* disposition of the racks containing the experimental mesocosms and (C) detailed view of one of these structures into the lake. Map was created using Ocean Data View v.4.7.6 (http://odv.awi.de) and the photographs were taken by M.J.C.

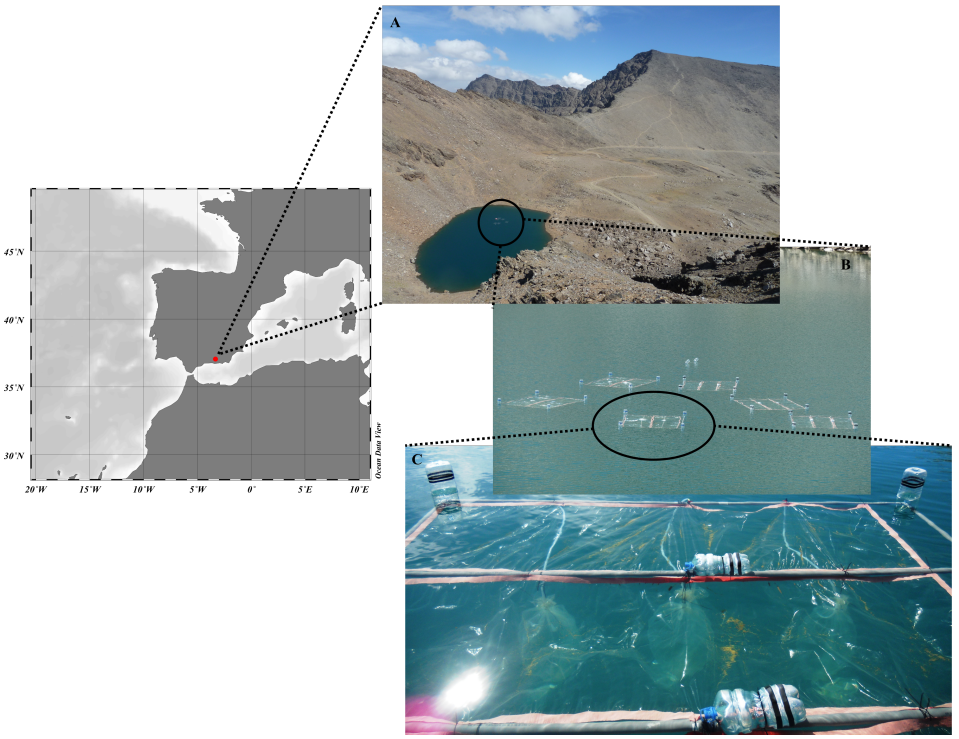

Figure 2: (A) Temperature and (B) solar irradiance as a function of depth in lake La Caldera. Irradiance data in the UVR portion are expressed in μW cm^{-2} nm^{-1}, PAR is in μmol photons m^{-1} s^{-1}.

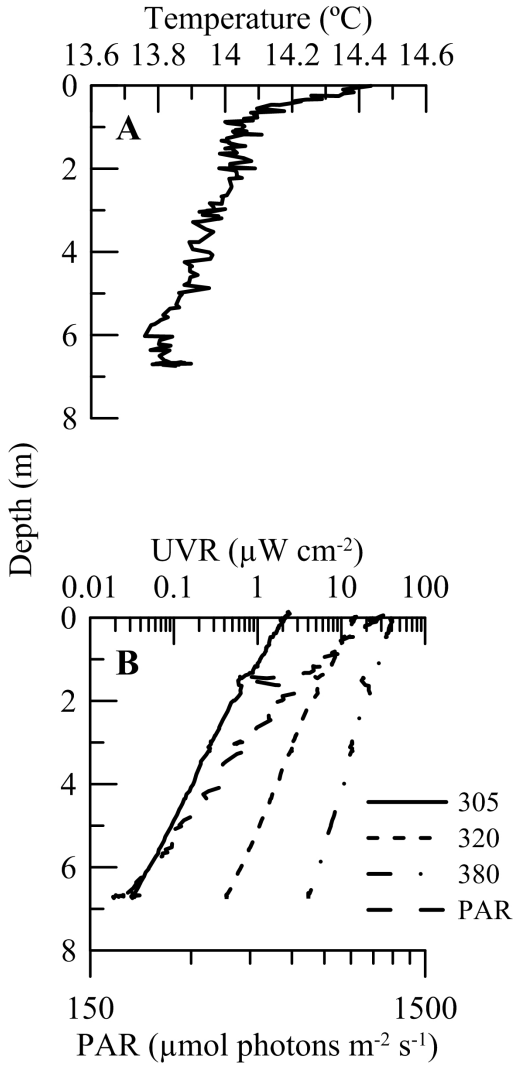

Figure 3: Mean (± SD) bacterial carbon demand:excretion of organic carbon (BCD : EOC) ratio under two radiation treatments, PAB (> 280 nm, white bars) and PAR (> 400 nm, black bars), and two pulsed nutrient regimes: (A) intensity, with ambient (amb), moderate (mod), and intense (int) pulse treatments; and (B) frequency, with ambient (amb), *press* and *pulse* treatments.

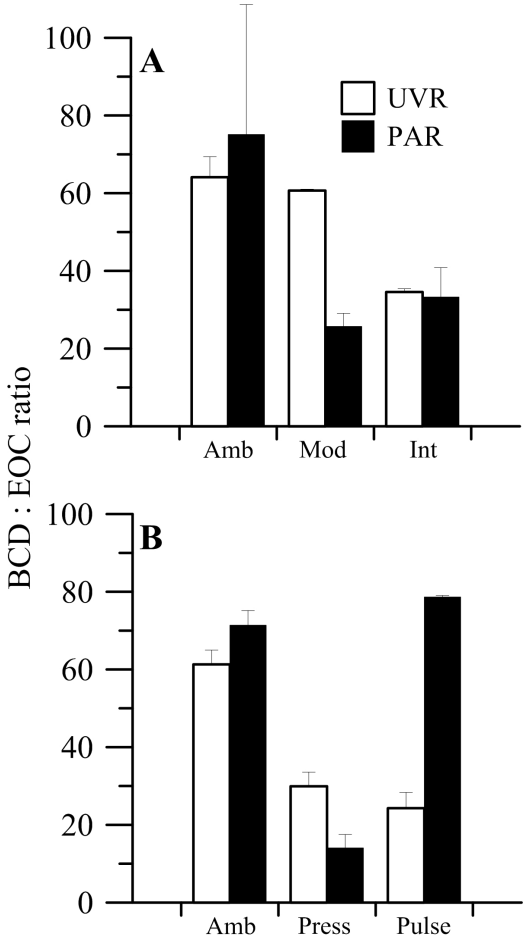

Figure 4: (A) Sestonic phosphorus (P) concentrations (in μg L^{-1}), (B) sestonic carbon:phosphorus ratio (C:P ratio), (C) bacterial production (BP, μg C L^{-1} h^{-1}), (D) primary production (PP, μg C L^{-1} h^{-1}), (E) excretion of organic carbon (EOC, μg C L^{-1} h^{-1}), (F) bacterial respiration (BR, < 0.7 μm; μM O_2 h^{-1}), (G) bacterial growth efficiency (BGE) and (H) percentage of photosynthetic excreted gross assimilation (%PEGA) in lake La Caldera under the two radiation treatments: PAB (white bars) and PAR (black bars) and the three nutrient treatments: ambient (amb), moderate (mod) and intense (int). The bars represent mean values of three replicates and lines on top of the bars are the standard deviation. Letters indicate differences among treatments by Bonferroni *post hoc* test. Note that these results represent responses observed over the short term when communities received different amounts of nutrients (Mod, 5 μg P L^{-1} and Int, 30 μg P L^{-1}.

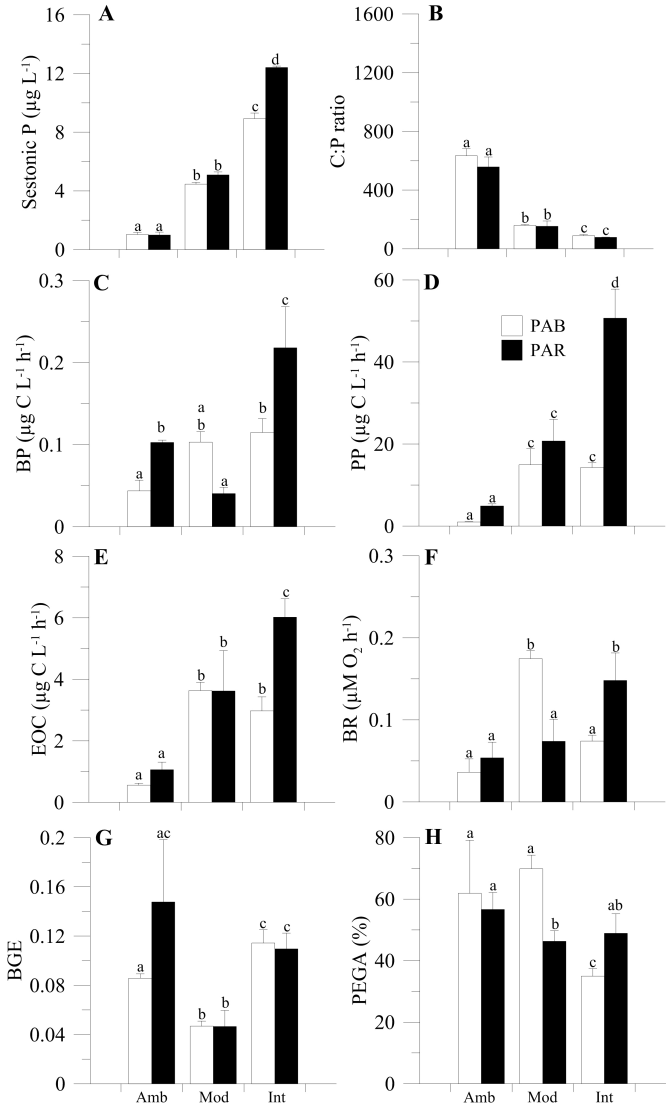

Supplementary references

Acker, J.G., Leptoukh, G., 2007. Online analysis enhance NASA Earth science data. *EOS, Trans. AGU* **88**, 14-17.

APHA, 1992. Standard methods for the examination of water and wastewater. American Public Health Association, Washington.

Bell, R.T., 1993. Estimating production of heterotrophic bacterioplankton via incorporation of tritiated thymidine, in: Kemp, P.F., Sherr, B.F., Cole, J.J. (Eds.), Handbook of methods in aquatic microbial ecology. Lewis Publishers, Boca Ratón, Florida, USA, pp. 495-503.

Benner, R., Strom, M., 1993. A critical evaluation of the analytical blank asociated with DOC measurements by high-temperature catalytic oxidation. *Mar. Chem.* **41**, 153-160.

Bullejos, F.J., Carrillo, P., Villar-Argaiz, M., Medina-Sánchez, J.M., 2010. Roles of phosphorus and ultraviolet radiation in the strength of phytoplankton–zooplankton coupling in a Mediterranean high mountain lake. *Limnol. Oceanogr.* **55**, 2549–2562.

Carrillo, P., Medina-Sánchez, J.M., Villar-Argaiz, M., 2002. The interaction of phytoplankton and bacteria in a high mountain lake: Importance of the spectral composition of solar radiation. *Limnol. Oceanogr.* **47**, 1294-1306.

Carrillo, P., Reche, I., Sánchez-Castillo, P., Cruz-Pizarro, L., 1995. Direct and indirect effects of grazing on the phytoplankton seasonal succession in an oligotrophic lake. *J. Plankton Res.* **17**, 1363-1379.

Dorado-García, I., Medina-Sánchez, J.M., Herrera, G., Cabrerizo, M.J., Carrillo, P., 2014. Quantification of carbon and phosphorus co-limitation in bacterioplankton: New insights on an old topic. *PloS One* **9**, e99288.

Gasol, J.M., del Giorgio, P., 2000. Using flow cytometry for counting natural planktonic bacteria and understanding the structure of planktonic bacterial communities. *Sci. Mar.* **64**, 197-224.

Iriondo, J.M., Albert, M.J., Escudero, A., 2003. Structural equation modelling: An alternative for assessing causal relationships in threatened plant populations. *Biol. Conserv.* **113**, 367-377.

Lee, S., Fuhrman, J.A., 1987. Relationships between biovolume and biomass of naturally derived marine bacterioplankton. *Appl. Environ. Microbiol.* **53**, 1298-1303.

Lohelin, J.C., 1992. Latent variable models. An introduction to factor, path and strutural analysis. Lawrence Erlbaum Associates.

Medina-Sánchez, J.M., Villar-Argaiz, M., Carrillo, P., 2006. Solar radiation - nutrient interaction enhances the resource and predation algal control on bacterioplankton: A short-term experimental study. *Limnol. Oceanogr.* **51**, 913-924.

Morales-Baquero, R., Pulido-Villena, E., Reche, I., 2006. Atmospheric inputs of phosphorus and nitrogen to the southwest Mediterranean region: Biogeochemical responses of high mountain lakes. *Limnol. Oceanogr.* **51**, 830-837.

Posch, T., Loferer-Krößbacher, M., Gao, G., Alfreider, A., Pernthaler, J., Psenner, R., 2001. Precision of bacterioplankton biomass determination: A comparison of two fluorescent dyes, and of allometric and linear volume-to-carbon conversion factors. *Aquat. Microb. Ecol.* **25**, 55-63.

Rocha, O., Duncan, A., 1985. The relationship between cell carbon and cell volume in freshwater algal species used in zooplankton studies. *J. Plankton Res.* **7**, 279-294.

Tanaka, J.S., 1987. How big is enough? sample size and goodness of fit in structural equation models with latent variables. *Child Devel.* **58**, 134-146.

Zar, J.H., 1999. Biostatistical analysis, 4th ed. Prentice Hall, Englewood Cliffs, NJ.

Zubkov, M.V., Burkill, P.H., 2006. Syringe pumped high speed flow cytometry of oceanic phytoplankton. *Cytom. A* **69**, 1010-1019.

Zubkov, M.V., Burkill, P.H., Topping, J.N., 2007. Flow cytometric enumeration of DNA-stained oceanic planktonic protists. *J. Plankton Res.* **29**, 79-86.

Chapter VI

Saharan dust inputs and high UVR levels jointly alter the metabolic balance of marine oligotrophic ecosystems

Abstract

The metabolic balance of the most extensive bioma on the Earth is a controversial topic of the global-change research. High ultraviolet radiation (UVR) levels by the shoaling of upper mixed layers and increasing atmospheric dust deposition from arid regions may unpredictably alter the metabolic state of marine oligotrophic ecosystems. We performed an observational study across the south-western (SW) Mediterranean Sea to assess the planktonic metabolic balance and a microcosm experiment in two contrasting areas, heterotrophic nearshore and autotrophic open sea, to test whether a combined UVR $\times$ dust impact could alter their metabolic balance at mid-term scales. We show that the metabolic state of oligotrophic areas geographically varies and that the joint impact of UVR and dust inputs prompted a strong change towards autotrophic metabolism. We propose that this metabolic response could be accentuated with the global change as remote-sensing evidence shows increasing intensities, frequencies and number of dust events together with variations in the surface UVR fluxes on SW Mediterranean Sea. Overall, these findings suggest that the enhancement of the net carbon budget under a combined UVR and dust inputs impact could contribute to boost the biological pump, reinforcing the role of the oligotrophic marine ecosystems as CO_2 sinks.

Introduction

Several global studies during the last two decades have shown the high prevalence of heterotrophic metabolism into the ocean, particularly in oligotrophic ocean areas (del Giorgio et al., 1997; Duarte & Agustí, 1998). Currently, however, the metabolic balance of oceans poses a heated debate, as reflected in the studies of Duarte et al. (2013) and Williams et al. (2013) where their autotrophy or heterotrophy, respectively, are defended. Nevertheless, both perspectives agree that the oligotrophic ocean

is a 'single steady-stable' ecosystem where the metabolic balance remains roughly invariant across spatio-temporal scales. By contrast, Serret et al. (2015) question the paradigm of the heterotrophy and propose that the oligotrophic ocean is "neither auto- nor heterotrophic, but functionally diverse." Most of the results published to date on this issue derive from oceanographic transects and short-term (hours) experiments. Moreover, most of these studies have involved almost exclusively open-ocean areas, whereas less (or scarce) attention has been directed towards coastal areas, where previous studies have shown a contrasting response of planktonic metabolism (autotrophy or heterotrophy) (Regaudie-de-Gioux & Duarte, 2013).

Global climate change is expanding the stratification in nearshore and open-sea oligotrophic areas (i.e., oceanic gyres) (Polovina et al., 2008) and increasing faster respiration rates than photosynthesis, as the Metabolic Theory of Ecology predicts (Brown et al., 2004) and as observations have confirmed (Yvon-Durocher et al., 2010). Global-change research also predicts higher climate variability, with greater nutrient availability due to severe droughts and harsher aridity, and increases in solar radiation exposure due to shallower upper mixed layers (IPCC, 2013). Deserts supply prodigious amounts of dust that affect both human concerns (i.e., weather, climate and health) (Jickells et al., 2005; Vinoj et al., 2014) and ecosystem productivity by providing key nutrients to stimulate the growth of planktonic communities (Gunnarsson et al., 2015; Moore et al., 2013). Particularly in aquatic ecosystems, studies have reported that nutrients associated with dust inputs tend to stimulate primary production (PP) (Bonnet et al., 2005; Mills et al., 2004; Ridame et al., 2014) and bacterial production (Bonilla-Findji et al., 2010), altering the structure of microbial planktonic communities (Lekunberri et al., 2010; Pulido-Villena et al., 2014) or biogeochemical cycles (Ridame & Guieu, 2002). Other studies, however, have also shown negative effects of dust on marine biota, due to the presence of high concentrations of toxic elements for growth (e.g., copper, cadmium or lead) (Hoffmann et al., 2012).

Together with dust-derived nutrient inputs, the other key factor that modulates the plankton responses is solar radiation. Within the euphotic zone, autotrophic organisms use photosynthetically active radiation (PAR) to drive photosynthesis, but in the upper part of this layer, cells are also exposed to high levels of ultraviolet radiation (UVR). A huge body of literature has shown their negative effects on metabolism and physiology of autotrophs (Williamson et al., 2014) and heterotrophs (Ruiz-González et al., 2013). However, positive effects of UVR on both compartments have also been shown, such as increased photorepair DNA damage (Helbling et al., 2003; Matallana-Surget et al., 2009) or enhanced photosynthesis (Gao et al., 2007).

Thus, understand the impact of these stressors (dust deposition and UVR) on planktonic communities is central for predicting the effects of global change on the metabolic balance, and consequently, determine whether planktonic communities act as net sinks or sources of CO_2 affecting the atmosphere-ocean transfer (Duarte & Prairie, 2005). In fact, a growing body of literature shows that the stressors can interact suppressing or amplifying their effects; hence their impacts can differ from their additive or single effects leading to ecological surprises (Brennan & Collins, 2015; Boyd et al., 2016). However, currently there is no direct empirical evidence quantifying how the effects of dust inputs and UVR on the planktonic metabolic balance shifts across temporal and spatial scales in environments with heterogeneous physical, chemical and biological characteristics (Hewitt et al., 2007; Sandman et al., 2013), such as nearshore and open-sea areas. Comparatively, nearshore areas usually have higher concentrations of organic and inorganic materials than does the open sea due to the great influence of riverine and continental runoff inputs, which also diminish the penetration of UVR into the water column (Häder et al., 2014). Thus, nearshore plankton communities are commonly more sensitive to UVR impact than are those of the open sea as the cells are adapted to darker environments and possess fewer protective mechanisms (Buma et al., 2009).

With this background, in this work we quantified for the first time (i) total PP (PP_{total}) and community respiration (CR) rates and the production / respiration metabolic balance (P/R ratio) across the South-western Mediterranean Sea (Alboran Sea); and (ii) the combined impact of Saharan dust inputs under high UVR levels on metabolic balance of planktonic communities through a microcosm experiment from two contrasting areas, one heterotrophic and other autotrophic. Ultimately, our aim was to identify whether the interaction of the two stressors will change the metabolic balance in these oceanic areas over short and mid-term scales in a future global-change scenario.

Material and Methods

Remote-sensing data

Daily area-average aerosol index (AI) and surface short-wave (SW) fluxes (i.e., UVR) for all Alboran Sea region (36° 43′ 5.1594" – 35° 22′ 0.4794" N, 5° 5′ 51.7194" – 1° 59′ 58.2" W) (SW Mediterranean Sea) were downloaded from Giovanni v 4.18.3 (http://disc.sci.gsfc.nasa.gov/giovanni). For 1979 – 2016 period, AI data used were provided by TOMS Nimbus-7 (January 1, 1979 – May 5, 1993), TOMS EP (July 22, 1996 – December 13, 2005) and OMI (December 14, 2005 – March 13, 2016) satellites. For 1980 – 2016, surface UVR-flux data used were provided by the MERRA-2 model. Previous studies in Mediterranean ecosystems have shown a highly positive correlation of AI with total phosphorus (TP) and particulate matter linked to dry atmospheric dust deposition (Morales-Baquero et al., 2006). We used annual means of area-average AI and SW-flux data as a measure of intensity of atmospheric dust deposition and incident irradiance on surface waters of Alboran Sea, respectively. Moreover, because previous studies in Mediterranean ecosystems have established that an AI = 1 constitutes the threshold between mild and intense events of dust deposition and AI $\geq$ 1

are the main contributors to the total annual AI (Bullejos et al., 2010), only AI ≥ 1 were considered during the 1978-2015 period. We also estimated the annual frequency of these events as the number of days per year affected by intense deposition events.

Observational and experimental study

Our study was conducted aboard of the Spanish B. O. Francisco de Paula Navarro cruiser from 16 to 21 June of 2014 during the MICROSENS campaign. The observational study comprised a total of 14 stations over the SW Mediterranean Sea to quantify the metabolism of planktonic communities. At each station, surface (5 m depth) seawater samples were collected using 10-L Niskin bottles and screened with 200 μm Nitex mesh to remove mesozooplankton (see all details about measurements below). In addition, additional integrated samples from the surface up to 15 m depth (300 L per area) in a nearshore (outside the West anticyclonic gyre, 36° 37′ N, 4° 24′ W - heterotrophic 1) and open-sea station (area inside this gyre, 35° 59′ N, 4° 19′ W – autotrophic 1) were also used in an experimental manipulation study, to assess the interactive effect of heavy Saharan dust inputs and high UVR fluxes, as expected in a global-change scenario (see details below). The rationale behind mixing water samples from various depths was to ensure a composite sample representative of the UML characterized by nearly uniform conditions. The sampling at discrete depths up to 15 m was also well justified by: (1) we did not found significant differences in P/R ratios between surface and at 15 m depth for both areas (data not shown) and (2) because a recent study in Alboran Sea during 1969-2012 have showed that during our sampling period the UML oscillate between 15 ($\pm$ 10) – 30 ($\pm$ 15) meters (Houpert et al., 2015). In addition, we also considered previous findings by Marañón et al. (2010) and Pulido-Villena et al. (2008) that showed that a dust enrichment caused by a high deposition event can reach up to 10 – 15 m depth.

The original integrated seawater samples from each area were sorted, mixed and placed in two different opaque containers (150 L), one with seawater with ambient nutrient conditions and the other enriched with Saharan dust-nutrient inputs. Immediately after dust additions, the seawater was dispensed into microcosms consisting in 15-L UVR-transparent low-density polyethylene bags (LDPE) (Plasticos Andalucia, Spain). To assess interactive effects of UVR and Saharan dust inputs, a 2 × 2 matrix in triplicate was implemented with: 1) two radiation treatments, PAB (UVR + PAR, > 280 nm, microcosms covered with LDPE) and P (PAR, > 400 nm, microcosms covered with Ultraphan UV 395 Opak Difegra film) and 2) two dust treatments, ambient (amb) (nutrient conditions at the sampling moment) and dust (i.e., enriched with 4.1 mg L^{-1} final concentration of Saharan dust). The LDPE used transmits 90% of photosynthetic active radiation, 75% of UV-A and 60% of UV-B, whereas Ultraphan UV 395 Opak Difegra film transmits > 90% of PAR but screens out UVR (< 390 nm). At the laboratory, and prior to the in situ experiment, the Saharan soil collected *in situ* in Merzouga (Tafilalet, Morocco; 31° 06′.00 N 3° 59′.24 W) was dry-sieved with a custom column knotted with wire mesh cloth of 1 mm and 100 mm pore size and dust was collected on a steel foil underneath the nest of sieves. The particles collected were then winnowed near a tilted glass and particles that adhered to the glass were gently collected with a fine brush. The size distributions of the sieved particles (1 – 10 μm) (Leitz Fluovert FS, Leica, Wetzlar, Germany) were broadly comparable with those of mineral dust collected in rain samples (5 – 10 μm), although had a slightly smaller size (10 – 20 µm) than sieved dust samples of Marañón et al. (2010). We used sieved dust samples within this range because of dust particles > 20 μm are rapidly removed during the atmospheric transport; in addition, at a certain distance from its source, soil-derived dust constitutes a coarse aerosol mode with a mean range of particle size between 2-7 μm (Guieu et al., 2010).

The dust concentration simulated the dust enrichment caused by an event of high deposition (61.5 g m^{-2}) in a 15-m surface-water layer. Recent observations show that annual dust-deposition rates vary widely (spatially

and temporally) across the Mediterranean Sea, with values ranging between 2 to 27 g m^{-2} yr^{-1} in the western basin (Vincent et al., 2015). In addition, most of the Saharan dust-deposition events tend to occur in pulses, and hence sometimes a single event can account for 40-80% of the annual flux registered into an ecosystem (Guerzoni et al., 1997). Therefore, in our experimental addition we simulate a plausible future deposition scenario which represents increases of more than 2-fold with respect to the total dust deposition received by the Mediterranean basin every year currently. After the microcosms were filled and amended with dust, they were suspended in two large black-painted tanks (ca. 800 L each; 1 for nearshore samples and 1 for open-sea samples) where were incubated during five days. We maintained the *in situ* temperature in both tanks by continuously pumping surface sea water. In addition, we manually shook the microcosms every hour to avoid that organisms settle so that they would receive homogeneous irradiances. The samples used in the incubations were taken using a manual vacuum syringe connected to an acid-washed silicone tube inserted in each microcosm.

Analyses and measurements

Solar radiation and physico-chemical characteristics of the water column

Incident solar radiation on microcosms was monitored daily using a BIC Compact multichannel radiometer (Biospherical Instruments Inc., CA, USA) installed on the top of the ship-deck with 3 channels for UVR portion, one for UV-B (305 nm) and two for UV-A (320 and 380 nm) and one broad-band channel for PAR (400-700 nm). At each station, underwater profiles of solar radiation were made with a submergible-BIC Compact multichannel radiometer (Biospherical Instruments Inc., CA, USA) with the same 4 radiation channels that mentioned above. Vertical profiles of temperature, pH, salinity and conductivity (down to 25 m) were taken using a sealogger

CTD SBE 25 (Sea-Bird Electronics, Inc., WA, USA).

Chlorophyll *a*

At each station (3 L) and every day at sunrise from each microcosm (3 L on June 17^{th}, and 1 L the following days), seawater samples for chlorophyll *a* (Chl *a*) determinations were immediately filtered onto Whatmann GF/F filters (25 mm diameter) and stored at -20°C until analysed. At the laboratory, the photosynthetic pigments were extracted in absolute methanol in darkness at 4°C for 24 h (Jeffrey & Humphrey, 1975) and were measured using a fluorometer (Perkin Elmer, model LS 55) which is routinely calibrated using a Chl *a* standard (Chl *a* from spinach, Sigma-Aldrich).

Autotrophic plankton counting

During the first and the last day, water samples from each microcosm were taken and preserved in brown glass bottles (125 mL) using alkaline Lugol's reagent (ca. 1% vol/vol) to identify and quantify autotrophic nanoplankton (ANP). An aliquot of 50 mL from each sample was settled in an Utermöhl chamber of 2.6 cm diameter for 48 h to ensure complete sedimentation of the smallest phytoplankton species and counts were made at 400× and 1000× magnification under an inverted microscope (Carl Zeiss AX10, LCC, USA). Also, 1.5 mL of sample was fixed with 75 μL of particle-free 20% (w/v) paraformaldehyde (1% final concentration) and immediately frozen in liquid nitrogen until analysed to quantify cell abundance of autotrophic picoplankton (APP) using a flow cytometer (FACSCanto II, Becton Dickinson Biosciences, Oxford, UK) (see details below). For ANP samples, at least 400 cells of the most abundant species were counted, and 20 cells of each species were measured to estimate cell volume according to a corresponding geometrical shape (Hillebrand et al., 1999), whereas biovolume for APP was calculated following Ribés et al. (1999). Biovolumes were

converted into carbon biomass using the formulas and coefficients proposed by Verity et al. (1992).

Heterotrophic plankton counting

Heterotrophic picoplankton (HPP) abundance was determined by the flow cytometry technique (FACSCanto II, Becton Dickinson Biosciences, Oxford, UK), fixing 1.5 mL of sampling water with 75 μL of particle-free 20% (w/v) paraformaldehyde (1% final concentration) and immediately frozen in liquid nitrogen until analysis. Before being analysed, unfrozen samples were stained using Syber–Green I DNA (Sigma-Aldrich, Co Ltd) 1:5000 final dilution (Gasol & del Giorgio, 2000; Zubkov et al., 2007). In addition, yellow-green 1 μm beads at standard concentration (10^5 particles mL^{-1}) (Fluoresbrite Microparticles, Polysciences, PA, USA) were also added to determine the absolute cellular concentrations (Zubkov et al., 2007; Zubkov & Burkill, 2006). Phycoerythrin and Chl *a* fluorescence signals were used to distinguish between APP and HPP (Mercado et al., 2006). HPP biomass values were estimated by approximating cell volume to their geometric shape and afterwards transform it to carbon units following suitable conversion factors (Posch et al., 2001).

Nutrient and dissolved organic carbon analyses

Triplicate samples from each station and microcosm were placed in 300 mL PET plastic bottles and frozen (-20°C) until nutrient analyses. To determine total nitrogen (TN), total dissolved nitrogen (TDN), total phosphorus (TP) and total dissolved phosphorus (TDP) concentrations, the samples were processed using the simultaneous persulphate oxidation method proposed by Koroleff (1977). For dissolved organic carbon (DOC) determination from each station and microcosm, triplicate seawater samples (150 mL) were filtered through pre-combusted (500°C during 2h) GF/F Whatmann

filters (25 mm diameter). Afterwards, they were acidified with HCl 1N (2%) and stored in darkness at 4°C until analysis. At the laboratory, DOC concentrations were measured with a TOC analyzer (Shimandzu, model 5000) following the procedure of Benner & Strom (1993).

^{14}Carbon incorporation measurements

One set of 42 samples in total for the observational study (duplicate clear bottles and one dark per station) plus one set of 32 daily samples for the experimental study (triplicate clear bottles and one dark bottle) were taken and inoculated with 5 μCi of labelled sodium bicarbonate to measure carbon incorporation as primary production (PP) following the method proposed by Steemann-Nielsen (1952). The experimental bottles were 35-mL UV-transparent Teflon FEP narrow-mouth bottles (Nalgene), uncovered (clear bottles) or covered with opaque adhesive foil (black bottles). All Teflon FEP bottles were then placed in the same tank of controlled-temperature as the microcosms and exposed for 4 h to solar radiation. Particulate PP was determined by filtering 30 mL through Whatmann GF/F filters (25 mm in diameter) at low pressure (< 100 mmHg) to avoid cell breakage, whereas a subsample of 4 mL of the filtrate was directly collected in scintillation vials to assess ^{14}C activity in the dissolved organic carbon fraction (i.e., DO^{14}C). After this, filters and filtrates were exposed to acid fumes for 24 h by adding 1N HCl (2%) to eliminate the non-assimilated ^{14}C. Finally, each sample was measured using a scintillation counter LS-6000 TA (Beckman). The total CO_2 in seawater samples was calculated from the alkalinity and pH measurements (APHA, 1992). In all calculations, the dark values were subtracted from the corresponding light values. PP_{total} was calculated as the sum of particulate PP plus the DOC fraction released by phytoplankton.

Oxygen concentration measurements

One set of 28 samples in total for the observational study (in duplicate per station) plus one set of 24 daily samples, for each experimental day (in triplicate per experimental treatment and area), were used to fill (without bubbles) 35-mL UV-transparent Teflon FEP narrow-mouth bottles (Nalgene) equipped with sensor spots (SP-PSt3-NAU-D5-YOP), sealed to avoid gas exchanges and incubated in darkness to measure the oxygen concentration during 12 h using an oxygen transmitter (Fibox 3, Presens GmbH, Germany) equipped with Oxyview 6.02 software to register data. Previously, the system was calibrated by a two-point calibration (0% and 100% oxygen saturation) together with temperature and atmospheric pressure data. From the resulting oxygen concentration data, we calculated the community respiration (CR) rates as the slope of the regression fit for decreases in oxygen concentration *vs.* time. The CR rates (in oxygen units) were converted into C units assuming a respiratory quotient of 1 (del Giorgio & Cole, 1998).

Data and statistical analyses

We evaluated the effect size of UVR under both dust treatments on PP_{total} and CR as:

$$\text{Effect size of UVR} = \text{PAB}_X/\text{P}_X,$$

being X the ambient or dust treatment. A value > 1 mean a stimulatory ultraviolet radiation (UVR) effect, whereas < 1 an inhibitory UVR effect for each nutrient treatment.

Statistical analyses for each experimental area (nearshore and open sea) were done separately. The effects of UVR, dust and their interaction on planktonic biomass of ANP, APP and HPP at the end of the experiment

were tested by a two-way analysis of variance (ANOVA). Because several interactions occurred within each planktonic group, these are highlighted in the text accordingly. A one-way repeated measures ANOVA (RM-ANOVA) was used to test whether the dust addition modified the effect size of UVR on PP_{total} and CR over the experiment. When significant interactions were detected, a *post hoc* least significant differences (LSD) test was performed. Also, a linear regression analysis was applied to relate the trend in the number of events of AI ≥ 1 *vs.* time. When appropriate, some of the data (e.g., DOC) were tested for significant differences using Student's t-test. Data were checked for normality (Shapiro-Wilk's test), and homoscedasticity (Levene's test) assumptions. All data are reported as mean values and standard deviations, whereas error propagation was used in the effect size of UVR on PP_{total} and CR. The metabolic balance data for each station across the SW Mediterranean Sea were represented using Ocean Data View v. 4.7.6 (Schlitzer, 2015).

Results

Long-term trends in AI and short-wave fluxes on SW Mediterranean Sea

The daily area-average AI and monthly area-average surface SW fluxes varied greatly through the 1979 and 1980 – 2016 period (Fig. S1). This variability resulted in alternating years with a characteristically strong seasonality in aerosol inputs (i.e., increasing AI values from May to September and maximum peaks in July – August) (e.g., year 2012, Fig. S1) followed by years where a slightly constant input of aerosols occurred (e.g., year 2013 – 2014, Fig. S1). AI also showed a clear oscillation in the total number of events, as well as, in the annual values over the study period (Fig. 1). Thus, we found periods of 6 – 8 years where total number of AI > 1 events significantly increased or decreased (Fig. 1). Despite these oscillating peri-

odic cycles, a significantly increasing frequency in the events registered was found over a long-term scale (Fig. 1; $R^2 = 0.28$, $F_{12.51}$, $p < 0.01$). For SW fluxes, a marked intra-annual seasonality was found (Fig. S1); however, these fluxes did not exhibit a clear trend over the time (Fig. 1).

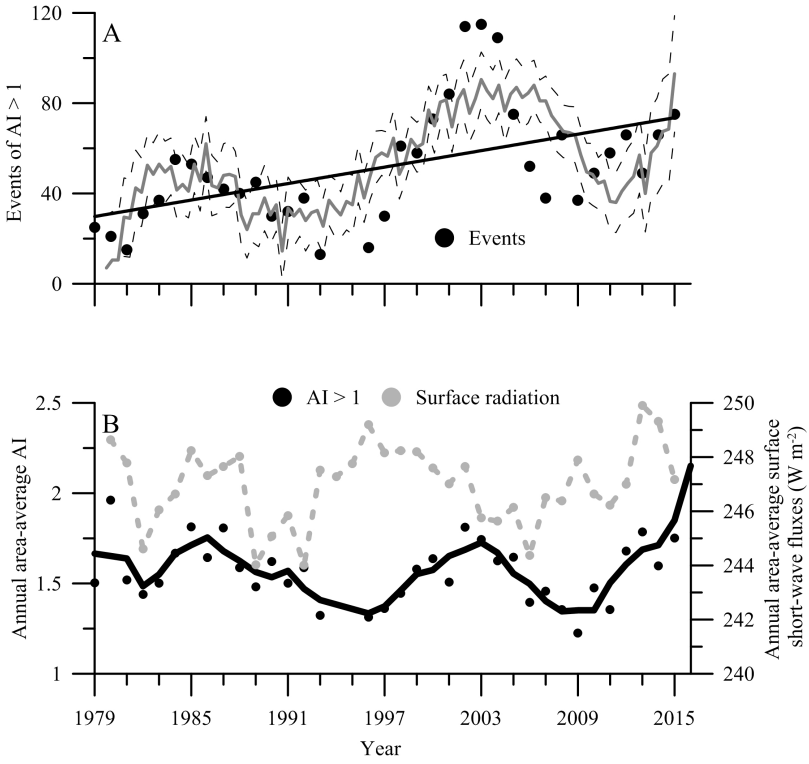

Figure 1: (A) Temporal pattern of total events of area-average aerosol index (AI > 1) for the 1979-2016 period. Solid grey trend line denotes the temporal response pattern using a non-linear fit of annual AI > 1 events vs. time with the Levenberg-Marquardt model. Dashed lines represent 95% confidence bands and the solid black line the regression line. (B) Mean annual area-average aerosol index (black circles, AI > 1, relative units) and surface short-wave radiation fluxes (grey circles, in W m^{-2}) on Alboran Sea for 1979-2016 period. Solid lines represent smoothed trend for both measurements using a polynomial Savitzky-Golay fitting model.

Observational study

Metabolic balance

In relation to the underwater radiation field, the profiles in all stations showed a high transparency to UVR (kd_{305} = 0.32 – 0.44, kd_{320} = 0.23 – 0.77, kd_{380} = 0.1 – 0.93) and PAR (kd_{PAR} = ranging between 0.01 – 0.14). Seawater temperature was relatively uniform across the SW Mediterranean Sea with mean values 21.47°C (± 0.71), from surface to 25 m deep across the study section (Table S1). Chl *a* concentrations were very low, with values below 1 μg L^{-1}, excepting four cases (stations 3, 5, 6 and 7), where Chl *a* concentrations rose to ca. 2 μg L^{-1} (Table S1). Nutrient concentrations were also generally low (Table S1), particularly TP with values < 0.9 μM, whereas TN showed values ranging between 228 and 357 μM across the Mediterranean Sea section studied. DOC concentrations averaged 197 μM, although with concentrations varying between 119 and 323 μM (Table S1). PP_{total} varied between 10 (± 1) and 118 (± 1) mmol C m^{-3} d^{-1}, whereas, CR did between 33 (± 12) and 105 (± 0.10) mmol C m^{-3} d^{-1}. This range of values in PP_{total} and CR rates was translated into P/R ratios that ranged between 0.15 and 1.84, indicating an alternation between auto and heterotrophic stations across the studied section (Fig. 2; Table S1).

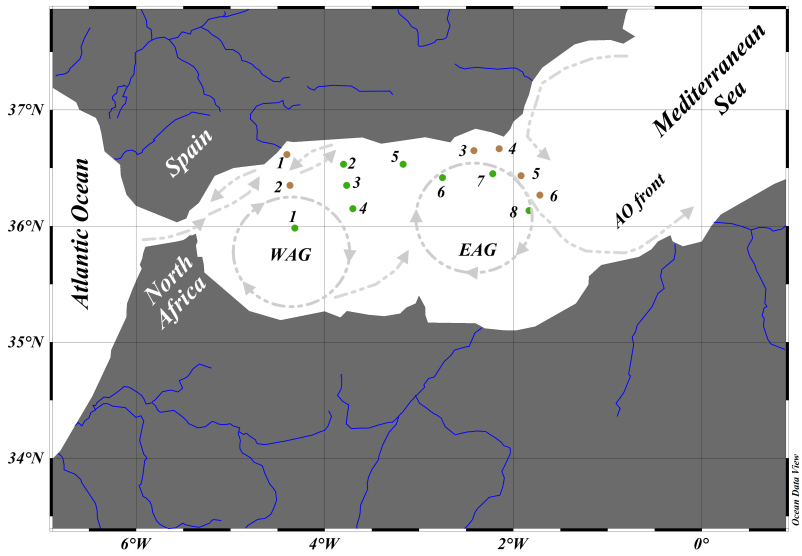

Figure 2: Geographical distribution of the different stations where the planktonic metabolism was measured during the Microsens campaign. Brown and green circles represent heterotrophic and autotrophic stations, respectively, whereas uppercase abbreviations means Western anticyclonic (WAG), Eastern anticyclonic (EAG) gyres and Almeria-Oman front (AO) and blue lines the main rivers in southern Spain and North Africa. Map was created using Ocean Data View v. 4.7.6 (https://odv.awi.de). Note that gyres are represented in relative magnitude and shape.

Experimental study

Physical, chemical and biological conditions

Sky conditions during the experimental period were characterized by slightly overcast days, particularly on June, 19^{th} and 20^{th}. Maximum irradiance received by samples during the experiment reached 6.4 (for 305 nm), 35.1 (for 320 nm) and 93.6 (for 380 nm) μW cm^{-2} and 534.9 (for PAR) W m^{-2}, whereas mean daily irradiance during the exposure period oscillated

between 2.03 – 2.82, 15.60 – 19.30 and 41.60 – 52.30 μW cm^{-2} and 225.60 – 282.30 W m^{-2}, respectively, for 305, 320, 380 nm, and PAR (Fig. S2). At the beginning of the experiments, both areas showed high TN and low TP concentrations, and high sestonic N:P ratios which were 2-fold higher in heterotrophic than in autotrophic communities (Table S2). By contrast, DOC concentrations were similar in both areas at the beginning (t-test = 1.45, p > 0.05) and overall decreased through the experiments, up to mean concentrations of 188.65 (± 2.26) and 196.68 (± 9.43) μM for heterotrophic and autotrophic communities, respectively. In terms of biomass, the autotrophic nanoplankton (ANP) fraction dominated the community in both areas and in all treatments with respect to the heterotrophic picoplankton (HPP) (< 40 μg C L^{-1}) and autotrophic picoplankton (APP) fraction (< 2 μg C L^{-1}) over the experiment. However, only in open sea did UVR negatively affect the ANP and HPP fractions regardless the dust treatment, significantly lowering values by ca. 50% (Fig. 3; Table S3).

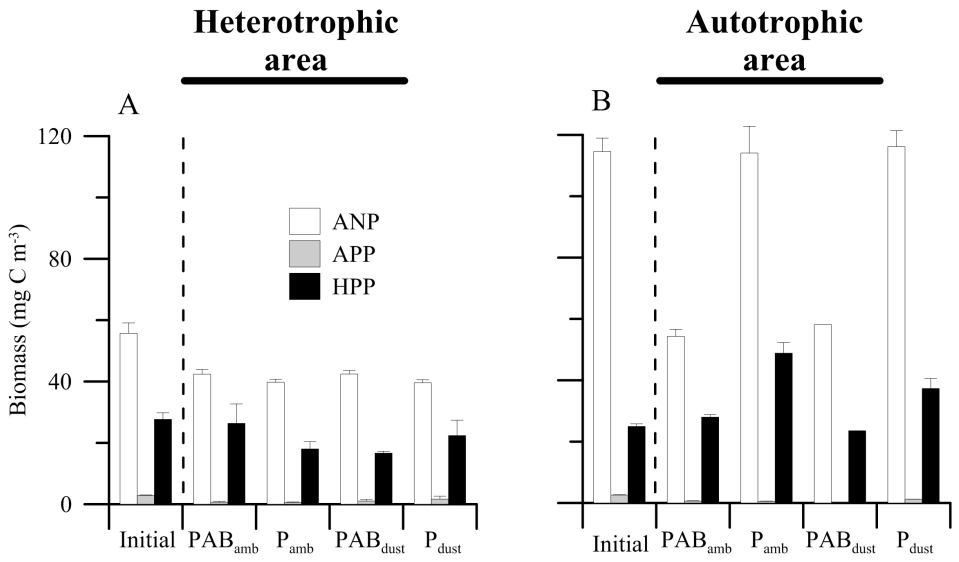

Figure 3: Mean (± SD) biomass (in mg C m^{-3}) (A, B) of autotrophic nanoplankton (ANP), autotrophic picoplankton (APP) and heterotrophic picoplankton (HPP) in the microcosms at the beginning of the experiment (initial) and after 5 days of exposure under PAB (> 280 nm) and PAR (P, > 400 nm) radiation treatments and two dust treatments, ambient (amb) and dust treatments in the heterotrophic and autotrophic area. The letters and numbers on top of the bars indicate the result of the LSD *post hoc* test.

UVR and Dust effects on the metabolic balance

In the heterotrophic area, PP_{total} significantly increased in all treatments, with values ranging between ca. 10 at the beginning and up to ca. 55 – 60 mmol C m^{-3} d^{-1} at the end of experiment (Fig. S3; Table S4). In the autotrophic area, PP_{total} slightly increased only under PAB_{amb} and P_{dust} treatments with respect to the initial conditions (Fig. S3) but significantly decreased under a combined impact of UVR × Dust. In both areas, the effect size of UVR was stimulatory on PP_{total} under ambient nutrient conditions, although dust addition significantly altered this stimulatory effect of UVR on PP_{total} over the experiment, generating an inhibitory effect that ranged between 30 – 57% and 38 – 74%, for the heterotrophic and autotrophic area, respectively (Fig. 4). By contrast, CR showed significantly higher values at the beginning (heterotrophic area, ca. 28 – 40 mmol C m^{-3} d^{-1} and autotrophic area, 30 – 70 mmol C m^{-3} d^{-1}), which declined over the experiment up to similar rates in both areas regardless of the treatment considered (except PAB_{amb} in autotrophic area) (Fig. S3; Table S4). As with PP_{total}, UVR increased the CR in both areas, whereas the dust also significantly altered the effect size of UVR on CR, increasing the inhibition of CR by between 20 – 60% and 2 – 88% in the heterotrophic and autotrophic area, respectively (Fig. 4; Table S4).

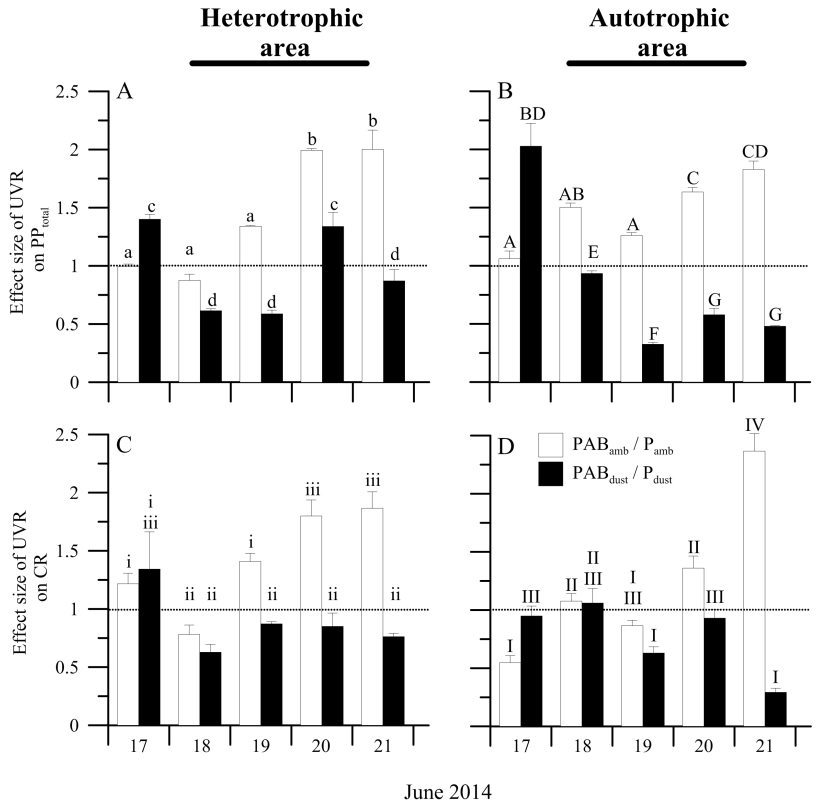

Figure 4: Effect size of UVR (as PAB / PAR ratio) on the mean (± SD) total primary production (A, B) (PP_{total}, in mmol C m^{-3} d^{-1}) and (C, D) mean (± SD) community respiration (CR) rates (in mmol C m^{-3} d^{-1}) in the microcosms during the experiment under two dust treatments, ambient (amb) and dust, in the heterotrophic and autotrophic area. The letters on top of the bars indicate the result of the LSD *post hoc* test, and the horizontal dashed line delineates the positive (> 1) or negative (< 1) ultraviolet radiation effects.

From PP_{total} and CR data (Fig. S3) we calculated the P/R ratio during the experiments, which show a similar response pattern in both areas (Fig. 5). Thus, at short-term P/R ratio was < 1 in both areas and for

all treatments (with the exception of PAB_{amb} in autotrophic area, P/R = 1.09), indicating a clear heterotrophy. Conversely, from the third day to the end of the experiment the P/R ratio was > 1, particularly under PAB_{dust} treatments, due to a surge in PP_{total} coupled with a fall in the CR rates. However, P/R ratio was ca. 1 or consistently < 1 in the autotrophic compared to the heterotrophic area (P/R > 1) under ambient conditions, due to higher CR than PP_{total}, as consequence of increased bacterial respiration under these conditions (data not shown). The metabolic balance changed from heterotrophy (or steady stable communities, P/R = 1) towards strong autotrophy at the end of the experiment under the joint effect of UVR and dust treatments (values between 3.3 - 4.4 for the heterotrophic and autotrophic area, respectively).

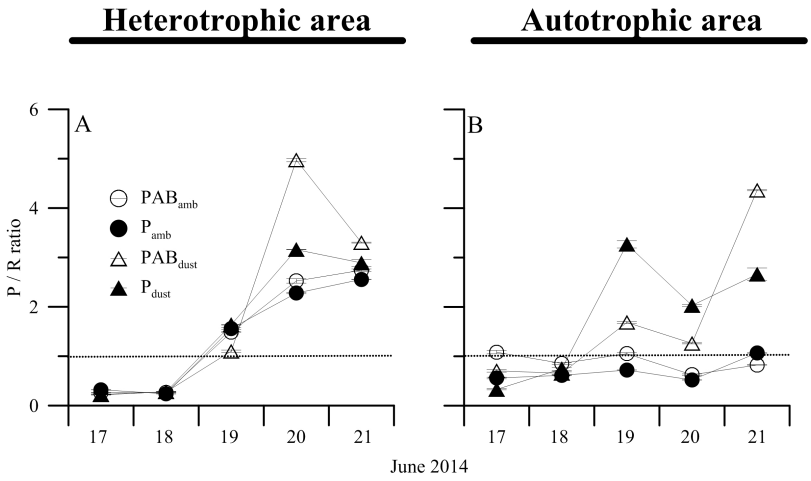

Figure 5: Mean (± SD) total production / respiration (P / R) ratios (A, B) under two radiation treatments, PAB (> 280 nm) and PAR (P, > 400 nm) and two nutrient treatments, ambient (amb) and dust during the experiments in the heterotrophic and autotrophic area.

Discussion

In this study, we report that the metabolic balance of strongly P-limited oligotrophic marine areas vary geographically between heterotrophic and autotrophic states, challenging the mainstream view of oligotrophic ocean as a 'single steady-state' ecosystem with an invariant metabolism across spatio-temporal scales (Duarte et al,. 2013; Williams et al., 2013). However, this spatial pattern showed is consistent with the recent results of Serret et al. (2015) who showed that the Atlantic Ocean (i.e., Oceanic gyres) is neither autotrophic nor heterotrophic but metabolically diverse.

In addition, the values of the metabolic balance of the SW Mediterranean Sea are also in line with previous estimates for other oligotrophic areas worldwide, such as NW and East basin of the Mediterranean Sea (mean P/R = 0.74), the North (mean P/R = 0.75) and South Pacific Ocean (mean P/R = 1.17) and the Indian Ocean (mean P/R = 1.78) (Regaudie-de-Gioux & Duarte, 2013). However, our findings in unproductive waters were between 4 to 7-fold lower that those reported for strongly productive areas in high-latitude environments, i.e. Southern Ocean and Arctic waters. The differences between both areas may be due not only to higher nutrients availability but also the fact that most of studies in the latter areas have been performed during the boreal / austral spring or summer in absence of a dark period in these latitudes. One underlying mechanism that likely can explain these contrasting results may be a strong stimulation of the bacterial respiration and dark-repair processes (Zenoff et al., 2006) during the night at temperate latitudes. However, these processes are inhibited under the midnight sun in the spring-summer Arctic day as recent studies have reported (Agustí et al., 2014; García-Corral et al., 2014).

In view of the metabolic variability observed in our survey and in previous reports over the last two decades (Regaudie-de-Gioux & Duarte, 2013) we investigated whether the metabolic state from two contrasting areas, one heterotrophic and the other autotrophic, could be altered by the joint

action of two major environmental stressors, i.e. Saharan dust inputs and UVR, in a future global-change scenario. Our data further suggests that the trophic state of both areas at the beginning of the experiments was most likely associated with plankton physiological conditions. Thus, not only Chl *a* concentrations were lower, but also the P-limitation was higher and the sestonic C:P and N:P ratios were 2-fold higher in the heterotrophic than the autotrophic area.

We found an inhibitory effect of the two stressors acting together on PP_{total}. These findings partially agree with previous studies in oligotrophic ecosystems (fresh and marine) that showed a higher negative UVR effect after nutrient enrichment on PP due to a decoupling between photosynthesis and growth (Carrillo et al., 2015; Durán et al., 2016). Likewise, a negative synergistic interactive effect of UVR and dust on CR was found. This finding contrasts with recent results showing a rise in respiratory processes under UVR due to an enhanced heterotrophic metabolism (Agustí et al., 2014). By contrast, although dust addition inverted the stimulatory UVR effect, we found that the planktonic metabolic balance showed a clear response pattern towards autotrophy in SW Mediterranean Sea communities at the mid-term, regardless of the area considered. Therefore, greater dust pulses due to a higher frequency and intensity of dust export events from Sahara, as reported here (see Fig. 1), together with high UVR fluxes by shallower upper mixed layers (UML) owing to increased surface temperatures, may induce significant changes in the metabolic state of oligotrophic marine ecosystems.

Despite that the UVR and dust inputs acting in concert depressed the respiratory processes, we found no biomass accumulation in any area over the experiment. The absence of stimulation in the autotrophic biomass compartment agrees with previous results that showed a very small biomass response after similar inorganic nutrient or dust additions (Marañón et al., 2010; Olsen et al., 2006). The most believable explanation behind this observation could be a high lysis rates undergone by phytoplankton during this period, late spring / early summer, as previously shown by Agustí &

Duarte (2000) in Mediterranean coastal waters. Nevertheless, based on our results we can rule out the idea that the stability found in phytoplankton biomass was due to: (i) a potential to toxic effect of metals contained in dust inputs as recent studies have proposed (Paytan et al., 2009), as in our study those concentrations were below detection limits (González-Olalla et al., submitted); or (ii) competition with HPP by nutrients as we found no stimulation of this compartment, either, over the experiment in terms of biomass.

The trend towards an autotrophic balance reported through our experimental study suggests that the combined impact of UVR and dust would bolster the biological pump. Thus, we can speculate that the fate of a larger fraction of carbon fixed by phytoplankton could not be remineralization and release as CO_2 into the atmosphere, as several previous works have suggested for unproductive waters (García-Corral et al., 2015; Regaudie-de-Gioux & Duarte, 2009) but rather it could be exportation from the euphotic zone, contributing the biological pump and reinforcing the marine ecosystems as CO_2 sinks (Agustí et al., 2015). However, we also should consider the potential role that mesozooplankton grazing and respiration play to remove marine primary production and increase carbon losses, respectively, as we directly excluded mesozooplankton in our study. If we assumed that mesozooplankton potentially consume ca. 23% of the total PP (Calbet, 2001; Duarte & Cebrián, 1996) and the respiratory losses of mesozooplankton represent on average the 25% of C ingested from PP (Hernández-León & Ikeda, 2005), zooplankton feeding activity would not substantially alter the trend reported (see Fig. S4).

Conclusion

Finally, and although the metabolic balance in these areas continues to be a great challenge for oceanographic research, observational studies combined with mid-term multi-stressors experiments in contrasting marine areas con-

stitute useful approaches to inform how future alterations due to the global climate change could alter the biotic regulation of CO_2. Despite that we should be cautious in extrapolating these results from a regional scale to a global oceanic scale, they underscore the need to consider that these oligotrophic areas, which suppose about half of the Earth's surface (Serret et al., 2015) could potentially become carbon sinks, at least during certain periods of the annual cycle (e.g., high UVR fluxes, peaks dust inputs) in the upcoming future.

References

Agustí, S., Duarte, C.M., 2000. Strong seasonality in phytoplankton cell lysis in the NW Mediterranean littoral. *Limnol. Oceanogr.* **45**, 940-947.

Agustí, S., González-Gordillo, J.I., Vaqué, D., Estrada, M., Cerezo, M.I., Salazar, G., Duarte, C.M., 2015. Ubiquitous healthy diatoms in the deep sea confirm deep carbon injection by the biological pump. *Nat. Commun.* **6**, 8.

Agustí, S., Regaudie-de-Gioux, A., Arrieta, J.M., Duarte, C.M., 2014. Consequences of UV-enhanced community respiration for plankton metabolic balance. *Limnol. Oceanogr.* **59**, 223-232.

APHA, 1992. Standard methods for the examination of water and wastewater. American Public Health Association, Washington.

Benner, R., Strom, M., 1993. A critical evaluation of the analytical blank asociated with DOC measurements by high-temperature catalytic oxidation. *Mar. Chem.* **41**, 153-160.

Bonilla-Findji, O., Gattuso, J.P., Pizay, M.-D., Weinbauer, M.G., 2010. Autotrophic and heterotrophic metabolism of microbial planktonic communities in an oligotrophic coastal marine ecosystem: Seasonal dynamics and episodic events. *Biogeosciences* **7**, 3491-3503.

Bonnet, S., Guieu, C., Chiaverini, J., Ras, J., Stock, A., 2005. Effect of atmospheric nutrients on the autotrophic communities in a low nutrient, low chlorophyll system. *Limnol. Oceanogr.* **50**, 1810-1819.

Boyd, P.W., Dillingham, P.W., McGraw, C.M., Armstrong, E.A., Cornwall, C.E., Feng, Y.-y., Hurd, C.L., Gault-Ringold, M., Roleda, M.Y., Timmins-Schiffman, E., Nunn, B.L., 2016. Physiological responses of a Southern Ocean diatom to complex future ocean conditions. *Nat. Clim. Change* **6**, 207-213.

Brennan, G., Collins, S., 2015. Growth responses of a green alga to multiple environmental drivers. *Nat. Clim. Change* **5**, 892-897.

Brown, J.P., Gillooly, F., Allen, A.P., Savage, V.M., West, G.B., 2004. Toward a metabolic theory of ecology. *Ecology* **85**, 1771-1789.

Bullejos, F.J., Carrillo, P., Villar-Argaiz, M., Medina-Sánchez, J.M., 2010. Roles of phosphorus and ultraviolet radiation in the strength of phytoplankton–zooplankton coupling in a Mediterranean high mountain lake. *Limnol. Oceanogr.* **55**, 2549–2562.

Buma, A.G.J., Visser, R.J., Van de Poll, W., Villafañe, V.E., Janknegt, P.J., Helbling, E.W., 2009. Wavelength-dependent xanthophyll cycle activity in marine microalgae exposed to natural ultraviolet radiation. *Eur. J. Phycol.* **44**, 515-524.

Calbet, A., 2001. Mesozooplankton grazing effect on primary production: A global comparative analysis in marine ecosystems. *Limnol. Oceanogr.* **46**, 1824-1830.

Carrillo, P., Medina-Sánchez, J.M., Herrera, G., Durán, C., Segovia, M., Cortés, D., Salles, S., Korbee, N., Figueroa, F.L., Mercado, J.M., 2015. Interactive effect of UVR and phosphorus on the coastal phytoplankton community of the Western Mediterranean Sea: Unravelling eco-physiological mechanisms. *PloS One* **10**, e0142987.

del Giorgio, P.A., Cole, J.J., 1998. Bacterial growth efficiency in natural aquatic systems. *Ann. Rev. Ecol. Syst.* **29**, 503-541.

del Giorgio, P.A., Cole, J.J., Cimbleris, A., 1997. Respiration rates in bacteria exceed phytoplankton production in unproductive aquatic systems. *Nature* **385**, 148-151.

Duarte, C.M., Agustí, S., 1998. The CO_2 balance of unproductive aquactic ecosystems. *Science* **281**, 234-236.

Duarte, C.M., Cebrián, J., 1996. The fate of the marine autotrophic production. *Limnol. Oceanogr.* **41**, 1758-1766.

Duarte, C.M., Prairie, Y.M., 2005. Prevalence of heterotrophy and atmospheric CO_2 emissions from aquatic ecosystems. *Ecosystems* **8**, 862-870.

Duarte, C.M., Regaudie-de-Gioux, A., Arrieta, J.M., Delgado-Huertas, A., Agustí, S., 2013. The oligotrophic ocean is heterotrophic. *Ann. Rev. Mar. Sci.* **5**, 551-569.

Durán, C., Medina-Sánchez, J.M., Herrera, G., Carrillo, P., 2016. Changes in the phytoplankton-bacteria coupling triggered by joint action of UVR, nutrients, and warming in Mediterranean high-mountain lakes. *Limnol. Oceanogr.* **61**, 413-429.

Gao, K., Wu, Y., Li, G., Wu, H., Villafañe, V.E., Helbling, E.W., 2007. Solar UV radiation drives CO_2 fixation in marine phytoplankton: A double-edged sword. *Plant Physiol.* **144**, 54-59.

García-Corral, L.S., Agustí, S., Regaudie-de-Gioux, A., Luculano, F., Carrillo-de-Albornoz, P., Wassmann, P., Duarte, C.M., 2014. Ultraviolet radiation enhances Arctic net plankton community production. *Geophys. Res. Lett.* **41**, 1-8.

García-Corral, L.S., Martínez-Ayala, J., Duarte, C.M., Agustí, S., 2015. Experimental assessment of cumulative temperature and UV-B radiation effects on Mediterranean plankton metabolism. *Front. Mar. Sci.* **2**, 48.

Gasol, J.M., del Giorgio, P., 2000. Using flow cytometry for counting natural planktonic bacteria and understanding the structure of planktonic bacterial communities. *Sci. Mar.* **64**, 197-224.

Guerzoni, S., Molinaroli, E., Chester, R., 1997. Saharan dust inputs to the western Mediterranean Sea: Depositional patterns, geochemistry and sedimentological implications. *Deep Sea Res. Pt. II* **44**, 631-654.

Guieu, C., Dulac, F., Desboeufs, K., Wagener, T., Pulido-Villena, E., Grisoni, J.-M., Louis, F., Ridame, C., Blain, S., Brunet, C., Bon Nguyen, E., Tran, S., Labiadh, M.J., Dominici, J.-M., 2010. Large clean mesocosms and simulated dust deposition: A new methodology to investigate responses of marine oligotrophic ecosystems to atmospheric inputs. *Biogeosciences* **7**, 2765-2784.

Gunnarsson, T.G., Arnalds, O., Appleton, G., Méndez, V., Gill, J.A., 2015. Ecosystem recharge by volcanic dust drives broad-scale variation in bird abundance. *Ecol. Evol.* **5**, 2386-2396.

Häder, D.P., Villafañe, V.E., Helbling, E.W., 2014. Productivity of aquatic primary producers under global climate change. *Photochem. Photobiol. Sci.* **13**, 1370-1392.

Helbling, E.W., Gao, K., Gonçalves, R.J., Wu, H., Villafañe, V.E., 2003. Utilization of solar UV radiation by coastal phytoplankton assemblages off SE China when exposed to fast mixing. *Mar. Ecol. Prog. Ser.* **259**, 59-66.

Hernández-León, S., Ikeda, T., 2005. A global assessment of mesozooplankton respiration in the ocean. *J. Plankton Res.* **27**, 153-158.

Hewitt, J.E., Thrush, S.F., Dayton, P.K., Bonsdorff, E., 2007. The efect of spatial and temporal heterogeneity on the design and analysis of empirical studies of scale-dependent systems. *Am. Nat.* **169**, 398-408.

Hillebrand, H., Dürselen, C.D., Kirschtel, D., Pollingher, U., Zohary, T., 1999. Biovolume calculation for pelagic and benthic microalgae. *J. Phycol.* **35**, 403-424.

Hoffmann, L.J., Breitbarth, E., Ardelan, M.V., Duggen, S., Olgun, N., Hassellöv, M., Wängberg, S.-Å., 2012. Influence of trace metal release from volcanic ash on growth of *Thalassiosira pseudonana* and *Emiliania huxleyi*. *Mar. Chem.* **132**, 28-33.

Houpert, L., Testor, P., Durrieu de Madron, X., Somot, S., D'Ortenzio, F., Estournel, C., Lavigne, H., 2015. Seasonal cycle of the mixed layer, the seasonal thermocline and the upper-ocean heat storage rate in the Mediterranean Sea derived from observations. *Progr. Oceanogr.* **132**, 333-352.

http://disc.sci.gsfc.nasa.gov/giovanni.

IPCC, 2013. Climate Change. The Physical Science Basis. Cambridge University Press, New York, USA.

Jeffrey, S.W., Humphrey, G.F., 1975. New spectrophotometric equations for determining chlorophylls *a*, *b*, c_1 and c_2 in higher plants, algae and natural phytoplankton. *Biochem. Physiol. Pflanzen (BBP)* **167**, 191-194.

Jickells, T.D., An, Z.S., Andersen, K.K., Baker, A.R., Bergametti, C., Brooks, N., Cao, J.J., Boyd, P.W., Duce, R.A., Hunter, K.A., Kawahata, H., Kubilay, N., LaRoche, J., Liss, P.S., Mahowald, N., Prospero, J.M., Ridgwell, A.J., Tegen, I., Torres, R., 2005. Global iron connections between desert dust, ocean biogeochemistry, and climate. *Science 308*, 67-71.

Koroleff, F., 1977. Simultaneous persulphate oxidation of phosphorous and nitrogen compounds in water., in: Grasshoff, K. (Ed.), Report on the Baltic intercalibration workshop, Kiel, Germany.

Lekunberri, I., Leport, T., Romero, E., Vázquez-Domínguez, E., Romera-Castillo, C., Marrasé, C., Peters, F., Weinbauer, M., Gasol, J.M., 2010. Effects of a dust deposition event on coastal marine microbial abundance and activity, bacterial community structure and ecosystem function. *J. Plankton Res.* **32**, 381-396.

Marañón, E., Fernández, A., Mouriño-Carballido, B., Martínez-García, S., Teira, E., Cermeño, P., Chouciño, P., Huete-Ortega, M., Fernández, E., Calvo-Díaz, A., Morán, X.A.G., Bode, A., Moreno-Ostos, E., Varela, M.M., Patey, M.D., Achterbergf, E.P., 2010. Degree of oligotrophy controls the response of microbial plankton to Saharan dust. *Limnol. Oceanogr.* **55**, 2339-2352.

Matallana-Surget, S., Douki, T., Cavicchioli, R., Joux, F., 2009. Remarkable resistance to UVB of the marine bacterium *Photobacterium angustum* explained by an unexpected role of photolyase. *Photochem. Photobiol. Sci.* **8**, 1313-1320.

Mercado, J.M., Ramírez, T., Cortés, D., Sebastián, M., Reul, A., Bautista, B., 2006. Diurnal changes in the bio-optical properties of the phytoplankton in the Alboran Sea (Mediterranean Sea). *Estuar. Coast. S. Sci.* **69**, 459-470.

Mills, M.M., Ridame, C., Davey, M., La Roche, J., Geider, R.J., 2004. Iron and phosphorus co-limit nitrogen fixation in the eastern tropical North Atlantic. *Nature* **429**, 292-294.

Moore, C.M., Mills, M.M., Arrigo, K.R., Berman-Frank, I., Bopp, L., Boyd, P.W., Galbraith, E.D., Geider, R.J., Guieu, C., Jaccard, S.L., Jickells, T.D., La Roche, J., Lenton, T.M., Mahowald, N.M., Marañón, E., Marinov, I., Moore, J.K., Nakatsuka, T., Oschlies, A., Saito, M.A., Thingstad, T.F., Tsuda, A., Ulloa, O., 2013. Processes and patterns of oceanic nutrient limitation. *Nat. Geosci.* **6**, 701-710.

Morales-Baquero, R., Pulido-Villena, E., Reche, I., 2006. Atmospheric inputs of phosphorus and nitrogen to the southwest Mediterranean region: Biogeochemical responses of high mountain lakes. *Limnol. Oceanogr.* **51**, 830-837.

Olsen, Y., Agustí, S., Andersen, T., Duarte, C.M., Gasol, J.M., Gismervik, I., Heiskanen, A.-S., Hoell, E., Kuuppo, P., Lignell, R., Reinertsen, H., Sommer, U., Stibor, H., Tamminen, T., Vadstein, O., Vaqué, D., Vidal, M., 2006. A comparative study of responses in plankton food web structure and function in contrasting European coastal waters exposed to experimental nutrient addition. *Limnol. Oceanogr.* **51**, 488-503.

Paytan, A., Mackey, K.R.M., Chen, Y., Lima, I.D., Doney, S.C., Mahowald, N., Labiosa, R., Post, A.F., 2009. Toxicity of atmospheric aerosols on marine phytoplankton. *Proc. Natl. Acad. Sci.* **106**, 4601-4605.

Polovina, J.J., Howell, E.A., Abecassis, M., 2008. Ocean's least productive waters are expanding. *Geophys. Res. Lett.* **35**, L03618.

Posch, T., Loferer-Krößbacher, M., Gao, G., Alfreider, A., Pernthaler, J., Psenner, R., 2001. Precision of bacterioplankton biomass determination: A comparison of two fluorescent dyes, and of allometric and linear volume-to-carbon conversion factors. *Aquat. Microb. Ecol.* **25**, 55-63.

Pulido-Villena, E., Baudoux, A.-C., Obernosterer, I., Landa, M., Caparros, J., Catala, P., Georges, C., Harmand, J., Guieu, C., 2014. Microbial food web dynamics in response to a Saharan dust event: Results from a mesocosm study in the oligotrophic Mediterranean Sea. *Biogeosciences* **11**, 5607-5619.

Pulido-Villena, E., Wagener, T., Guieu, C., 2008. Bacterial response to dust pulses in the western Mediterranean: Implications for carbon cycling in the oligotrophic ocean. *Glob. Biogeochem. Cy.* **22**, GB1020.

Regaudie-de-Gioux, A., Duarte, C.M., 2009. Patterns in planktonic metabolism in the Mediterranean Sea. *Biogeosciences* **6**, 3081-3089.

Regaudie-de-Gioux, A., Duarte, C.M., 2013. Global patterns in oceanic planktonic metabolism. *Limnol. Oceanogr.* **58**, 977-986.

Ribés, M., Coma, R., Maria-Gili, M., 1999. Seasonal variation of particulate organic carbon, dissolved organic carbon and the contribution of microbial communities to live particulate organic carbon in a shallow near-bottom ecosystem at the Northwestern Mediterranean Sea. *J. Plankton Res.* **21**, 1077-1100.

Ridame, C., Dekaezemacker, J., Guieu, C., Bonnet, S., L´Helguen, S., Malien, F., 2014. Contrasted saharan dust events in LNLC environments: Impact on nutrient dynamics and primary production. *Biogeosciences* **11**, 4783-4800.

Ridame, C., Guieu, C., 2002. Saharan input of phosphate to the oligotrophic water of the open western Mediterranean Sea. *Limnol. Oceanogr.* **47**, 856-869.

Ruiz-González, C., Simó, R., Sommaruga, R., Gasol, J.M., 2013. Away from darkness: A review on the effects of solar radiation on heterotrophic bacterioplankton activity. *Front. Microbiol.* **4**, 1-24.

Sandman, A.N., Wikström, S.A., Blomqvist, M., Kautsky, H., Isaeus, M., 2013. Scale-dependent influence of environmental variables on species distribution: A case study on five coastal benthic species in the Baltic Sea. *Ecography* **36**, 354-364.

Schlitzer, R., 2015. Ocean Data View, http://odv.awi.de.

Serret, P., Robinson, C., Aranguren-Gassis, M., García-Martín, E.E., Gist, N., Kitidis, V., Lozano, J., Harris, C., Thomas, R., 2015. Both respiration and photosynthesis determine the scaling of plankton metabolism in the oligotrophic ocean. *Nat. Commun.* **6**, 6961.

Steemann-Nielsen, E., 1952. The use of radio-active carbon (C^{14}) for measuring organic production in the sea. *J. Cons. Perm. Int. Explor. Mer.* **18**, 117-140.

Verity, P.G., Robertson, C.Y., Tronzo, C.R., Andrews, M.G., Nelson, J.R., Sieracki, M.E., 1992. Relationships between cell volume and the carbon and nitrogen content of marine photosynthetic nanoplankton. *Limnol. Oceanogr.* **37**, 1434-1446.

Vincent, J., Laurent, B., Losno, R., Bon Nguyen, E., Roullet, P., Sauvage, S., Chevaillier, S., Coddeville, P., Ouboulmane, N., di Sarra, A.G., Tovar-Sánchez, A., Sferlazzo, D., Massanet, A., Triquet, S., Morales Baquero, R., Fornier, M., Coursier, C., Desboeufs, K., Dulac, F., Bergametti, G., 2015. Variability of mineral dust deposition in the western Mediterranean basin and South-East of France. *Atmos. Chem. and Phys. Discuss.* **15**, 34673-34717.

Vinoj, V., Rasch, P.J., Wang, H., Yoon, J.-H., Ma, P.-L., Landu, K., Singh, B., 2014. Short-term modulation of Indian summer monsoon rainfall by West Asian dust. *Nat. Geosci.* **7**, 308-313.

Williams, P.J.l.B., Quay, P.D., Westberry, T.K., Behrenfeld, M.J., 2013. The oligotrophic ocean is autotrophic? *Ann. Rev. Mar. Sci.* **5**, 535-549.

Williamson, C.E., Zepp, R.G., Lucas, R.M., Madronich, S., Austin, A.T., Ballaré, C.L., Norval, M., Sulzberger, B., Bais, A.F., McKenzie, R.L., Robinson, S.A., Häder, D.P., Paul, N.D., Bornman, J.F., 2014. Solar ultraviolet radiation in a changing climate. *Nat. Clim. Change* **4**, 434-441.

Yvon-Durocher, G., Jones, J.I., Trimmer, M., Woodward, G., Montoya, J.M., 2010. Warming alters the metabolic balance of ecosystems. *Philos. T. Roy. Soc. B* **365**, 2117-2126.

Zenoff, V.F., Heredia, J., Ferrero, M., Siñeriz, F., Farías, M.E., 2006. Diverse UV-B resistance of culturable bacterial community from high-altitude wetland water. *Curr. Microbiol.* **52**, 359-362.

Zubkov, M.V., Burkill, P.H., 2006. Syringe pumped high speed flow cytometry of oceanic phytoplankton. *Cytom. A* **69**, 1010-1019.

Zubkov, M.V., Burkill, P.H., Topping, J.N., 2007. Flow cytometric enumeration of DNA-stained oceanic planktonic protists. *J. Plankton Res.* **29**, 79-86.

Supplementary information

Supplementary tables

Table 1: Mean (± SD) of the planktonic metabolic rates, total primary production (PP_{total}) and community respiration (CR) (in mmol C m^{-3} d^{-1}) and of the production (P) / respiration (R) ratio of the planktonic communities in the Southwestern Mediterranean Sea. The number of stations sampled and their trophic nature (autotrophic or heterotrophic), position (latitude and longitude), depth (in m), *in situ* temperature (T, °C), the dissolved organic carbon (DOC, in μM), total phosphorus (TP, in μM) and nitrogen (TN, in μM) and chlorophyll *a* (Chl *a*, in μg L^{-1}) concentrations in each station are shown. Note that samples in each station were taken from surface waters (5 m depth).

Station	Position	Depth	*in situ* T	DOC	TP	TN	Chl *a*	PP_{total}	CR	P/R
Autotrophic 1	35° 59'N, 4° 19' W	284	16.84 (±0.77)	213 (±31)	0.09 (±0.03)	357 (±0.30)	1.90 (±0.30)	36 (±2)	33 (±12)	1.09
Autotrophic 2	36° 32' N, 3° 48' W	113	21.58 (±1.37)	193 (±45)	0.60 (±0.04)	313 (±69)	0.68 (±0.12)	55 (±1)	40 (±0)	1.38
Autotrophic 3	36° 21' N, 3° 46' W	430	20.15 (±1.66)	323 (±176)	0.48 (±0.08)	309 (±14)	2.24 (±1.47)	66 (±8)	43 (±12)	1.53
Autotrophic 4	36° 09' N, 3° 42' W	289	18.05 (±0.60)	229 (±80)	0.65 (±0.09)	256 (±11)	1.47 (±0.42)	64 (±8)	46 (±12)	1.39
Autotrophic 5	36° 32' N, 3° 10' W	200	20.45 (±1.20)	189 (±70)	0.50 (±0.04)	297 (±21)	1.50 (±0.93)	81 (±24)	81 (±19)	1
Autotrophic 6	36° 25' N, 2° 45' W	995	22.06 (±0.76)	119 (±10)	0.24 (±0.03)	292 (±5)	0.63 (±0.04)	79 (±16)	43 (±11)	1.84
Autotrophic 7	36° 27' N, 2° 13' W	180	23.18 (±0.41)	123 (±8)	0.50 (±0.03)	248 (±33)	0.37 (±0.00)	118 (±1)	96 (±2)	1.23
Autotrophic 8	36° 08' N, 1° 50' W	830	23.64 (±0.03)	150 (±56)	0.50 (±0.04)	228 (±17)	0.47 (±0.09)	113 (±0)	105 (±0.1)	1.08
Heterotrophic 1	36° 37' N, 4° 24' W	76	17.78 (±1.14)	322 (±89)	0.10 (±0.00)	348 (±10)	0.75 (±0.09)	10 (±1)	38 (±13)	0.26
Heterotrophic 2	36 ° 21' N, 4° 22' W	740	22.19 (±0.95)	281 (±12)	0.80 (±0.11)	307 (±10)	0.80 (±0.21)	32 (±18)	86 (±27)	0.37
Heterotrophic 3	36° 39' N, 2° 25' W	338	23.50 (±0.05)	137 (±40)	0.51 (±0.07)	268 (±5)	0.34 (±0.07)	21 (±6)	66 (±23)	0.32
Heterotrophic 4	36° 40' N, 2° 09' W	87	23.65 (±0.30)	177 (±80)	0.45 (±0.08)	237 (±5)	0.47 (±0.00)	21 (±0.10)	63 (±16)	0.33
Heterotrophic 5	36° 26' N, 1° 55' W	1438	23.75 (±0.66)	147 (±15)	0.38 (±0.03)	272 (±4)	0.50 (±0.05)	36 (±1)	86 (±19)	0.42
Heterotrophic 6	36° 16' N, 1° 43' W	1973	23.69 (±0.04)	162 (±17)	0.78 (±0.13)	319 (±49)	0.47 (±0.06)	11 (±4)	74 (±32)	0.15

Table 2: Mean (± SD) of chlorophyll *a* (Chl *a*, in μg L^{-1}), total phosphorus (TP, in μM), total nitrogen (TN, in μM), sestonic carbon (in μM), nitrogen (in μM) and phosphorus (in μM), sestonic C:P and N:P ratio and dissolved organic carbon concentrations (DOC, in μM) at the beginning of the experiment for the heterotrophic and autotrophic area.

	Heterotrophic area	Autotrophic area
Chl *a*	0.75 (±0.09)	1.90 (±0.30)
TP	0.10 (±0.00)	0.09 (±0.03)
TN	348 (±10)	357 (±0.30)
Sestonic C	58 (±6)	34 (±4)
Sestonic N	8.49 (±0.45)	4.38 (±0.47)
Sestonic P	0.02 (±0.00)	0.02 (±0.00)
Sestonic C:P ratio	2915 (±271)	1681 (±296)
Sestonic N:P ratio	425 (±19)	219 (±12)
DOC	322 (±89)	213 (±31)

Table 3: Results from two-way analysis of variance (ANOVA) for cell biomass (in mg C m^{-3}) of autotrophic nanoplankton (ANP), autotrophic picoplankton (APP) and heterotrophic picoplankton (HPP) in the heterotrophic and autotrophic area with radiation, Rad (PAB, > 280 nm and P, > 400 nm) and dust (ambient [amb] and dust), as factors. *F* values represent *F*-test, and the asterisks *****, ****** and ******* represent the $p < 0.05$, $p < 0.01$ and $p < 0.001$, respectively.

	ANP	APP	HPP
Treatment	*F*	*F*	*F*
Heterotrophic area			
Rad	0.15	0.60	0.29
Dust	0.02	5.34*	1.22
Rad×Dust	0.04	1.46	8.42**
Autotrophic area			
Rad	71.27***	3.81	155.14***
Dust	4.78	0.01	33.5*
Rad×Dust	116.92***	0.01	6.43*

Table 4: Results from one-way repeated measures analysis of variance (RM-ANOVA) for the effect size of UVR on the total primary production (PP_{total}) and community respiration (CR) in the heterotrophic and autotrophic area with dust (ambient [amb] and dust) and time, as factors. F values represent F-test, and the asterisks *****, ****** and ******* represent the $p < 0.05$, $p < 0.01$ and $p < 0.001$, respectively.

	PP_{total}	CR
Treatment	F	F
Heterotrophic area		
Dust	4.13	1.43
Time	10.18***	2.02
Dust×Time	6.48**	2.0*
Autotrophic area		
Dust	7.12*	0.75
Time	5.24*	11.11***
Dust×Time	15.16***	13.69***

Supplementary figures

Figure 1: (A) Daily area-average aerosol index (triangles, AI > 1, relative units), (B) inter-annual succession of AI events from 2012 - 2014 and (C) monthly area-average surface short-wave radiation fluxes (W m^{-2}) on Southwestern Mediterranean Sea from 1979 – 2016 period.

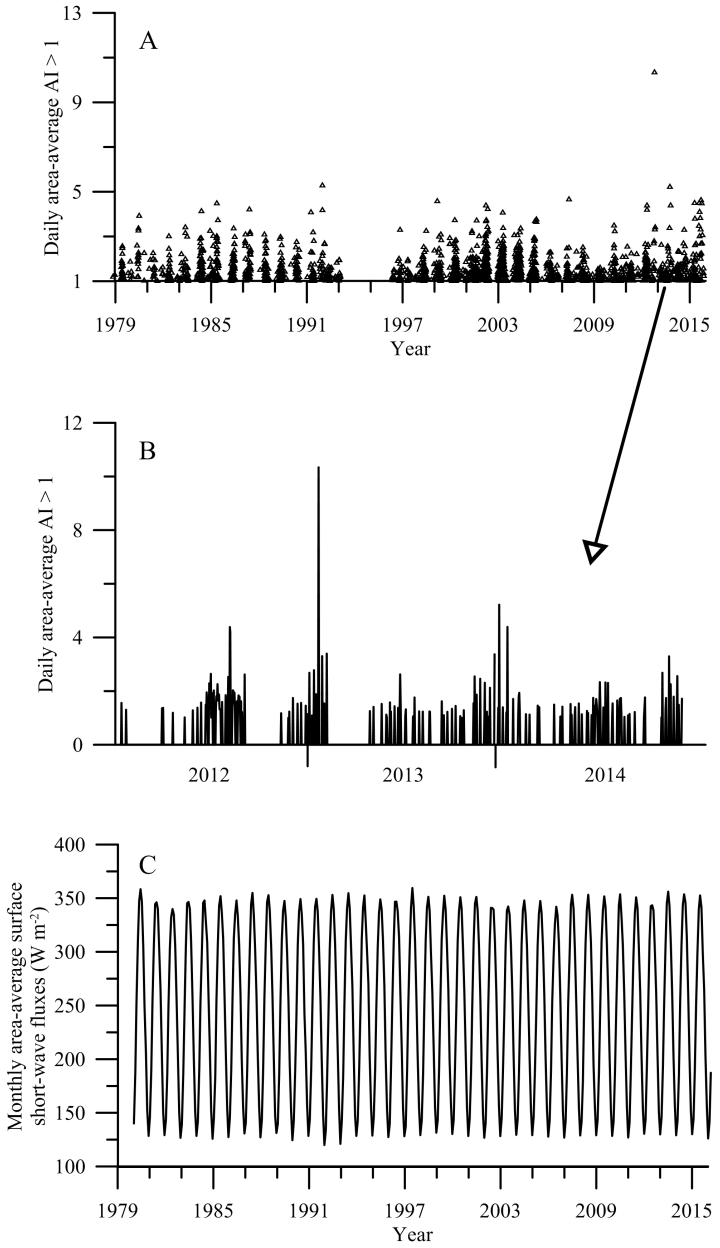

Figure 2: Surface solar radiation for: (A) PAR, 400-700 nm (in W m^{-2}) and (B) UV-B (305 nm, solid line) and UV-A (320 nm, large dashed line and 380 nm, small dashed line) (in μW cm^{-2}) during the exposure period (June 17^{th} – 21^{th}, 2014).

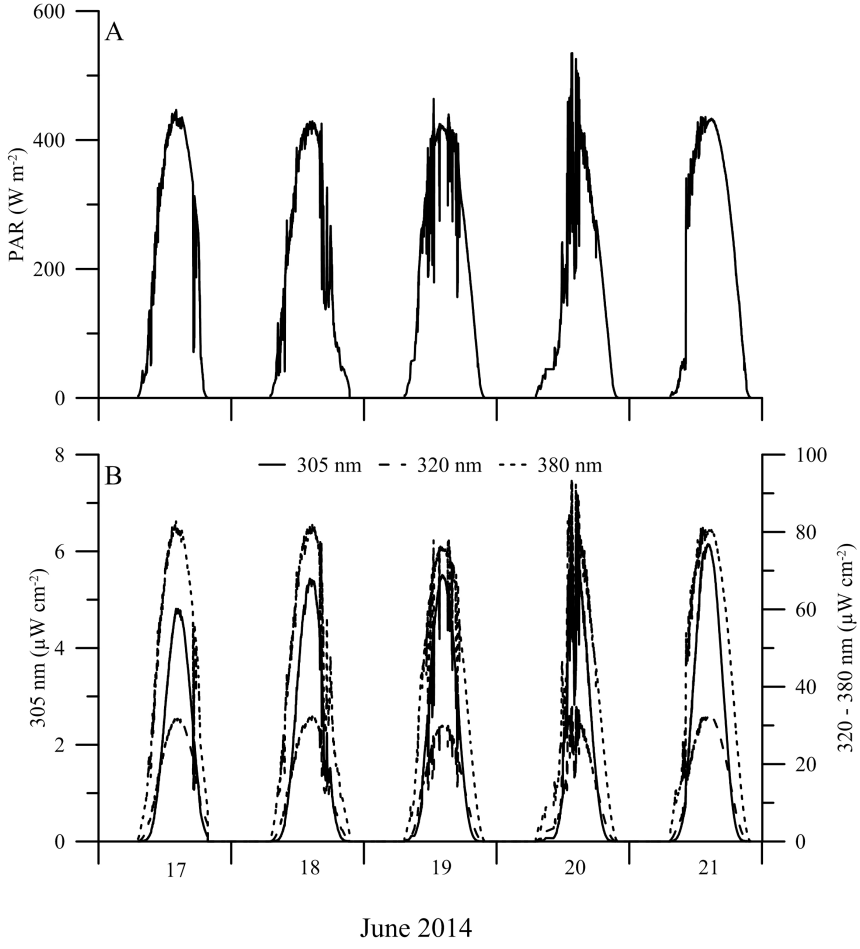

Figure 3: (A, B) Mean (± SD) total primary production (PP_{total}, in mmol C m^{-3} d^{-1}) and (C, D) community respiration (CR) rates (in mmol C m^{-3} d^{-1}) in the microcosms during the experiment under two radiation treatments, PAB (> 280 nm) and PAR (> 400 nm) and two dust treatments, ambient (amb) and dust in the heterotrophic and autotrophic area.

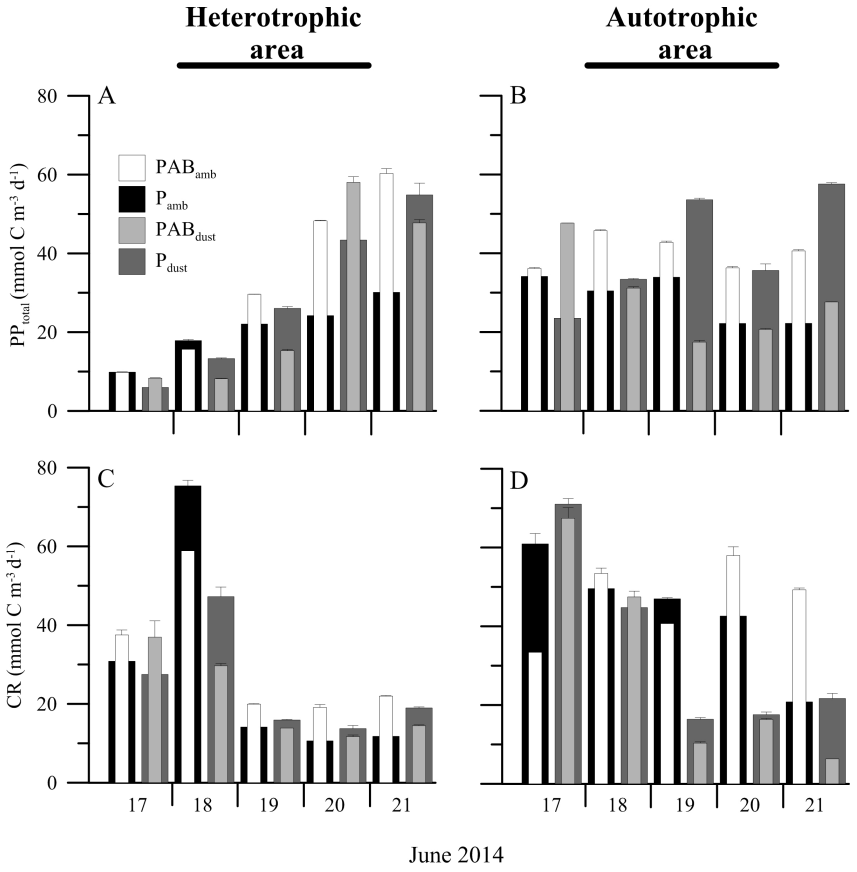

Figure 4: Mean (± SD) total primary production / community respiration (PP_{total} / CR) ratios under two radiation treatments, PAB (> 280 nm) and PAR (P, > 400 nm) and two nutrient treatments, ambient (amb) and dust during the experiments in the heterotrophic and autotrophic area, considering the potential mesozooplankton grazing and respiration in unproductive marine waters.

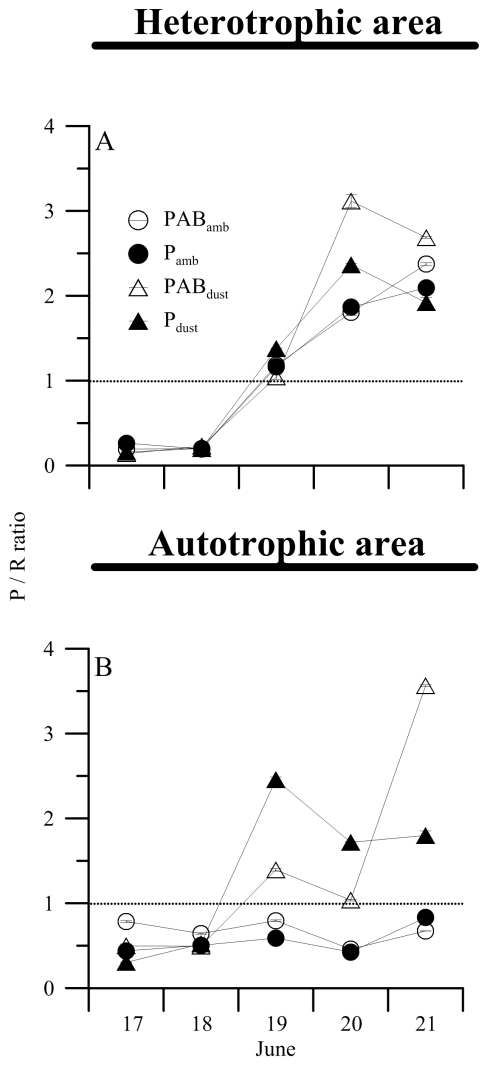

Chapter VII

Increased dust deposition and riverine nutrients under high UVR decrease the CO_2-sink capacity of coastal South Atlantic waters

Abstract

Increased nutrient concentrations by anthropic activities and alterations in atmospheric dust deposition together with enhanced ultraviolet radiation (UVR) levels due to the shoaling of surface water layers by the global warming, are unpredictably altering the ecosystems functioning. However, studies dealing with the impacts of interactions between multiple global change factors on planktonic primary producers and heterotrophs are uncertain. Here we test how increases in nutrient concentrations either through riverine or dust-aerosol inputs under high UVR levels could alter the metabolic balance of coastal ecosystems. We conducted an experiment with surface plankton communities from coastal waters of South Atlantic Ocean and combined these results with remote-sensing data. We found that both factors acting jointly reduced 18% the carbon (C) sink capacity of these areas, and prompted shifts toward communities dominated by nanoflagellates regardless of the origin of the nutrients source. This declined C uptake suggests that the decreasing trend observed in the productivity of this area during the last years could be accentuated with the global change. Therefore, this discovery highlight that avoid bias in the metabolic balance estimates under future complex environmental conditions require longer-term scales and considering both shifts in the structure as the metabolic status of planktonic communities.

Introduction

The growth of human population and their activities (e.g., agriculture, herding, deforestation, industries) are resulting in substantial transfers of nutrients, mainly nitrogen (N) and phosphorus (P) to adjacent freshwater bodies, followed by transport to coastal waters (Peñuelas et al., 2013). In fact, Peñuelas et al. (2012) showed that the current global demand of P and N by human activities are growing, hence it would be expected that

the riverine nutrient inputs into marine ecosystems would be intensified in the future (Rabalais et al., 2009). Together with these massive human-caused additions, the increasingly climate variability due to global change (i.e., higher droughts, storms and alterations in wind patterns) is also producing increases in the atmospheric N and P deposition into coastal waters (Mahowald et al., 2008). Thus, as a result of these perturbations, marine coastal habitats are being confronted with several alterations (i.e., low dissolved oxygen, reduced water clarity) which are triggering cascading effects on the ecosystem functioning (i.e., less suitable habitats for feeding and reproduction, increasing harmful phytoplankton blooms) (Harding et al., 2016; Maar et al., 2016).

Previous studies conducted with planktonic communities have shown variable effects of nutrient inputs, from a stimulation of the PSII performance (Φ_{PSII}) (Browning et al., 2014), primary (Marcoval et al., 2008; Ridame et al., 2014) and bacterial production (Lekunberri et al., 2010; Teira et al., 2016) or organism's growth, to inhibition of these responses that, as in the case of dust inputs, can be due to inputs of companying toxic elements (e.g., copper, lead) (Dao & Beardall, 2016; Hoffmann et al., 2012). In addition to the nutrient inputs, solar radiation in the water column is greatly altered by global change. Due to the global warming, the increasing stratification of the water column is producing increases in the solar radiation levels (particularly the ultraviolet radiation portion, UVR, 280–400 nm) that organisms are receiving in the surface waters (Williamson et al., 2014). A huge body of literature have reported that UVR, at current or enhanced levels due to global change, has a well-known inhibitory effect on the metabolism (e.g., primary production, nutrients uptake) (Helbling et al., 2015b; Hessen et al., 2012; Villafañe et al., 2015a) and physiology (e.g., Φ_{PSII}, DNA repair) (Harrison et al., 2015; Jeffrey et al., 2000; Villafañe et al., 2016) of planktonic organisms. However, other studies have also shown some positive effects of UVR i.e. increases in phytoplankton biomass (Cabrera et al., 1997; Yamaguchi et al., 2015), net community production (García-Corral et al., 2014) and in the carbon (C) incorporation (Barbieri et al., 2002; Gao et al., 2007).

In spite of that coastal systems constitute the most productive areas of the biosphere (Rousseaux & Gregg, 2014) and that N and P together with solar radiation are pivotal for the functioning of the C-cycle, one of the unresolved issues in global change research is if a rising nutrients availability, by riverine or dust-aerosol inputs, and high UVR fluxes could impact the C-uptake by phytoplankton and its remineralization by respiration of the total planktonic community. As consequence of potential unbalance between both processes, the capacity of these ecosystems as C-sinks of the human-induced carbon dioxide (CO_2) emissions could be greatly altered in the future. To shed new lights about the metabolic functioning of coastal areas under future global change scenarios, we experimentally increased the nutrient concentrations, mimicking future dust deposition and riverine inputs, under high UVR exposure to determine physiological and metabolic responses and shifts in the structure of a microplanktonic community in Patagonian coastal waters. The South Atlantic Ocean to the east of Patagonia not only is one of the most productive regions worldwide with a rich and diverse community (Acha et al., 2004; Romero et al., 2006) but also it is considered as one of the most intense CO_2 sinks per unit area in the global Ocean (Bianchi et al., 2009). For all that we used this area as model ecosystem to quantify variations in the net primary production (NPP), community respiration (CR) and gross primary production (GPP) at short and mid-term scales. From this data, we quantify how increased nutrient inputs from different origin and high UVR levels could alter the capacity of South Atlantic coastal ecosystems to sequester CO_2 in the future.

Material and Methods

Study area and sampling

The Chubut River estuary, together with its area of influence, is a mesotidal and highly productive estuary (Piccolo & Perillo, 1999) characterized

by a variable range of physico-chemical and biological conditions due to the interaction between the end of Chubut River and the South of Atlantic Ocean (Helbling et al., 2010). The study area has been the focus of several investigations during the last two decades which have been centered in the single effects of UVR (Helbling & Villafañe, 2014) or in combination with other global change variables (Helbling et al., 2015a; Villafañe et al., 2015b) on phytoplankton community throughout the annual succession. Surface seawater (0.5 m depth and salinity > 33) was collected at the mouth of the Chubut River estuary (Egi station, 43° 18.8′S, 65° 02.0′W) during high tide on the afternoon of October 19^{th}, 2014 using an acid-cleaned (1N HCl) bucket. The sample (200 L in total) was pre-screened through a 180 μm Nitex mesh to eliminate mesozooplankton, placed in 25-L opaque acid-washed containers and transported to Estación de Fotobiología Playa Unión (EFPU, 10 – 15 min away from the sampling site).

Experimental set up

The set up consisted in eighteen 10L-UVR-transparent microcosms where seawater samples were dispensed (Alpax Trade Lab, São Paulo, Brazil, 72% transmission at 280 nm). A 2 × 3 factorial design was implemented with: a) Two solar radiation treatments, 1) PAB (PAR + UV-A + UV-B, > 280 nm; uncovered microcosms), and 2) P (PAR > 400 nm; microcosms covered with Ultraphan 395 nm filter), and b) three nutrient treatments, 1) ambient (amb), whose nutrient concentrations at the moment sampling were: nitrite + nitrate (N) = 2.4 μM, phosphate (P) = 1.76 μM and silicate (Si) = 1.7 μM, 2) riverine inputs (riv) through the addition of inorganic nutrients i.e. $NaNO_3$, NaH_2PO_4 and Na_2SiO_3 as N, P and Si sources, respectively, 61.98 μM (N), 30.84 μM (P) and 135.37 μM (Si) and 3) atmospheric dust inputs, whose addition increased the nutrient concentrations in 0.31 μM (N), 1.15 μM (P) and 4.90 μM (Si) with respect to ambient conditions.

The experimental addition of riverine inorganic nutrients used in this study was based on the historical nutrient concentrations registered in the

study area, with mean concentrations of N, P and Si ranging 0.20 – 21 μM, 0.19 – 6.4 μM and 1.7 – 236 μM for N, P and Si, respectively (Helbling et al., 2010). Hence our additions simulated increases of 3 and ca. 5-fold for N and P compared to the maximal concentrations registered in the area. Si concentrations, however, were in the mean range of those received over the year so that diatoms, which are an important component of this planktonic community, were not limited by this nutrient during the experiment. The dust added was collected *in situ* in Merzouga (Tafilalet, Morocco, 31° 6′.00 N, 3° 59′.24 W). Previously to their addition, the dust was dry-sieved using a custom column knotted with a wire mesh cloth of 1 mm and 100 mm pore size, and was collected on a steel foil underneath the nest of sieves. The size of particles used ranged between 1 – 10 μm (Leitz Fluovert FS, Leica, Wetzlar, Germany), which are broadly comparable with those used in previous reports that showed that dust particles larger than this size are rapidly removed during the atmospheric transport (Guieu et al., 2010). The rationale to add Saharan dust as a continental dust model source is due to that the Sahara desert is responsible for 58% of the global dust emissions each year (Tanaka & Chiba, 2006). Currently, very few studies worldwide have directly quantified the impacts that atmospheric dust deposition in combination with other global change drivers has on the functioning as well as on the trophic status of ecosystems. Moreover, recent results by Brahney et al. (2015) underscore that under a future global change scenario these impacts will be particularly relevant in areas where major dust (and ash) sources are closer, as in the case of the Southern Hemisphere ecosystems, where the experimental evidences are still absent. The amount of dust added in the experiment (4.1 mg L^{-1}) simulates a deposition scenario of 61.5 mg m^{-2} into a 15-m-depth water layer, which constitute the layer potentially affected after intense dust deposition events (Marañón et al., 2010; Pulido-Villena et al., 2008). Thus, if we consider that: (1) mean number of dust deposition events per year on the area during the last two decades is approx. 100 (see below in results); (2) the annual dust deposition rates on South Atlantic is 500 mg m^{-2} yr^{-1} (Jickells & Moore, 2015) and (3) that most of these deposition events occur in strong pulses (Guerzoni et al., 1997), we simulate a future scenario of increases of up to 12-fold

in dust inputs respect to the current conditions on this area. Moreover, our experimental additions of dust are also in line with recent reports over different marine areas worldwide that used concentrations ranging between 1 – 7.3 mg L^{-1} (Cabrerizo et al., 2016; Chien et al., 2016; Meng et al., 2016; Westrich et al., 2016).

All microcosms (triplicates per radiation and nutrient treatments) were placed in 200-L tanks with running water to maintain the *in situ* temperature (14.5 °C) and exposed to natural solar radiation during five days. The thin water layer (ca. 0.5 m) that covered all microcosms simulated the worst possible scenario with a shallow upper mixed layer (UML). The microcosms were shaken manually five times a day so that plankton received homogeneous irradiances during the exposure by avoiding that organisms settle at the bottom of the microcosms. Sub-samples for different measurements / analyses were taken daily [for Chlorophyll *a* (Chl *a*) determinations, oxygen (O_2) concentration and effective photochemical quantum yield (Φ_{PSII}) measurements] or every other day [taxonomic composition of community, nutrient analyses] using a syringe attached to a silicone tube inserted into each microcosm to prevent their tampering. The procedures are described below:

Analyses and measurements

Remote-sensing data

Data from daily aerosol index (AI) and monthly particulate organic carbon (POC) for Egi station were downloaded from Giovanni v 4. 18. 3 Earth database of National Aeronautics and Space Administration (NASA) (Acker & Leptoukh, 2007). For the period 1996 – 2015, AI data were provided by the Total Ozone Mapping Spectrometer – Earth Probe (TOMS-EP) (July 22, 1996 to December 31, 2003) and by the Ozone Monitoring Instrument (OMI) (January 1, 2004 to December 31, 2015) satellites, re-

spectively. As previous studies (Bullejos et al., 2010) established that an AI > 0.5 constitutes a deposition event, we also considered the annual dust deposition events as the number of days per year affected by events of AI > 0.5. For monthly POC, data were provided by sea-viewing wide field-of-view sensor (SeaWiFS, September 4, 1997 to December 31, 2010) and by moderate resolution imaging spectroradiometer (MODIS, January 1, 2011 to October 31, 2016).

Solar radiation measurements

We monitored the incident solar radiation during the experiments using an ELDONET (Real Time Computers, Germany) broadband filter radiometer that measures UV-B (280–315 nm), UV-A (315–400 nm) and PAR (400–700 nm) every second, averages the data over a 1-min interval, and stores them in a computer. The radiometer is routinely calibrated (once a year) using a solar calibration procedure. For this calibration, the irradiance data during clear sky conditions are compared with the output of models for transfer of atmospheric radiation (Björn & Murphy, 1985). Daily PAR doses in the study area for the 1999 – 2015 period were obtained from the EFPU online database (see http://www.efpu.org.ar).

Chl *a* measurements

Water samples (100 mL) to determine Chl *a* concentration were taken from each microcosm every day early in the morning and filtered onto M-GF (25 mm) filters (Muntkell, Sweden). After this, photosynthetic pigments were extracted in absolute methanol as described in Holm-Hansen & Riemann (1978), and a scan between 250-750 nm was done using a spectrophotometer (Hewlett Packard, model HP 8453E). Chl *a* concentrations were calculated using the equations of Porra (2002).

Taxonomic analyses

Samples for the identification and / or counting of autotrophic nanoplankton (ANP), autotrophic picoplankton (APP) and heterotrophic picoplankton (HPP) cells were obtained at the beginning and the last day of exposure to solar radiation from each microcosm. For ANP, samples were placed in 125 mL brown glass bottles and fixed with buffered formalin (final concentration 0.4% of formaldehyde in the sample). Aliquots of 25 mL were settled for 24 h in a Utermöhl chamber (Hydro-Bios GmbH, Germany) and species were identified and enumerated using an inverted microscope (Leica, model DM IL, Germany) following the technique described by Villafañe & Reid (1995). The biovolumes of the phytoplankton species were estimated by adjusting their shape to known geometric forms following Hillebrand et al. (1999), and by measuring the main cell dimensions of at least 10 cells per species. From these biovolumes, C biomass were calculated with the equations of Strathmann (1967). For APP and HPP, 1.5 mL of sample was fixed with 75 μL of particle-free 20% (w/v) paraformaldehyde (1% final concentration) and immediately frozen (–20 °C) until analysis to quantify cell abundance using a flow cytometer (FACSCanto II, Becton Dickinson Biosciences, Oxford, UK). Previous to analysis, all samples were thawed and stained with Syber–Green I DNA (Sigma-Aldrich Co Ltd) 1:5000 final dilution (Gasol & del Giorgio, 2000; Zubkov et al., 2007). After this, yellow-green 1-µm beads at standard concentration (10^5 particles mL^{-1}; Fluoresbrite Microparticles, Polysciences, PA, USA) were also added to determine the absolute cellular concentration (Zubkov et al., 2007; Zubkov & Burkill, 2006). As with the same samples we quantified APP and HPP, we used the phycoerythrin and Chl *a* signals to distinguish between autotrophic and heterotrophic picoplankton groups (Mercado et al., 2006). From cell abundances we estimated the biovolumes of both picoplanktonic groups following Zubkov et al. (1998), which were converted into C biomass by using conversion factors of 0.22 (Booth, 1988) and 0.35 pg C μm^{-3} (Bjørnsen, 1986) for the APP and HPP fractions, respectively.

Growth rates

The specific growth rates of ANP, APP and HPP (μ, in d^{-1}) under the different experimental conditions were calculated from cell concentration as:

$$\mu = \ln (N_5/N_1)/(t_5 - t_1)$$

where N_5 is the cellular concentration (in cells $mL^{-1} \times 10^3$) the last day of the experiment (t_5) and N_1 is the cellular concentration at the first day of the experiment (t_1).

Nutrient analyses

Samples from each microcosm were collected at t_1, after two days of exposure and at t_5 and placed in 125 mL HDPE bottles and frozen (-20 °C) until analyses, to determine N, P and Si concentrations by spectrophotometric techniques, as described in Strickland & Parsons (1972).

Dust elemental composition and elements concentrations

Seventeen elements (i.e., Na, Mg, Al, K, Ca, Ti, V, Cr, Mn, Fe, Ni, Cu, Zn, Br, Sr, Pb, P) were analyzed by an ICP-OES system (Perkin Elmer Inc, OptimaTM 8300, USA) equipped with the software WinLab32TM (v. 4.0). All the elements were extracted from dust samples (6.15×10^{-2} mg) by previously dissolving them during five days in 15 mL of autoclaved seawater at 14.5 °C. In this way we simulated similar dilution conditions as those performed in our experiment (see above). Prior to analysis, the ICP-OES system was calibrated with a series of monoelement standard solutions (Perkin Elmer Inc, USA) together with internal standards (Perkin Elmer Inc, USA) to drift correction.

O_2 concentration measurements

Samples from each microcosm were taken daily (before sunrise) and placed into Teflon FEP narrow-mouth bottles (Nalgene – 35 mL) without bubbles. Each Teflon bottle (18 in total) equipped with an O_2 sensor-spot (SP-PSt3-NAU-D5-YOP, PreSens GmbH, Germany) was exposed to the same radiation treatment than imposed to the corresponding mesocosm from which it came and were put inside a temperature-controlled water bath to keep the in situ temperature. The O_2 concentrations were measured during 24 daily cycles using a Fibox 3 optode-probe oxygen transmitter (PreSens GmbH, Germany) furnished with the Oxyview 6.02 software and a fiber-optic. Measurements started at dawn and were done hourly until dusk, and then every 4-6 hours during the night until completing the daily cycle. Each sample was measured for 30 seconds collecting one datum per second. Every day, previous to the measurements, the probe was calibrated using a two-point (0% and 100% saturation) calibration procedure, at the *in situ* temperature and taking into account the atmospheric pressure.

Fluorescence measurements

To determine the dynamics of Φ_{PSII} along the experimental period, aliquots of 3 mL were taken daily and directly from each microcosm at dawn, noon and dusk to measure in vivo PSII photochemical parameters using a pulse amplitude modulated (PAM) fluorometer (Walz, Water PAM, Effeltrich, Germany). Each sample was measured six times immediately after sampling without any dark-adaptation, with each measurement lasting 10 seconds; thus the total time for measuring each sample was 1 min. Effective photochemical quantum yield of PSII was calculated using the equations of Genty et al. (1989) and Maxwell & Johnson (2000) as:

$$\Phi_{PSII} = \Delta F/F'm = (F'm - Ft)/F'm$$

where F′m is the maximum fluorescence induced by a saturating light pulse (ca. 5300 μmol photons m^{-2} s^{-1} in 0.8 seconds) and Ft the current steady state fluorescence induced by a red actinic light pulse (492.2 μmol photons m^{-2} s^{-1} – peak at 660 nm) in light-adapted cells.

Data and statistical analyses

From monthly POC data, we fitted a linear regression model POC *vs.* time for the 1997-2014 and 2015-2016 periods based on the distinct trends for each (see results section). In addition, from daily light-darkness Φ_{PSII} measurements, we fitted a polynomial regression model to the values at noon and dawn versus time for each radiation and nutrient treatments to assess: (1) the Φ_{PSII} inhibition experienced by the communities at noon when received maximal irradiances; and (2) the recovery capacity of these communities from the dusk to the following dawn to counteract the potential photodamage experienced during the previous day. Likewise, we also fitted a polynomial regression model with oxygen concentration values at noon versus time for each radiation and nutrient treatment to calculate the changes in the net primary production (NPP, in mmol O_2 m^{-3} d^{-1}) throughout the experiment as:

$$\mathrm{NPP} = [\mathrm{O_2}]\mathrm{t_5} - [\mathrm{O_2}]\mathrm{t_1}/(\mathrm{t_5} - \mathrm{t_1})$$

being $[O_2]t_5$ the modeled O_2 concentrations the last day of the experiment (t_5) and $[O_2]t_1$ the modeled concentrations for the first day (t_1) of exposure.

From the O_2 concentrations measured during the night, we calculated the dark community respiration (dark CR, in mmol m^{-3} h^{-1}) for each radiation and nutrients treatments as difference between the O_2 concentrations measured before dawn of the following experimental day and those measured during the dusk of the experimental day considered.

Then, we assessed the UVR effect on NPP and dark CR under ambient, dust or riverine treatments as:

$$\text{UVR effect (\%)} = (\text{P} - \text{PAB})/\text{P} \times 100$$

being PAB and P the NPP or dark CR under UVR + PAR and only PAR treatments, respectively.

The daily CR_{PAB} rates (mmol O_2 m^{-3} d^{-1}) for each nutrients treatment and day were calculated as:

$$\text{Daily CR}_{PAB} = \text{dark CR}_{PAB} + \text{light CR}$$

where the dark CR_{PAB}, represents the respiration values measured during the night in samples previously exposed to full solar radiation. The light CR was estimated after obtaining the UVR effect on respiration (see above) and applying this factor to the dark CR_{PAB} as:

$$\text{Light CR} = \text{dark CR}_{PAB} \times (1 - \text{UVR effect})$$

By doing this, we obtained more realistic measurements of daily CR as other experimental studies (Agustí et al., 2014; Medina-Sánchez et al., 2017) has shown that the respiration rates of planktonic communities can be enhanced or inhibited under UVR exposure. Finally, we estimated the gross primary production (GPP) under ambient, dust and riverine treatments as:

$$\text{GPP} = \text{NPP} + (\text{daily CR}_{PABt5 \; - \; PABt1})$$

From the GPP and daily $\text{CR}_{PABt5 \; - \; PABt1}$ (see table 1) data we evaluated the CO_2-sink capacity of our model coastal ecosystem, as the ratio between both parameters, under ambient, dust and riverine treatments after

an acclimation period of 5 days. We used a two-way analysis of the variance (ANOVA) to test interactions between UVR and nutrient (amb, dust and riv) treatments on NPP, cell abundances and growth rates of ANP, APP and HPP. We used a one-way ANOVA to test significant differences between nutrient treatments on the UVR effect on NPP (%) and on CO_2-sink capacity. Two-way repeated (RM) measures ANOVA was performed to test interactions between UVR and nutrients treatment on dark CR, whereas that one-way RM-ANOVA was used to test significant differences among nutrient treatments on UVR effect on dark CR (%) and daily CR. Normality (by Shapiro-Wilk's test) and homoscedasticity (by Cochran's and Levene's tests) or sphericity (by Mauchly's test) was checked for each variable to verify the ANOVA and RM-ANOVA assumptions (Zar, 1999). When interactive effects were significant, Least Significant Differences (LSD) Fisher *post hoc* tests were performed. Student's tests were used to test significant differences between the slopes of the polynomial regression fits of Φ_{PSII}. All data are reported as mean and standard deviation, whereas error propagation was used to calculate the error for the UVR effects (%) on NPP and dark CR.

Results

Long-term trends in POC and AI on coastal South Atlantic waters

Monthly POC exhibited a characteristic response pattern through 1997-2016 period (Fig. S1A), with increasing values from pre-bloom to bloom period when maxima values are found (peaks ranging between approx. 600 to 1000 mg C m^{-3}) followed by decreasing values during the post bloom period. Overall, maxima POC values matched with the lowest monthly PAR doses characteristic of the austral winter in this area (Fig. S1A) whereas the lowest POC values occurred in austral summer when de PAR

doses reached high values. Despite these annual cycles, our results showed a steady increase in POC over the time which lasted up to 2014 (R^2 = + 0.17, $F_{5.11}$, p < 0.001). Noticeably, this trend was significantly inverted (R^2 = – 0.35, $F_{0.01}$, p < 0.001) in the last two years (2014-2016). Likewise, both the intensity (AI > 0.5, Fig. S1B) as the frequency (events, Fig. S1C) in AI increased from 1997 to 2016 on this area.

Plankton physiological and metabolic responses

Our experimental manipulation determined a typical V-shaped pattern of Φ_{PSII} over daily light-darkness periods, with decreases in Φ_{PSII} as light intensities increased during the day followed by increases in Φ_{PSII} at lower light intensities during the evening (Fig.1; Table S1). Overall, at noon there was an increasing photoinhibition (i.e., decreasing polynomial slopes) over the experiment which was coupled with the higher radiation levels experienced by communities, particularly on the last two days when maximal mean irradiances were registered. Thus, mean daily irradiances were ca. 152, 21 and 0.50 during the three first days and 223, 32 and 0.7 W m^{-2} during the last two days of the experiment, for PAR, UV-B and UV-A, respectively. Moreover, this enhanced inhibition found towards the end of the experiment was not only dependent of the radiation treatment but also of the nutrients source considered. In fact, we found that mean noon Φ_{PSII} values decreased 2-fold (ca. 0.17 relative units [r.u.]; Fig. 1C) at the end of the experiment period under riverine treatments regardless of the radiation treatment considered. Also noon Φ_{PSII} values were significant lower (2-fold) under these conditions than under dust or ambient treatments (Fig. 1A, B) where they had values ca. 0.33 on average during the same period (*t*-test riv *vs.* amb=6.92, p<0.001; *t*-test riv *vs.* dust=3.62, p<0.001). Conversely, dawn Φ_{PSII} exhibited similar or even higher values (i.e., increasing polynomial slopes), particularly under riverine treatments, with increases ranging between 0.01-0.11 r.u. over the experiment. These increases in Φ_{PSII} denote that night recovery was enough to counteract the daily inhibition, avoiding any chronic damage into the PSII.

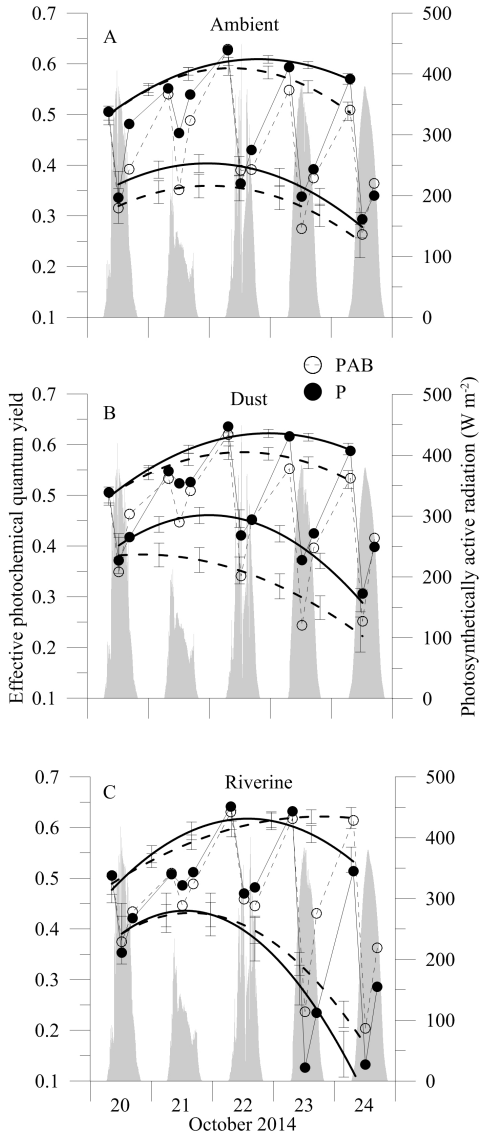

Figure 1: Daily cycles of mean effective photochemical quantum yield values under two radiation treatments, PAB (> 280 nm, open circles) and P (PAR, > 400 nm, solid circles) and three nutrient treatments, (A) ambient, (B) dust and (C) riverine inputs during the experimental period (October 20-24th). Note that grey areas represent daily irradiances of photosynthetically active radiation (PAR, in W m^{-2}). Dashed (samples under PAB) and solid (samples under P) lines represent the polynomial regression fit during the dawn (upper part of each panel) and noon day (lower part of each panel) during the incubation period whereas the vertical lines represent the 95% confidence intervals. For simplicity, error bars of mean effective photochemical quantum yield are omitted.

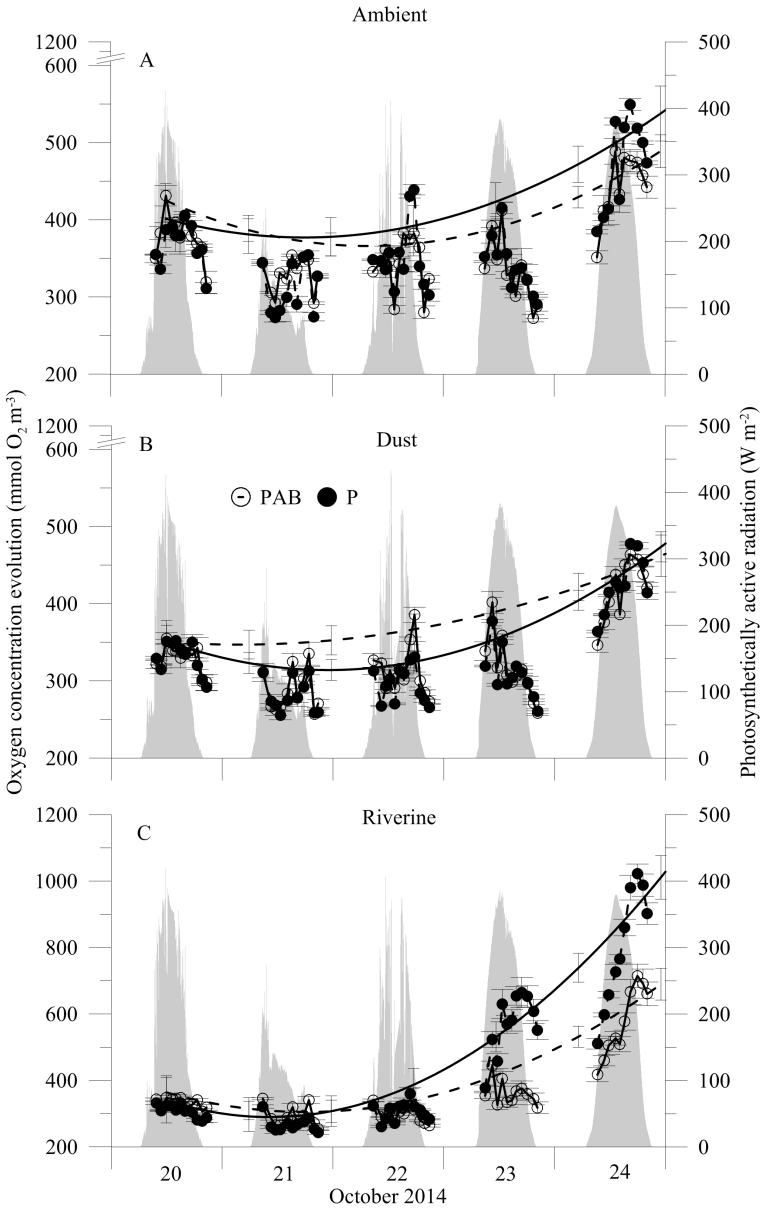

Figure 2: Daily cycles of mean (± SD) community oxygen evolution (in mmol O_2 m^{-3}) under two radiation treatments, PAB (> 280 nm, open circles) and P (PAR, > 400 nm, solid circles) and three nutrient treatments, (A) ambient, (B) dust and (C) riverine inputs during the experimental period (October 20-24^{th}). Note that grey areas represent daily irradiances of photosynthetically active radiation (PAR, in W m^{-2}). Dashed (samples under PAB) and solid (samples under P) lines represent the polynomial regression fit during the incubation period whereas the vertical lines represent the 95% confidence intervals.

Similarly as for the Φ_{PSII} measurements, the O_2 evolution exhibited a response modulated by the light-darkness diel cycle. In fact, during the first three days, the evolution of O_2 showed an increasing-decreasing response pattern due to the cloudy conditions that dominated; however, during the last two days, O_2 exhibited a characteristic response with increases from the dawn up to dusk, followed by a continuous decrease during the darkness period (Fig. 2; Table S1). Overall, the O_2 concentrations showed an increasing response over the experiment, being particularly higher under riverine (Fig. 2C, $>$ 500 mmol O_2 m^{-3}) than under ambient or dust treatments at the end of the experiment (Fig. 2A, B, similar or $<$ 500 mmol O_2 m^{-3}). As consequence, the NPP was 2-4-fold higher under riverine treatments, whereas similar values were found in ambient and dust conditions (ca. 40 mmol O_2 m^{-3} d^{-1}; Fig. 3A). Noticeably, UVR exerted a similar inhibitory effect (50%) on NPP under ambient and riverine treatments, but it significantly enhanced (ca. -10%) the NPP under dust treatments (Fig. 3B).

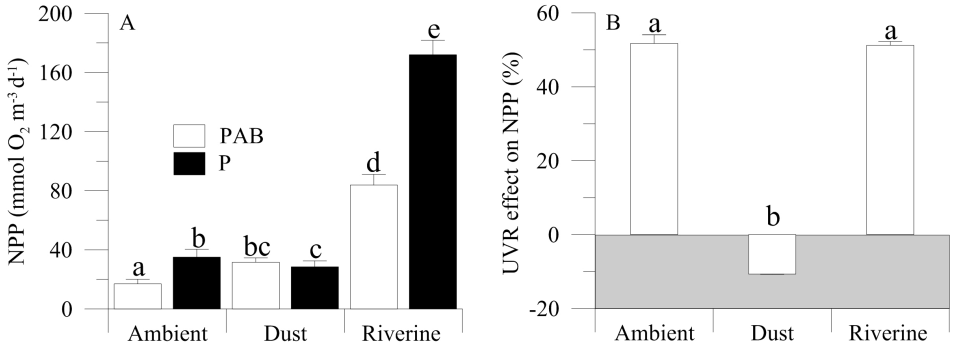

Figure 3: (A) Mean (± SD) net primary production (NPP, in mmol O_2 m^{-3} d^{-1}) in samples exposed to two radiation treatments, PAB ($>$ 280 nm) and P (PAR, $>$ 400 nm) and three nutrient treatments, ambient (amb, circles), dust (triangles) and riverine (riv, diamonds) over the experimental period (October 20-24th). (B) Mean (± SD) UVR effects (%) on the total NPP under ambient, dust and riverine treatments. The letters on the top of bars indicate significant differences by LSD *post hoc* test.

For dark CR, there was an interactive UVR × Nut × Time (Table S2). From the beginning up to the third day of the experiment, dark CR exhibited a slightly constant response pattern in all conditions (10 mmol O_2 m^{-3} h^{-1}). Thereafter, these rates significantly increased (LSD *post hoc*, $p < 0.01$) only under riverine treatments where maximal values were determined, whereas they remained with similar values than mentioned above under ambient and dust treatments (Fig. 4A). Regarding to UVR impacts on dark CR, our results showed a significant Nut × Time effect (Table S3); thus, while dust inputs exerted a stimulatory effect over the experiment (-50 to -15%), riverine inputs changed from an enhancement of the dark CR at short-term (-78%) to a great inhibition at mid-term, reaching similar values as those found under ambient conditions (ca. 35%, Fig. 4B). There was also a significant Nut × Time effect on daily CR (Table S3). In fact, under ambient conditions the daily CR exhibited an unimodal response pattern, whereas that under enriched nutrient conditions the daily CR significantly increased over the experiment (LSD *post hoc*, $p < 0.001$). Despite these increasing daily CR rates registered under enriched conditions, they were 1.5-fold higher under riverine than dust treatments.

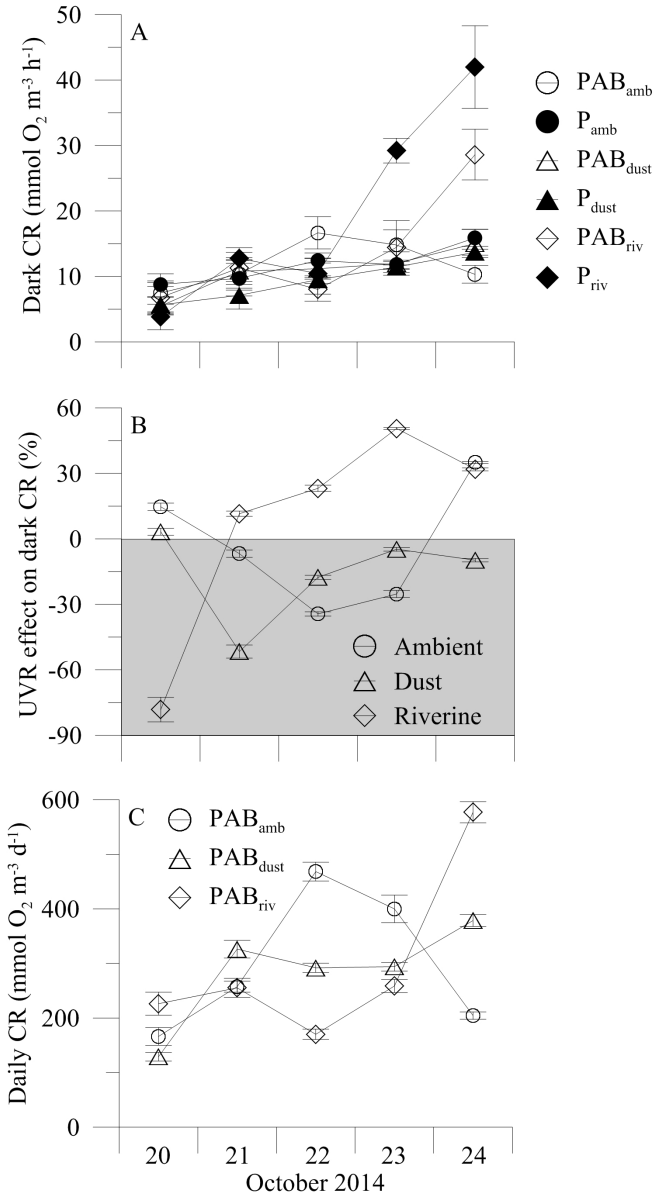

Figure 4: (A) Mean (± SD) rates of dark community respiration (CR, in mmol O_2 m^{-3} h^{-1}) in samples exposed to two radiation treatments, PAB (> 280 nm) and P (PAR, > 400 nm) and three nutrient treatments, ambient (amb, circles), dust (triangles) and riverine (riv, diamonds) inputs during the experimental period (October 20-24th). (B) Mean (± SD) UVR effects (%) on dark CR and (C) daily CR rates (CR, in mmol O_2 m^{-3} d^{-1}) under ambient (amb) dust and riverine (riv) treatments over the experimental period.

Plankton metabolic balance: Nutrients source and UVR interaction

The CO_2-sink capacity showed values > 1 in all treatments, denoting a net autotrophic metabolism in our coastal model ecosystem (Fig. 5; Table 1). Nevertheless, we found significant decreases in the CO_2-sink capacity for the dust and riverine treatments as compared to their respective values under ambient conditions. In fact, these decreases in the sink capacity after an acclimation period indicate a significant reduction of the CO_2 uptake by communities acclimated to the future conditions, by as much as ca. 18% on average, regardless of the nutrient source considered.

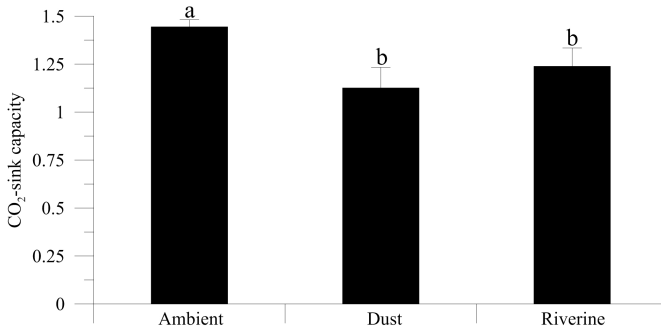

Figure 5: Mean (± SD) CO_2-sink capacity in a model coastal ecosystem after an acclimation period of five days under ambient, dust and riverine inputs. The letters on the top of bars indicate significant differences by LSD *post hoc* test.

Table 1: Mean (± SD) gross primary production (GPP), net primary production (NPP) and daily community respiration (daily CR) (in mmol O_2 m^{-3} d^{-1}) after five days of incubation under ambient, dust or riverine treatments.

	Ambient	Dust	Riverine
GPP	54.97 (±2.12)	281.31 (±0.99)	434.73 (±2.75)
NCP	16.93 (±0.63)	31.61 (±0.59)	83.85 (±1.43)
CR	38.03 (±1.49)	249.70 (±0.40)	350.88 (±1.32)

Plankton community structure

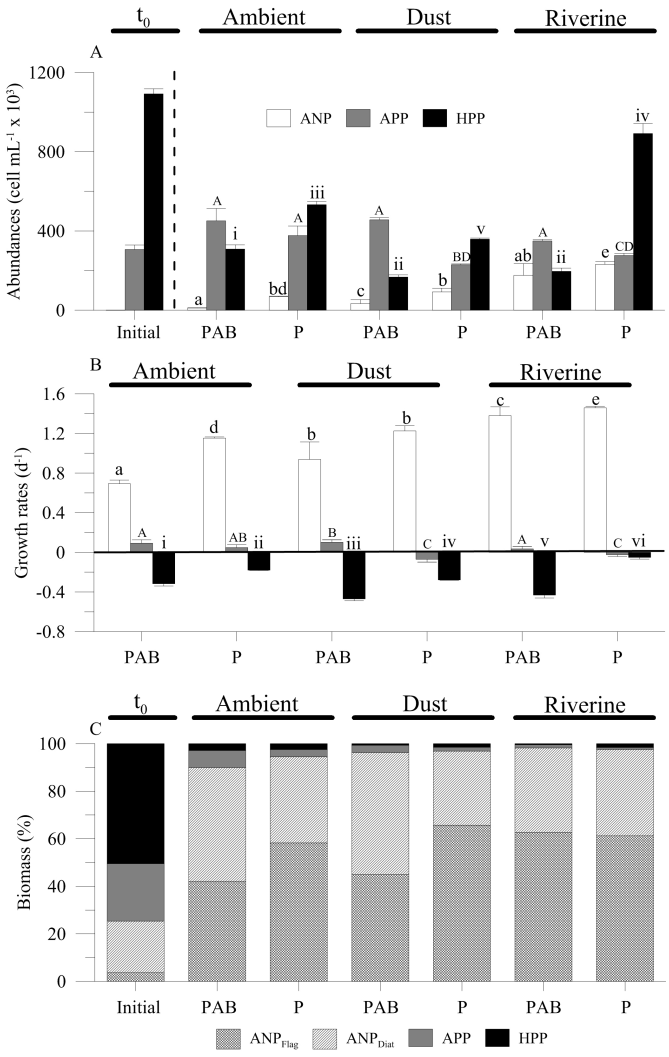

Figure 6: Mean (± SD) (A) cell abundances (in cell $mL^{-1} \times 10^3$), (B) growth rates (in d^{-1}) and carbon biomass (C) (in percentage) of autotrophic nano (ANP) and picoplankton (APP) and heterotrophic picoplankton (HPP) at the beginning (initial) and after five days of exposure to two radiation treatments, PAB (> 280 nm) and P (PAR, > 400 nm) and three nutrient treatments, ambient (amb), dust and riverine (riv) inputs. Note that for carbon biomass, ANP fraction was divided into the two main contributors to the total biomass, flagellates (Flag) and diatoms (Diat). The letters on the top of bars indicate significant differences by LSD *post hoc* test.

After five days of acclimation to the conditions imposed, our results also showed shifts in the planktonic community structure faced to the interaction UVR × dust or riverine; thus, the HPP decreased whereas ANP (and APP) abundances increased (or not varied) over the incubation time (Fig. 6A). Moreover, ANP and HPP showed significant higher abundances in samples receiving only PAR regardless nutrients treatment, whereas APP abundances showed the opposite pattern (excepting under ambient nutrients; Fig. 6A; Table S4). These shifts in the autotrophic fraction were also paralleled with increasing Chl *a* concentrations which exhibited a similar response pattern than NPP and were on average 4-fold higher (88 mg m^{-3}) under riverine than under ambient and dust treatments, where not significant differences were found (ca. 19 and 21 mg m^{-3}), respectively (data not shown).

These different response in cell abundances resulted in diverse growth rates of the different fractions (Fig. 6B), exhibiting positive values in the ANP (approx. 1.5 d^{-1}), negative in the HPP (-0.5 d^{-1}) and variable in the APP. Notwithstanding, whereas the dust and riverine inputs counteracted the negative UVR effects on ANP growth, both nutrient sources accentuated these effects on HPP growth (Fig. 6B). APP did not show a clear response pattern to radiation and nutrient treatments. In terms of biomass (Fig. 6C), the plankton community was co-dominated by autotrophs and heterotrophs at the beginning of experiment (ca. 20 mg C m^{-3} for each group); however, after 5 days of incubation ANP dominated the community (i.e., 548.7 mg C m^{-3} on average) respect to APP (ca. 11.5 mg C m^{-3}) and HPP (ca. 7.8 mg C m^{-3}), regardless of the treatment considered (Fig. 6C). Within the ANP fraction, unidentified flagellates < 10 μm co-dominated or dominated the community faced to diatoms (mainly pennates). The contribution of dinoflagellates was almost negligible ($< 1\%$ of the total biomass) in all treatments. The shifts mentioned in the plankton community were coupled with acute decreases during the experiment in the nutrient concentrations, particularly in the N and P fractions under ambient and dust inputs treatments where such concentrations ranged from ca. 2.60 and 2.34 μM at the beginning of the experiment to 0.03 and 0.40 μM at the end for

N and P, respectively. For Si, we found a moderate consumption between 25 (amb and dust) – 50% (riv) respect to the initial conditions (Table S5).

Discussion

This study reports for the first time that in a future scenario of increased dust-aerosol deposition or riverine input of nutrients and high UVR fluxes a reduction in the CO_2-sink capacity of coastal South Atlantic Ocean could occur. Our results also show that this reduction in the CO_2 sinking was accompanied by a shift in planktonic communities, particularly in riverine treatments, towards a predominance of nanoplanktonic flagellates, supporting the existing feedback between functioning (metabolic balance) and structure (specific composition) in marine ecosystems (Viviani et al., 2011). Thus, this study provides a framework for understand the changes that are occurring in the primary production of this area (POC; Fig. S1A), and show how future variations in physical (UVR) and chemical (nutrient inputs) conditions could alter the role that the South Atlantic Ocean plays as CO_2 sink in the global Ocean (Bianchi et al., 2009). In the following paragraphs, we will disentangle the processes that could underlie to the physiological, metabolic and structural responses reported in this study.

The decrease reported in the CO_2 sink capacity under enriched nutrient conditions and high UVR levels is in line with a recent global change model that predict strong reductions in the C-downward fluxes between 38% and 50% in surface waters of low (LNLC) and high (HNLC) latitude ecosystems, respectively (Boyd, 2015). However, it contrasts with recent reports in coast Mediterranean waters where the combination of high UVR levels and dust deposition (Cabrerizo et al., 2016) or nutrient (Carrillo et al., 2015) inputs determined a shift the metabolic balance from heterotrophy toward autotrophy. The plausible explanation to these contrasting results may lies in the different trophic state of both marine areas, a highly productive and non-limited by nutrients area (i.e., coastal South Atlantic Ocean)

versus an unproductive and strongly nutrient-limited area (i.e., coasts of Southwestern Mediterranean Sea). The reduction in the sink capacity was determined by an increase relatively higher in CR than NPP under nutrient enriched conditions (dust and riverine). This higher energetic expenditure seem to be linked to the dominance of flagellates in the (nano)planktonic community due to: (1) they have higher specific respiration / production ratios than that of nonflagellated ones, as the active movement capacity requires an increased metabolic activity (Striebel et al., 2009); and (2) their potential mixotrophic metabolism which combine phototrophic and phagotrophic abilities to grow into the same organism (Fischer et al., 2016; Raven, 1997), and therefore, constitute an energetically more demanding trophic strategy in terms of C (Litchman et al., 2007; Mitra et al., 2014; Raven, 1997). Although we did not quantify mixotrophy *sensu stricto*, supporting this latter explanation we found a decreased bacterial biomass and growth rates throughout the incubation period, which could be interpreted as a control top down by mixotrophics flagellates.

This selection towards flagellates found under our experimental conditions could have also been favored by: (1) their lower susceptibility to photoinactivation than picoplankton cells as posses lower radiation exposure per unit pigment or per cell volume, and therefore, have greater resistance to high irradiances (Key et al., 2010; Li et al., 2011); (2) their higher nutrient uptake ability when their availability is increased (Mercado et al., 2014); and (3) their motility, which seems to make them better competitors than nonflagellated cells (e.g., diatoms) in shallower UMLs, as simulated here. In fact, previous experimental (Jäger et al., 2008) and observational (Lee & Yoo, 2016) studies investigating the influence of the UML depth and the turbulence on community structure support our interpretation.

The stimulatory effect of both nutrient sources on phytoplanktonic biomass (Fig. 6C) was linked to increases in the NPP and daily CR, however, this effect was stronger under riverine inputs. The underlying mechanism underpinning this different intensity of response to nutrient sources seems to be related with a more efficient photochemical performance of phytoplank-

ton under riverine than dust treatments. In fact, despite that the highest dynamic photoinhibition occurred under riverine conditions, it was counteracted during the darkness, and even under these conditions the communities exhibited an increased dark-recovery capacity over the study period (Fig. 1C). Thus, our findings show that the interaction between abiotic factors, nutrient inputs and UVR, and dark periods is critical so that the species can obtain the needed energy through dark respiration and proteins, amino acids and ATP synthesis to can repair the damaged PSII. A higher recovery capacity would permit increases in Φ_{PSII} activity and consequently, would explain the increased NPP reported over the experimental period; however, it also would suppose a higher energetic expenditure in terms of C through respiration to sustain this capacity. This proposal is supported by a recent report by Li et al. (2016) who found that phytoplankton cells are able to maintain a continued PSII protein cycling during darkness to retrieve from the damage experienced during the radiation exposure period, permitting them sustain the photosynthetic activity in subsequent exposures.

By contrast, the lower recovery capacity of Φ_{PSII} (approx. 0.1, in relative units; Fig. 1B, C) during the darkness under dust compared to riverine inputs could be related to scarce N supply observed under these conditions. The N limitation is supported by the low concentrations of this nutrient found in dust treatments at the end of the experiment along with low Chl *a* concentrations, which were not significantly different of those measured under ambient conditions. In addition, we can also rule out the presence of toxic elements (e.g., lead, copper) as potential constrainers of NPP and CR under dust treatments [see Jordi et al., (2012) and Paytan et al., (2009)], because the concentration of such elements were below detection limits during all the incubation period (data not shown).

Conclusion

Overall, the combination of our experimental and remote-sensing results provide strong evidences about the fact that coastal South Atlantic Ocean, considered as a strong CO_2-sink (Padín et al., 2010), could decrease their C uptake in a future scenario of greater human and / or climate-derived pressures. We are fully aware that our experimental setup simulates extreme events of nutrients inputs and high levels of UVR, however, our results are not deprived of ecological signicance because the longer-term scales considered here allow us avoiding bias (above or below) in the estimates of the metabolic balance of ecosystems (see Duarte et al., 2013; Regaudie-de-Gioux & Duarte, 2013). In addition, in this study we also took into account both the plankton metabolic status and their acclimation ability (García-Corral et al., 2016) as the shifts occurred in the community structure (Villafañe et al., 2016), which are key factors that also influence the metabolic balance of ecosystems. Therefore, the development of these approaches supposes an improvement in the understanding about how aquatic ecosystems will respond to future complex global change conditions.

References

Acker, J.G., Leptoukh, G., 2007. Online analysis enhance NASA Earth science data. *EOS, Trans. AGU* **88**, 14-17.

Acha, E.M., Mianzan, H., Guerrero, R.A., Favero, M., Bava, J., 2004. Marine fronts at the continental shelves of austral South America: Physical and ecological processes. *J. Mar. Syst.* **44**, 83-105.

Agustí, S., Regaudie-de-Gioux, A., Arrieta, J.M., Duarte, C.M., 2014. Consequences of UV-enhanced community respiration for plankton metabolic balance. *Limnol. Oceanogr.* **59**, 223-232.

Barbieri, E.S., Villafañe, V.E., Helbling, E.W., 2002. Experimental assessment of UV effects upon temperate marine phytoplankton when exposed to variable radiation regimes. *Limnol. Oceanogr.* **47**, 1648-1655.

Bianchi, A.A., Ruiz Pino, D., Isbert Perlender, H.G., Osiroff, A.P., Segura, V., Lutz, V., Clara, M.L., Balestrini, C.F., Piola, A.R., 2009. Annual balance and seasonal variability of sea-air CO2 fluxes in the Patagonia Sea: Their relationship with fronts and chlorophyll distribution. *J. Geophys. Res.: Oceans* **114**, C03018.

Björn, L.O., Murphy, T.M., 1985. Computer calculation of solar ultraviolet radiation at ground level. *Physiol. Veg.* **23**, 555-561.

Bjørnsen, P.K., 1986. Automatic determination of bacterioplankton biomass by image analysis. *Appl. Environ. Microbiol.* **51**, 1199-1204.

Booth, B.C., 1988. Size classes and major taxonomic groups of phytoplankton at two locations in the subarctic Pacific Ocean in May and August, 1984. *Mar. Biol.* **97**, 275-286.

Boyd, P.W., 2015. Toward quantifying the response of the oceans' biological pump to climate change. *Front. Mar. Sci.* **2**, 77.

Brahney, J., Mahowald, N., Ward, D.S., Ballantyne, A.P., Neff, J.C., 2015. Is atmospheric phosphorus pollution altering global alpine Lake stoichiometry? *Glob. Biogeochem. Cy.* **29**, GB5137.

Browning, T.J., Bouman, H.A., Henderson, G.M., Mather, T.A., Pyle, D.M., Schlosser, C., Woodward, E.M.S., Moore, C.M., 2014. Strong responses of Southern Ocean phytoplankton communities to volcanic ash. *Geophys. Res. Let.* **41**, 2851-2857.

Bullejos, F.J., Carrillo, P., Villar-Argaiz, M., Medina-Sánchez, J.M., 2010. Roles of phosphorus and ultraviolet radiation in the strength of phytoplankton–zooplankton coupling in a Mediterranean high mountain lake. *Limnol. Oceanogr.* **55**, 2549–2562.

Cabrera, S., López, M., Tartarotti, B., 1997. Phytoplankton and zooplankton response to ultraviolet radiation in a high-altitude Andean lake: Short - versus long-term effects. *J. Plankton Res.* **19**, 1565-1582.

Cabrerizo, M.J., Medina-Sánchez, J.M., González-Olalla, J.M., Villar-Argaiz, M., Carrillo, P., 2016. Saharan dust and high UVR jointly alter the metabolic balance in marine oligotrophic ecosystems. *Sci. Rep.* **6**, 35892.

Carrillo, P., Medina-Sánchez, J.M., Herrera, G., Durán, C., Segovia, M., Cortés, D., Salles, S., Korbee, N., Figueroa, F.L., Mercado, J.M., 2015. Interactive effect of UVR and phosphorus on the coastal phytoplankton community of the Western Mediterranean Sea: Unravelling eco-physiological mechanisms. *PloS One* **10**, e0142987.

Chien, C.-T., Mackey, K.R.M., Dutkiewicz, S., Mahowald, N., Prospero, J.M., Paytan, A., 2016. Effects of African dust deposition on phytoplankton in the western tropical Atlantic Ocean off Barbados. *Glob. Biogeochem. Cy.* **30**, 716-734.

Dao, L.H.T., Beardall, J., 2016. Effects of lead on growth, photosynthetic characteristics and production of reactive oxygen species of two freshwater green algae. *Chemosphere* **147**, 420-429.

Duarte, C.M., Regaudie-de-Gioux, A., Arrieta, J.M., Delgado-Huertas, A., Agustí, S., 2013. The oligotrophic ocean is heterotrophic. *Ann. Rev. Mar. Sci.* **5**, 551-569.

Fischer, R., Giebel, H.-A., Hillebrand, H., Ptacnik, R., 2016. Importance of mixotrophic bacterivory can be predicted by light and loss rates. *Oikos* **in press**.

Gao, K., Li, G., Helbling, E.W., Villafañe, V.E., 2007. Variability of UVR effects on photosynthesis of summer phytoplankton assemblages from a tropical coastal area of the South China Sea. *Photochem. Photobiol.* **83**, 802-809.

García-Corral, L.S., Agustí, S., Regaudie-de-Gioux, A., Luculano, F., Carrillo-de-Albornoz, P., Wassmann, P., Duarte, C.M., 2014. Ultraviolet radiation enhances Arctic net plankton community production. *Geophys. Res. Lett.* **41**, 1-8.

García-Corral, L.S., Holding, J., Carrillo-de-Albornoz, P., Steckbauer, A., Pérez-Lorenzo, M., Navarro, N., Serret, P., Duarte, C.M., Agustí, S., 2017. Effects of UVB radiation on net community production in the upper global ocean. *Glob. Ecol. Biogeogr.* **26**, 54-64.

Gasol, J.M., del Giorgio, P., 2000. Using flow cytometry for counting natural planktonic bacteria and understanding the structure of planktonic bacterial communities. *Sci. Mar.* **64**, 197-224.

Genty, B.E., Briantais, J.M., Baker, N.R., 1989. The relationship between the quantum yield of photosynthetic electron transport and quenching of chlorophyll fluorescence. *Biochim. Biophys. Acta* **990**, 87-92.

Guerzoni, S., Molinaroli, E., Chester, R., 1997. Saharan dust inputs to the western Mediterranean Sea: Depositional patterns, geochemistry and sedimentological implications. *Deep Sea Res. Pt. II* **44**, 631-654.

Guieu, C., Dulac, F., Desboeufs, K., Wagener, T., Pulido-Villena, E., Grisoni, J.-M., Louis, F., Ridame, C., Blain, S., Brunet, C., Bon Nguyen, E., Tran, S., Labiadh, M.J., Dominici, J.-M., 2010. Large clean mesocosms and simulated dust deposition: A new methodology to investigate responses of marine oligotrophic ecosystems to atmospheric inputs. *Biogeosciences* **7**, 2765-2784.

Harding, L.W., Gallegos, C.L., Perry, E.S., Miller, W.D., Adolf, J.E., Mallonee, M.E., Paerl, H.W., 2016. Long-Term trends of nutrients and phytoplankton in Chesapeake Bay. *Estuar. Coast.* **39**, 664-681.

Harrison, J.W., Silsbe, G.M., Smith, R.E.H., 2015. Photophysiology and its response to visible and ultraviolet radiation in freshwater phytoplankton from contrasting light regimes. *J. Plankton Res.*, **37**: 472-488.

Helbling, E.W., Banaszak, A.T., Villafañe, V.E., 2015a. Differential responses of two phytoplankton communities from the Chubut river estuary (Patagonia, Argentina) to the combination of UVR and elevated temperature. *Estuar. Coast.* **38**, 1134-1146.

Helbling, E.W., Banaszak, A.T., Villafañe, V.E., 2015b. Global change feed-back inhibits cyanobacterial photosynthesis. *Sci. Rep.* **5**, 14514.

Helbling, E.W., Pérez, D.E., Medina, C.D., Lagunas, M.G., Villafañe, V.E., 2010. Phytoplankton distribution and photosynthesis dynamics in the Chubut River estuary (Patagonia, Argentina) throughout tidal cycles. *Limnol. Oceanogr.* **55**, 55-65.

Helbling, E.W., Villafañe, V.E., 2014. Ultraviolet radiation studies upon phytoplankton from freshwater and marine ecosystems of Argentina, in: Tell, G., Izaguirre, I., Ofarrell, I. (Eds.), Freshwater Phytoplankton of Argentina: Phytoplankton Diversity and Ecology in Different Aquatic Systems, pp. 375-392.

Hessen, D.O., Frigstad, H., Færøvig, P.J., Wojewodzic, M.W., Leu, E., 2012. UV radiation and its effects on P-uptake in arctic diatoms. *J. Exp. Mar. Biol. Ecol.* **411**, 45-51.

Hillebrand, H., Dürselen, C.D., Kirschtel, D., Pollingher, U., Zohary, T., 1999. Biovolume calculation for pelagic and benthic microalgae. *J. Phycol.* **35**, 403-424.

Hoffmann, L.J., Breitbarth, E., Ardelan, M.V., Duggen, S., Olgun, N., Hassellöv, M., Wängberg, S.-Å., 2012. Influence of trace metal release from volcanic ash on growth of *Thalassiosira pseudonana* and *Emiliania huxleyi*. *Mar. Chem.* **132**, 28-33.

Holm-Hansen, O., Riemann, B., 1978. Chlorophyll *a* determination: Improvements in methodology. *Oikos* **30**, 438-447.

Jäger, C.G., Diehl, S., Schmidt, G.M., 2008. Influence of water-column depth and mixing on phytoplankton biomass, community composition and nutrients. *Limnol. Oceanogr.* **53**, 2361-2373.

Jeffrey, W.H., Kase, J.P., Wilhelm, S.W., 2000. Ultraviolet radiation effects on bacteria and viruses in marine ecosystems, in: de Mora, S., Demers, S., Vernet, M. (Eds.), The Effects of UV Radiation on Marine Ecosystems. Cambridge University Press, pp. 206-236.

Jickells, T.D., Moore, C.M., 2015. The importance of atmospheric deposition for ocean productivity. *Ann. Rev. Ecol. Evol. Syst.* **46**, 481-501.

Jordi, A., Basterretxea, G., Tovar-Sánchez, A., Alastuey, A., Querol, X., 2012. Copper aerosols inhibit phytoplankton growth in the Mediterranean Sea. *Proc. Natl. Acad. Sci.* **109**, 21246-21249.

Key, T., Mccarthy, A., Campbell, D.A., Six, C., Roy, S., Finkel, Z.V., 2010. Cell size trade-offs govern light exploitation strategies in marine phytoplankton. *Environ. Microbiol.* **12**, 95-104.

Lee, S., Yoo, S., 2016. Interannual variability of the phytoplankton community by the changes in vertical mixing and atmospheric deposition in the Ulleung Basin, East Sea: A modelling study. *Ecol. Model.* **322**, 31-47.

Lekunberri, I., Leport, T., Romero, E., Vázquez-Domínguez, E., Romera-Castillo, C., Marrasé, C., Peters, F., Weinbauer, M., Gasol, J.M., 2010. Effects of a dust deposition event on coastal marine microbial abundance and activity, bacterial community structure and ecosystem function. *J. Plankton Res.* **32**, 381-396.

Li, G., Gao, K., Gao, G., 2011. Differential Impacts of Solar UV Radiation on Photosynthetic Carbon Fixation from the Coastal to Offshore Surface Waters in the South China Sea. *Photochem. Photobiol.* **87**, 329-334.

Li, G., Woroch, A.D., Donaher, N.A., Cockshutt, A.M., Campbell, D.A., 2016. A hard day's night: Diatoms continues recycling Photosystem II in the dark. *Front. Mar. Sci.* **3**, 218.

Litchman, E., Klausmeier, C.A., Schofield, O.M., Falkowski, P.G., 2007. The role of functional traits and trade-offs in structuring phytoplankton communities: Scaling from cellular to ecosystem level. *Ecol. Lett.* **10**, 1170-1181.

Maar, M., Markager, M., Madsen, K.S., Windolf, J., Lyngsgaard, M.M., Andersen, H.E., Møller, E.F., 2016. The importance of local versus external nutrient loads for Chl *a* and primary production in the Western Baltic Sea. *Ecol. Model.* **320**, 258-272.

Mahowald, N., Jickells, T.D., Baker, A.R., Artaxo, P., Benitez-Nelson, C.R., Bergametti, G., Bond, T.C., Chen, Y., Cohen, D.D., Herut, B., Kubilay, N., Losno, R., Luo, C., Maenhaut, W., McGee, K.A., Okin, G.S., Siefert, R.L., Tsukuda, S., 2008. Global distribution of atmospheric phosphorus sources, concentrations and deposition rates, and anthropogenic impacts. *Glob. Biogeochem. Cy.* **22**, GB4026.

Marañón, E., Fernández, A., Mouriño-Carballido, B., Martínez-García, S., Teira, E., Cermeño, P., Chouciño, P., Huete-Ortega, M., Fernández, E., Calvo-Díaz, A., Morán, X.A.G., Bode, A., Moreno-Ostos, E., Varela, M.M., Patey, M.D., Achterbergf, E.P., 2010. Degree of oligotrophy controls the response of microbial plankton to Saharan dust. *Limnol. Oceanogr.* **55**, 2339-2352.

Marcoval, M.A., Villafañe, V.E., Helbling, E.W., 2008. Combined effects of solar ultraviolet radiation and nutrients addition on growth, biomass and taxonomic composition of coastal marine phytoplankton communities of Patagonia. *J. Photochem. Photobiol. B* **91**, 157-166.

Maxwell, K., Johnson, G.N., 2000. Chlorophyll fluorescence - a practical guide. *J. Exp. Bot.* **51**, 659-668.

Medina-Sánchez, J.M., Herrera, G., Durán, C., Carrillo, P., 2017. Optode use to evaluate microbial planktonic respiration in oligotrophic ecosystems as an indicator of environmental stress. *Aquat. Sci.* **in press**.

Meng, X., Chen, Y., Wang, B., Ma, Q.W., Wang, F.J., 2016. Responses of phytoplankton community to the input of different aerosols in the East China Sea. *Geophys. Res. Lett.* **43**, 7081-7088.

Mercado, J.M., Ramírez, T., Cortés, D., Sebastián, M., Reul, A., Bautista, B., 2006. Diurnal changes in the bio-optical properties of the phytoplankton in the Alborán Sea (Mediterranean Sea). *Estuar. Coast. S. Sci.* **69**, 459-470.

Mercado, J.M., Sala, I., Salles, S., Cortés, D., Ramírez, T., Liger, E., Yebra, L., Bautista, B., 2014. Effects of community composition and size structure on light absorption and nutrient uptake of phytoplankton in contrasting areas of the Alboran Sea. *Mar. Ecol. Progr. Ser.* **499**, 47-64.

Mitra, A., Flynn, K.J., Burkholder, J.M., Berge, T., Calbet, A., Raven, J.A., Granéli, E., Glibert, P.M., Hansen, P.J., Stoecker, D.K., Thingstad, F., Tilmann, U., Vage, S., Wilken, S., Zubkov, M.V., 2014. The role of mixotrophic protist in the biological carbon pump. *Biogeosciences* **11**, 995-1005.

Padín, X.A., Vázquez-Domínguez, M., Castaño, M., Alonso-Pérez, F., Gago, J., Gilcoto, M., Álvarez, M., Pardo, P.C., de la Paz, M., Ríos, A.F., Pérez, F.F., 2010. Air-Sea CO_2 fluxes in the Atlantic as measured during boreal spring and autumn. *Biogeosciences* **7**, 1587-1606.

Paytan, A., Mackey, K.R.M., Chen, Y., Lima, I.D., Doney, S.C., Mahowald, N., Labiosa, R., Post, A.F., 2009. Toxicity of atmospheric aerosols on marine phytoplankton. *Proc. Natl. Acad. Sci.* **106**, 4601-4605.

Peñuelas, J., Poulter, B., Sardans, J., Ciais, P., van der Velde, M., Bopp, L., Boucher, O., Godderis, Y., Hinsinger, P., Llusia, J., Nardin, E., Vicca, S., Obersteiner, M., Janssens, I.A., 2013. Human-induced nitrogen-phosphorus imbalances alter natural and managed ecosystems across the globe. *Nat. Commun.* **4**, 2934.

Peñuelas, J., Sardans, J., Rivas-ubach, A., Janssens, I.A., 2012. The human-induced imbalance between C, N and P in Earth's life system. *Glob. Change Biol.* **18**, 3-6.

Piccolo, M.C., Perillo, G.M.E., 1999. Estuaries of Argentina: A review, in: Perillo, G.M.E., Piccolo, M.C., Pino Quivira, M. (Eds.), Estuaries of South America: Their geomorphology and dynamics. Springer-Verlag, Berlin, pp. 101-132.

Porra, R.J., 2002. The chequered history of the development and use of simultaneous equations for the accurate determination of chlorophylls *a* and *b*. *Photosynth. Res.* **73**, 149-156.

Pulido-Villena, E., Wagener, T., Guieu, C., 2008. Bacterial response to dust pulses in the western Mediterranean: Implications for carbon cycling in the oligotrophic ocean. *Glob. Biogeochem. Cy.* **22**, GB1020.

Rabalais, N.n., Turner, R.E., Díaz, R.J., Justic, D., 2009. Global change and eutrophication of coastal waters. *ICES J. Mar. Sci.* **66**, 1528-1537.

Raven, J.A., 1997. Phagotrophy in phototrophs. *Limnol. Oceanogr.* **42**, 198-205.

Regaudie-de-Gioux, A., Duarte, C.M., 2013. Global patterns in oceanic planktonic metabolism. *Limnol. Oceanogr.* **58**, 977-986.

Ridame, C., Dekaezemacker, J., Guieu, C., Bonnet, S., L´Helguen, S., Malien, F., 2014. Contrasted saharan dust events in LNLC environments: Impact on nutrient dynamics and primary production. *Biogeosciences* **11**, 4783-4800.

Romero, S.I., Piola, A.R., Charo, M., Eiras-Garcia, C.A., 2006. Chlorophyll-*a* variability off Patagonia based on SeaWiFS data. *J. Geophys. Res.* **111**, C05021.

Rousseaux, C.S., Gregg, W.W., 2014. Interannual variation in phytoplankton primary production at a global scale. *Remote Sens.* **6**, 1-19.

Strathmann, R.R., 1967. Estimating the organic carbon content of phytoplankton from cell volume or plasma volume. *Limnol. Oceanogr.* **12**, 411-418.

Strickland, J.D.H., Parsons, T.R., 1972. A practical handbook of seawater analysis. *Fish. Res. Board Can. Bull.* **167**, 1-310.

Striebel, M., Bartholmé, S., Zernecke, R., Steinlein, C., Haupt, F., Diehl, S., Stibor, H., 2009. Carbon sequestration and stoichiometry of motile and nonmotile green algae. *Limnol. Oceanogr.* **54**, 1746-1752.

Tanaka, T.Y., Chiba, M., 2006. A numerical study of the contributions of dust source regions to the global dust budget. *Glob. Planet. Change* **52**, 88-104.

Teira, E., Hernández-Ruiz, M., Barber-Lluch, E., Sobrino, C., Teixeira, I.G., Álvarez-Salgado, X.A., Nieto-Cid, M., Martínez-García, S., Figueiras, F.G., Fernández, E., 2016. Bacterioplankton responses to riverine and atmospheric inputs in a coastal upwelling system (Ría de Vigo, NW Spain). *Mar. Ecol. Progr. Ser.* **542**, 39-50.

Villafañe, V.E., Cabrerizo, M.J., Erzinger, G.S., Bermejo, P., Strauch, S.M., S., V.M., Helbling, E.W., 2016. Photosynthesis and growth of temperate and sub-tropical estuarine phytoplankton in a scenario of nutrient enrichment under solar ultraviolet radiation exposure. Estuar. Coast. **in press**.

Villafañe, V.E., Guendulain-García, S.D., Valadez, F., Rosiles-González, G., Helbling, E.W., Banaszak, A.T., 2015a. Antagonistic and synergistic responses to solar ultraviolet radiation and increased temperature of phytoplankton from cenotes (sink holes) of the Yucatán Peninsula, Mexico. *Freshwater Sci.* **34**, 1282-1292.

Villafañe, V.E., Reid, F.M.H., 1995. Métodos de microscopía para la cuantificación del fitoplancton, in: Alveal, K., Ferrario, M.E., Oliveira, E.C., Sar, E. (Eds.), Manual de Métodos Ficológicos. Universidad de Concepción, Concepción, Chile, pp. 169-185.

Villafañe, V.E., Valiñas, M.S., Cabrerizo, M.J., Helbling, E.W., 2015b. Physio-ecological responses of Patagonian coastal marine phytoplankton in a scenario of global change: Role of acidification, nutrients and solar UVR. *Mar. Chem.* **177**, 411-420.

Viviani, D.A., Björkman, K.M., Karl, D.M., Church, M.J., 2011. Plankton metabolism in surface waters of the tropical and subtropical Pacific Ocean. *Aquat. Microb. Ecol.* **62**, 1-12.

Westrich, J.R., Ebling, A.M., Landing, W.M., Joyner, J.L., Kemp, K.M., Griffin, D.W., Lipp, E.K., 2016. Saharan dust nutrients promote *Vibrio* bloom formation in marine surface waters. *Proc. Natl. Acad. Sci.* **113**, 5964-5969.

Williamson, C.E., Zepp, R.G., Lucas, R.M., Madronich, S., Austin, A.T., Ballaré, C.L., Norval, M., Sulzberger, B., Bais, A.F., McKenzie, R.L., Robinson, S.A., Häder, D.P., Paul, N.D., Bornman, J.F., 2014. Solar ultraviolet radiation in a changing climate. *Nat. Clim. Change* **4**, 434-441.

Yamaguchi, H., Hirade, N., Higashizono, K., Tada, K., Kishimoto, K., Oyama, K., Ichimi, K., 2015. Light and nutrient limitation on phytoplankton production in the strait of an enclosed coastal sea (Bisan Strait, eastern Seto Inland Sea, Japan). *J. Sea Res.* **103**, 75-83.

Zar, J.H., 1999. Biostatistical analysis, 4th ed. Prentice Hall, Englewood Cliffs, NJ.

Zubkov, M.V., Burkill, P.H., 2006. Syringe pumped high speed flow cytometry of oceanic phytoplankton. *Cytom. A* **69**, 1010-1019.

Zubkov, M.V., Burkill, P.H., Topping, J.N., 2007. Flow cytometric enumeration of DNA-stained oceanic planktonic protists. *J. Plankton Res.* **29**, 79-86.

Zubkov, M.V., Sleigh, M.A., Tarran, G.A., Burkill, P.H., Leakey, R.J.G., 1998. Picoplanktonic community structure on an Atlantic transect from 50°N to 50°S. *Deep Sea Res. Pt I* **45**, 1339-1355.

Supplementary information

Supplementary tables

Table 1: Results of polynomial regression fits of effective photochemical quantum yield (Φ_{PSII}) *versus* time during the dawn and at noon and daily cycles of oxygen concentration evolution under two radiation treatments: PAB (> 280 nm) and P (PAR, > 400 nm) and three nutrient treatments: ambient (amb), dust and riverine (riv) inputs. F represents F-test values, R^2 the determination coefficient, and the asterisks *, ** and *** represent the $p < 0.05$, $p < 0.01$ and $p < 0.001$, respectively.

Dawn Φ_{PSII}		
Treatment	F	R^2
PAB_{amb}	1.02***	0.65
P_{amb}	32.7***	0.84
PAB_{dust}	8.08**	0.57
P_{dust}	38.96***	0.86
PAB_{riv}	14.51***	0.71
P_{riv}	10.08**	0.63
Noon Φ_{PSII}		
PAB_{amb}	3.50*	0.40
P_{amb}	7.63**	0.56
PAB_{dust}	7.40**	0.55
P_{dust}	9.54**	0.61
PAB_{riv}	19.68***	0.77
P_{riv}	12.94***	0.68
Oxygen concentration evolution		
PAB_{amb}	43.95***	0.88
P_{amb}	27.22***	0.82
PAB_{dust}	25.66***	0.81
P_{dust}	87.29***	0.94
PAB_{riv}	86.59***	0.93
P_{riv}	167.19***	0.97

Table 2: Results of statistical analysis of the two-way repeated measures analysis of the variance (ANOVA) of each factor considered and their interaction on the dark community respiration (CR) over the experimental period (October, 20-24th). The labels indicate: Rad (PAB [> 280 nm] and P [> 400 nm] treatments), Nut, nutrients (ambient, dust and riverine) and Time, the experimental period. F represents the F-test values, and the asterisks *, ** and *** represent the $p < 0.05$, $p < 0.01$ and $p < 0.001$, respectively.

Dark CR	
Treatment	F
Rad	2.28
Nut	15.67***
Time	346.34***
Rad×Nut	5.11*
Rad×Time	27.90***
Nut×Time	134.71***
Rad×Nut×Time	22.50***

Table 3: Results of statistical analysis of the one-way repeated measures analysis of the variance (ANOVA) of the UVR effects (%) on dark community respiration (CR) and daily CR over the experimental period (October, 20-24th) under three nutrients conditions: ambient, dust and riverine inputs. The labels indicate: Nut, nutrients source and Time, the experimental period. F represents the F-test values, and the asterisks *, ** and *** represent the $p < 0.05$, $p < 0.01$ and $p < 0.001$, respectively.

	UVR effect on dark CR	Daily CR
Treatment	F	F
Nut	4363.21***	0.07
Time	31590.82***	114.38***
Nut×Time	58376.17***	105.17***

Table 4: Results of statistical analysis of two-way analysis of the variance (ANOVA) of each factor considered and their interaction on autotrophic nanoplankton (ANP), autotrophic picoplankton (APP) and heterotrophic picoplankton (HPP) abundances after five days of incubation. The labels indicate: Rad (PAB [> 280 nm] and P [> 400 nm] treatments), Nut, nutrients (ambient, dust and riverine). F represents the F-test values, and the asterisks *, ** and *** represent the $p < 0.05$, $p < 0.01$ and $p < 0.001$, respectively.

	ANP	APP	HPP
Treatment	F	F	F
Rad	19.85***	16.26**	252.10***
Nut	63.79***	3.75	48.66***
Rad×Nut	0.10**	2.73*	48.94***

Table 5: Mean (± SD) nitrate + nitrite, phosphate and silicate concentrations (in μM) at the beginning, middle and at the end of the experiment (October 20-24th, 2014) under two radiation treatments, PAB (> 280 nm) and P (PAR, > 400 nm) and three nutrient treatments, ambient (amb), dust and riverine (riv) inputs.

Treatment	Oct 20	Oct 22	Oct 24
		Nitrate + Nitrite	
PAB_{amb}	2.44 (±0.00)	0.05 (±0.03)	0.01 (±0.01)
P_{amb}		0.07 (±0.03)	0.06 (±0.03)
PAB_{dust}	2.75 (±0.00)	1.23 (±0.65)	0.04 (±0.01)
P_{dust}		0.05 (±0.02)	0.01 (±0.00)
PAB_{riv}	64.42 (±0.00)	55.36 (±0.36)	63.81 (±0.80)
P_{riv}		54.37 (±4.13)	62.61 (±3.80)
		Phosphate	
PAB_{amb}	1.76 (±0.00)	1.78 (±0.04)	0.27 (±0.06)
P_{amb}		1.28 (±0.14)	0.42 (±0.01)
PAB_{dust}	2.91 (±0.00)	0.64 (±0.03)	0.30 (±0.06)
P_{dust}		0.85 (±0.19)	0.60 (±0.08)
PAB_{riv}	32.60 (±0.00)	24.76 (±2.95)	25.16 (±2.38)
P_{riv}		23.81 (±2.28)	13.98 (±1.73)
		Silicate	
PAB_{amb}	58.53 (±0.00)	76.74 (±5.33)	43.69 (±2.34)
P_{amb}		50.59 (±0.03)	40.24 (±3.30)
PAB_{dust}	63.43 (±0.00)	55.13 (±2.50)	44.91 (±0.55)
P_{dust}		58.54 (±7.26)	43.26 (±5.74)
PAB_{riv}	198.79 (±0.00)	118.29 (±8.48)	106.86 (±11.68)
P_{riv}		112.97 (±5.85)	93.27 (±10.25)

Supplementary figures

Figure 1: (A) Mean (± SD) monthly particulate organic carbon (POC, in mg C m^{-3}) from 1997-2016 and monthly photosynthetically active radiation doses (PAR, in MJ m^{-2}) from 1999-2015 period , (B) mean (± SD) annual aerosol index > 0.5 (AI > 0.5, relative units) and (C) total number of AI > 0.5 events from 1995-2015 period on Egi station (43° 18.8′S, 65° 02.0′W). Solid and dashed lines represent the linear regression fit.

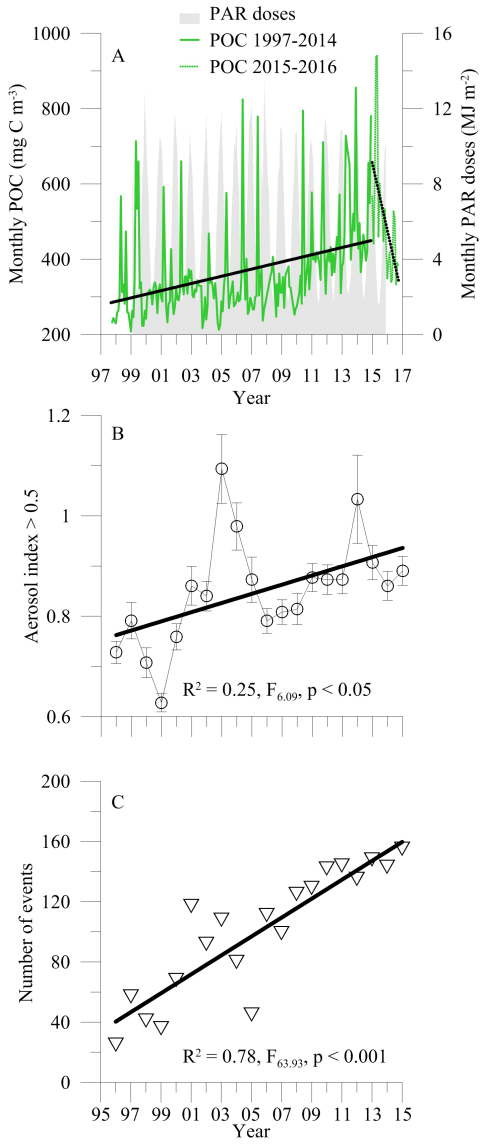

Chapter VIII

Synthesis

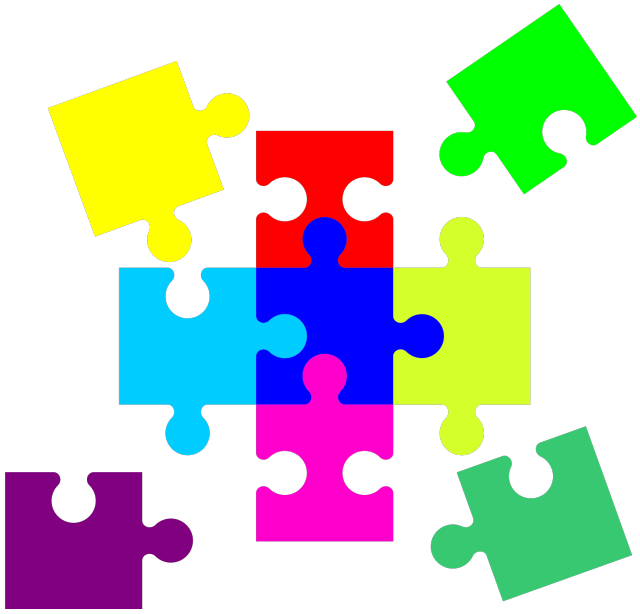

This thesis presents an empirical evaluation of the interactive effects of three of the main global-change factors that are affecting aquatic ecosystems: ultraviolet radiation (UVR), nutrient inputs (Nut), and temperature (T). From this complex environmental scenario, an ambitious approach was developed combining laboratory and field experiments and remote-sensing data, different spatio-temporal scales, and levels of biological organization in order to quantify the plankton responses to multiple global-change drivers. With these premises in mind the first question raised is:

1. How do key phytoplankton groups respond to a predicted global-change scenario?

Under current environmental conditions UVR was found to consistently inhibit the photosynthesis and PSII performance of all species assessed (i.e., Bacillariophyceae, Chlorophyceae, Dinophyceae, and Haptophyceae) whereas strongly increasing the respiration of the four phytoplankton species (Chapter III). However, in a future global-change scenario under UVR, simulated warming of up to 4°C and increased nutrient concentrations (20-fold), two opposite specie-specific responses were determined: (1) an antagonistic response of Bacillariophyceae and Haptophyceae, with an increased photosynthetic activity and repair rates together with depressed respiration rates. The underlying mechanism was a suitable functioning of the oxygen-evolving complex (OEC), which could have favored an increased electron gradient and consequently greater NPQ activity; and (2) a synergistic response of Chlorophyceae and Dinophyceae with an accentuated harmful UVR effect on all the processes mentioned above. The reason behind these responses may be a damaged OEC or even, in the case of Chlorophyceae, the fact that the xanthophyll cycle is based in the violaxanthin, which involves two de-epoxidation stages and thus implies a longer response time to cope with the stress than in the case of Dinophyceae, where the diadinoxanthin cycle requires only one de-epoxidation stage. These opposite responses to the interaction among multiple drivers reveal that it might not only affect the primary production (PP) of aquatic ecosystems but

may also alter community structure; benefiting certain populations of organisms (e.g., Bacillariophyceae and Haptophyceae) as opposed to others (e.g., Chlorophyceae and Dinophyceae).

Noticeably, these responses were deduced at the populational level under constant stress, although the extrapolation to natural conditions requires an approach that also considers the seasonal variability of the environmental conditions. Hence the following question is:

2. Can the natural environmental variability of ecosystems alter the magnitude of response of phytoplankton communities to global change?

When the timing of the three global-change drivers acting together over the phytoplankton succession was considered, our experimental results showed increasing inhibition of the NCP and PSII performance towards bloom compared to pre-bloom (Chapter IV). The increased inhibition during the most productive stage of the succession matched a stronger dominance of larger organisms such as diatoms, but also with low solar radiation doses received and *in situ* T. This higher inhibitory effect found during the bloom under the UVR × Nut × T interaction was not accompanied by a stimulation of processes such as PSII repair or respiration to attenuate the detrimental effects of a global-change scenario. These observed differences between pre-bloom and bloom periods and the diminished NCP (and PSII) towards bloom under a global-change scenario suggest direct harmful effects on phytoplankton. Nevertheless, the NCP assessed in our study constitutes a community-level response that integrates not only phytoplankton responses but all of the processes affecting the balance between production and respiration. Because these studies were focused on primary producers, and did not consider the role that decomposers may have in the C cycle, our next challenge was examine how the joint effect of nutrient inputs and UVR might affect the coupling phytoplankton-bacteria in nature (Chapter V). Therefore, the third question to solve is:

3. Can a future global-change scenario alter the planktonic dynamics and consequently the producer-decomposer coupling?

Our observational results through a long-term whole-lake study (6 years) indicated that planktonic community dynamics depend strongly on the schedule of nutrient inputs, with high-intensity pulses prompting shifts towards communities dominated by photoautotrophs, whereas low-intensity but high-frequency pulses promote changes towards communities dominated by mixotrophic nanoflagellates (MNFs) (Chapter V). Surprisingly, the heterotrophic compartment showed no clear response pattern over time, regardless of the timing of nutrients regime. From these observational results, it was experimentally tested (3 weeks) whether the nutrient-input timing and high UVR levels could alter both the planktonic dynamic as well as the coupling between phytoplankton and bacteria. Our results imply that the joint action of the two drivers may reinforce the commensalistic phytoplankton-bacteria interaction, particularly under a growing frequency of pulsed nutrients. The coupling of phytoplankton and bacteria by a greater release of organic C stimulated a higher bacterial growth and a subsequent consumption of them by MNFs because: (1) they are able to combine phototrophy and phagotrophy within the same cell; and (2) they are competitively more successful than other groups (i.e., photoautotrophs, ciliates or heterotrophic nanoflagellates) under low-nutrient and high-light conditions. Thus, taking into account all the aspects described above from population to community level and from short- to mid-term scales (Chapters III to V), the last level of complexity to test the potential global-change impact are the ecosystems, and thus the final question to answer becomes:

4. How might temperate ecosystems of both hemispheres with contrasting trophic state perform in the future?

Traditionally, it has been associated the predominance of heterotrophy with unproductive marine (i.e., open ocean) and freshwater (i.e., high-mountain lakes) ecosystems, whereas a strong autotrophy has been related

to highly productive areas (i.e,. coasts). In the Chapter VI, it was demonstrated that oligotrophic ecosystems of the Northern Hemisphere can be autotrophic or heterotrophic, i.e. metabolically diverse. Conversely, a future environmental scenario with enhanced nutrient inputs through atmospheric dust deposition and high UVR levels may not only stimulate the activity of the biological pump with respect to the heterotrophic processes but may also even shift the trophic state of these areas. Hence, coastal ecosystems could act as major CO_2 sinks in the future instead of as CO_2 sources. By contrast, when a future environmental scenario of increased nutrient concentrations and UVR levels was simulated, but in a highly productive coastal ecosystem of the Southern Hemisphere, the results indicated that although these environmental conditions did not reverse the CO_2 sink capacity of these ecosystems, it severely decreased their ability to take up CO_2 from the atmosphere (Chapter VII).

In view of the fact that ecosystems of both hemispheres showed a dual response to the interaction between increased nutrient inputs and high UVR levels, our results point out that if this trend continues in the coming decades, the current role that unproductive ecosystems (as CO_2 sources) and highly productive ones (as CO_2 sinks) have in the global C cycle could be severely altered. Concluding remarks are exposed in the following chapter.

Chapter IX

Conclussions

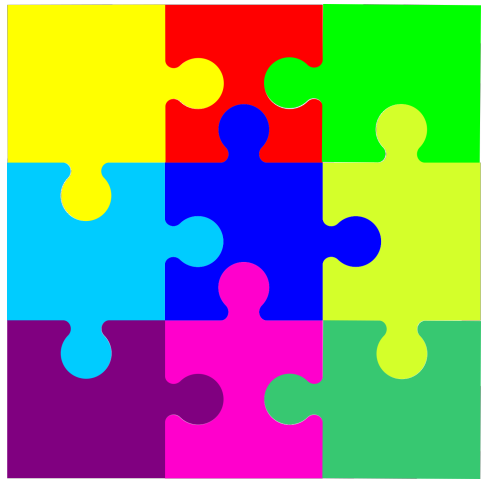

1. At the population level, the photosynthetic activity of all taxonomic groups assayed, Bacillariophyceae, Chlorophyceae, Dinophyceae, and Haptophyceae, was highly sensitive to ultraviolet radiation (UVR) whereas that the processes of respiration and PSII repair did not show a clear response. The interaction among UVR, nutrients, and temperature attenuated the harmful UVR effect (antagonistic effect) on photosynthetic activity of Bacillariophyceae and Haptophyceae but accentuated it (synergistic effect) on Chlorophyceae and Dinophyceae.

2. At the community level, the inhibitory UVR effect on net community production from pre-bloom to bloom period was progressively accentuated by the interaction with increased nutrients and temperature, and it also matched with the predominance of larger diatoms, lower *in situ* T and solar irradiances.

3. Within planktonic communities, the interaction producer-decomposer was strengthened by a rising frequency of nutrient inputs and high UVR levels. This reinforcing was caused by an increase of dual control through the release of photosynthetic C and the predatory pressure exerted by mixotrophic nanoflagellates.

4. At the ecosystem level, the metabolic balance in unproductive areas was altered by dust deposition and high UVR fluxes towards an enhanced autotrophy, increasing the activity of the biological pump. However, in highly productive ecosystems nutrient inputs under stressful UVR fluxes decreased the CO_2 sink capacity regardless of the origin of the nutrients source, riverine or atmospheric aerosol.

1. A nivel poblacional, la actividad fotosintética de todos los grupos taxonómicos considerados, Bacilariofíceas, Clorofíceas, Dinofíceas y Haptofíceas, fue muy sensible a la radiación ultravioleta (RUV) mientras que los procesos de respiración y reparación del PSII no mostraron un patrón de respuesta claro. La interacción entre RUV, nutrientes y temperatura atenuó el efecto dañino de la RUV (efecto antagónico) sobre la actividad fotosintética de Bacilariofíceas y Haptofíceas pero lo acentuó (efecto sinérgico) sobre Clorofíceas y Dinofíceas.

2. A nivel de comunidad, el efecto inhibitorio de la RUV sobre la producción neta de la comunidad desde el periodo de pre-bloom al bloom fue progresivamente acentuado por la interacción entre incrementos en las concentraciones de nutrientes y temperatura; además, esto también coincidió con una predominancia de grandes diatomeas, menor T *in situ* e irradiancias solares.

3. Dentro de las comunidades planctónicas, la interacción productor-consumidor fue fortalecida por una creciente frecuencia de entradas de nutrientes y altos niveles de RUV. Este reforzamiento fue causado por una potenciación del control dual que nanoflagelados mixotróficos ejercieron sobre bacterias a través de la liberación de C fotosintético y de una mayor presión de depredación.

4. A nivel ecosistémico, el balance metabólico de áreas improductivas fue alterado por la deposición de polvo atmosférico y altos flujos de RUV hacia una potenciada autotrofia, incrementando la actividad de la bomba biológica. Sin embargo, en ecosistemas altamente productivos, las entradas de nutrientes bajo niveles de RUV estresantes llevó a una disminución en la capacidad como sumidero de CO_2 de estas áreas con independencia del origen de las fuente de nutrientes, ya sea fluvial o bien de aerosoles atmosféricos.


Erkjennelsene
Agradecimientos
Remerciements
Dankwoord
Eskertza
Acknowledgements
Penghargaan
Riconoscimenti
Danksagungen
Reconeixements

A lo largo de este capítulo de esta historia llamada vida, los avatares de la misma me han otorgado el privilegio (y hasta me atrevería a decir que por qué no la suerte) de cruzar mi camino con otras muchas (y variadas) historias, en muchos casos anónimas; sin embargo, todas y cada una de ellas comparten un nexo común de unión, un bien preciado y escaso, el tiempo, su tiempo; tiempo que cada una de esas historias decidió regalarme y compartir conmigo a sabiendas de que jamás podrán volver a recuperarlo. Por ello, y ya que siempre estaré en deuda con todos/as y cada uno de vosotros/as, y por si mi memoria me falla en este preciso y efímero instante de exaltación emocional, recibid mi más sincero agradecimiento.

En primer lugar, quiero agradecer a mis padres la oportunidad de ser, sentir y padecer, de enseñarme el camino pero dejarme tropezar, caer y volverme a levantar tantas veces como haya sido necesario, por la libertad de decidir siempre cómo, dónde, por qué, para qué y con quién, por no cuestionar ninguna de mis decisiones, y a pesar de no haberlas compartido, y en muchas ocasiones ni siquiera comprendido, apoyarme sin más.

A Rosa, por ser una MADRE con mayúsculas, por dar su alma desde el principio, por ser un ejemplo de fortaleza, lucha y superación constante, y por no dejar de estar ahí nunca. A mis tres hermanos, a mi hermana y a sus respectivos/as por tanto a pesar de mis ausencias, de mis idas, venidas y de mis vueltas a ir, de mis infinitos "tengo muchas cosas que hacer" o "es que tengo que terminar unas cosillas", por esos días en los que uno puede verse desayunando en lugares insospechados (¡Eh!, Alba) y por esos déjà vu en los que uno dice, y si sí?...o, y si no?...y al final la realidad (o la llave girando en la cerradura de la puerta) te devuelve justo a ese lugar del que quisieras escapar. A mis sobrinos/as y primillos/as, por recordarme que nunca jamás deje de mirar las cosas (y la vida) con esos ojos, sus ojos.

A mis abuelos, Fermín y María, por soportar durante mi infancia y en años mozos mis incesantes por qué y por dejarme ser un "cazoletero" incansable en ese corral que hacía las veces de laboratorio/invernadero/sala de juegos. A mi tíos, María y Rafael, por demostrar que uno siempre tiene

que dar lo mejor de sí, pase lo que pase, pese a quien pese y cueste lo que cueste, sin esperar nunca nada a cambio, y por esos años de haza y acequía que uno tanto echa menos.

A Roquito e Isabel, por la oportunidad de empezar a ganarme la vida con bandeja, mandil y pajarita, por esos mejillones a la marinera, foie y calderetas de verano inolvidables, por las cervecitas que os debo y deberé hasta el fin de mis días (jijiji), y por tantos buenos momentos alrededor de esa mesa y piscina. También a Jose y Susana, por estar ahí a pesar de la distancia, y por no dejar nunca de invitarme a ir a Barcelona a pesar de que el invitado nunca (casi) cumpla con su dicha.

A Rubencito, por ser la otra parte del dúo Chivitas en la farándula mollera, por la ayuda a "romper" vitros, planchas y PCs, a "comernos" cajones de Cheesecake y Almendrados, por tirar limones a maceteros, hacerle la competencia a BMW (por las líneas me refiero) y ver como a Mariano se le ilumina la cara al pensar en nuestro aguinaldo, por tener que soportar juntos oír el Arrebato y esa aspiradora golpeando la puerta tantas y tantas mañanas en las que uno era un sucedáneo de "muñequito", después de una larga noche como "hombrecito". Neeeennnnaaa, eso, lo sabía yo! (tienes que leerlo con voz de Isabelita). A Mari Paz, la única e inigualable, por soportarnos a lo largo de todos estos años al resto de chicos de la familia.

A los de siempre, Alex (Kantal), Javi Nuñez, Paquito, Martita, Patris (Puerta y Mesa) y Sarita, por estar ahí a pesar de no hacer mucho ruido ni pedir nunca explicaciones, por esas mañanas, tardes y noches de sancajeo del bueno, y del no tan bueno. A Javi Heredia, al que las vicisitudes de la Biología hace más de una década nos hizo unirnos, pero aquellas de la vida nos hizo separarnos, sin embargo, y pese a todo este largo espacio-tiempo, has estado y sigues estando ahí. Gracias, por tu amistad sincera y por ser un AMIGO de verdad, por esos Macarrones Boloñesa y por aquello de que los capítulos tienen un principio y por supuesto, siempre han de tener un final.

A los Bereberes (o Berebercios), por la acogida de este extraño que se coló en vuestro viaje, y en muchas de vuestras vidas, por los momentos vividos a lomos de una duna, nuestra duna, por las interminables horas de autobús jugando a lobo, y por las noches de azotea en un lugar perdido en mitad de la nada, donde esa nada te hace sentir lo pequeños que podemos llegar a ser en la inmensidad de este maravilloso lugar llamado Universo.

A Aida (sin tilde, por supuesto), Dani, Gaby, Greta, Laura, Víctor, Cande, Tashin, Gina y Esme (la vecina), por tantísisma buena indecencia junta, por esos días en los que uno sabe cómo y dónde empieza todo, pero no cómo y dónde puede acabar; eso sí, de la música ni os preocupeis, hacedme caso por una vez y olvidaos por completo, ya que siempre acabará sonando la misma banda sonora. Ahora me pregunto, ¿Quién dio vela a este Enrique para tanto "entierro"?.

A todos aquellos/as que hay o ha habido tanto en el Instituto del Agua, como a uno y otro lado de la frontera, de esa delgada línea roja, la puerta interdepartamental Ecología-Genética, gracias por dejarnos ocupar vuestro nicho ecológico, a veces, más allá de la capacidad de carga, por esos días (y tardes-noches-mañanas) de tés y cafés, de comedores, Zahor o tupper y patio, de cineclub ecológico, tapas y Perro (con su perrito), de Marisma (y sus pipas), de Sidrería, de campo, playa y barbacoas. A Javi Valverde, por cambiar mi concepción de lo que es un/a liberal (8 = 80, forever and ever), a Emilio y Laura por demostrarme empíricamente que se puede "hablar mal" de alguien justo a sus espaldas (recordad el Peatón), y por enseñarme pequeños-grandes lugares (El Vini), a Alba porque "submitir" o "atachar" algo puede hacerte famoso de entre los famosos en sus citas para Whatsapp, a Carlitos por no decir NO a casi nada sea el día y la hora que sea, por enseñarnos que el café SIEMPRE va con dos azucarillos ("Maaammaaá querida!!") y que el dulce de leche pega con cualquier cosa (¡Ay!, la puucchhaa!), simplemente hay que tener el paladar adecuado. A Diego y Gema, a pesar de no deleitarnos más con su excelsa presencia. A Ana Funes, por su carisma y por ponerle siempre el punto positivo a las cosas, a pesar de que a veces un mismo no se lo encuentre. A Ana Mellado, por esas discusiones

sobre interacciones tróficas y recursos pulsados, y por esos momentos sencillos (¡Ay!, las termas) que jamás uno olvida; a Lucía, porque volar alto y lejos es cuestión de "liarse la manta a la cabeza y tirar pa'lante" y a Raquel, Martín, Mode, Alex, Eli y Ada por devolverme en muchas ocasiones a la cotidianidad de las cosas y del día a día. A Irene y Guille (y sus Alegrías), Silvia, Eva, Paulita y Fran Bullejos por ser parte de mis inicios en este mundo llamado ciencia y sus intríngulis. A Kina, por hacerme mirar las migas edulcoradas, las lentejas de lata y las tartas con todos sus estabilizantes ($\pm$ 10 como mínimo, si no 'nanai') made in Mercadona con mejores ojos (Ohhhhh, mother 'main'), y a Sergio, por enseñarme que los zumos de cristal unidos con enebro destilado y paseo en bici pueden llegar a ser compañeros de viaje poco recomendables. Gracias a ambos por aquellas tardes y momentos tan buenos en esos días algo nublados para los tres ;).

A Ismael, por permitirme obtener una visión dispar, en ocasiones alguien diría que hasta descabellada, de una misma realidad, y por hacerme recordar en mi fuero interno su genealogía a 3.000 metros tratando de inflar una zodiac con un inflador de muy dudosa eficiencia, mientras en mi cabeza sonaba "sí, sí, está todo perfectamente preparado y controlado para mañana" (jajaja); y a Juanma Olalla, por su ser y buen hacer, y por aceptar el reto de embarcarse en un crucero de "ensueño", que no de lujo, a través del Mediterráneo para hacer "cosas de polvos y luces (de colores)".

Y cómo no a los genéticos, María, Caro y a Merce ('alias' la niña de los churros), y Paquillo y Rubén, porque uno puede acabar sin quererlo, pero si bebiéndolo, enjaulado o dando explicaciones a un "mili-troncho" sobre los pormenores del mayor o menor fitness reproductor de los alopécicos frente al resto de los mortales.

A Bea, Bibi, Araceli, Sergio Mesa (y Niaka), Belenchu, David, Kenia, César (y su para qué), Paco, Gianlu, Senda y Rodrigo por tantas y tantas risas, ilusiones y buenos momentos, por esas interminables tardes de juegos y noches sin fin. A Juanmi Olivares y a Laurita, por recordarme que si algo es susceptible de ser comprado, ¿para que invertir tiempo en hacerlo

por uno mismo? (jijiji); y porque la impuntualidad, siendo sincero, puede ir reñida con el buen ser, buen hacer y hacer sentir bien a uno, gracias a vosotros!.

A Carmen, por hacerme cambiar con su fugaz presencia e impronta muchas de las respuestas, y cuestionarme muchas de las preguntas (quién sabe si hallaré respuesta a todas ellas), por aparecer sin más, sin ni siquiera pedir permiso, pero también sin pedir nada a cambio a pesar de dar lo mejor de sí misma, por ser y estar, por su impaciente paciencia, por sus innumerables "eres un petardillo", y por ser a *perfect stranger*. Who knows the secret tomorrow will hold?.

Una de las cosas importantes (mucho) y bonitas de una tesis doctoral es que es un trabajo (sí, los escépticos han leído bien, sí, T-R-A-B-A-J-O) que no sólo es fruto del esfuerzo, paciencia, constancia y perseverancia del que se quiere doctorar, sino que también es el resultado (al menos en mí caso puedo asegurarlo con total certeza) del esfuerzo de otras personas que día a día, codo a codo, están a tú lado. Con estas líneas quisiera mostrar mi agradecimiento a todas y cada una de ellas.

En primer lugar, a mis directores, Pre por aceptar el reto de dirigir esta tesis, por aceptar todas y cada una de mis propuestas, sugerencias, "locuras" y presiones a golpe de nudillo y buenos días en tu puerta durante este tiempo, por dejarme elegir dónde quiero ser y sentir, por la oportunidad de ser marinero (y no en tierra precisamente), surcar el Mediterráneo e ir hasta el otro lado del Atlántico casi la mitad de este periplo doctoral, y no precisamente buscando a mi madre con Amedio, por no dejar nunca de alentarme y por poner cada uno de tus días (bueno y malos) lo mejor de tí misma para que aquella "propuesta deshonesta" un buen día de Septiembre, a día de hoy sea una realidad tangible en tiempo y hora. A Walter, por dar lo mejor de tí profesional y personalmente desde el inicio, por tu honestidad y sinceridad en todo esto, por la oportunidad de poder trabajar en esa fábrica de sueños llamada EFPU, por las charlas en la estación, en la chacra o través de skype cualquier día y hora ante mis dudas científicas

interminables, por hacerme dudar de que dudo y ver que uno tiene que ser muy crítico consigo mismo, por "currarme" y hacerme "enamorar" a la argentina infinidad (o más) de veces, y por demostrarme que absolutamente todo (o casi) puede lograrse si uno cree lo suficiente en ello.

Alrededor de estas dos grandes personas, he tenido también la posibilidad de conocer y compartir horas de laboratorio, mar y lagos, ideas, papers, proyectos y por supuesto, asados, cervezas y nesteas (o Terma, en su caso) con otras grandísismas personas. A Juanma Medina y Mani, por darle luz a los días grises, alegrías a las penas, y recordar que uno no por puede estar en un grupo y doctorarse siendo un bebedor nato de té y sus derivados (ahí os dejo la inquietud). A Vir, por haber sido un apoyo constante e incesante cuando uno está tan lejos de casa tratando de construir sobre algo en lo que cree profundamente, por los consejos de vida y ciencia, por las tardes de "cocina y receta elegida", por enseñarme las bondades del fuerte viento Patagónico, que los problemas tienen que tener los minutos contados (5', pies en agua fría, a tomar lo que se pueda y a seguir adelante sin mirar atrás) y que hay que dejarse llevar siempre. A Tomy, quién me preguntó si aparecería algún día justo aquí, sí, en esta sección. Gracias, por esas mañanas de equitación, Petaca y Manuela (jijiji), por tardes de Merlín y por las noches de adivinanzas y acertijos, por hacerme un lugar en esa habitación llamada leonera y preparar (calentar) esas media lunas dulces/saladas. A Amalia y Darío, por estar siempre en el lugar adecuado a la hora justa, y a Estela, no sólo por tu tarta de queso (aún guardo tú maravillosa e inigualable receta) si no por ser un ejemplo de que los años no tienen por qué ser sinónimo de impedimento, si no que son las alas para poder seguir volando hasta el lugar donde uno quiera. A Pau, Ro y Cris por ser compañeros de "fatigas", muestreos y experimentos, y de días y días de facturas, mate, comidas, cenas y Stellas y ballenas.

A Maca, por su cariño, sus ganas y predisposición para todo, por plantearnos experimentos en lo que dura un viaje PU–Rawson o vice versa (jijiji), y por las bondades culinario-resposteras de aquellos lares; y a Balado, por ese chivito al asador que nunca llegó (jijiji), por currar a este "gassshhheeego

de Ezpaña" (Ché, Manolillo, dejate [sin tilde] de joder!) una y mil veces, y porque salir a dar una vueltita, aunque sea la del perro, implica planchar una camisa de las de verdad, pero siempre acompañada de bombachas de campo y alpargatas. A esos "viejitos" que un día decidieron abrir las puertas de su casa para acogerme, y compartir conmigo sus historias de vida, y a Mabel por sacarme una sonrisa diaria cada vez que uno llegaba a casa y encontraba atada al pomo de su puerta una bolsita con delicias caseras de ultramar.

En último lugar, a tí, querido/a, osado/a y anónimo/a lector/a no sólo porque has decidido (o eso espero) llegar hasta la última página de este "librito" escrito en la lengua de Shakespeare, en donde la tónica general de interacciones entre medioambiente y organismos invisibles (pero esenciales) a los ojos prima, sino porque con tu esfuerzo diario, muchas veces me auguro que incluso incosciente, me has dado la gran oportunidad de sumergirme y aproximarme cada día un poco más al conocimiento del mundo real. A todos/as y cada uno/a de vosotros, muchas GRACIAS!.